Transactions of the ASME

TRANSACTIONS OF THE AMERICAN SOCIETY OF MECHANICAL ENGINEERS

VOLUME 77 APRIL 1955 NUMBER 3

Transactions

of The American Society of Mechanical Engineers

Published on the tenth of every month, except March, June, September, and December

Published monthly by The American Society of Mechanical Engineers. Publication office at 20th and Northampton Streets, Easton, Pa. The editorial department is located at the headquarters of the Society, 29 West Thirty-Ninth Street, New York 18, N. Y. Cable address, "Dynamic," New York. Price $1.50 a copy, $12.00 a year for Transactions and the *Journal of Applied Mechanics;* to members and affiliates, $1.00 a copy, $6.00 a year. Add $1.50 for postage to all countries outside the United States, Canada, and Pan-American Union. Changes of address must be received at Society headquarters seven weeks before they are to be effective on the mailing list. Please send old as well as new address.... By-Law: The Society shall not be responsible for statements or opinions advanced in papers or...printed in its publications (B13, Par. 4).... Entered as second-class matter March 2, 1928, at the Post Office at Easton, Pa., under the Act of August 24, 1912....

Visualization Studies of Secondary Flows With Applications to Turbomachines

By H. Z. HERZIG[1] and A. G. HANSEN,[1] CLEVELAND, OHIO

The investigation reported in this paper is intended mainly as an exploratory inquiry into some fundamental aspects of the boundary-layer flows in turbomachines. These studies are preliminary to a more complete analysis of the flow in turbomachines. Nevertheless, the insight obtained into the secondary-flow patterns and behavior is fundamental in nature. Thus it may provide a basis for correlation and interpretation of other experimental data. When flow conditions are sufficiently similar to those which existed in these studies, the conclusions drawn from these tests may likewise serve to extend the understanding and correlation of other experimental data. It is further anticipated that the flow behavior observed experimentally in the various configurations may prove useful as a means for evaluating the reasonableness of various simplifying assumptions used in theoretical analyses. In particular, it might serve as a criterion both in the initial selection of the assumptions and in estimations of the physical validity of analytically obtained results.

INTRODUCTION

PRESENT-day blade design is based mainly on modified two-dimensional or quasi three-dimensional flow theories of perfect inviscid flows. The design is then refined by allowing for such factors as boundary-layer thickness and growth by use of formulas developed from classical studies of simple-flow configurations. Inherent in this procedure is the assumption that such corrections for the effects of viscosity can yield good approximations to the real fluid behavior in the actual turbomachines. Verification of this assumption theoretically can be accomplished only by comparison of the results with a solution for the complete viscous-flow equations in the turbomachine. At the present time (at least), such complete solutions have not been obtained because of the mathematical complexity of the problem. Nevertheless, the combination of simplified-flow theories with adjustments for boundary-layer effects has made it possible to achieve fairly satisfactory design procedures for turbomachines that operate at low and moderate flow speeds.

However, with the trend toward high-speed high-mass-flow turbomachines, these boundary-layer effects become increasingly significant. As transonic velocities are approached, the boundary-layer accumulations and three-dimensional boundary-layer flows, together with their effects upon the main-stream flow, give rise to such large deviations from desired conditions in turbomachines, based on simplified-flow design methods, that the ordinary, rough, qualitative adjustments are no longer adequate. With useful solutions of the complete flow equations still quite remote, it becomes important for the designer to be able to refine his qualitative adjustment procedures in order to compensate successfully for the increased boundary-layer deviations. This, in turn, requires more fundamental information concerning the boundary-layer flow patterns in turbomachines.

These considerations motivated a series of experimental investigations (1, 2, 3, 4, 5, 6)[2] at the NACA Lewis Laboratory. This paper presents and considers applications of the combined results of these investigations, which used flow-visualization techniques as well as total pressure and flow-angle measurements in order to obtain an insight into the three-dimensional boundary-layer flow patterns in typical axial-flow turbomachines. The particular boundary-layer phenomena considered are (*a*) secondary flows in the shroud region (secondary flows are defined as any motions of boundary-layer fluid having components normal to the through-flow directions); (*b*) radial transport of boundary-layer material; and (*c*) blade-tip-clearance-region secondary flows with and without relative motion between the blades and end walls or shrouds.

Applications of the results of these fundamental investigations are the main concern of this report. Accordingly, the emphasis is placed upon reporting the results as succinctly as is possible consistent with understanding the flow phenomena involved. Comprehensive descriptions of the methods employed to obtain the results can be found in the Bibliography.

One secondary purpose of this paper is to indicate possible directions for further studies in experimental research. Another is to indicate the kinds of simplifying assumptions that may be made with regard to theoretical solutions of the flow equations, which will lead to physically valid and useful results.

APPARATUS AND PROCEDURES

A brief general description of the basic apparatus and procedures used for flow visualization is presented. More detailed information, together with a discussion of the validity of the results obtained by flow-visualization techniques, have been presented (1).

Two-Dimensional Cascade

Fig. 1 presents a sketch of the two-dimensional cascade-flow rig. The nozzle section was so designed that the solidity, angle of attack, aspect ratio, turning angle, and blade-stagger angle could be varied quite readily. The entire nozzle assembly was easily removable and for some of these tests the cascade was replaced by sheet-metal cascades of blades or by sheet-metal rectangular bends.

The two-dimensional cascades were used for tests at Mach numbers below 0.4.

Other Configurations

Annular Cascades. A schematic view of the annular nozzle-cascade test unit is shown in Fig. 2. The nozzles investigated therein include: Set A of blades with constant discharge angle designed for smooth two-dimensional velocity profiles, set B of commercially designed blades with constant discharge angle, and set C of vortex blades with smooth velocity-profile design.

---

[1] Lewis Flight Propulsion Laboratory, National Advisory Committee for Aeronautics.

Contributed by the Hydraulic Division and presented at the Annual Meeting, New York, N. Y., November 29–December 4, 1953, of The American Society of Mechanical Engineers.

Note: Statements and opinions advanced in papers are to be understood as individual expressions of their authors and not those of the Society. Manuscript received at ASME Headquarters, July 28, 1953 Paper No. 53—A-56.

[2] Numbers in parentheses refer to the Bibliography at the end of the paper.

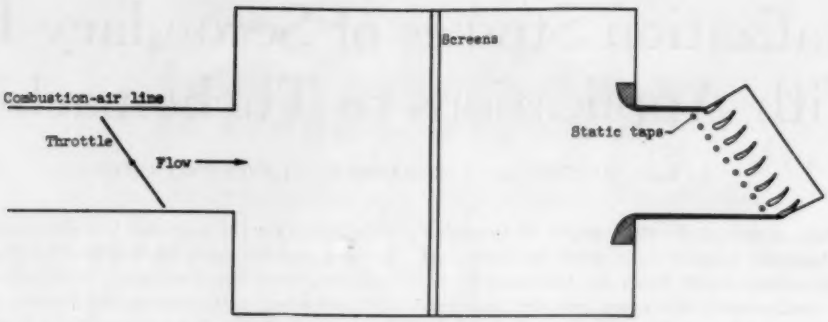

FIG. 1 TWO-DIMENSIONAL STEADY-FLOW CASCADE

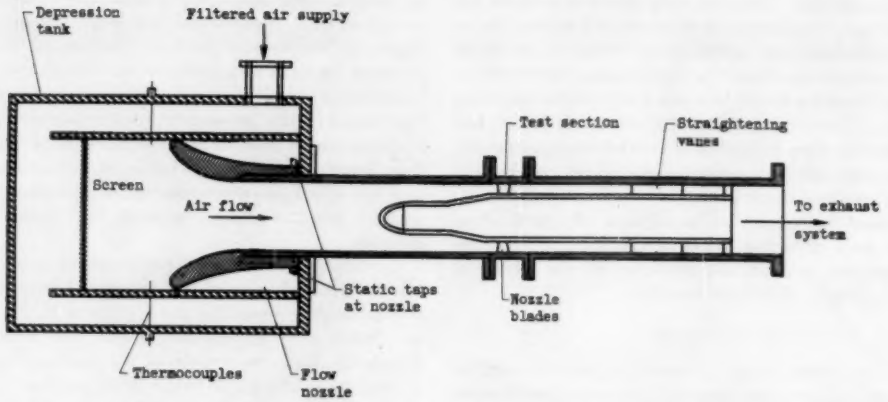

FIG. 2 SCHEMATIC VIEW OF ANNULAR-NOZZLE CASCADE TEST UNIT; FIG. 1, REFERENCE (4)

The annular nozzle cascades were used for a range of hub-discharge Mach numbers up to about 1.5.

Tip-Clearance Configurations. Because one end wall of the two-dimensional cascade was adjustable, it was possible to provide variable blade-tip clearances. For the studies of the effects of relative blade-to-wall motion on the tip-clearance flows, the end wall was replaced by the endless belt of a belt sander whose direction and speed could be varied at will, Fig. 3.

FLOW-VISUALIZATION PROCEDURES

Smoke Studies. The smoke used for flow-visualization studies was generated by burning oil-soaked cigars using compressed air. This simple device, Fig. 4, provided intense nontoxic smoke with no fire hazard. Proper use of the pressure regulators, bleeds, and settling bottles made it possible to inject the smoke in such fashion as to match the local flow velocities.

The smoke flow-visualization method was used at the lowest flow velocities, (about 30 fps). The particular advantage of this method is that it permits an observer to see the actual stream tubes within the flow field as well as on the boundaries.

Hydrogen-Sulphide Traces. The brown trace made by hydrogen-sulphide gas on a lead-carbonate-base paint was used for flow visualization at Mach numbers in the range of 0.4 to 1.5. The traces are of sufficiently high contrast for photographing. Hydrogen sulphide is corrosive and toxic and must be handled accordingly. The chief disadvantage of this method is that it provides indications of flows along the boundaries only. Because of the turbulence at the higher Mach numbers, the hydrogen-sulphide traces indicate the flow paths of a region of the boundary layer instead of individual streamline paths. For these reasons interpretations of the significance of hydrogen-sulphide traces, and the paint traces described in the following section, are made only on the basis of previous information which is obtained either by the smoke-visualization method or by quantitative measurements.

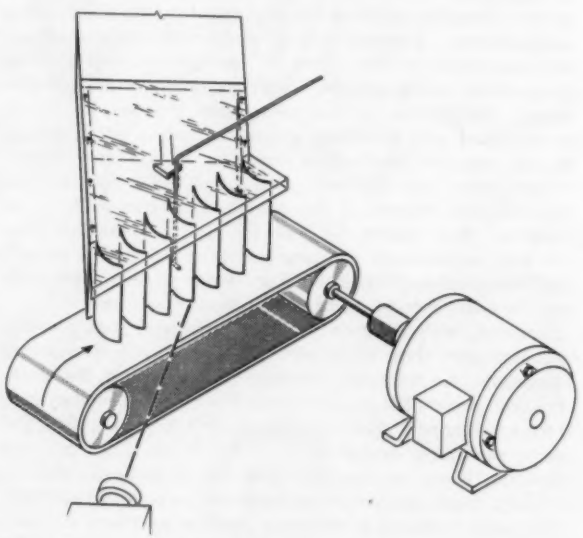

FIG. 3 SCHEMATIC DIAGRAM OF APPARATUS USED FOR STUDYING TIP-CLEARANCE EFFECTS WITH RELATIVE MOTION BETWEEN WALL AND BLADES

Paint Flow Traces. The lead-carbonate paint used for the

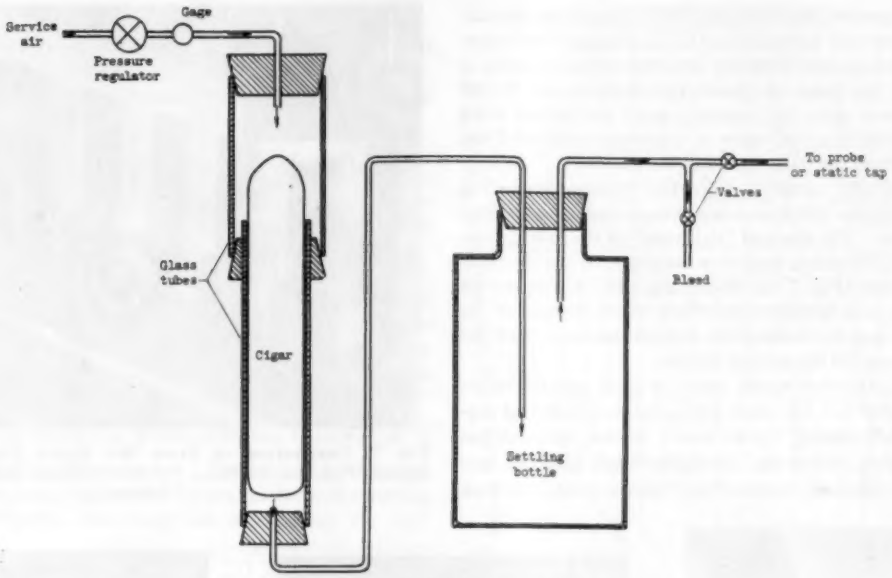

FIG. 4 SMOKE GENERATOR

paint-trace tests was deliberately made nondrying and capable of flowing with surface-flow gradients at the higher Mach numbers investigated. The qualitative results are considered valid only when confirmed by additional experimental evidence.

INSTRUMENTATION

Total pressures, flow angles, and wall static pressures were measured at a discharge-measuring station in the annular cascade investigations. The measuring probes and hot-wire anemometers used are described elsewhere (4). Great care was taken in the fabrication and use of these instruments in order to make the results as reliable and accurate as possible. Nevertheless, because of the large pressure and angle gradients involved in the flow regions of chief interest in this report, the results are discussed in qualitative terms only.

SECONDARY FLOWS IN SHROUD REGIONS

For simplicity the boundary-layer flow study was begun with the visualization of the end-wall inlet boundary layer of a two-dimensional cascade at low air speeds. It was intended, by using the smoke-flow-visualization method, to isolate and to evaluate the effects of main-stream turning upon the wall boundary layer by eliminating such complicating considerations as radial flows and shock phenomena.

Fig. 5 demonstrates the overturning in the end-wall boundary layer that results from imposition of the main-stream static-pressure gradients upon the low-momentum boundary-layer fluid. The smoke was introduced at the wall by means of the probe.

Passage-Vortex Formation. A downstream view of a boundary-layer streamline crossing the 45-deg channel, Fig. 6, shows that as the streamline approaches the suction surface, it deflects spanwise and then rolls up into a vortex-type flow. (The insert shows the entire streamline pattern schematically.) It was found by probe surveys that all the streamlines in the wall boundary layer converged to approximately the same region and rolled up into the flow vortex. The pattern of vortex formation was such that, as the point of smoke introduction was shifted

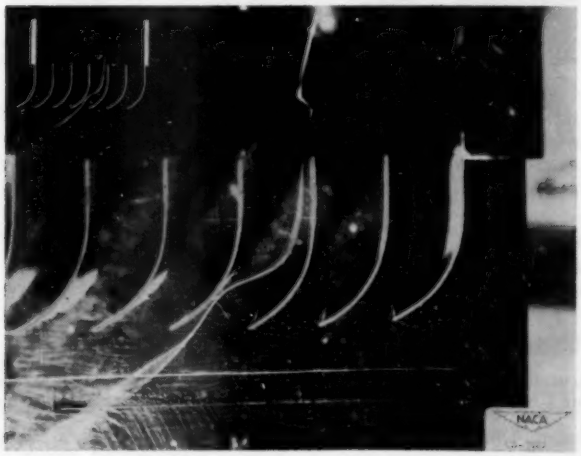

FIG. 5 OVERTURNING IN END-WALL BOUNDARY LAYER DUE TO SECONDARY FLOW
(Smoke introduced through probe on wall in passage at inlet.)

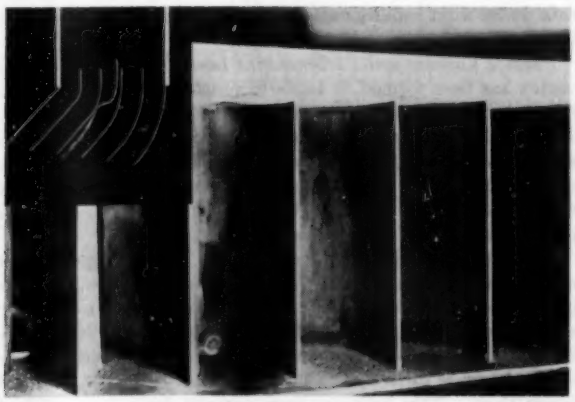

FIG. 6 DOWNSTREAM VIEW SHOWING PASSAGE-VORTEX FORMATION RESULTING FROM ROLL UP OF END-WALL BOUNDARY LAYER
(Smoke introduced on wall near blade pressure surface.)

toward the suction side, the spanwise deflections of the streamlines along the end wall increased as they approached the region of convergence where they rolled up into the central portions of the vortex. As the point of smoke introduction was shifted toward the pressure side, the boundary-layer streamlines along the end wall approaching the region of convergence deflected less spanwise and formed the outer layers of the vortex.

This secondary-flow vortex is called the "passage vortex" in order to emphasize the fact that it is a passage and not a trailing-edge phenomenon. The size and "tightness" of the passage vortex increase with increasing main-flow turning. When the turning is large enough (Fig. 7 for 60-deg cascade), the outermost layer may come from boundary-layer flow which deflects off the pressure surface and flows along the wall all the way across the channel until it reaches the suction surface.

At low air speeds where smoke could be used, passage-vortex formation was observed for other configurations, including cascades of 65(12)-10 blades, vortex nozzle blades, constant-discharge-angle blades, and so on. At higher Mach numbers, surface indications, obtained by use of hydrogen-sulphide traces on

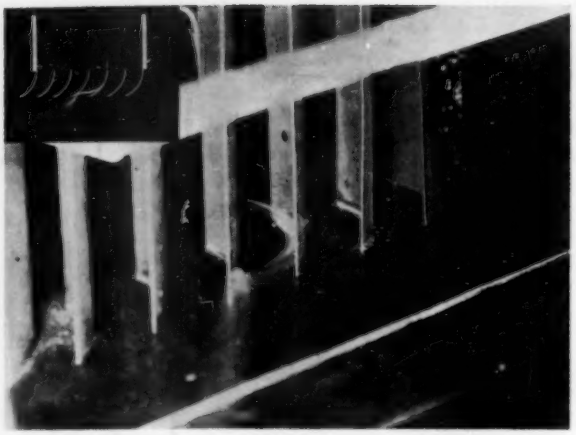

FIG. 7 DEFLECTION OF FLOW OFF BLADE PRESSURE SURFACE, ACROSS PASSAGE, TO ROLL UP INTO OUTER LAYERS OF PASSAGE VORTEX

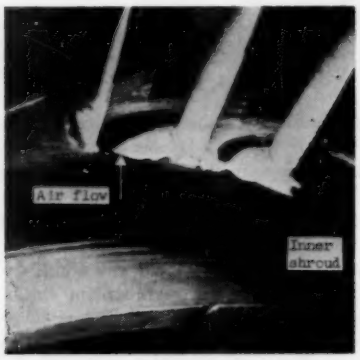

(a) Inner shroud at entrance

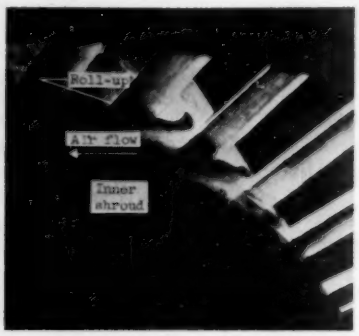

(b) Inner shroud at exit

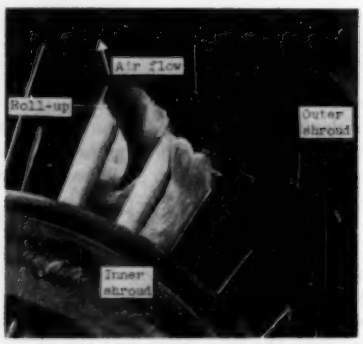

(c) Outer shroud at exit

FIG. 8 HYDROGEN-SULPHIDE TRACES THROUGH BLADE CHANNEL SHOWING CROSS-CHANNEL DEFLECTION PATTERN IN SHROUD REGIONS OF ANNULAR-NOZZLE CASCADE

white-lead paint, show that the cross-channel deflection pattern remains unchanged, Fig. 8, for an annular cascade. The range of velocities investigated is extended to Mach numbers of approximately 1.5 in annular nozzle cascades as discussed in the section Secondary Flows in Turbine-Nozzle Cascades. At that time sufficient additional information is presented to indicate under what conditions a discrete passage vortex is likely to be formed at the higher Mach numbers.

Passage Vortezes and Turbomachine Losses. Once the passage vortex has been formed, it tends to resist turning and does not follow subsequent main-stream turnings as it proceeds downstream. Fig. 9 shows how in tandem cascades a vortex formed in the upstream cascade resists the turning in the downstream cascade. An observer at the tests could see the passage vortex ricochet off a pressure surface of the downstream cascade causing flow separation in the region of impact.

Thus not only does the accumulation of low-energy material near the suction surface of a turbomachine passage cause flow disturbances and losses leading to flow-angle deviations and poor angles of attack in subsequent blade rows, but also the vortex behavior, as it passes downstream, can lead to flow disturbances on the pressure surfaces that it impinges upon and to additional losses there. This behavior may account for a large part of the losses variously attributed to secondary flows. The mixing action of the vortex behavior likewise represents a large deviation from the kind of simplified boundary-layer behavior assumed in some design procedures.

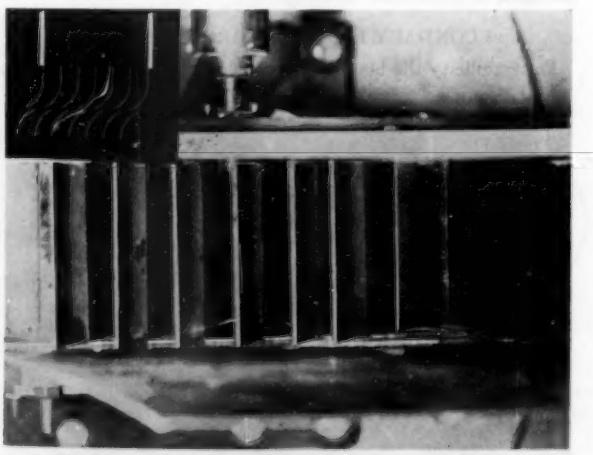

FIG. 9 RESISTANCE TO TURNING OF PASSAGE VORTEX GENERATED BY UPSTREAM CASCADE CAUSES IT TO STRIKE PRESSURE SURFACE OF BLADE IN DOWNSTREAM CASCADE
(Smoke introduced through probe on wall at inlet to upstream cascade.)

SECONDARY FLOWS IN TURBINE-NOZZLE CASCADES

The effects of radial pressure gradients and higher flow Mach numbers were studied in the annular turbine-nozzle cascade test unit, Fig. 2. The three sets of nozzle blades used were typical of the blading of modern high-speed-turbine nozzles.

Secondary Flows in Shroud Regions

The traces of hydrogen-sulphide on white lead, Fig. 8, indicate the same type of cross-channel deflections seen in the end-wall boundary layer of the two-dimensional cascade (1, 4, 5, 6). These tests were conducted at hub Mach numbers up to nearly 1.5, as indicated in the figures. Because of the high velocities and higher turbulence levels involved here, the hydrogen-sulphide trace spread out somewhat rather than defining a sharp line. The results which are now presented for set C of turbine nozzle blades were duplicated for sets A and B as well.

Radial Secondary Flows in Vortex-Nozzle Blades, Set C

Indications Based on Measurements. Contours of local energy loss (4) at the exit measuring station for the vortex blades (set C), are presented in Fig. 10. The energy loss is defined by

$$\text{Loss} = 1 - \frac{V_a^2}{V_i^2} = \frac{\left(\frac{p_2}{P_2}\right)^{\frac{\gamma-1}{\gamma}} - \left(\frac{p_2}{P_1}\right)^{\frac{\gamma-1}{\gamma}}}{1 - \left(\frac{p_2}{P_1}\right)^{\frac{\gamma-1}{\gamma}}}$$

where

V_a = actual velocity as determined from exit static pressure and local total pressure at exit
V_i = ideal velocity as determined from exit static pressure and reference inlet total pressure
p_2 = exit static pressure
P_2 = local exit total pressure
γ = ratio of specific heats
P_1 = reference inlet total pressure

It is noted that the hub-loss accumulation is much larger than the outer shroud-loss accumulation for both the subsonic and supersonic-flow conditions, despite the fact that the "wetted" area is the greater in the outer half of the passages. This is taken to indicate radial flow of boundary-layer material along the blade trailing edge and along the suction surface. The decrease in outer-shroud loss core and increase in inner-shroud core with increasing Mach number indicate the development of additional or larger paths for radial transport of low-energy fluid at the higher flow Mach number.

Visual Indications of Radial Flow. In the presence of a radial pressure gradient in the annular cascade, the radial transport of sizable quantities of low-energy material requires boundary-layer regions, with low-viscous-shear forces, extending from hub to tip on the blades. The blade-trailing-edge regions provide such paths. Another possible radial pathway is provided on the suction surface of each blade at the supersonic-flow conditions when a shock exists across the passage to cause thickening of the blade suction-surface boundary layer. Fig. 11(*a*) shows the location of this shock wave by its effect on paint on the blades and shroud. Fig. 11(*b*) shows the thickened boundary-layer paths along which low-energy material might be transported radially on the blade suction surfaces. For this photograph the suction surfaces of blades 1, 2, and 3 were given narrow bands of paint at the inner-shroud, mid-span, and outer-shroud radial positions, respectively.

Evaluation of Radial Components of Secondary Flow. The existence of radial flow of low-energy material as indicated in the

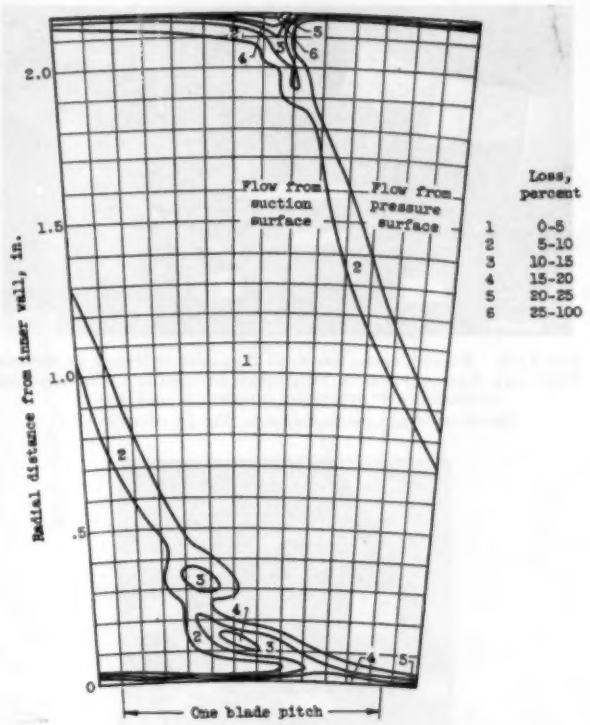

Fig. 10(*a*) Contours of Energy Loss at Exit Measuring Station of Vortex Blades, Set C; Fig. 5, Reference (4)
(Subsonic flow condition; hub Mach number, 0.94.)

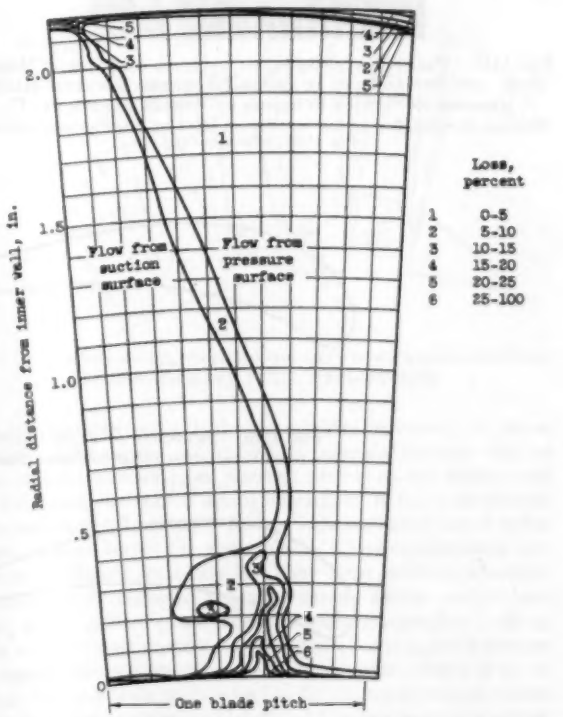

Fig. 10(*b*) Contours of Energy Loss at Exit Measuring Station of Vortex Blades, Set C; Fig. 5, Reference (4)
(Supersonic flow condition; hub Mach number, 1.46.)

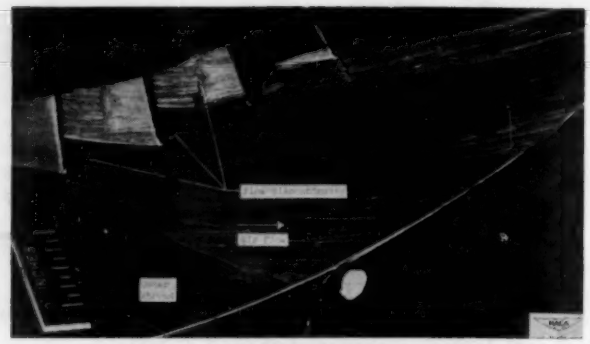

FIG. 11(*a*) PAINT TRACES SHOWING LOCATION OF SHOCK AT NOZZLE EXIT AND RADIAL FLOW IN THICKENED BOUNDARY-LAYER REGIONS ON SUCTION SURFACES OF VORTEX BLADES, SET C
[Shock pattern at nozzle discharge; Fig. 10, reference (4).]

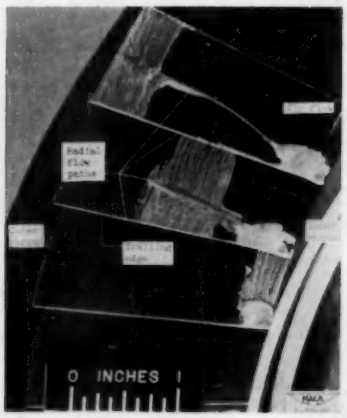

FIG. 11(*b*) PAINT TRACES SHOWING LOCATION OF SHOCK AT NOZZLE EXIT AND RADIAL FLOW IN SHOCK-THICKENED BOUNDARY-LAYER REGIONS ON SUCTION SURFACES OF VORTEX BLADES, SET C
[Regions of radial flow of low-momentum fluid on blade suction surfaces; Fig. 11(*b*), reference (4).]

previous section was proved and the quantity of such flows at the supersonic-flow condition was evaluated by the following quite simple device (5):

Flow fences were fastened to the blades at the mid-span position, as in Fig. 12. The flow fence in Fig. 12(*a*) was intended to interrupt radial flows both along the trailing edge and in the thickened boundary-layer region indicated in Fig. 11. The modified fence, Fig. 12(*b*), which was distorted somewhat during modification, affected only the trailing-edge radial flows. The results are presented in Fig. 13. Because of possible losses due to the fences themselves, the reduction in inner-shroud loss core is used to measure the quantities of radial transport. It was found that, at the supersonic-flow condition for this set of vortex turbine-nozzle blades, radial transport of boundary layer accounted for 65 per cent of the low-energy material in the inner-shroud loss core at the blade-exit station. Thirty-five per cent came through along the trailing edge, and 30 per cent through the thickened boundary-layer paths on the suction surfaces.

Summarizing this portion of the secondary-flow study, the core of low-energy fluid found near the suction surface at the inner shroud of a turbine-nozzle passage is an accumulation of losses that for the most part originate elsewhere in the passage. The paths by which the secondary-flow mechanism transports this boundary-layer material are indicated schematically in Fig. 14. These secondary flows can be diverted, for example, by simple barriers in the flow paths. Thus the degree of underturning at the inner wall, caused by blockage resulting from loss accumulations due to secondary flow, can be reduced, with the secondary flow material being distributed elsewhere in the passage.

SECONDARY FLOWS IN NOZZLE BLADES OF CONSTANT DISCHARGE ANGLE, SETS A AND B

Figs. 15 and 16 [reference (6), Figs. 4(*a* and *d*)] present the loss-core patterns at the exit-measuring stations for the constant-discharge-angle nozzles (sets A and B). The same shift in loss-core sizes is observed for these blades as was observed previously for the vortex blades; this shift again indicates radial secondary-flow components here too. Because paint traces at the supersonic-flow conditions for sets A and B were found to be practically identical with those for set C, Fig. 11, they are not

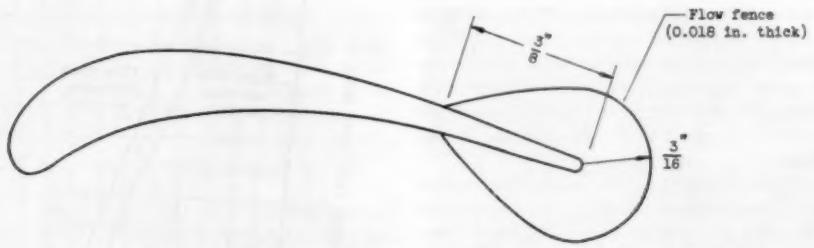

FIG. 12(*a*) SKETCHES OF FLOW FENCES LOCATED ON BLADES AT MID-SPAN POSITION
(Flow fence to interrupt radial flow along blade trailing edge and in thickened boundary-layer region.)

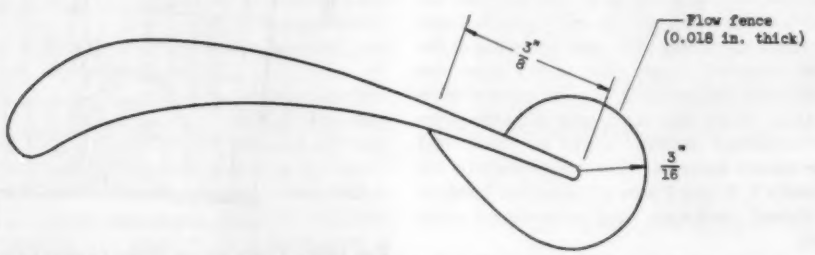

FIG. 12(*b*) SKETCHES OF FLOW FENCES LOCATED ON BLADES AT MID-SPAN POSITION
(Modified flow fence to interrupt radial flow along blade trailing edge only.)

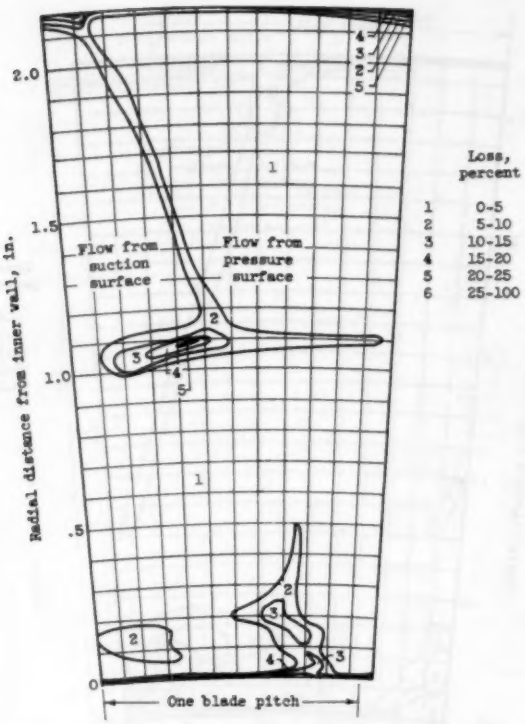

FIG. 13(*a*) CONTOURS OF ENERGY LOSS AT EXIT OF VORTEX BLADES, SET C, SHOWING RESULTS OF RADIAL-FLOW FENCES, HUB MACH NUMBER 1.46; FIG. 12, REFERENCE (5)
(Flow fence interrupting radial flow along trailing edge and along suction surface.)

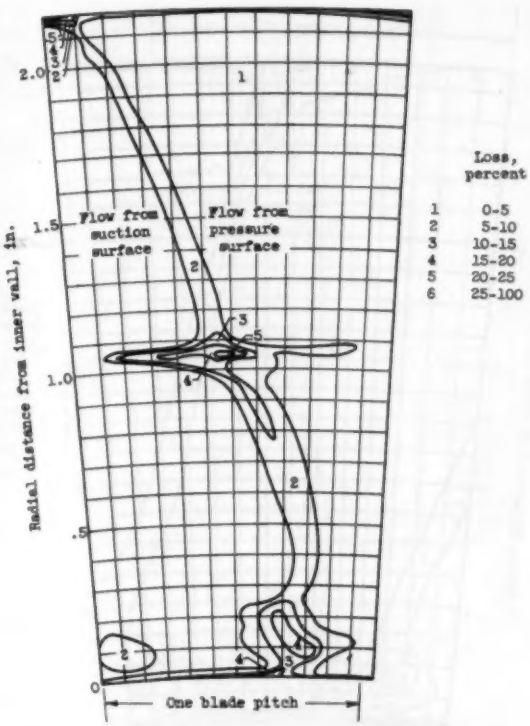

FIG. 13(*b*) CONTOURS OF ENERGY LOSS AT EXIT OF VORTEX BLADES, SET C, SHOWING RESULTS OF RADIAL-FLOW FENCES, HUB MACH NUMBER 1.46; Fig. 12, REFERENCE (5)
(Modified flow fence interrupting radial flow along trailing edge only.)

presented here. Fig. 17 shows the radial trailing-edge flow at the subsonic-flow condition for set A of turbine-nozzle blades.

BLADE VELOCITY PROFILES AND LOSSES IN THREE TURBINE-NOZZLE CASCADES

The radial-flow indications for nozzle set B are qualitatively the same as for nozzle sets A and C. However, the presence of the comparatively large outer-shroud loss cores for set B, particularly at the subsonic-flow condition, calls for a closer scrutiny of the aerodynamic differences between the three sets of blades (6).

Blade Velocity Profiles. The suction-surface velocity profiles for the tip sections of three sets of blades are presented in Fig. 18. Whereas the velocity profiles for sets A and C are smooth, the velocity distributions for set B show two velocity peaks at midspan and three peaks along the suction surface near the outer shroud. According to boundary-layer theory, such velocity peaks and subsequent decelerations lead to relatively large or separated boundary-layer regions on the blades downstream of these peaks. Smooth velocity profiles such as those for blades A and C are more likely to result in relatively thin, unseparated, blade-boundary layers. Smoke-flow tests at low Mach numbers did indicate a large separated region on the suction surfaces of set B and smooth flow over set A, Fig. 19. This was indicated by the slow dissipation of the smoke on the suction surface of set B when the introduction of smoke was interrupted suddenly, thereby indicating a large stagnant flow region on these blades; no such region was observed for set A. These smoke tests were not conducted on set C.

Loss Accumulations and Passage Vortexes. The small-size outer-shroud loss cores for both set A and set C of turbine-nozzle

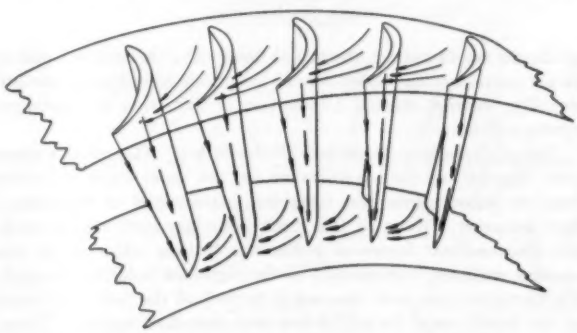

FIG. 14 SCHEMATIC SKETCH OF SECONDARY FLOW PATHS IN ANNULAR NOZZLE CASCADE; FIG. 6, REFERENCE (5)

blades, together with hydrogen-sulphide evidence of cross-channel flows on the outer shrouds, strongly indicate that as fast as the boundary-layer material arrives at the suction side of the passage most of it drains off radially to the inner shroud. The experimental evidence did not indicate formation of a discrete passage vortex for these blades. The experimental evidence is different for blade B. Here there exists a separated boundary-layer region at the outer-shroud section and at least part of the shroud cross-channel boundary-layer flow rolls up into a well-formed passage vortex. Once formed, the resistance to turning demonstrated by the passage vortex causes it to diverge from the blade surface and to be separated from the blade boundary-layer regions in which radial transport normally occurs. Therefore the passage vortex comes off downstream near the outer shroud. With increased Mach number, the radial pressure

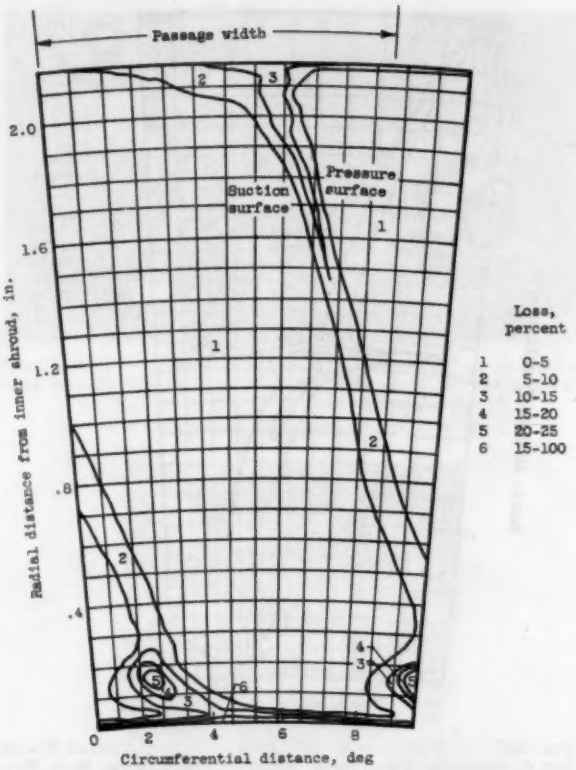

FIG. 15(a) CONTOURS OF ENERGY LOSS AT EXIT MEASURING STATION OF CONSTANT DISCHARGE-ANGLE BLADES, SET A; FIG. 4(a), REFERENCE (6)
(Lower Mach number.)

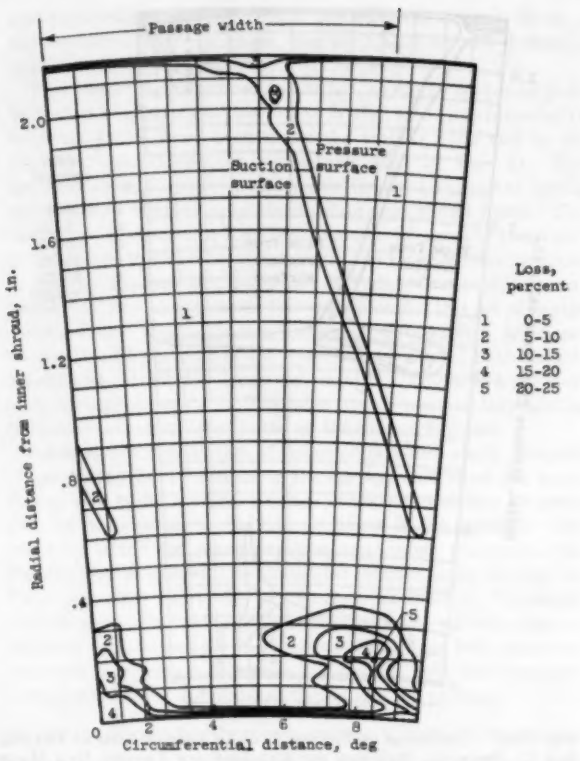

FIG. 15(b) CONTOURS OF ENERGY LOSS AT EXIT MEASURING STATION OF CONSTANT DISCHARGE-ANGLE BLADES, SET A; FIG. 4(b), REFERENCE (6)
(High Mach number.)

gradients are increased, the radial-flow paths are enlarged, and a larger portion of the outer-shroud loss material is drained inward radially, thereby causing a reduction of the size of the passage-vortex roll up.

Radial Secondary Flows and Blade Wakes. The relative sizes and "depths" of the blade wakes for the three kinds of blades tend to substantiate the foregoing explanation of secondary-flow behavior. Even in the thick boundary-layer regions with low-viscous-shear forces at either the trailing edges or on the suction surfaces, components of through-flow velocity do exist. Furthermore, the main flow tends to peel off the boundary layer at the interfaces of the radial-flow and main-flow regions. These two effects are largely responsible for the wakes behind blades. It should then be possible to correlate the size and quantity of low-energy radial flows with the extent and "depth" of the wakes measured downstream. A comparison of Figs. 10, 15, and 16 shows that the wakes for set B are indeed smaller than for sets A and C. This appears to follow logically from the observations that with the blades of set B only a fraction of the outer-shroud boundary-layer material flows radially inward.

It is concluded then that the extent and depth of the wake measured at any radial position are a measure of both the quantity of the radial secondary-flow components and the blade-profile losses.

Remarks on Turbine-Nozzle Performance. Mass-averaged nozzle-blade efficiencies (which typically are on the order of 0.98) are not good indexes of nozzle-blade performance. Better indications of the seriousness of the flow disturbances involved are gained from examining the effects on the discharge flow angles. For example, at the higher Mach numbers, the flow-angle variations across a passage at a radial distance of 0.1 in. from the inner shroud were 8.9, 25.0, and 9.5 deg for blades A, B, and C, respectively. Nozzle-discharge-angle variations as high as 25 deg near the inner shroud can easily result in losses of 3 per cent in turbine efficiency. A further indication is obtained by noting that the maximum-loss parameters (4) found were 21, 67, and 25 per cent for the three sets of blades.

Several positive recommendations can be made to the designer of turbine-nozzle blades from these considerations of secondary flows in turbine-nozzle cascades. Mass-averaged efficiencies notwithstanding, it is worth the time and effort to design blades with favorable velocity profiles. This will result in less severe local flow disturbances and smaller deviations from design discharge angles. It also will serve to put the secondary-flow mechanism to good use by transferring part or all of the loss cores away from the outer shroud where they could aggravate the already disturbed tip-flow region in the rotors downstream.

Nor is it necessary to permit all the loss-core material to pile up near the inner shroud and result in large disturbances in that region. It was demonstrated that the radial flows of low-energy fluids can be interrupted fairly easily.

FLOW IN BLADE-END REGIONS

PRELIMINARY REMARKS

In the blade passages of turbines and axial-flow compressors, there is a tendency for large flow disturbances to occur in blade-end regions. Furthermore, in passages having blade end clearance, the magnitude of the clearance has a direct influence on calculated losses and flow behavior in the blade-tip regions. In

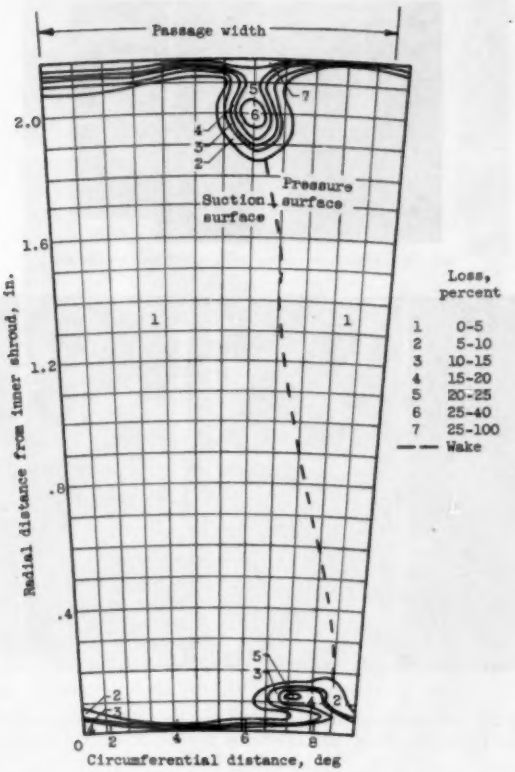

FIG. 16(*a*) CONTOURS OF ENERGY LOSS AT EXIT MEASURING STATION OF CONSTANT DISCHARGE-ANGLE BLADES, SET B; FIG. 4(*c*), REFERENCE (6)
(Lower Mach number.)

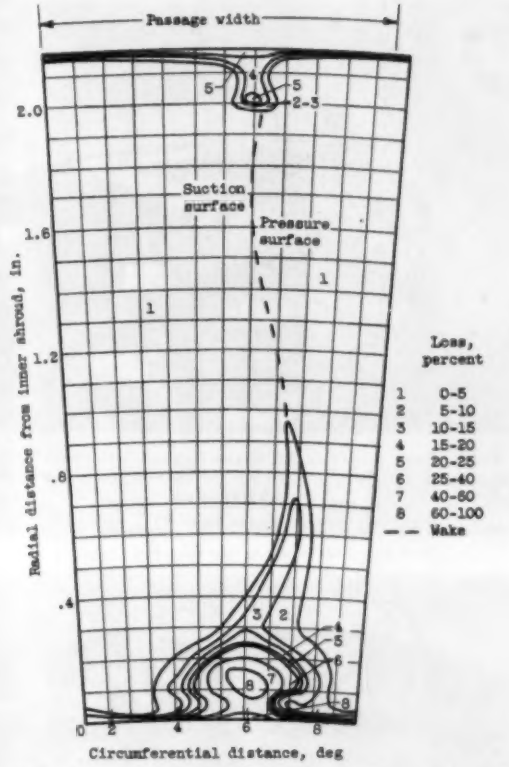

FIG. 16(*b*) CONTOURS OF ENERGY LOSS AT EXIT MEASURING STATION OF CONSTANT DISCHARGE-ANGLE BLADES, SET B; Fig. 4(*d*), REFERENCE (6)
(High Mach number.)

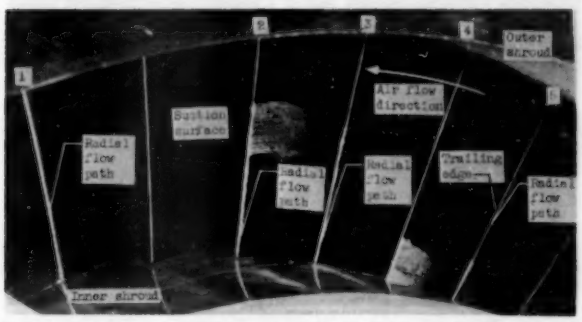

FIG. 17 PAINT TRACES INDICATING RADIAL TRAILING-EDGE FLOW AT SUBSONIC-FLOW CONDITION FOR CONSTANT DISCHARGE-ANGLE BLADES, SET A; Fig. 11(*c*), REFERENCE (6)

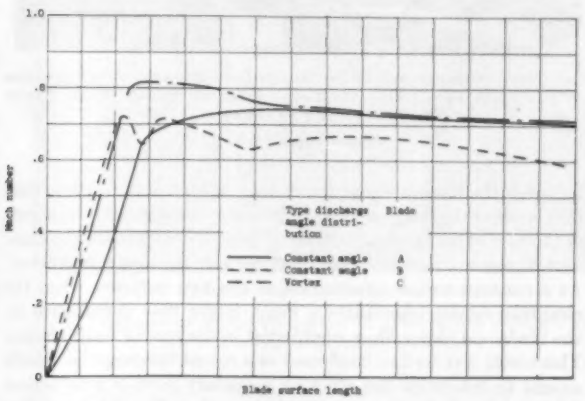

FIG. 18 BLADE SUCTION-SURFACE VELOCITY PROFILES AT TIP SECTIONS FOR THREE SETS OF NOZZLE BLADES; FIG. 2(*c*), REFERENCE (6)

order to understand better the manner in which tip clearance influences flow behavior, flow-visualization studies were made in two-dimensional cascades provided with tip clearance and in a two-dimensional cascade modified to provide relative motion between the blades and an end wall. This latter case was chosen to approximate more closely conditions that exist in an actual compressor or turbine.

TIP CLEARANCE

The initial studies of blade-tip-clearance regions were made in two-dimensional cascades having 0.060 and 0.014-in. tip clearances (1.7 and 0.4 per cent span, respectively). These studies disclosed that flow along the blade pressure surface in the tip vicinity and in the wall boundary layer near the pressure surface deflected under the tip and formed a vortex lying against the suction surface. This deflection and vortex formation is shown in Fig. 20(*a*) for 0.060-in. clearance and in Fig. 20(*b*) for 0.014-in. clearance. Fig. 21 shows that the passage vortex previously described still exists; however, it has been displaced by the tip-clearance vortex. These two vortexes rotate side by side in opposite directions with little apparent mixing. Furthermore, the formation of the tip-clearance vortex appeared to

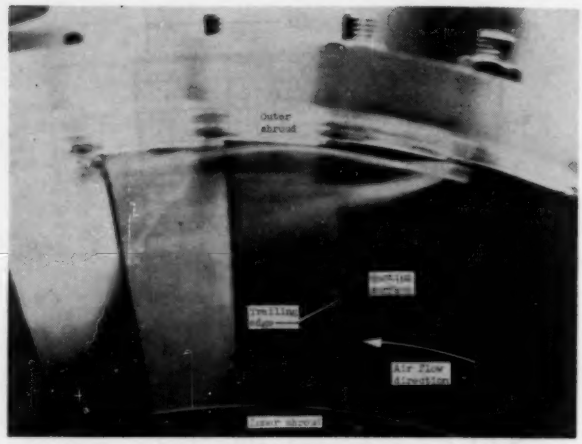

FIG. 19(a) COMPARISON OF BOUNDARY LAYERS ON SUCTION SURFACES OF BLADES A AND B OBTAINED BY INJECTING SMOKE NEAR THEIR OUTER SHROUDS

(Smoke traces, blade A.)

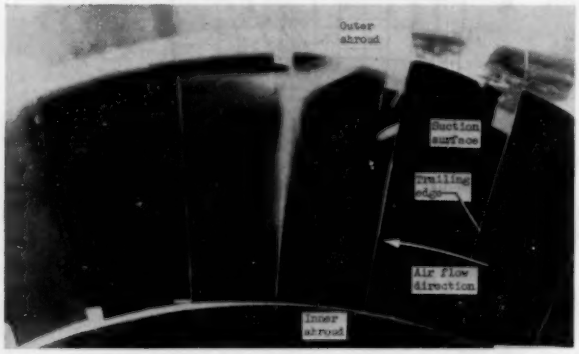

FIG. 19(b) COMPARISON OF BOUNDARY LAYERS ON SUCTION SURFACES OF BLADES A AND B OBTAINED BY INJECTING SMOKE NEAR THEIR OUTER SHROUDS

(Smoke traces, blade B.)

influence the magnitude of the passage vortex only to the extent that some of the flow, on or near the blade pressure surface, which in the case of no tip clearance would have flowed into the passage-vortex region, now becomes part of the tip-clearance vortex. As a consequence, the formation of the two vortexes, when tip clearance exists, constitutes a much larger flow disturbance in the blade-end region than would exist in the case of no clearance. This result was further confirmed in a recent investigation which sought to determine the effect on secondary flows of a reduction in turning at turbine-nozzle blade ends. The blade-section profiles, in this instance, were faired to nonturning sections at the blade ends by cutting back the blade leading and trailing edges starting 0.040 in. from the end wall.

Loss parameters, calculated on the basis of total pressure measurements downstream of the nozzle blades, were found to have increased greatly because of tip-clearance effects that exist when the blades are cut back.

The results of these tests have direct application to stator-blade-row fabrication. They indicate that blade clearance, either arising from improper blade fitting or purposely provided, as in the case previously discussed, generally results in the formation of larger loss regions in the blade passage. This also leads to increased flow disturbances in a downstream rotor.

(a) Tip-clearance vortex with 0.060 inch clearance

(b) Tip-clearance vortex with 0.014 inch clearance

FIG. 20 DEFLECTION OF FLOW OFF PRESSURE SURFACE AT BLADE END, THROUGH TIP-CLEARANCE REGION TO ROLL UP AS VORTEX NEAR SUCTION SURFACE

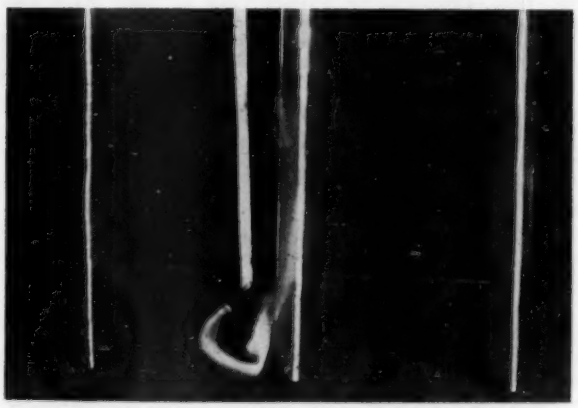

FIG. 21 DISPLACEMENT OF PASSAGE VORTEX BY TIP-CLEARANCE VORTEX

RELATIVE MOTION BETWEEN BLADES AND WALL

As mentioned previously, in order to study flow in a blade-end region when relative motion exists between the blades and an end wall, one of the end walls of a two-dimensional cascade was replaced by an endless moving belt whose direction and speed could be varied at will, Fig. 3. Visualization tests were conducted in this modified cascade for the following wall speeds: Slow (well below air speed); moderate (approximately equal to air speed); and fast (well above air speed).

The tests disclosed two interesting phenomena (3). The first was that a blade surface, which was "leading" relative to the wall motion, exerted a scraping effect on boundary layer entrained on the moving wall. This phenomenon is depicted in Fig. 22(a),

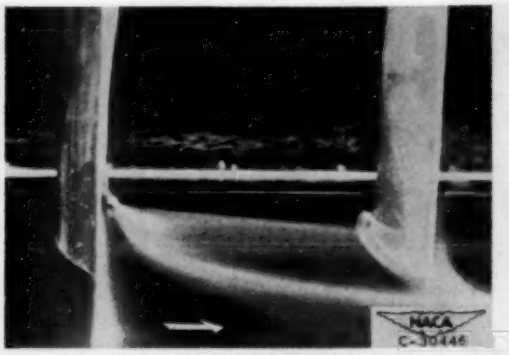

(a) Suction surface leading

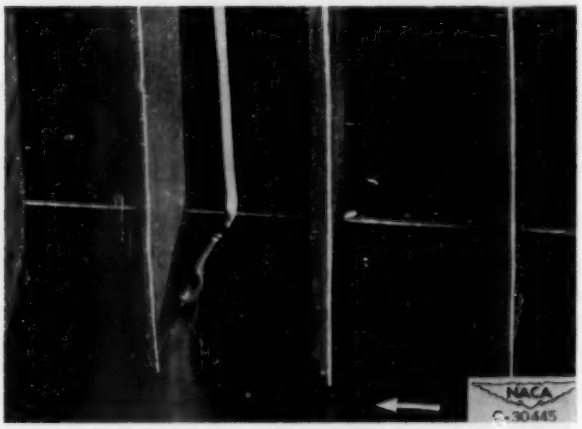

(b) Pressure surface leading

FIG. 22 STREAMLINE PATTERNS SHOWING SCRAPING EFFECTS AT LEADING SURFACES OF BLADES WITH RELATIVE MOTION BETWEEN BLADES AND WALL

where the suction surface is the leading surface, and in Fig. 22(*b*), where the pressure surface is leading. (The latter figure particularly indicates the rolling motion imparted to the incoming air by the blade surface.) One consequence of this scraping action, when the pressure surface is leading, is that flow along the blade surface which normally would have deflected under the blade tip with a stationary wall is deflected away from the wall when relative motion exists.

This flow deflection is shown for a stationary wall in Fig. 23(*a*) and for a wall moving at moderate speed in Fig. 23(*b*): The second result of interest was that the motion of the wall exerted an "aspirating" effect on low-momentum air on the blade surface which was trailing relative to the wall motion and deflected this air toward the wall. Fig. 24 shows this aspirating effect on flow on the blade-pressure surface for a slow wall speed. Fig. 25 depicts the significant increase in flow deflection toward the wall caused by aspiration on the suction surface.

APPLICATIONS TO TURBOMACHINES

The net effects of the phenomena described in the previous section on flow in the blade-tip region of the configuration tested can be outlined as follows:

1 In the case where the pressure surface was leading (as, for example, in a compressor), the indicated flow behavior acted: (*a*) To improve flow conditions in the blade-tip region in the sense that it prevented flow on the pressure surface from deflecting under the tip and thereby indicated an increase in blade-tip loading as compared with the stationary case; (*b*) to improve conditions on the suction surface by aspirating low-energy air off the suction surface thereby to reduce the tendency for flow to separate in the trailing-edge region.

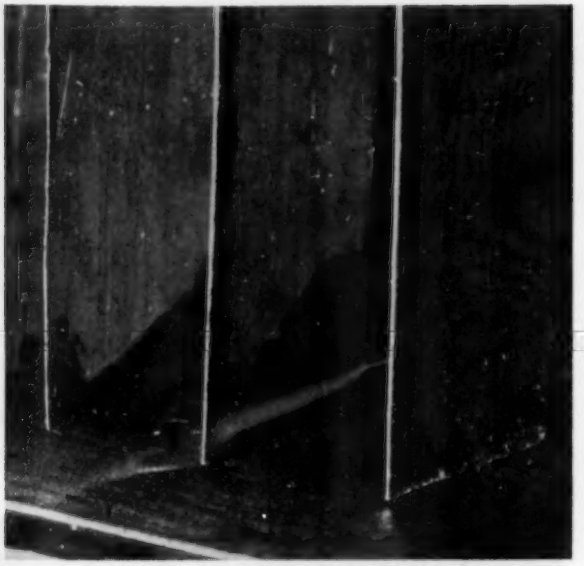

(a) Probe on nose of blade; stationary wall

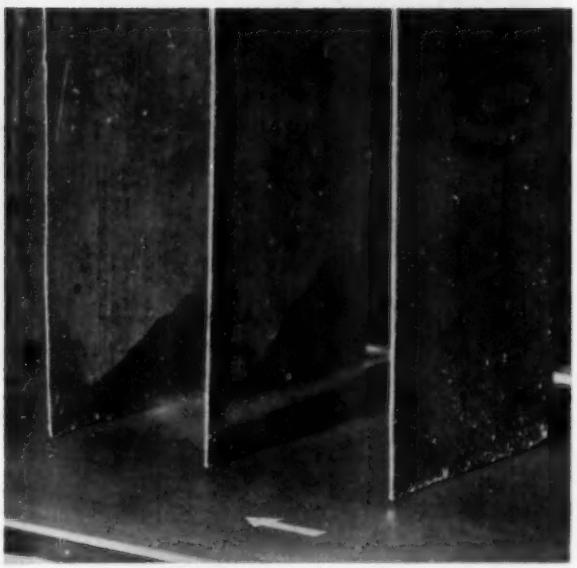

(b) Probe on nose of blade; slow-speed wall

FIG. 23 EFFECTS OF SCRAPING ACTION ON STREAMLINE DEFLECTIONS ON PRESSURE SURFACE OF BLADE

2 When the suction surface was leading (as, for example, in a turbine) the flow behavior acted: (*a*) To aggravate tip effects by decreasing the static pressure in the pressure surface tip region (as indicated by increased flow deflection toward the wall) and thereby to reduce blade loading at the tip; (*b*) to worsen flow conditions at the suction surface by piling up fluid on and near the surface and, consequently, to increase the tendency toward flow separation in the trailing-edge region. This piling up of air also resulted in a greater disturbance to flow in the passage than resulted from the original secondary-flow effects.

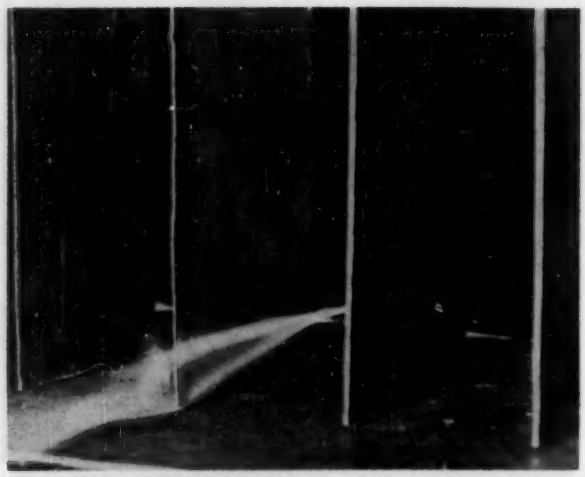

(a) Probe on nose of blade; stationary wall

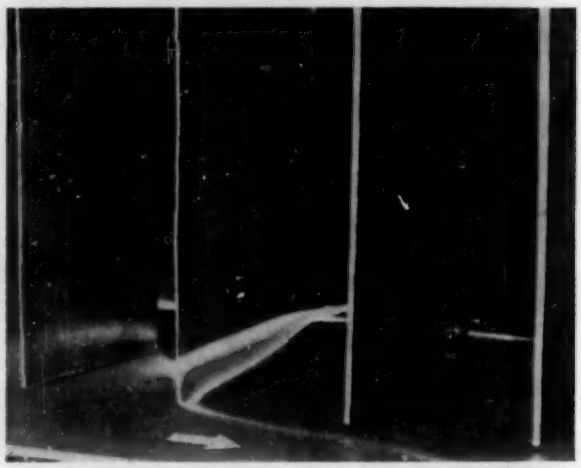

(b) Probe on nose of blade; slow-speed wall

FIG. 24 EFFECTS OF ASPIRATING ACTION ON STREAMLINE DEFLECTIONS ON PRESSURE SURFACE OF BLADES

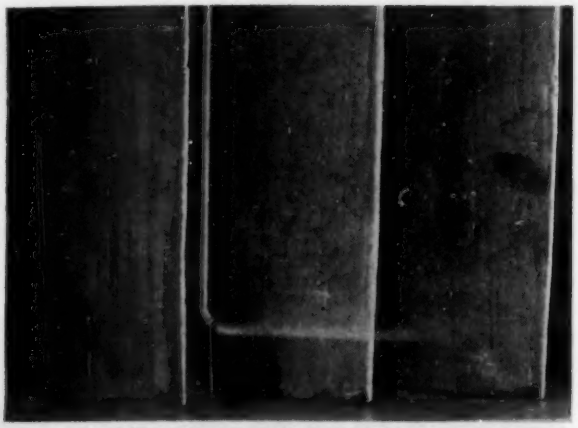

(a) Probe on nose of blade; stationary wall

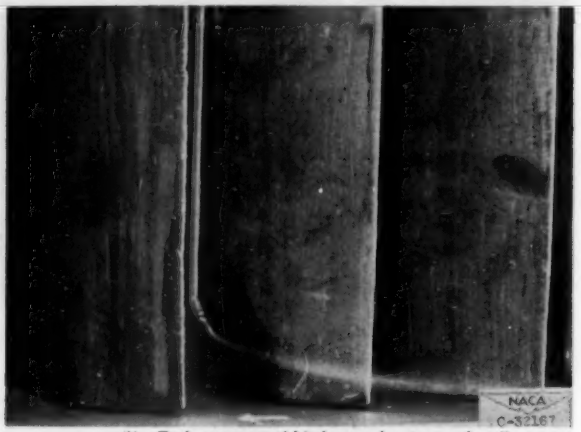

(b) Probe on nose of blade; moderate-speed wall

FIG. 25 ASPIRATING EFFECTS ON STREAMLINE DEFLECTIONS ON SUCTION SURFACE OF BLADES

The patterns of the flow obtained with the pressure surface leading simulate to a degree, the absolute fluid motion in an axial-flow compressor stator or the relative motion in a compressor rotor. The patterns obtained with the suction surface leading simulate to a degree the relative motion of the fluid at the blade tips of a turbine rotor.

Moderate Tip-Stagger Configurations. In all the previously discussed cases of wall motion, the observed scraping effect completely masked the secondary and tip-clearance flows which exist when the wall is stationary. In the compressor case, that is, with the pressure surface leading, the scraping action appears to be beneficial to tip loading. Therefore the use of blade shrouding to improve flow conditions would be undesirable in an axial-flow compressor. On the other hand, shrouding might be helpful in the case of moderate-speed turbines having blade-tip staggers comparable to those of the configuration tested. Even if this hypothesis is accepted, however, the problem still remains as to how to reduce unfavorable tip effects when rotor speed is sufficiently great to make shrouding inadvisable from stress and weight considerations. Research on possible solutions to this problem is discussed in the following section.

High Tip-Stagger Configurations. Investigations of several turbines have disclosed a large variation in blade-tip efficiencies which apparently cannot be too well explained on the basis of two-dimensional cascade analysis. In particular, certain of these rotor configurations had unusually good tip efficiencies in comparison to the others. These rotors were characterized by having relatively high flow turning and blade-tip stagger. The question therefore arises as to how high flow turning and blade-tip stagger might affect the type of flow patterns mentioned in the foregoing. General considerations indicate that high turning (or high circulation) would give rise to a large pressure differential across the blade tip and hence to a tendency for strong tip-clearance flows to form. High turning also would result in larger cross-channel pressure gradients which should tend to increase secondary-flow components (although this might be partially offset by the previously mentioned tendency toward increased flow into the tip-clearance region).

Finally, if the blade-tip stagger were large, the blade surface near the tip would exert more of a "slicing" rather than a "scraping" effect on the boundary layer entrained on the casing; that is, this boundary layer would have an appreciable velocity component parallel to the blade-suction surface. This should serve to reduce the scraping effect. Therefore it is possible that in certain high-turning and/or high-tip-stagger configurations a sort of balance might be achieved between tip-clearance forces on one hand, and secondary-flow forces and scraping effects on the

other hand, that might lead to a considerable reduction in flow disturbance in the blade-tip region. In order to examine this possibility in detail, smoke studies were conducted in a 45-deg-stagger-angle, two-dimensional cascade, with a moving wall.

Fig. 26 presents photographs of the results of an investigation of blades with approximately 125 deg turning; the insert depicts the orientation of the blades. Because of the high turning of the cascade blades, the camera had to be directed broadside at the smoke, Fig. 3, and could not be aimed along smoke paths. This necessitated the use of large quantities of smoke to obtain any photographs at all. Those that were obtained are photographs of projected smoke patterns only.

In Fig. 26(*a*) the smoke was introduced through the probe at the leading edge of the middle cascade blade spanwise about one third of the way up the blade on the pressure-surface side (the photographs show suction surfaces only). The wall was stationary. Some of the smoke deflected down the pressure surface and through the tip-clearance space forming a very large tip-clearance-flow region on the suction side of the middle blade. This tip-clearance flow can be seen near the wall against the suction surface of the middle blade in Fig. 26(*a*). The excess of smoke, which did not follow this pattern, can be seen passing downstream to the right in the photograph. No suitable photographs could be obtained of the passage-vortex roll up that was observed to occur in the upstream third of the passage and to roll around the large region occupied by the tip-clearance flow, making a sharp surface of demarcation defining this region.

With the wall moving at moderate speed, Fig. 26(*b*), the tip-clearance flow, which is against the suction surface, was observed to have been reduced considerably in magnitude. The region occupied by this flow was correspondingly reduced with the result that smoke introduced in the boundary layer at the passage inlet could now approach closer to the suction surface than with the wall stationary.

With the wall at a higher speed, Fig. 26(*c*), no tip-clearance flow to the suction surface was observed. Smoke introduced in the inlet boundary layer, for the most part, flowed quite smoothly downstream. This indicated that such a balance was established between the secondary flow and the scraping effects on the one hand, with the powerful forces tending to create tip-clearance flow on the other hand, as to produce relatively undisturbed flow throughout the passage. As a matter of fact, the flow through the passage under these conditions was smoother than in earlier configurations where less turning and smaller tip-clearance forces were involved.

In this preliminary sort of investigation the possibility was therefore substantiated that a balance could be achieved between secondary-flow forces, tip-clearance forces, and scraping effects that would lead to improved flow conditions throughout the blade passage and its boundary-layer regions. This result implies that high-speed turbine-rotor configurations might be designed in such a fashion as to prevent reduced loading on the blades at the tip section by evaluating and regulating the relative sizes of the secondary and blade-end-clearance effects. It also suggests a reason for apparently conflicting experimental results found in the literature concerning the effects of tip clearance on turbomachine performance.

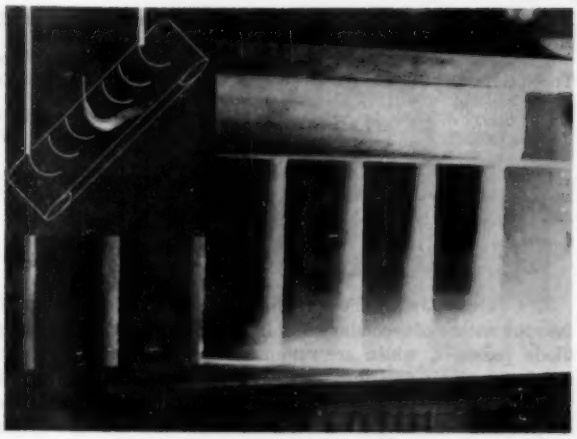

FIG. 26(*a*) BALANCING TIP-CLEARANCE EFFECTS WITH SCRAPING EFFECTS DUE TO RELATIVE MOTION BETWEEN WALL AND HIGH TURNING BLADES TO GIVE IMPROVED FLOWS NEAR BLADE ENDS (Stationary wall. Smoke introduced on pressure surface of middle blade.)

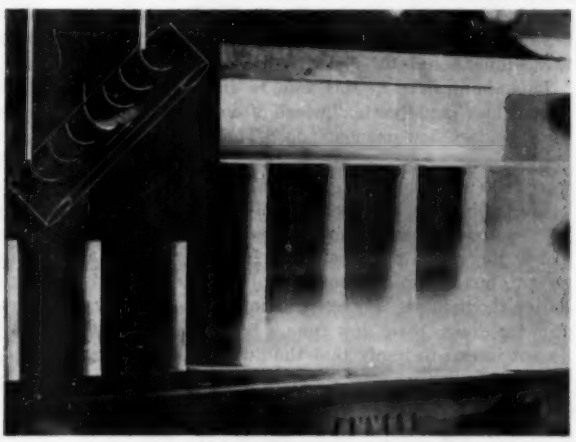

FIG. 26(*b*) BALANCING TIP-CLEARANCE EFFECTS WITH SCRAPING EFFECTS DUE TO RELATIVE MOTION BETWEEN WALL AND HIGH TURNING BLADES TO GIVE IMPROVED FLOWS NEAR BLADE ENDS (Moderate-speed wall. Smoke introduced on pressure surface of middle blade.)

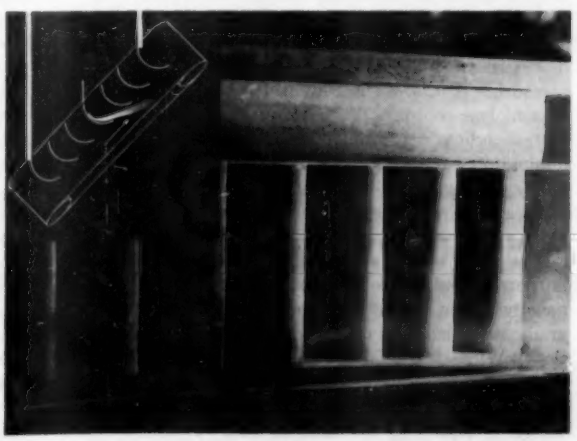

FIG. 26(*c*) BALANCING TIP-CLEARANCE EFFECTS WITH SCRAPING EFFECTS DUE TO RELATIVE MOTION BETWEEN WALL AND HIGH TURNING BLADES TO GIVE IMPROVED FLOWS NEAR BLADE ENDS (High-speed wall. Smoke introduced on pressure surface of middle blade.)

BIBLIOGRAPHY

1 "Visualization of Secondary-Flow Phenomena in Blade Rows," by H. Z. Herzig, A. G. Hansen, and G. R. Costello, NACA RM E52F19, 1952.

2 "Effect of Geometry on Secondary Flows in Blade Rows," by A. G. Hansen, G. R. Costello, and H. A. Herzig, NACA RM E52H26, 1952.

3 "Smoke Studies of Secondary Flows in Bends, Tandem Cas-

cades, and High-Turning Configurations," by A. G. Hansen, H. Z. Herzig, and G. R. Costello, NACA RM E52L24a, 1953.

4 "Experimental Investigation of Loss in an Annular Cascade of Turbine-Nozzle Blades of Free-Vortex Design," by H. W. Allen, M. G. Kofskey, and R. E. Chamness, NACA TN 2871, 1953.

5 "Study of Secondary-Flow Patterns in an Annular Cascade of Turbine-Nozzle Blades With Vortex Design," by H. E. Rohlik, H. W. Allen, and H. Z. Herzig, NACA TN 2909, 1953.

6 "Comparison of Secondary Flows and Boundary-Layer Accumulations in Several Turbine Nozzles," by M. G. Kofskey, H. W. Allen, and H. Z. Herzig, NACA TN 2989, 1953.

Discussion

R. C. Dean, Jr.[3] The revealing investigations of the NACA into the nature of secondary flow in accelerating and decelerating blade passages, which are summarized in this paper, present the first realistic description of this phenomenon. The authors, who have done much to guide the research program as well as to prepare this summary, deserve credit for their pioneering work. Until this time, little general appreciation of the nature of secondary flow has been evident, the several analytical attacks notwithstanding. Thus any attempt to describe such a flow analytically or to take it into account pragmatically in turbomachine design has been handicapped. The work of the authors has opened avenues for significant progress in the treatment of three-dimensional turbomachine flows.

It is appropriate, at this time, to discuss the semantics of the words "loss" and "vortex" which often are employed to describe the secondary-flow phenomenon. These words can have broader implications than, it is believed, the authors intend. Their use, relative to secondary flow, has given rise to confusion in the past.

The word loss implies dissipation or irreversibility in the process under consideration. "Loss material" may refer to fluid of low stagnation pressure or low velocity relative to the main stream, but it also commonly implies a dissipation in this fluid during the process. By construction of "loss contours" to represent the downstream flow from a blade row, the authors surely do not intend to imply that the fluid has only suffered dissipation during the secondary-flow process. The contours actually indicate that the fluid possesses lower stagnation pressure, or kinetic energy, than the main flow. The cause of the local defects cannot be traced to dissipation in the blade passage except under special conditions.

Fluid may arrive at the blade row with spatially nonuniform stagnation pressure; this nonuniformity is responsible, in fact, for the inception of secondary flow. Such fluid displaces three-dimensionally as it traverses the blade row. If stagnation pressure is measured upstream and at a "corresponding" position downstream of the blade row, it is highly likely that the two measuring points will not lie on the same streamline. For this reason, loss contours plotted from the difference between two corresponding readings of stagnation pressure would indicate dissipation even in a reversible flow arriving at the blade row with spatially nonuniform stagnation pressure.

Local dissipation can only be measured along a streamline. Such measurements are very difficult and unsatisfactory today.

The word vortex also may imply other properties than the authors intend. The predominant characteristic of a vortex is usually taken to be significant circulation with strong shear gradients which, in a real fluid, give rise to high rates of dissipation. While the fluid accumulated in the wall-suction-surface corner of a blade passage certainly possesses some vorticity, its predominant characteristic is low stagnation pressure, or low velocity, relative to the main stream. Detailed measurements, undertaken in the M.I.T. Gas Turbine Laboratory and elsewhere, indicate relatively small vorticity in this fluid and, surprisingly, that only 0.2 to 1 per cent of the main-stream kinetic energy is associated with the secondary flow.

That the accumulated fluid cannot possess strong vorticity may be deduced also from the fact that it was shed from the low-velocity boundary layer. Its original low stagnation pressure and low velocity preclude the generation of the high velocities associated with a strong vortex.

The conception of a vortex applied to this region of low stagnation pressure makes its resistance to turning in a tandem blade row seem mysterious. If attention is focused instead on the characteristically low velocity, it becomes clear that the fluid cannot flow through a diffusing cascade without an increase in its stagnation pressure. The larger the size of this low-velocity core, the smaller will be the increase in its stagnation pressure due to momentum exchange with the main flow. Therefore this fluid tends to travel on a path which avoids an impossible pressure rise. Eventually it may approach a blade of the tandem row and spread into a thin sheet, but eventually it must be energized by the main flow and carried downstream. Indefinite accumulation at any one location is inconsistent with the continuity condition.

Careful regard for the semantics of these two words—vortex and loss—should facilitate use of the authors' excellent data and aid future progress toward a complete understanding of the phenomenon.

H. P. Eichenberger.[4] The paper contains a great amount of interesting observations of secondary flow in turbomachines. A commendable work has been done by drawing conclusions of immediate use to the designer.

The tests seem to show that it is hopeless to approach the problem with a linearized theory which makes a perturbation on a simple flow pattern because the displacement of the low-energy fluid occurs in an essentially nonlinear manner (rolling up in a vortex). If the actual streamlines are known, however, it should be easy to explain why they must behave as they do.

In order to illustrate this qualitatively, let us consider the acceleration $\rho(V^2/R)$ in the direction of the principal normal to a streamline, where R is the radius of curvature of the streamline.

This acceleration is, in absence of friction, balanced by the pressure gradient $\partial P/\partial n$, where n indicates the direction of the principal normal. For two neighboring streamlines with different velocities V (i.e., different stagnation pressures) the pressure gradient $\partial P/\partial n$ must be the same. Thus in order to satisfy

$$\rho \frac{V^2}{R} = \frac{\partial P}{\partial n}$$

the streamline with lower velocity must have a smaller radius of curvature R and turn toward n. It is helpful for the imagination to notice that instead of considering streamlines with various velocities (stagnation pressures), we can consider streamlines with various densities. High-stagnation-pressure streamlines behave as if they consisted of a denser material and vice versa.

This was overlooked in the past, when the centers of vortices were called "cores of high losses"; these centers are just the collections of fluid whose stagnation pressure has been reduced previously when near the solid walls.

The authors state that a "passage vortex tends to resist turning." In the light of the foregoing discussion this observation of the authors should be interpreted as showing that the fluid which has formed the passage vortex and has been shed into the main

[3] Assistant Professor of Mechanical Engineering, Massachusetts Institute of Technology, Cambridge, Mass.

[4] Fluid Dynamics Research Project, AiResearch Manufacturing Company, Los Angeles, Calif.

stream at the trailing edge of the blades has, in the next cascade, a stagnation pressure which is above the average of the free-stream stagnation pressure. This at first surprising fact shows a desirable side of the secondary flow; the vehement momentum exchange between the boundary layer and the free stream, which allows higher pressure rise along the hub and casing of axial-flow compressors than would be possible without secondary flow.

DEAN RAINS.[5] The authors' contributions already have become standard references in the field of secondary flows. This paper represents an admirable summary and application of their previous NACA reports.

The recent construction of an axial-flow-pump facility in the Hydrodynamics Laboratory at the California Institute of Technology[6] gave the writer an opportunity to investigate in a machine, problems similar to those discussed by the authors. The facility consists of a pump of compressorlike geometry operating in a closed water-filled circuit. A lucite window forms a portion of the outside case for the full length of the pump. Provisions were made for the injection of tracing oil-droplet streams at various points both in the rotor and stator-blade rows. The first study of this type was made in the rotor-blade passages. The oil, mixed to a specific gravity of one, was injected through a probe attached to the rotor and was observed in the rotating reference frame by a stroboscopic light.

Fig. 27 illustrates an example of this technique and shows the secondary flow on the rotating hub. The type of flow is the same as that shown in stationary passages by the authors. The strong crossflows are confined roughly to the ten per cent of the secondary layer closest to the wall.

[5] Graduate Student, California Institute of Technology, Pasadena, Calif. Student Mem. ASME.

[6] "Report on Design and Construction of the Axial Flow Pump Test Facility," by T. W. Fuller and A. J. Acosta, California Institute of Technology, Hydrodynamics Laboratory Report E-12.13, June, 1953.

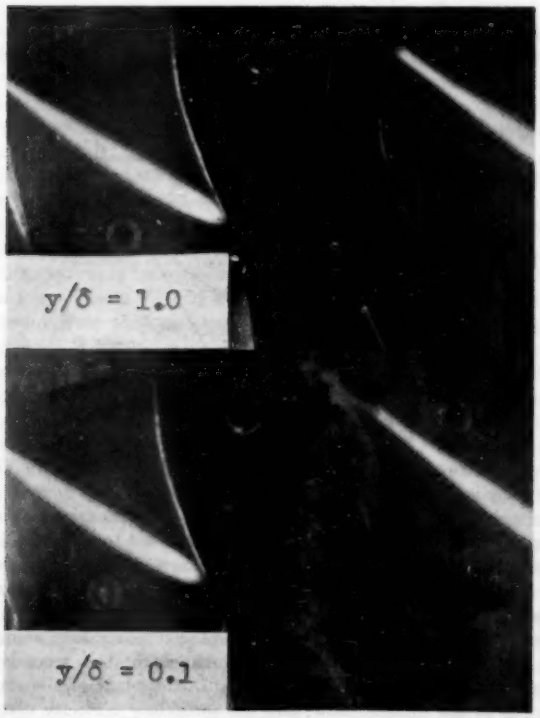

FIG. 27

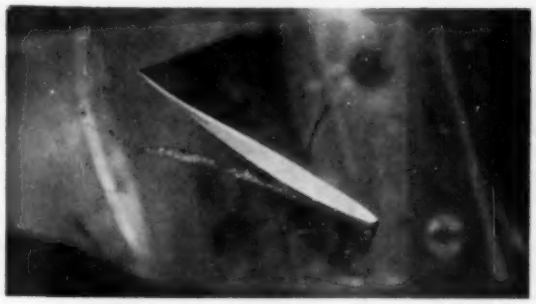

FIG. 28

The existence of a tip-clearance vortex has been shown by the authors. The rotational flow of the vortex causes a low-pressure region at its center which may cavitate. Fig. 28 is a photograph of such cavitation and shows that the tip vortex is strong and concentrated enough to measurably increase the losses in a machine.

This work is sponsored by Navy Bureau of Ordnance and the Office of Naval Research, and is under the general direction of Prof. W. D. Rannie.

EDWARD SILBERMAN.[7] Both visualization and quantitative studies of secondary flows in blade rows have been conducted at the St. Anthony Falls Hydraulic Laboratory.[8,9] These studies have been performed in two-dimensional channels using water and air at low speeds. The results are essentially in agreement with those presented by the authors. There are some details of the secondary flow observed by the writer and not brought out by the authors, however, which should be mentioned.

Fig. 29(*b*) of this discussion shows the measured total head distribution obtained behind a two-dimensional blade row. For comparison, Fig. 29(*a*) shows the total head distribution obtained at the same location in a straight duct. This figure shows strikingly how the passage vortex cores of low total head are composed of fluid which was in the wall boundary layer upstream of the blades, while the wall region downstream of the blades is occupied by fluid of high total energy which originally was in the interior of the duct. The low-energy cores should not be thought of as representing energy losses produced by the blade row.

The passage vortexes were not observed beyond the blade trailing edges even though the low-energy cores did persist. However, small trailing vortexes were detected behind the blades; these were generated by the passage vortexes at the trailing edges and were of opposite sign to them. Downstream of the blades the wall boundary-layer fluid (of high total energy) was considerably overturned while the cores were slightly underturned. The overturning was still evident several chord lengths downstream.

Quantitative measurements showed that the rate of energy loss immediately downstream of the blades is of the same order or larger than that in the blades. This higher rate of loss is attributed to the wall shear produced by the high-energy fluid in

[7] Associate Professor, St. Anthony Falls Hydraulic Laboratory, University of Minnesota, Minneapolis, Minn.

[8] "Secondary Flows in Guide Vane Bends With Some Notes on the Primary Two-Dimensional Flow," by E. Silberman, University of Minnesota, St. Anthony Falls Hydraulic Laboratory Project Report No. 36, January, 1953.

[9] "Importance of Secondary Flow in Guide Vane Bends," by E. Silberman, Proceedings, Third Midwestern Conference on Fluid Mechanics, June, 1953, pp. 669–686.

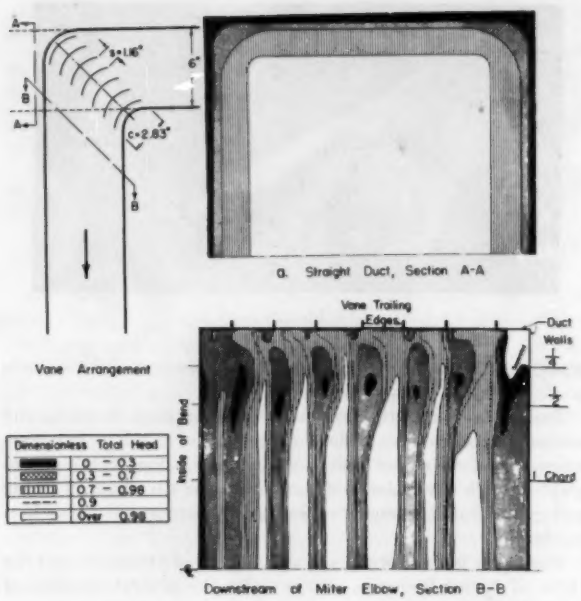

FIG. 29 TOTAL HEAD DISTRIBUTION BEHIND A TWO-DIMENSIONAL BLADE ROW

the wall boundary layers behind the blades. For the fixed two-dimensional cascade, at least, it is this new wall boundary layer rather than the low-energy cores which is important in determining loss attributable to the blades. The cores along with the blade wakes were smoothed out within 5 to 10 chord lengths downstream and the loss in the process was too small to measure in the present experiments.

The writer observed one place where the secondary flow actually improved the main flow. This was in connection with separated blade boundary layers mentioned by the authors in discussing radial flow. In this case the secondary flow served to prevent separation near the blade ends even though separation occurred over the central part of the span.

L. H. SMITH, JR.[10] The work done by the authors is indeed a valuable contribution to the literature on secondary flows, and the results which they have found present a challenge to those of us who try to explain such flows theoretically.

The analytical treatment of the problem in any exact fashion is difficult because the flow is highly rotational. Thus the conventional assumption that the vorticity is transported by the primary flow (the flow which would exist if two-dimensional-cascade data were used at each spanwise section of the blades ignoring the flow normal to the wall) is no longer a good approximation because the secondary velocities are of the same order of magnitude as the primary velocities. It is therefore necessary to consider the vorticity as being transported by the actual flow to get a more accurate picture. This leads to an integral equation because the actual flow is not known until the secondary vorticity has been integrated.

Rather than attempting to solve the problem as a whole, we can study the flow at several stations along the flow path, the first of these being in the blade passage near the inlet and the others following periodically. The location of these stations is shown in Fig. 30, herewith. Up to the first station, the secondary

[10] Department of Mechanical Engineering, The Johns Hopkins University, Baltimore, Md. Assoc. Mem. ASME.

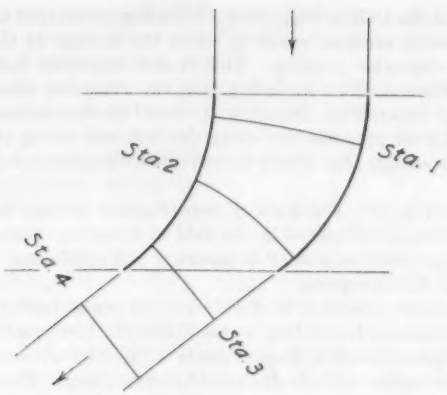

FIG. 30

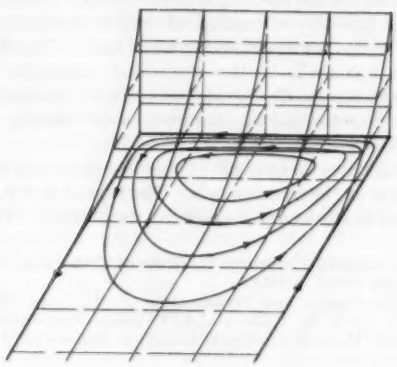

FIG. 31

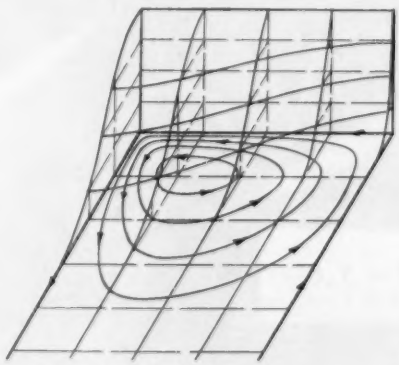

FIG. 32

velocities are small so that it is permissible to neglect them. The vorticity is considered as transported by the primary flow up to this point, and from this the secondary velocities calculated. For the next station the vorticity is transported by the primary flow plus the secondary flow found at the first station. For each succeeding station the vorticity is transported by the complete flow as determined at the station preceding it.

In Figs. 31 and 32 we see the first and second stations in isometric view. The streamlines corresponding to the secondary flow at each station are shown plotted in the plane of a surface normal to the primary flow, and the secondary vorticity distributions which induce the secondary flows are plotted vertically

above the surfaces. In Fig. 31 the secondary vorticity is constant from blade to blade so that the streamlines are symmetrical about the center line of the passage. In Fig. 32, however, the vorticity distribution has shifted in accordance with the secondary velocities in Fig. 31. This new vorticity distribution induces secondary velocities represented by the streamlines in Fig. 32. The crowding of the streamlines in the corner indicates that the secondary velocities are higher there. This corner is at the suction side of the vane.

In Fig. 33 we see a spiral which indicates the path which a particle might take as it comes successively under the influences of the streamlines in Figs. 31 and 32 and the flow at the stations which follow these. This type of flow corresponds to the passage vortex which has been observed by the authors. The well-known trailing vortex sheet (which quickly rolls up into a trailing vortex) is of course also present, and this turns in the opposite direction to that of the passage vortex.

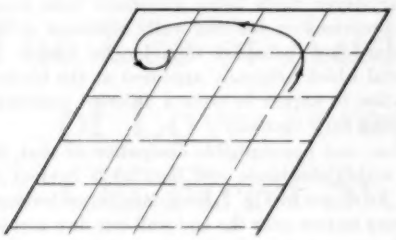

FIG. 33

C. H. WU.[11] The authors are to be complimented for a fine exploration of the boundary-layer flows in two and three-dimensional cascades. The result on the three turbine nozzles is particularly significant. It shows that in the actual three-dimensional viscous flow the nozzle blades designed by the method of two-dimensional potential flow for smooth velocity distributions behave much better than nozzle blades having irregular velocity distributions as obtained by the method of two-dimensional potential flow. This finding would encourage turbine designers to employ more refined blade-design methods to design their blades.

The smoke traces show very clearly the passage vortex for flow velocities below 30 fps, which correspond to very low Reynolds numbers and Mach numbers. At high Reynolds number and high Mach number the hydrogen-sulphide and the lead-carbonate traces indicate only the path of the boundary-layer flow very close to the end wall. The flow above it may be quite different from that obtained by the smoke trace at low flow velocity. It would be interesting to know if there is any indication that the direction of these traces at the wall tends toward the main-flow direction when the main flow velocity is increased.

In the pictures made for the effects of the tip clearance and the relative motion between blade tip and end wall, it seems that the smoke probes are placed at a considerable distance away from the wall. It would be interesting to see the fluid motion with probes placed very close to the wall. It also would be interesting to view the changes in the scraping and aspiration effects of the moving wall when the wall speed is increased from below air speed to above air speed.

In order to facilitate the application of the results obtained by the authors to similar cascades and nozzles, it would be useful to have more information regarding these experiments, such as the Reynolds number, the Mach number, the ratio of air velocity to wall velocity, the air-inlet angle, and the cascade geometry.

The basic equations describing the three-dimensional flow of either a nonviscous fluid or a viscous fluid in a rotating-blade passage (when these equations are expressed in terms of the relative velocity) are not the same as those describing corresponding flows in a stationary-blade passage (when these equations are expressed in terms of the absolute velocity). Therefore the secondary flow in a rotating-blade passage may or may not be approximately the same as those obtained in a stationary-blade passage of the same geometry and subjected to the same relative flow at inlet. It would be useful to obtain secondary-flow data in three-dimensional passages of rotating blades which are of the same geometry as the stationary blades and subjecting them to the same relative inlet flow as that in the stationary case. For this investigation, in addition to the usual dimensionless parameters, another dimensionless parameter containing the angular speed of the blade such as $W_z/\omega r$ (where W_z is the axial component of the relative velocity, ω is the angular speed of the blade, and r is the radial distance of the blade section under consideration measured from the axis of rotation) would be an important one for similarity consideration.

AUTHORS' CLOSURE

The authors wish to extend their appreciation to the writers of discussions for their carefully considered comments and additions, and for the evident expenditures of time and effort which they so generously contributed.

As noted in the Introduction, this paper was intended to present an over-all view of the authors' experimental secondary-flow investigations. Accordingly, many of the details deleted in this paper were presented in references (1 to 6) which partially answer some of the comments received.

The nature and behavior of "passage vortexes" and the subject of "losses" receive considerable attention in several of the discussions. The authors would prefer to group the comments, as it were, and to discuss each of these two topics as a whole, rather than deal with various ramifications of the same considerations separately.

Vortexes. By way of explanation to Professor Dean, the term "vortex" as used by the authors is applied to "flow vortexes" in which the fluid can be seen to be spiralling as it flows. There is an actual circulatory motion involved. Furthermore, in many cases these circulatory components are observed to attain high velocities which at present are being studied by means of high-speed motion pictures.

Dr. Eichenberger's comments touch upon the interesting problem of the influence of static pressure gradients on the motion of low momentum air. If attention is confined to a streamline in the main flow and a neighboring streamline in the boundary layer which are parallel approaching a turning section, both streamlines will experience the same lateral pressure gradient $\partial P/\partial n$ at the instant the main stream turns. As is pointed out in the comments, the streamline in the boundary layer (which has a velocity lower than the main stream) must turn more sharply to satisfy

$$\rho \frac{V^2}{R} = \frac{\partial P}{\partial n}$$

where R = radius of curvature of boundary-layer streamline. Once the boundary layer has turned to flow in a different direction from the main stream, the pressure gradient imposed by the main flow has components tangent to the boundary-layer streamline as well as normal to it. Consequently $\partial P/\partial n$ for the boundary-layer streamline may be considerably smaller than that of a

[11] Professor of Mechanical Engineering, Polytechnic Institute of Brooklyn, Brooklyn, N. Y.

neighboring main flow streamline; so small in fact that the radius of curvature determined from

$$R = \rho V^2 \Big/ \frac{\partial P}{\partial n}$$

may exceed that of the main stream at a given point (cf. Fig. 5, center of passage.) Unfortunately, therefore, it would be quite difficult to draw any conclusions about relative velocities of neighboring streamlines based on the curvatures of the streamlines alone. If it is assumed that the over-all pressure gradient is the same for two such streamlines, it still would be necessary to know the respective tangential components of the gradient before a calculation of streamline velocities could be made.

With regard to the flow vortexes formed in the passages, the authors know only that the centers of these vortexes contain low stagnation-pressure fluids originally found in the boundary layers upstream of the roll-up region. For the type of flow under consideration, it is highly improbable that the stagnation pressures in the vortexes ever could exceed that of the main stream. The comment in the discussion touching upon this point perhaps refers to the well-known fact that low-momentum fluid entering the rotor of a typical compressor has a higher relative stagnation pressure than nearby fluid in the main stream.

It is noted that measurements in compressor rotors indicate higher pressure rises (and higher efficiencies) in the hub region of axial-compressor rotors than might be expected. It is believed that this is predominantly the result of the outward flow of low-energy fluid under the action of centrifugal forces.

Professor Silberman's discussion brings out several interesting aspects of vortex formation and flow behavior. Not only do the low-energy cores persist downstream as he notes, but as shown in Fig. 26 of another report,[12] the passage vortexes also are seen to continue twisting well downstream of the cascade. The small trailing vortexes of opposite sign to the passage vortexes have been observed by the authors too and are photographed and discussed in proposed reports by Milton Kofskey and Hubert Allen, associated with the authors in the NACA secondary flow-research program.

In connection with these small trailing vortexes, it must be noted that the cross-channel component of boundary-layer flow can be considered as a "double" boundary layer. The component normal to the main stream must have zero velocity at the wall, rise to some maximum value, and then fall to zero again in the main stream. The outer portion of this cross-channel boundary layer rolls up to form the so-called passage vortex. The "sublayer" next to the wall has vorticity of opposite sign to the outer portion and when it rolls up produces vortexes opposite in direction to passage vortexes. As has been indicated by Henk G. Loos,[13] under some conditions, the diffusion of vorticity from this sublayer may be larger than from the remaining part of the boundary layer and so the sublayer vorticity will then disappear rapidly. The important thing is that these oppositely directed vortexes arise as part of the same secondary-flow behavior that produces the passage vortexes and have not been observed as being directly "generated" by the passage vortexes.

[12] "Visualization Studies of Secondary Flow," by A. G. Hansen, H. Z. Herzig, and G. R. Costello, NACA TN 2947.

[13] "Analysis of Secondary Flow in the Stator of an Axial Turbomachine," by H. G. Loos, Technical Report No. 3, N-25949, Daniel and Florence Guggenheim Jet Propulsion Center, California Institute of Technology.

Losses. The authors agree wholeheartedly of course that they "do not intend to imply that the fluid has only suffered dissipation during the secondary-flow process." The authors regard the secondary-flow process as serving mainly to redistribute and collect the low-momentum fluid in the passages. This is strikingly brought out by the experimental investigations of the annular nozzle cascade losses which showed that for one typical configuration the secondary-flow process acted to transport boundary-layer material from the outer-shroud inlet and the pressure surface of one cascade blade to the suction-surface inner-shroud region of the adjoining blade near the passage exit. It is stated explicitly in references (1 to 6) and in this paper as well, that the loss cores are collections of boundary-layer fluids from other portions of the passages.

The smoke-visualization procedures merely make it possible to see the secondary-flow processes at work within the blade row; the measured "loss contours" likewise merely indicate a state of affairs at a measuring station. Often the major part of the boundary-layer fluids being visualized were generated by dissipative processes on the end walls upstream of the blades. The secondary-flow behavior then largely causes boundary-layer material which originally appeared at the blade-row inlet in one location to appear in quite a different position from the "corresponding exit" location.

Dissipation, and nonnegligible dissipation at that, does occur frequently within the blade row itself as is evident in several instances. As shown in Fig. 7, boundary layer developed on the blade pressure surface near the end wall can flow across the passage into the passage vortex. At some indefinite position on the blade, a little further spanwise from the end wall, the boundary developed on the blade pressure surface will still deflect to the end wall but will not be able to cross to the roll-up region. Instead, it will move off downstream as part at least of the new end-wall boundary layer. These particular dissipative effects have been chosen from among those which occur within the passage because they serve to clarify another point raised in a discussion. The boundary layer developed on a relatively short distance along the blade pressure surface has high total energy as compared with inlet boundary layer in general. However, its total energy (and velocity) is certainly not as high as the main stream total energy by the time it becomes part of the new end-wall boundary layer. If this occurs within the passage where blade-to-blade pressure gradients exist, then this new "high-energy" boundary layer must overturn, albeit not as much as the inlet-wall boundary layer overturns before it rolls up.

Professor Dean observes, as is indicated in the present paper and references (3 to 6) and footnote 13, that the kinetic energy associated with secondary flows is quite small. It bears repeating once more that the chief concern here is with the sizable deviation in main stream turning angle, especially in blade end regions, caused by flow-area blockage resulting from secondary-flow behavior.

Professor Wu's pertinent remarks and suggestions are noted with interest. The experimental investigations he recommends are in progress at the NACA Lewis Laboratory. We are studying the secondary flows by means of visualization procedures in an annular rotating turbine configuration. Similar experiments on rotating compressors are being readied and will include most, if not all, of the experimental results in which Dr. Wu expresses interest.

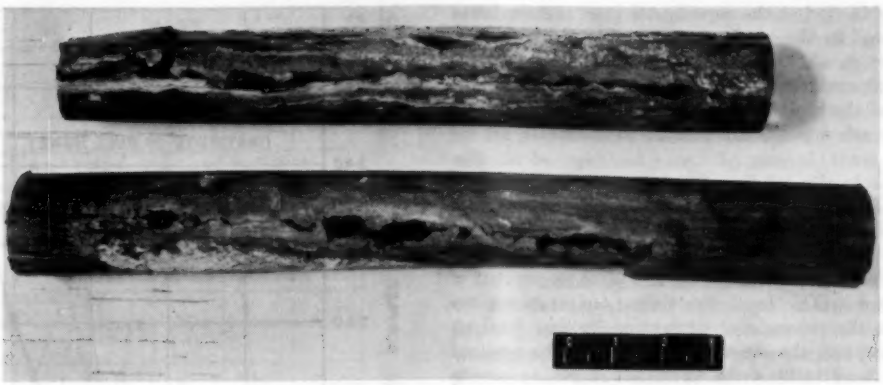

FIG. 1 EXAMPLES OF AIR-HEATER CORROSION

The Use of Additives for the Prevention of Low-Temperature Corrosion in Oil-Fired Steam-Generating Units

BY E. C. HUGE[1] AND E. C. PIOTTER,[2] ALLIANCE, OHIO

Low-temperature corrosion has become an important consideration and presents a real problem in the design and operation of oil-fired steam-generating units. It is caused by the presence of sulphur trioxide in the combustion gases which unites with water vapor and forms sulphuric acid on the cooler surfaces of the unit. Various ways of combating this condition are discussed, with particular emphasis on the use of dolomite as an additive. Test data and the results of actual operating experience are presented which show that additives are effective in reducing the amount of acid formed and, in some cases, practically eliminating cold-end pluggage and corrosion. The economics of their use and the design of units for higher efficiency when using additives also are discussed.

INTRODUCTION

A YEAR ago, the results of tests on fuel-oil additives for reducing ash-deposit troubles in the high-temperature zones of steam-boiler units were reported.[3] At that time it was stated that the use of additives also resulted in a reduction of air-heater corrosion. This paper reviews the operating experience on these units and presents later test data which show the influence of the additive on the corrosive nature of the flue gases.

In recent years, corrosion in the low-temperature zones of oil-fired boilers has become increasingly serious, particularly in the cold section of the air heaters. Examples of service failures are shown in Fig. 1. These tubes were removed after less than 1 year of service from a unit firing a fuel oil containing $2^1/_2$ to 3 per cent sulphur. Although this illustration does not show the ash deposits within the tubes, pluggage usually occurs with corrosion.

Primarily, two factors have been responsible for the increased difficulties with air-heater corrosion. One is the decrease in air-heater metal temperatures which has resulted from the demand for more efficient boilers. The second is the change in the quality of the residual oil available for central-station consumption. There has been a significant increase in the sulphur and ash content of the oil. In addition, the amount of vanadium and alkalies in the ash has increased. This has been brought about by changes in refinery processes and the utilization of oil from new fields.

The sulphur and ash constituents in the oil are important in corrosion because they are responsible for the formation of sulphur trioxide (SO_3) in boiler flue gases. When the oil is burned, practically all of the sulphur in the fuel is oxidized to SO_2, a relatively harmless compound under conditions normally encountered in boiler practice. However, at some point in the unit, small quantities of SO_3 also are formed. Various theories have been advanced as to the cause of this SO_3 formation. It appears at this time that the theory which is most applicable to conditions encountered in a steam-generating unit is that catalytic oxidation of SO_2 to SO_3 occurs as the flue gases pass through the unit. There is considerable evidence which indicates that an appreciable portion of the SO_3 found in flue gases is formed in this manner. Field tests on oil-fired units have shown consistently an increase in SO_3 content of the gases between the 2000-deg

---

[1] Project Engineer, The Babcock & Wilcox Company, Research Center. Mem. ASME.

[2] Research Engineer, The Babcock & Wilcox Company, Research Center.

[3] "The Application of Additives to Fuel Oil and Their Use in Steam-Generating Units," by J. B. McIlroy, E. J. Holler, Jr., and R. B. Lee, Trans. ASME, vol. 76, 1954, pp. 31–46.

Contributed by the Research Committee on Low Temperature Flue Gas Corrosion and Deposits and presented at the Annual Meeting, New York, N. Y., November 29–December 4, 1953, of THE AMERICAN SOCIETY OF MECHANICAL ENGINEERS.

NOTE: Statements and opinions advanced in papers are to be understood as individual expressions of their authors and not those of the Society. Manuscript received by ASME Headquarters, December 9, 1953. Paper No. 53—A-235.

temperature levels found at the superheater inlet and the lower temperatures found in the air heater. Equilibrium considerations for the reaction of SO_2 to SO_3 indicate a tendency to produce SO_3 as temperature levels are reduced. Catalytic surfaces consisting of the iron oxide of the tubes and the vanadium and iron-bearing ash deposits are present to accelerate the reaction.

In many respects the conditions existing in the boiler are similar to those employed in the manufacture of sulphuric acid. In this process SO_2 gas is passed over a catalyst, usually an oxide of vanadium or platinum, at a temperature of 800 to 1150 F. The contact time varies between 2 and 4 sec and 90 to 98 per cent of the SO_2 is converted to SO_3. In a boiler, similar temperature zones are present, but the presence of proportionally less catalyst, the low excess air, and the short contact time at the required temperatures all tend to limit the formation of SO_3 to minute quantities. Less than 5 per cent of the sulphur in the oil is converted to SO_3. This represents a concentration of SO_3 in the flue gas of not more than 0.005 per cent by volume or 50 ppm. The amount of SO_3 formed varies from unit to unit and is influenced mainly by the fuel fired, the ash characteristics, the condition of tube surfaces, and the boiler design.

Despite the low concentration of SO_3 in the flue gas, it may cause severe corrosion of low-temperature surfaces in the air heater. Fig. 2 shows the relationship between the SO_3 content

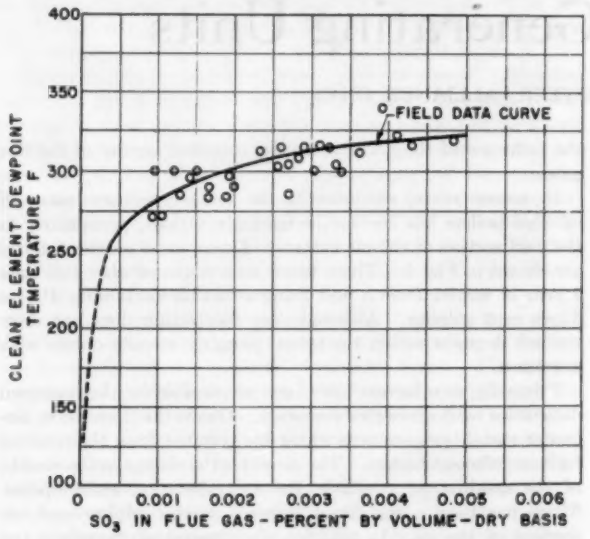

FIG. 2 RELATIONSHIP OF DEW-POINT TEMPERATURE TO SO_3 CONTENT OF FLUE GASES

and the dew-point temperature of the flue gas in a number of central-station boilers. It will be noted that even minute amounts of SO_3, in the range of 0.002 per cent by volume or 20 ppm, have a profound effect on the dew point, raising it from approximately 120 F to over 300 F. Frequently, metal temperatures in some sections of the air heater are below the dew-point temperature of flue gas containing SO_3. Under these conditions, the SO_3 combines with water vapor in the gas and condenses as sulphuric acid on the relatively cold surfaces. The acid condensed will be at a concentration in accordance with the equilibrium of sulphuric acid and water at the temperature of the condensing surface. The equilibrium characteristics of sulphuric acid are such that concentrated acid in a liquid form can be condensed from very dilute concentrations in the vapor phase.

The variation of acid strength with surface temperature is

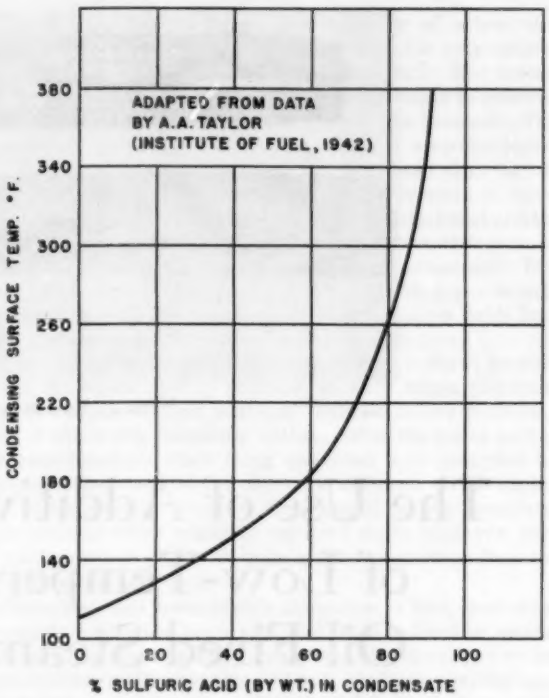

FIG. 3 CONCENTRATION OF SULPHURIC ACID CONDENSED FROM CLEAN FLUE GAS AT VARIOUS TEMPERATURES

shown in Fig. 3. In the corrosion section of the air heater, metal temperatures vary widely and, consequently, sulphuric acid of many different concentrations is encountered. As is shown later, this factor has an important bearing on the variations in service life of different materials.

METHODS OF PREVENTING OR REDUCING CORROSION

Owing to the many variables involved in a problem of this kind, there are various possible approaches to its solution. Those that are considered here deal with the materials of construction, air-heater design, fuels, and additives.

Materials. In the search for suitable materials for low-temperature service in air heaters, extensive tests have been conducted on numerous metals and acid-resistant tube coatings. Metals tested in field units have included admiralty metal, monel, Everdur, Cor-Ten, AISI 304 and 316 stainless steels, and several grades of aluminum. Although some have shown better corrosion resistance than others, none has been found which will withstand successfully the wide range of acid concentrations existing in air heaters.

Fig. 4 illustrates the corrosion rates of several common metals when immersed in boiling sulphuric-acid solutions of various strengths. It will be noted that each of the four materials has relatively good corrosion resistance in some concentrations of acid, but very poor resistance in others. This characteristic is believed to be the principal reason for the inconsistent performance of metals in field units. For example, on some oil-fired installations where steel tubes have corroded excessively, aluminum tubes have shown good life, while on other installations aluminum has shown no improvement. The use of Cor-Ten, a low-carbon steel containing small amounts of copper, chromium, and nickel, in some cases has resulted in an appreciable increase in service life over that of plain steel, but not to the extent of being corrosion-free.

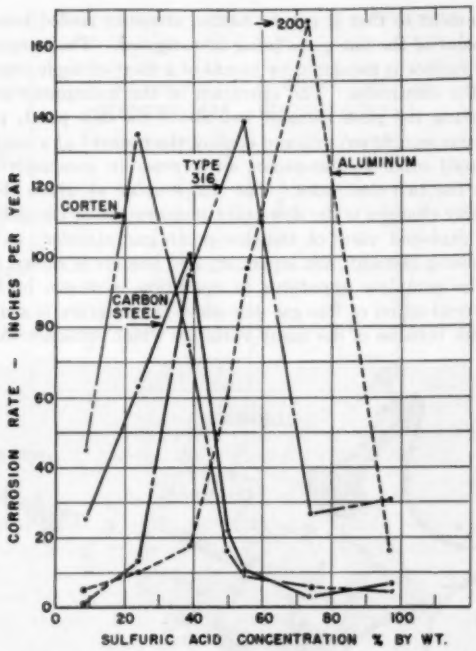

FIG. 4 CORROSION RATE OF VARIOUS METALS IMMERSED IN BOILING SULPHURIC-ACID SOLUTION

Type AISI 316 stainless steel has exhibited an advantage where low concentrations of acid are involved, but its corrosion resistance has been poor where high acid concentrations are prevalent. Results with the stainless steels, as well as other alloys, have indicated that there is as yet no single metal available which will be suitable for the variety of corrosive conditions encountered in an air heater.

In addition to the testing of metals, acid-resistant coatings have been explored. Over fifty organic and inorganic coatings have been tested in the laboratory or in various field installations. These coatings may be divided into the following four general classifications: (1) organic, (2) ceramic, (3) electrodeposited, and (4) spray-metallized.

Organic coatings, which composed the largest single group of compounds tested, included phenol-formaldehyde resins, coal tars, vinyls, furanes, and silicones. Of these, the phenol-formaldehyde group was found to be the only type exhibiting sufficient corrosion resistance for serious consideration. However, they were subject to a temperature limitation which in most cases was too low for air-heater applications. Field tests of resins of this type generally have been unsuccessful.

Ceramic coatings, such as porcelain, provide excellent resistance to corrosion if a perfect coating can be obtained. Unfortunately, these coatings are not completely reliable because pin holes and other minor defects are sometimes present. Special tube holders are necessary because the tubes cannot be expanded into the tube sheets without damaging the porcelain. Field tests of porcelain-coated tubes have indicated good performance but none has been in service a sufficient length of time to allow an evaluation.

Electrodepositing of silver, lead, and nickel, and spray-metallizing with Carpenter 20 stainless steel have been unsuccessful because of porosity of the coating.

Chemically inert materials such as graphite and glass also are being tested but the physical characteristics of these materials do not appear too well-suited for use in boilers.

Air-Heater Design. A common method of preventing or at least reducing corrosion is to increase metal temperature by one of the more conventional methods. Among these are cold-air by-passing, hot-air recirculation, and the use of steam to preheat air entering the air heater. The details of these arrangements are familiar to all of those interested in the corrosion problem and will not be discussed here. In general, these devices increase the capital investment and lower the efficiency of the boiler by increasing exit-gas temperature. However, they are usually intended for use only at reduced loads and are effective in many applications.

On an increasing number of units, wide spacing of air-heater tubes at the cold-air inlet is employed to reduce air mass flow and increase minimum metal temperatures without sacrificing efficiency. Combination counterflow-parallel-flow arrangements also are used occasionally to accomplish this.

A comprehensive discussion of the foregoing methods of increasing air-heater metal temperatures was presented in a paper by P. H. Koch.[4]

Fuels. An ideal way to prevent corrosion in oil-fired boilers would be the complete removal of sulphur and other undesirable constituents from the oil. Unfortunately, this is economically impractical at the present time, although further development might make such a solution feasible.

Additives. Another method of preventing corrosion, and the one which will be considered in detail, concerns the use of additives to either reduce the acid content of the flue gas or to neutralize its corrosive effect when it condenses on the metal surfaces. It has been known for some years that boilers fired with pulverized coal experience much less air-heater corrosion than boilers fired by other means, even with equal amounts of sulphur in the fuels. Since the main difference in conditions between pulverized coal and other methods of firing appeared to be the amount of fly ash passing through the boiler, tests were initiated by several investigators to determine the effects of introducing various additive materials into units troubled with corrosion.

A large portion of the early laboratory and field tests was sponsored by the British Boiler Availability Committee and other British investigators.[5] Although none of this work was conducted on oil-fired units, it will, nevertheless, be reviewed here as a background for the later work carried on in this country.

The British laboratory work on the low-temperature corrosion problem usually consisted of using a dew-point meter[6] and SO_2-SO_3 apparatus to determine the changes brought about by additives in a carefully controlled SO_3 bearing flue gas. Generally, the flue gas was formed by adding SO_2 or SO_3 to the flame of a Bunsen or other small gas burner. In this manner, relatively stable test conditions could be held for considerable periods of time. The additive material, usually in the form of a smoke, could be introduced at any desired point. Field tests were conducted on stoker-fired boilers which, in most cases, were of the chain-grate type. Since the laboratory and field results obtained were generally in agreement, no attempt to segregate them will be made in this summary.

Additives investigated by the British included pulverized-coal fly ash, carbon smoke, silica, zinc, coke particles, and magnetite (Fe_3O_4). Practically all of these materials had some beneficial effect on flue gases containing troublesome quantities of

[4] "Tubular Air-Heater Performance and Corrosion Problems," by Paul H. Koch, ASME Metropolitan Section, Applied Mechanics and Heat Transfer Division Meeting, March, 1951, New York, N. Y.

[5] Summaries of Published Papers—The Boiler Availability Committee Bulletin M/C 235 London, England, February, 1953.

[6] "Developments in the BCURA Dewpoint Meter," by P. F. Corbett, D. Flint, and R. F. Littlejohn, British Coal Utilisation Research Association Information Circular No. 55, April, 1952; also published in the *Journal of the Institute of Fuel*, vol. 25, 1952, pp. 246–252.

SO_3. The effects of adding zinc smokes or zinc concentrates to stoker-fired boilers were especially pronounced. In some tests in which a 50 per cent zinc-bearing concentrate was added to the coal in a ratio of 2 lb additive per 100 lb of coal, dew-point temperatures were lowered from acid values of 300 F to water dew points of approximately 120 F, and SO_3 quantities were reduced to one fourth of their original values.

Less pronounced but still helpful benefits were obtained when adding pulverized-coal fly ash. With this material, little change was noted in dew-point temperatures, but corrosion probe tests and measurements of the rate of acid deposition showed a positive reduction in potentially corrosive conditions. Firing pulverized coal over the fuel bed of stokers produced similar results. A combination of approximately 20 per cent pulverized-coal firing and 80 per cent stoker firing was found to be sufficient to decrease acid-deposition rates appreciably. The practice of firing pulverized coal in this manner has been applied in at least two British power stations to reduce sulphuric-acid corrosion.

Although the foregoing work was carried on in Great Britain on coal-fired units, extensive additive trials also have been conducted in this country at several stations firing fuel oil. The next section of this paper will deal with the experience at these plants, and the results of test data accumulated by the authors' company.

Tests of Additives on Field Units

Special Test Equipment. In order to measure the characteristics of the flue gas which cause corrosion, various instruments have been developed. Perhaps the most widely used of these are the dew-point meter and the apparatus for determining SO_2 and SO_3 contents of gases. The operation of these instruments will be reviewed briefly to clarify the discussion of the data.

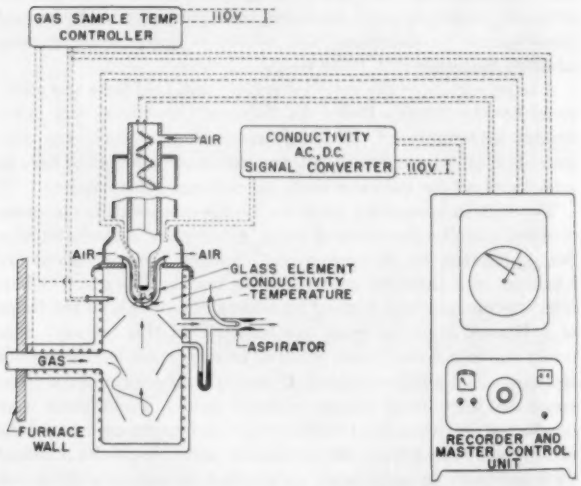

Fig. 5 Diagrammatic Arrangement of Dew-Point Apparatus

The dew-point instrument used in the test work conducted by the authors' company is shown schematically in Fig. 5. Basically, it is an electrical-conductivity instrument which measures dew-point temperature by the change in conductance between two electrodes embedded in a pyrex-glass condensing surface or element. This principle is well known and was demonstrated originally by Professor Johnstone in his work on dew-point measurement.[7] Air at a controlled temperature is supplied to the element so that it can be heated above or cooled below the dew point of the flue gases being investigated. The temperature of the surface is measured by means of a thermocouple embedded near the electrodes. The operation of the instrument consists of heating the glass element well above the dew point, passing a flue-gas sample over it, and cooling the element at a controlled rate until condensation causes an increase in conductivity between the two electrodes. The temperature at which the conductivity changes is the dew-point temperature of the gas.

An exploded view of the dew-point gas sampler, including the sensing element, ash separator, and heaters is shown in Fig. 6. The complete apparatus in operation is shown in Fig. 7.

Determination of flue-gas dew-point temperature is a difficult problem because of the many variables which influence the indi-

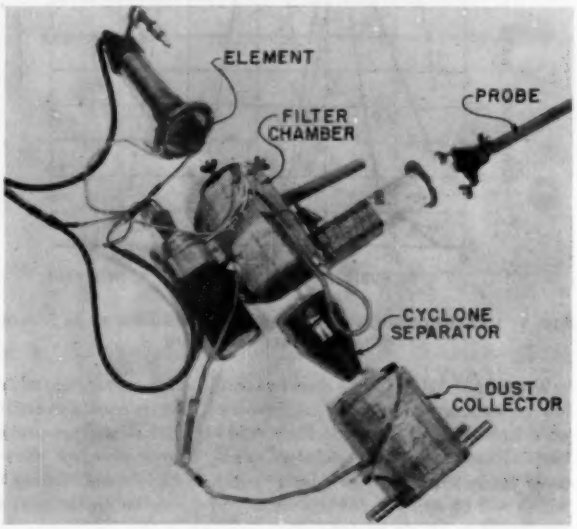

Fig. 6 Exploded View of Dew-Point Sampler

Fig. 7 Dew-Point Meter in Operation

[7] "Electrical Method for the Determination of the Dew-Point of the Gases," by H. F. Johnstone, University of Illinois Engineering Experiment Station, Circular No. 20, 1929.

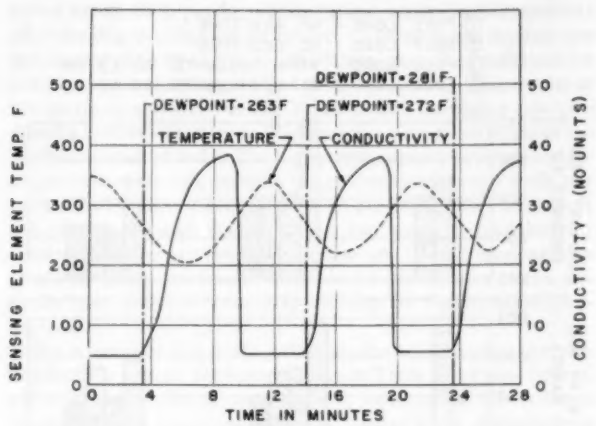

FIG. 8 TYPICAL DATA FROM DEW-POINT METER

cation. An example can be seen in Fig. 8 which illustrates typical data taken from a dew-point-meter chart. At the beginning of the test the sensing element was cleaned and heated to 350 F. The low-conductivity reading of the clean dry element is shown by the solid line on the chart. While exposed to the flue-gas sample, the element gradually was cooled until condensation took place, causing a sharp rise in conductivity. The temperature of 263 F at which this occurred is the dew point of this particular sample. The element was then dried but not cleaned and a second dew point taken which registered 272 F. Repeating this process a third time produced a 281 F value. Two additional successive readings, although not shown, registered 292 and 293 F. This phenomenon of higher readings when the element is not cleaned has been noted many times and apparently is due to the ability of the oil ash which accumulates on the element to absorb acid. Which of the values corresponds to the dew point affecting the actual air-heater surfaces is uncertain. In actual practice the dew-point indication obtained with the clean element is usually taken as the dew-point reading.

Other factors which have been found to influence the measured dew point are velocity of the gas over the sensing element, the rate at which the element is cooled, and the temperature of the gas sample. To eliminate as many of these variables as possible, the instrument is equipped with automatic controls which maintain constant temperature of the gas sample approaching the sensing element and a regulated rate of cooling of this element.

The dew-point meter has been used successfully on a number of operating boiler units, with a variety of fuel conditions. However, it is generally agreed that dew-point temperature alone does not necessarily present a true measurement of corrosion conditions. A principal reason for this is the fact that ash characteristics or other variables in the boiler can affect the rate of corrosion. Also, as previously illustrated in Fig. 2, the dew-point temperature of flue gas becomes relatively constant when the SO_3 content of the flue gas increases above approximately 20 ppm.

To supplement the data obtained with the dew-point meter, the measurement of SO_2 and SO_3 content is also desirable, and the apparatus for doing this is shown schematically in Fig. 9. The arrangement of this apparatus, including improvements in design and operation, were described in a recent paper.[8]

In brief, the equipment consists of a quartz sampling tube,

[8] "Improved Method for the Determination of SO_2 and SO_3 in Boiler Flue Gases," by R. E. Matty and E. K. Diehl, American Chemical Society, September, 1953. Copies may be obtained from R. E. Matty, Babcock & Wilcox Co., R&D Dept., Alliance, Ohio.

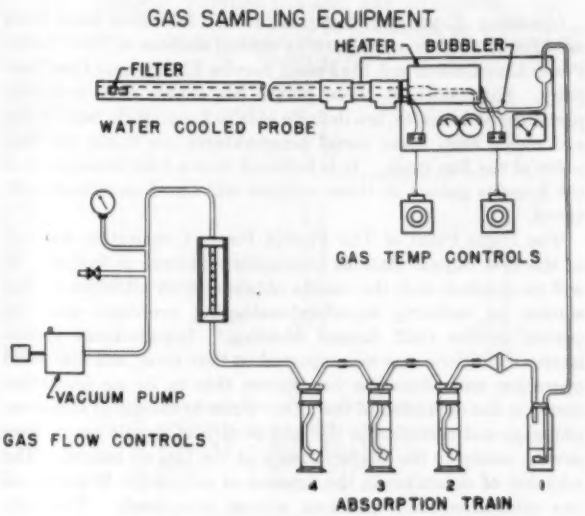

FIG. 9 DIAGRAM OF SO_2–SO_3 APPARATUS

an absorption train to collect SO_2 and SO_3, a means of measuring and controlling gas flow and temperature, and a vacuum pump to draw the gas from the boiler. The quartz tube is wrapped with a resistance heater to maintain the surface in contact with the gas sample at a temperature well above the dew point. The assembly is installed in a stainless-steel probe which has provisions for water cooling when testing in high-temperature zones. A kaolin wool filter is used in the furnace end of the sampler to insure clean gas to the absorption train. The gas temperature leaving the probe is approximately 600 F. The bubbler immediately following the probe is filled with isopropyl alcohol which serves to chill the gas and at the same time prevent oxidation of SO_2 to SO_3. From the bubbler, the flue gas passes to the first bottle of the absorption train where a fritted-glass filter once more bubbles the gas through isopropyl alcohol. The small holes in the filter trap the SO_3, which is now in the form of minute sulphuric-acid droplets. After leaving the first bottle, the gas passes through another fritted-glass filter to insure complete removal of the SO_3 and then through two absorption bottles containing a hydrogen-peroxide solution. The SO_3 is absorbed in the latter two bottles and is oxidized completely to SO_3 by the peroxide. The last bottle serves to prevent any carryover of liquid from entering the flowmeter.

The quantities of SO_2 and SO_3 in the flue gas are determined analytically by barium-sulphate precipitation and the use of a calibrated photoelectric turbidimeter. In this method of analysis, the amount of light transmitted through the solution containing the precipitate is used as a measure of the sulphur. The solutions in the bubbler, the first bottle, and the large fritted-glass filter are used to determine the SO_3 content of the flue gas, and a composite of all of the solutions is used for a total sulphur determination. The SO_2 quantity is determined by difference.

The main problem involved in any apparatus for determining sulphur oxides is the possibility of chemical changes in the sampling system. In this case, considerable care has been taken to prevent oxidation of SO_2 to SO_3 in the probe or the absorption train. By using a noncatalytic quartz tube, filtering fly ash from gases entering the probe, and employing isopropyl alcohol as an inhibitor, it is believed that such conversion has been essentially eliminated.

The use of the dew-point meter and the SO_2–SO_3 apparatus has made it possible more effectively to evaluate the variables responsible for low-temperature corrosion.

Operating Experience With Additives. Additives have been used for some time at oil-burning central stations of The Florida Power Corporation and the Public Service Electric and Gas Company. Experience at these plants has shown that additives, particularly dolomite, are definite aids in keeping air heaters dry and clean, even when metal temperatures are below the dew point of the flue gases. It is believed that a brief description of the benefits gained at these stations will be of considerable interest.

The Inglis Plant of The Florida Power Corporation was one of the first central stations to employ additives in fuel oil. It will be recalled that the results obtained with additives at this station in reducing superheater-slagging problems were reported at the 1952 Annual Meeting.[3] Improvement in air-heater conditions also was reported at that time, and continued operation with dolomite has shown this to be an important factor in the operation of the unit. Prior to the use of additives, pluggage and corrosion in the cold section of the air heater were severe, owing to the characteristics of the fuel oil burned. The addition of dolomite, in the amount of only 0.001 lb per lb oil has eliminated this problem almost completely. The only procedure now required to keep the air heater clean is the periodic use of the soot blowers at the gas outlet. The absence of corrosion is borne out by the fact that no tubes have been replaced since the start of the dolomite program 2½ years ago.

At the Inglis Plant, the additive is mixed with fuel oil to form a slurry and is then added to the main fuel-oil line ahead of the burners.

A second Florida Power Corporation Station, the Higgins Plant, has alleviated severe air-heater problems by introducing dry dolomite into the combustion-air stream at the burners. The effectiveness of this method of feeding is apparently about the same as the oil-slurry feed.

At the Kearny Station of the Public Service Electric and Gas Company, beneficial results have been obtained with dolomite on a plate-type regenerative air heater. The record at this plant also shows a past history of pluggage and corrosion. After dolomite was introduced, the air-heater surfaces were dry and clean. For a time the dolomite was added to the fuel in a manner similar to that used at the Inglis Plant, but for simplicity, the system was later changed to enable blowing the additive directly into the gas stream at a location ahead of the air heater. In both instances the results were beneficial.

The foregoing stations are mentioned specifically because field tests have been conducted at each to determine the changes in SO_3 content and dew-point temperature with additive. However, several other plants also are employing some type of additive system and are obtaining beneficial results.

Test Data and Results. The major portion of the data presented in this paper are from tests conducted at the Higgins Plant of the Florida Power Corporation. The boiler at this plant allowed an ideal comparison of conditions before and after introducing an additive, since none had been used prior to the test program. The unit tested is a 450,000-lb-steam per hr oil-fired radiant boiler equipped with a tubular air heater. It burns about 30,000 lb per hr of oil at full load. Tests were made at the air-heater inlet and outlet and in some cases at the superheater inlet. Four different conditions were investigated.

1 Full load without additive.
2 Half load without additive.
3 Full load with 0.001 lb dolomite per lb oil.
4 Full load with 0.002 lb dolomite per lb oil.

The latter conditions resulted in feeding rates of approximately 30 and 60 lb of dolomite per hr, respectively.

In Fig. 10 the flue-gas characteristics of the Higgins unit are shown before and after the use of dolomite. In examining these data, it will be noted that at full load without additive the dew point entering the air heater was 340 F while the quantity of SO_3 was approximately 0.004 per cent by volume or about 3 per cent of the total sulphur in the fuel. In passing through the air heater, approximately 25 per cent of the SO_3 was lost, presumably by condensation, lowering the flue-gas dew point some 30 deg. Thermocouples attached to air-heater tubes at the cold-air inlet revealed metal temperatures considerably below the dew point, so that the drop in SO_3 noted was not surprising.

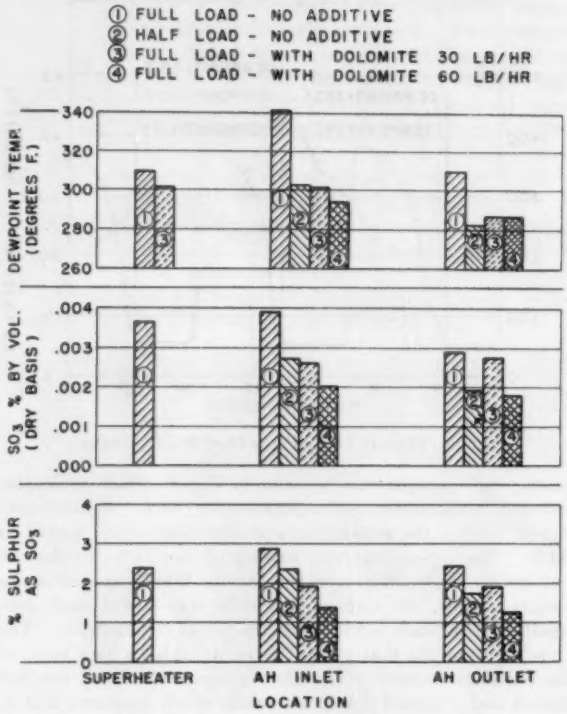

FIG. 10 SO_3 AND DEW-POINT VALUES AT HIGGINS STATION

The half-load tests showed the dew-point temperatures and SO_3 values to be lower than at full load. Although a portion of this change was attributed to dilution of SO_3 by higher excess air, the "per cent S as SO_3" also was lowered, indicating less formation of SO_3 than at the high-load condition. The amount of SO_3 condensed on the air heater was approximately 38 per cent of the total entering, but this quantity on a pounds per hour basis was only about one half that condensed at full load. The decrease with load in the amount of SO_3 lost in the air heater would indicate that air-heater corrosion on some units may be more serious at full load than at partial load. Although this is contrary to the usual conception of air-heater operation, the possibility is being investigated further.

The additive tests at the Higgins Plant were begun after dolomite had been fed for approximately 1 week at a rate of 30 lb per hr. An analysis of the dolomite showed it to contain 34 per cent CaO, 20.8 per cent MgO, and 38.6 per cent CO_2.

From Fig. 10 it can be seen that the addition of dolomite was reflected by decreases in the dew-point temperature and the SO_3 content of the flue gas entering the air heater. However, the most significant result was that the SO_3-values before and after the air heater became approximately the same, indicating little condensation on the air-heater surfaces.

Based on the values obtained without dolomite, the quantity

added at the 30-lb per hr rate would not neutralize theoretically all of the SO_3 entering the air heater. Therefore the feeding rate was increased to 60 lb per hr, which was more than sufficient for complete neutralization, if all of the SO_3 reacted. The results of this increase, also given in Fig. 10, show that the higher rate produced a further reduction in SO_3 level, but not proportional to the additional amount fed. The higher rate removed approximately 50 per cent of the SO_3 entering the air heater while the 30-lb per hr rate had removed slightly over 30 per cent. The amount of SO_3 passing through the air heater continued to be relatively constant, further confirming the reduction in acid condensation on the air-heater surfaces. Dew-point temperatures at the air-heater inlet were not lowered appreciably by the increased feeding rate.

The amount of SO_3 flowing through the boiler during the various tests in pounds per hour is given in Table 1. These figures, which are averages of several tests, again show the reduced amount of acid deposited in the air heater when dolomite was introduced.

TABLE 1 TABULATION OF SO_3 IN HIGGINS AIR HEATER

Boiler load	Additive rate, lb/hr	SO_3 entering air heater, lb/hr	SO_3 leaving air heater, lb/hr	SO_3 condensed, lb/hr
Full	None	50.0	38.0	12.0
Half	None	23	16.7	6.3
Full	30 lb/hr	33.4	36.2	−2.8
Full	60 lb/hr	25.5	22.8	2.7

It is of interest to note that the decreased condensation of sulphuric acid measured during the tests was substantiated by the marked improvement evidenced by the thin, light-colored, dusty deposits found in the air heater during an inspection immediately following the test program. Prior to the use of additives the deposits were dark-colored, moist, and greater in thickness.

Test results at the Inglis and Kearny Stations were similar to those at the Higgins Plant, although, since these plants were employing additives regularly, the large residual quantity of dolomite present in the units obscured the comparison of conditions with and without additive. An example of this was found at the Inglis Plant. There, the SO_3 level throughout the boiler was considerably lower than at Higgins even though the oil analyses were the same. Presumably, this difference was due to the accumulations of dolomite on the furnace walls and convection surfaces which may have continued to absorb SO_3 during the tests when the additive feeder was out of service.

Both the Higgins and Inglis Plants burn fuel oil containing 2.4–3.3 per cent sulphur and 10–20 per cent vanadium as V_2O_5 in the ash. For comparative purposes, tests were conducted at a third station, Hooker's Point of the Tampa Electric Company, where the sulphur content of the fuel oil was only 1.5 per cent and the vanadium low. Typical oil and ash analyses from these stations are shown in Table 2. The boiler tested at Hooker's Point was similar to that at Inglis except for the air heater, which was of the regenerative type. No additive system had ever been employed. The tests results at Hooker's Point revealed the dew points and SO_3 values to be high in proportion to the sulphur in the fuel. At both the superheater and air-heater inlet locations, the per cent of the total sulphur in the oil found as SO_3 was higher than at either of the other two plants without additive. This relationship is shown in Fig. 11. It is apparent from this graph that the amount of SO_3 existing in a boiler is not a direct function of the sulphur content of the fuel but is influenced by other factors.

The trends of the data obtained thus far indicate that sufficient SO_3 is formed ahead of the superheater to produce fairly high acid-dew-point temperatures. Additional SO_3 is produced by

TABLE 2 TYPICAL OIL AND ASH ANALYSES

	Fuel-oil analyses, per cent: Florida Power Corp. Higgins & Inglis plants	Fuel-oil analyses, per cent: Tampa Electric Co. Hooker's Point Station
Carbon	86.0	87.4
Hydrogen	10.2	10.6
Oxygen	1.4	0.5
Sulphur	2.4	1.5
Ash	0.10	0.04
	Ash analyses, per cent	
SiO_2	7.4	19.0
Al_2O_3	0.3	0.1
Fe_2O_3	5.1	16.8
MnO	...	0.1
NiO	3.2	0.9
V_2O_5	15.0	1.6
CaO	1.2	4.8
MgO	2.6	1.7
P_2O_5	...	0.1
SO_3	40.3	34.8
$Na_2O + K_2O$(as Na_2O)	26.4	19.8
Undetermined	...	0.3

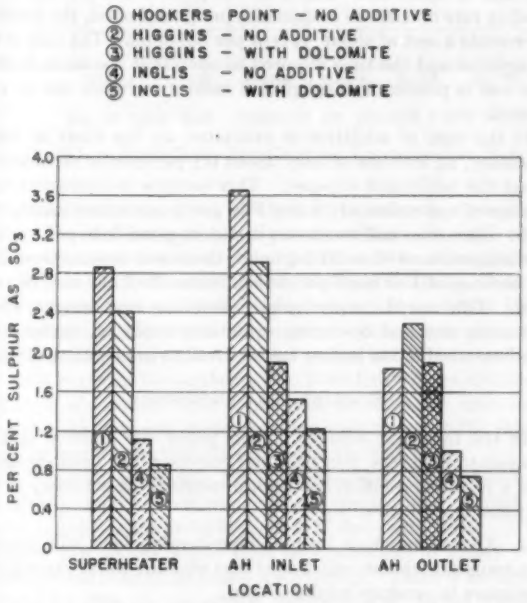

FIG. 11 COMPARISON OF SO_3 RESULTS AT THREE OIL-BURNING POWER STATIONS

catalytic conversion in the superheater and boiler banks. When dolomite is added, the SO_3 concentration and dew-point temperature of the flue gases are lowered. Although these changes are not sufficient to eliminate all of the potential acid flowing through the boiler, the reduction which does occur is sufficient to alleviate corrosion difficulties. In accomplishing this, it is believed the action of the dolomite is twofold:

1 By reducing the amount of free SO_3 in the flue gas and lowering the dew-point temperature, the amount of air-heater surface upon which acid will condense is reduced materially. In other words, many tubes formerly below the dew-point temperature will be above it when additives are introduced, even though the metal temperatures are unchanged. Furthermore, the quantity of SO_3 which condenses on the tubes that are still below the dew point will be reduced substantially since there is less potential acid available.

2 Beneficial effect of the dolomite occurs on the tube surfaces themselves. Since a portion of the tubes remains below the dew point even with additives, it is probable that some acid continues to condense. However, as soon as the condensation begins, the dolomite scrubbing over the tube surfaces neu-

tralizes the acid and keeps the surfaces dry. Because of the drying action, pluggage in the low-temperature zones also is reduced. Based on the Higgins test data, the condensation and neutralization which occur in the air heater must be relatively small, since measurements showed that little SO_3 was lost there.

It is anticipated that further test work will enable a more complete explanation of the physical and chemical action which occurs in the air heater when dolomite is used.

Economics of Additives for Corrosion Prevention

The savings which can be realized on existing boilers by preventing corrosion in low-temperature zones are obvious when a low-cost material such as dolomite can be used. Where an appreciable amount of cleaning and maintenance is required, the cost of an additive is small compared to that necessary to keep the unit in operation. Based on the price of $12 per ton and a feeding rate of 0.001 lb of dolomite per pound of oil, the additive represents a cost of about 1/4 cent per bbl of oil. The cost of the equipment and the time required to operate it are small, so that the cost is practically negligible if serious corrosion can be prevented.

If the cost of additives is evaluated on the basis of boiler efficiency, an increase of only about 0.1 per cent is necessary to offset the additional expense. This increase is equivalent to a change of approximately 4 deg F in gas temperature leaving the unit. Based on additive tests, it may be possible to reduce exit-gas temperatures 40 to 50 deg below those now obtainable so that an increase of 1 or more per cent in boiler efficiency may be realized. This would be particularly useful in new designs, where optimum size and operating conditions could be combined to produce a reduction in first costs as well as in operating costs.

Summary and Conclusions

In the foregoing sections of this paper the problem of low-temperature surface pluggage and corrosion has been discussed and a practical solution has been presented. A summary of the contents is as follows:

1 All boilers which burn sulphur-bearing fuels will produce some sulphur trioxide which combines with the water vapor in the flue gases to produce sulphuric acid.

The amount of corrosion in a specific unit depends primarily on the relationship of metal temperatures to the dew-point temperature of the flue gases and the balance between the sulphuric-acid condensing and the quantity of basic ash constituents.

2 Residual oil fuel is comparatively high in sulphur and its ash frequently contains a high proportion of constituents which may promote the formation of sulphur trioxide. In addition, oil ash contains limited quantities of materials which will absorb sulphur trioxide or neutralize sulphuric acid. For this reason the combustion gases from most residual oils are considered potentially corrosive.

3 The use of an additive, such as dolomite, will reduce the amount of sulphur trioxide present in the flue gases and will inhibit sulphuric-acid corrosion. Futhermore, dolomite will reduce the quantity of ash depositing in the air heater and the amount of work necessary to keep these surfaces clean.

4 The use of dolomite for the prevention of low-temperature corrosion is economically feasible and it is recommended where corrosion or pluggage is a problem.

It is anticipated that it will be possible further to lower exit-gas temperatures and realize gains in boiler efficiency which heretofore were denied because of prohibitive conditions.

Steam-generating-unit designers and operators realize that they are confronted with intensifying the search for a solution to the low-temperature corrosion problem and it is hoped that the material which has been presented in this paper will assist in that solution.

Acknowledgments

The results and data of the foregoing have been made possible by the interest and co-operation of the personnel of the companies involved, and their wholehearted help and support, as well as that of the authors' associates, are gratefully acknowledged.

Discussion

J. F. Barkley.[9] The Society is indebted to the authors for a logical attack on the difficult problem of corrosion in air preheaters. The problem is difficult from the standpoint of understanding theoretically the reactions involved and also from the standpoint of correcting the difficulty in a practical manner. The early Egyptians struggled for years learning how to use arithmetical fractions. Let us hope this problem will in time be solved as satisfactorily.

Fig. 4 of the paper shows the widely varying corrosion-resistance rates of several metals in boiling sulphuric-acid solutions of different strengths. The authors state their belief that this characteristic is "the principal reason for the inconsistent performance of metals in field units." It seems reasonable to assume that, with clean gases, this could, at least to some extent, be true, and even with dirty gases it may have some bearing. However, the curves in Fig. 4 for carbon steel and Cor-Ten steel are very close together, while experience shows these metals to vary widely in their relative resistance to field corrosion, particularly with dirty gases. Fig. 42 of the U. S. Bureau of Mines Report of Investigations 4996, "Corrosion and Deposits in Regenerative Air Preheaters," shows open-hearth steel to corrode about 75 per cent faster than Cor-Ten; this has been corroborated, in general, in many field installations.

Deposits covering the metal greatly affect the corrosion rate and also the theoretical thinking as to explanations of the chemical action. The sulphur moves toward the metal of the air preheater, and the metal moves away from it to form sulphates. The intensity of the acid action, which is that of the ionic hydrogen, is affected by the type of sulphate formed; the pH of solutions of sulphates varies appreciably. Laboratory tests, described in the Bureau of Mines Report of Investigations 4996, of corrosion rates of metals in sulphuric acid have shown that the addition of air-preheater deposits has changed the rate of corrosion up to 9000 per cent. In one case the addition essentially prevented corrosion, and in others caused it to appear. The problem is not so simple.

The authors are to be greatly commended on their work on dew-point meters. It is certainly a logical approach to the general problem. To determine just what can be done with some chosen type of reading obtained will require much field experience. Surely, some reading should provide some sort of tool, but it appears evident that a number of other factors are involved.

The successful use of dolomite in oil-fired units points to the necessity of determining the value of its use in coal-fired units. Is its adsorptive action greatly enhanced by its chemical nature? If so, it should be able to improve greatly on the adsorptive action of ordinary fly ash. How much will be required? Does not the quantity required depend upon its fineness? Possibly 90 per cent of its work is done by some 10 per cent of its amount occurring as the finest sizes. Is soft, easily ground dolomite therefore more desirable than hard? The authors' consideration of these questions would be appreciated greatly.

[9] Chief, Fuel Utilization Branch, Bureau of Mines, U. S. Department of the Interior, Washington, D. C. Fellow, ASME.

A. A. Berk.[10] The authors' company is to be congratulated on its research-minded staff and on the very considerable attack that its engineers have made on the problem of low-temperature flue-gas corrosion and deposits in oil-fired steam-generating units. A year ago, McIlroy, Holler, and Lee announced that a series of empirical field tests had proved that boiler availability could be greatly increased in several oil-fired systems through judicious use of additives, and that dolomite was especially effective. Several months ago, Matty and Diehl presented their field method for determining SO_2 and SO_3 in flue gases. Now Huge and Piotter have presented a third paper in this series, reporting analytical and dew-point data to show that the use of a relatively small quantity of dolomite has a considerable effect on the sulphur-trioxide content of the flue gases and therefore reasonably could be expected to affect corrosion and deposits in the low-temperature sections of air preheaters.

The purpose of this discussion is to examine the analytical and dew-point data in relation to the accumulated literature on the subject, especially the very fine fundamental work that has been done on clean gases by the British Coal Utilization Research Association. If the field-test methods described in this paper could be made to give results comparable to those obtained under more exactly known and carefully controlled laboratory conditions, the work of the ASME Special Research Committee on Low Temperature Flue Gas Corrosion and Deposits would be simplified, since important research tools would be available for plant surveys of sulphur trioxide in flue gases and of the dew point of such gases.

The authors summarize their field-test data in Fig. 2 to show the special relationship they found between the dew-point temperature and the SO_3 content of flue gases. They state that their dew-point values are not entirely accurate because the slight deposits of oil ash formed during the measurement may have caused the observed dew point to be slightly high. Also, the results were affected by the rate at which the metering element was cooled in relation to the temperature and rate of flow of the gas sample. Nevertheless, they conclude that the dew point becomes relatively constant when the SO_3 content increases above approximately 20 ppm.

This conclusion is not supported by the British work with clean gases. This is shown very clearly when a representative set of British data are superimposed on the author's Fig. 2. Fig. 12, herewith, shows on the same scale as the authors' data a portion of a curve that was published by A. A. Taylor (1)[11] in 1942. This curve has generally been accepted as valid for clean gases because it was obtained with synthetic mixtures of gases and was not based on chemical analyses of the gas mixtures. The curve has been confirmed by Dooley and Whittingham (2) and by others, including H. D. Taylor (3). H. F. Johnstone (4) predicted the upper end of it from the vapor pressure of concentrated sulphuric acid. Other investigators (5) have shown that dew points of flue gases from oil-fired furnaces follow the same general relationship to SO_3 concentration as that of the Taylor curve.

The outstanding characteristic of this Taylor curve is that it is not flat, the spread of dew points corresponding to 20 and 50 ppm SO_3 being 3 times the spread of the B&W data.

The second important difference is that the British dew points are considerably lower at the same SO_3 concentrations. The difference cannot be ascribed to a water-vapor effect, since both curves were plotted on a dry-gas basis and the water-vapor content of Taylor's synthetic gas mixtures was 8.5 per cent as against about 10 per cent for flue gas from an oil-fired furnace. Hygroscopic dust in the flue gases would tend to raise the dew point as shown by the meter but many workers have reported that field surveys show a reverse effect of dusts on the measurement (6). Johnstone (7) showed that the dew-point raising effect of a hygroscopic dust was serious only when the dust had been deposited on a metal surface in quantity. This may explain the high dew points observed with fouled probes but the values of the field-data curve in the authors' Fig. 2 evidently were obtained with clean electrodes. The comparison between the field-data curve and the clean-gas curve therefore indicates that the B&W dew-point meter was probably reading on the high side.

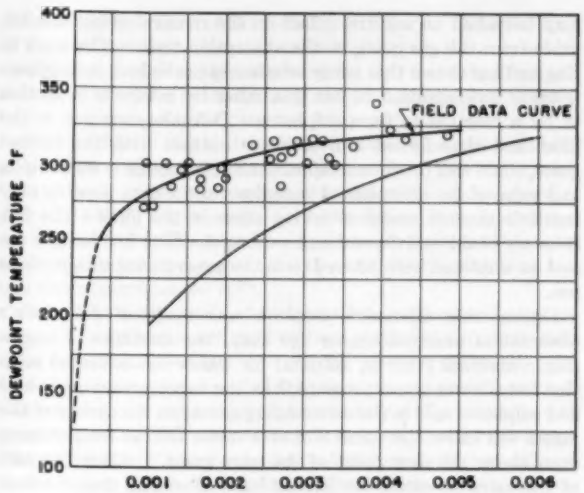

Fig. 12 SO_3 in Flue Gas—Per Cent by Volume—Dry Basis

One possible explanation for the difference between the two sets of data could be that some sulphur dioxide was oxidized to sulphur trioxide in the probe to the B & W dew-point meter. The measured dew points would then be equivalent to higher SO_3 concentrations than those found analytically. There is no direct evidence for such an assumption, however, and the description of the B&W dew-point meter and its use is not detailed enough for the writer to suggest where this evidence should be sought. It may be significant that the authors found their method sensitive to flue-gas temperature and gas-flow rate, whereas Corbett, Flint, and Littlejohn (8) state that the readings with the British dew-point instrument "were independent of gas temperature and velocity in the range of 600–1000 F and 5–50 fps, respectively."

Similarly, low SO_3 analytical values could cause a displaced SO_3-dew-point curve. The chief difficulty in analyzing flue gases for SO_3 in the presence of a considerably higher content of SO_2 has always been the tendency for some of the sulphur dioxide to be oxidized to sulphur trioxide after the sample was diverted from the gas stream and before the analysis was made. To prevent such oxidation, the B&W engineers use a special filter that cleans the gases at a relatively high temperature. In so doing they probably prevented the oxidation of SO_2 to SO_3 but they also may have promoted the reduction of SO_3 to SO_2.

Whittingham (9) showed that sulphuric acid reacts with deposited carbon at temperatures above 285 F. Considerable soot would be expected to be deposited in the filter of the sampling probe, and since the gases were passed through this filter at the comparatively slow rate of one liter per min during the 1-hr sampling period, SO_3 reduction would appear to be encouraged.

Other components in the oil ash (10) also retained on the filter,

[10] Chief Industrial Water Branch, Region VIII, Bureau of Mines, College Park, Md.

[11] Numbers in parentheses refer to the Bibliography at the end of this discussion.

may have had an additive effect on the removal of sulphur trioxide from the gas going to the absorption train. The work in England has shown that many substances can reduce the sulphur-trioxide concentration in flue gas either by catalyzed reduction or by a reaction to form sulphates. Dolomite, trapped in the filter and thus forced into intimate contact with the filtered gases, could well produce an apparent SO_3 reduction in the sample, and some of the unexplained variations in the data possibly may result from such reactions taking place in the filter. The SO_3 recovery could well depend on how long the filter had been in use and on what had been filtered from the gases during this previous use.

During this discussion mention was made of Johnstone's observation nearly 25 years ago that "the existence of hygroscopic material (that is, material for which the saturated solution has a lower vapor pressure than the vapor pressure of water and sulphuric acid in the surrounding gases) on the surface of the metal will cause the formation of a moist film at temperatures even above the dew point of the pure gases." After 12 years of intensive research, the British have concluded that the best they can do with their dew-point meters is to determine the rate at which sulphuric acid can build up on metal surfaces at temperatures below the dew point and so to anticipate where corrosion will be serious, or more frequently to explain why it occurred. The most serious build-up has been found to occur 40 to 80 F below the dew point. Therefore the determination of dew points as such may have little significance, in addition to being particularly difficult measurements to make in power plants.

This discussion in no way detracts from the very real and important finding that a relatively small quantity of dolomite greatly increases boiler availability in certain oil-fired steam-generating plants. This is an accomplishment that has considerably more practical importance than the cited British work. It is also possible that the dew point and analytical data are out of line with literature data because the latter are incorrect. However, it is much more reasonable to conclude that the field-testing equipment requires considerable improvement.

BIBLIOGRAPHY

1 "Relation Between Dewpoint and the Concentration of Sulfuric Acid in Flue Gases," by A. A. Taylor, *Journal of the Institute of Fuel*, vol. 16, 1942, pp. 25–28.

2 "Oxidation of Sulfur Dioxide in Gas Flames," by A. Dooley and G. Whittingham, Trans. Faraday Society, vol. 42, 1946, pp. 354–362.

3 "The Condensation of Sulfuric Acid on Cooled Surfaces Exposed to Hot Gases Containing Sulfur Trioxide," by H. D. Taylor, Trans. Faraday Society, vol. 47, 1951, pp. 1114–1120.

4 "An Electrical Method for the Determination of the Dewpoint of Flue Gases," by H. F. Johnstone, University of Illinois, Urbana, Ill., Circular No. 20, 1929.

5 "The Determination of SO_2 and SO_3 in Flue Gases," by P. F. Corbett, *Journal of the Institute of Fuel*, vol. 24, 1951, pp. 247–251.

6 "The Influence of Certain Smokes and Dusts on the SO_3 Content of the Flue Gases in Power-Station Boilers," by P. F. Corbett and D. Flint, *Journal of the Institute of Fuel*, vol. 26, 1953, pp. 410–417, 446.

7 "The Corrosion of Power Plant Equipment by Flue Gases," by H. F. Johnstone, University of Illinois, Urbana, Ill., Bulletin 229, 1931, p. 41.

8 "Developments in the BCURA Dewpoint Meter," by P. F. Corbett, D. Flint, and R. F. Littlejohn, *Journal of the Institute of Fuel*, vol. 25, 1952, pp. 246–252.

9 "The Influence of Carbon Smokes on the Dewpoint and Sulfur Trioxide Content of Flame Gases," by G. Whittingham, *Journal of Applied Chemistry*, vol. 1, 1951, pp. 382–388.

10 "The Reduction of Sulfur Trioxide by Constituents of Boiler Flue Dust," by H. E. Crossley, A. Poll, and F. Sweett, *Journal of the Institute of Fuel*, vol. 21, 1948, pp. 207–209, 213.

Hilmer Karlsson.[12] The authors are to be congratulated for their interesting presentation of means available for combating low-temperature corrosion by flue gases in the auxiliaries of the boiler such as economizers and/or air preheaters.

The facts disclosed by the development of comparatively new instrumentation are basic and open the road toward better understanding of the action that is taking place and which understanding will aid materially in the solution of this difficult and important problem. The data on a typical run with a dew-point meter are particularly interesting in that they show an increase in dew-point temperature from 263 to 293 F when the probe was alternately cooled and heated several times but not cleaned. This increase in dew point is due to dust deposition and indicates the difficulty in obtaining a really reliable dew point for use as an operating guide so long as fine particles or dust are present in the gas stream. Perhaps the definition of dew point given by Dr. Henry Frazier Johnstone, namely, "the highest temperature at which a liquid may exist in equilibrium with the gas," is more exact for these purposes since it takes into account the normal dusty condition of the surface as well as the hygroscopic nature of much of the deposited material. To get the same dew point in the air heater or economizer as that measured by the meter, it would be necessary to remove the dust from the entering gas just as is done in the meter.

The use of additives, especially those that neutralize the SO_3, appears to be an encouraging step in so far as protection of the low-temperature surface is concerned but eventually may have to be examined further in view of the increasing attention being given to air pollution.

With reference to the test reported on the corrosion resistance of different materials when exposed to low-temperature flue gases, we wish to confirm the authors' findings and refer to the U.S. Bureau of Mines Report of Investigations No. 4996 dated August, 1953, giving results of tests being carried out under a co-operative program between the Bureau and the writer's company. These tests are being continued.

R. B. Lee.[13] The difficulties of obtaining dependable data for determining corrosion troubles in an air heater have been explained clearly in this paper. The authors and their assistants should be complimented on designing test equipment that will give information which can be used in analyzing air-heater corrosion.

Most of our experience has been with tubular air heaters. Two boilers operating at 860 psig 900 F are equipped with air heaters having 39-ft tubes, single gas pass, four air passes. It has been necessary to retube these heaters every 18 months using carbon-steel tubes. Aluminum tubes were tried once but started to fail in 6 months. We have no results on the use of dolomite as an additive in these air heaters since the additive system has been in service only 2 months.

The installation at our Inglis Plant was described in the previous paper on additives. From September, 1947, until aluminum oxide was started in 1950, there was a continuous maintenance problem of removing the deposit from the tubes and replacing tubes whenever it was absolutely necessary. The cold end of this heater was completely retubed twice in this time with additional replacements at other times. Life of these tubes in some sections was 4 to 6 months. Some trouble was still experienced while using aluminum oxide as an additive. After dolomite was started and the correct proportions determined, it has not been necessary to replace any of the carbon-steel tubes and, furthermore, no

[12] Technical Manager, Air Preheater Corporation, Wellsville, N. Y. Fellow, ASME.

[13] Florida Power Corporation, St. Petersburg, Fla.

washing or cleaning is necessary other than that obtained with the air-puff soot blowers three times a day.

A boiler installed at the Higgins Plant in 1951, is equipped with two separate tubular air heaters having two gas passes and one air pass. This boiler has a capacity of 450,000 lb per hr of steam at 1260 psig 950 F. The tubes in the second gas pass or cold end were carbon steel, 16 ft long. There are 1566 tubes in each cold section. From September 10, 1951, until July 26, 1953, 4568 tubes were replaced besides approximately 500 tubes in each section blanked off to increase the velocity of the gas. Besides the cost of tubes, approximately $12,000 labor was required. Directional dampers were installed on both gas and air sides in an effort to increase tube-metal temperatures. A recirculating hot-air duct was installed on one heater without any noticeable decrease in tube pluggage. During this time, we were washing each heater with alkaline water every 3 weeks, thereby using approximately 25 tons of chemicals in less than 2 years.

In March, 1953, a system for blowing dolomite through the burner throats was installed. This appeared to stop corrosion but approximately one half of the tubes were either blanked off or failed as a result of the action before this date. In August, 1953, the cold ends of both air heaters were completely retubed with Cor-Ten tubes. Prior to this, a few Cor-Ten tubes had been installed and in a year of operation indicated practically no corrosive action. We are still washing these heaters once every 3 months, mainly because of an accumulation of dolomite caused partly by unequal distribution to the heaters and partly by not having determined the correct amount of feed at various boiler loads. However, there has been no indication of additional corrosion on tube sheets or ductwork after dolomite was started.

As stated in the paper, SO_3 is present in the air heaters, whether it is formed in the furnace or in the boiler. Any substance that will reduce the amount of SO_3 present or neutralize the deposit on the tube surfaces will reduce air-heater maintenance and tube replacement. It is our experience based on results that tubular air heaters with carbon-steel tubes installed on boilers burning the present residual fuel oil will be subject to considerable corrosion and pluggage unless a substance is added to reduce and neutralize the acid properties of the flue gas.

S. J. Zawadowicz.[14] Burning high sulphur and vanadium-bearing oils on steam-generating units involves the following problems:

1 Corrosion and plugging of cold-end surfaces.
2 Slagging of hot-end passages.
3 Wastage of hot-end surfaces.

The fuel oil burned at Kearny Generating Station has considerably more vanadium and sulphur than that reported in the paper for the Higgins Plant. Vanadium pentoxide in the ash averages about 30 per cent with the maximum running to 60 and 70 per cent, and the sulphur averages 3.0 per cent with the maximum running as high as 4.3 per cent.

On a Ljungström air preheater on the mercury unit at this station, dolomite mixed with pulverized-coal fly ash in 2 to 1 ratio by weight has been introduced at the gas inlet to the air preheater since January, 1953. Inspection during October showed the air heater was dry and clear with a thin white chalky deposit at the cold end. Draft loss has been practically constant over this period. The last washing of the surfaces was in November, 1952. Slight corrosion was found at the edge of cold-end elements in a few small areas where the plates were corroded away up to 1/2 in. in depth. Except for this corrosion, the condition of the air preheater was similar to that found in February. From the date of the last washing to the inspection in October, the unit was in service 5648 hr. During this period the unit was shut down and started 25 times for causes outside the air heater, subjecting the heater each time to cooling to room temperature.

Prior to the use of additive, the air preheater required washing at intervals averaging 2800 service hours.

Air-inlet and gas-outlet temperatures have been maintained at 150 and 350 F, respectively, by recirculating hot air and bypassing cold air. The soot blower, located at the cold-air inlet and using heated compressed air is operated 10 min each hour and one whole hour once per shift.

Dew-point temperature determination at Kearny showed no appreciable difference with and without the use of additive. Perhaps this results from the high sulphur content of the oil. Referring to the curve in Fig. 2 of the paper, showing relationship of SO_3 to dew-point temperature, there is only a slight drop in dew point when the SO_3 concentration is reduced in the high range. The improvement is probably due to the second effect mentioned in the paper, that is, drying and neutralization of the acid condensed on the surfaces.

There are indications that the boiler-tube surfaces also are benefiting from the dolomite and fly-ash injection at the air heater, the dolomite being transported into the furnace by the combustion air aided by soot blowing which is on the air side. This apparently scrubs the additive off the heating elements and it is carried by the combustion air into the furnace. Wall tubes are fairly clean with only a thin deposit which, in general, is brown in color. Gas spaces between fog-bank tubes are clear, deposit on fog-bank tubes varies from dark gray to brown color with powdery to sandy texture, overlaying a hard whitish-green scale. Without additive the deposits in the furnace and fog banks are black, hard, and very difficult to remove.

In the discussion of a paper by J. B. McIlroy, E. J. Holler, and R. B. Lee,[15] H. Weisberg reported that probes which had been in the furnace of the Kearny mercury boiler while firing oil with 1:1 and 2:1 dolomite to ash ratio indicated that dolomite did not prevent or reduce hot-end corrosion. Subsequently, ash analysis of the 2:1 dolomite-treated oil was compared with the specifications for noncorrosive residual fuel oil as given in Table 1 of a paper by B. O. Buckland, C. M. Gardiner, and G. D. Sanders,[16] of the General Electric Company. The ash analysis indicated that the ratio of the calcium to vanadium, with allowance for magnesium, barium, and nickel, was 4.5. This ratio fell below the specifications ratio of 6 or greater. In addition, the sodium-to-vanadium ratio was found to be 0.45. This exceeded the specifications ratio which requires a value not greater than 0.3. It would appear, therefore, that the General Electric specification for preventing high-temperature corrosion was not maintained. More work on this phase of the problem is indicated.

Authors' Closure

Mr. Barkley refers to the results of field tests with Cor-Ten and, while the Bureau of Mines results were obtained with coal, they follow the general pattern that the authors noted with oil. There is apparently more sulphur conversion to SO_3 in oil-fired units than in coal, and corrosion is consequently more severe with oil than with coal. This can be attributed, as Mr. Barkley points out, to the difference in the composition of the ash and the quantity.

[14] Engineer, Electric Engineering Department, Public Service Electric and Gas Company, Newark, N. J. Assoc. Mem. ASME.

[15] "The Application of Additives to Fuel Oil and Their Use in Steam-Generating Units," by J. B. McIlroy, E. J. Holler, and R. B. Lee, Trans. ASME, vol. 76, 1954, pp. 31–46.

[16] "Residual Fuel-Oil Ash Corrosion," by B. O. Buckland, C. M. Gardiner, and G. D. Sanders, Paper No. 52—A-161 (unpublished), presented at the 1952 Annual Meeting of The American Society of Mechanical Engineers.

The use of dolomite and other additives is under test on coal-fired units and the results appear to be promising. It always has been the authors' contention that fineness of the additive was very important. In fact, it has been specified that 100 per cent of the material should pass through a 325-mesh sieve. It is known that the soft, high-specific-surface type such as a dolomitic hydrate or magnesite can be used successfully in dry form, injected into the gas stream at the air-heater entrance.

Mr. Berk points out that the dew-point temperature curve appears to be high and flat in comparison with other known data. It is believed that the accumulation of additional data will substantiate the shape of the curve. Its exact magnitude is no doubt, as Mr. Berk suggests, a function of the fuel analysis and, as such, is influenced by many factors. Some of these which are enumerated have been recognized as important. These would include the formation of SO_3 in the sampling apparatus and the effective filtering of ash from the SO_2-SO_3 apparatus. Difficulties with soot formations have not been troublesome mainly because of the absence of soot. In general, either the dew-point meter or the SO_2-SO_3 apparatus will not produce consistent results if there is more than an occasional coke particle. On units where carbon has been encountered in the gas stream, a lower dew-point temperature has been recorded than when the carbon or coke was eliminated from the gas stream. It is believed that this lower dew-point temperature is due to the conductance of the carbon film on the probe and possibly to the absorption of some of the SO_3 by the carbon. However, the real dew-point temperature is of a magnitude determined in the absence of carbon.

The dew-point meter is a very sensitive instrument and will record minute quantities of moisture. When used in combination with the SO_2-SO_3 apparatus it can be a useful tool. If the dew-point temperature entering the air heater is substantially the same as that leaving, and the amount of SO_3 is also constant across the heater, it is reasonable to assume that there is no condensation and, therefore, no corrosion.

The authors agree with Mr. Karlsson that the determination of dew points with deposits is a difficult undertaking. In some instances, with a regular oil ash, the dew-point temperature will increase with an increase in deposits. On the other hand, an additive ash may have the opposite effect. The early observance of this phenomenon has led to the more extensive investigations which form the base of this paper.

Mr. Lee points out that the cost of maintenance as a result of corrosion is a real item and is well worth some preventative means, such as the use of a dolomite additive. An additional benefit which Mr. Lee [15] has mentioned in a previous paper is that of ease of washing when using dolomite.

Mr. Zawadowicz relates his experiences, which check those of Mr. Lee fairly closely, with regard to the elimination of air-heater pluggage and corrosion. He points out that there was no noticeable difference in dew-point temperature with and without dolomite. It is possible that even though the main body of gas is not affected appreciably, there is an effective layer of absorptive material deposited which insulates the steel surface against sulphuric-acid attack. Apparently there is not enough of the dolomite recirculated into the furnace to blanket effectively any of the catalytic surfaces in the generating unit, so that the amount of SO_3 to the air heater is fairly constant with and without dolomite.

Regarding the corrosion ratio as specified by Buckland, Gardiner, and Sanders[16] it is difficult to visualize that an increase in the calcium-to-vanadium ratio from 4.5 to 6 and a decrease in the sodium-to-vanadium ratio from 0.45 to 0.30 would eliminate high-temperature corrosion. It has been found that the rate of high-temperature corrosion was reduced in a test-basket installation at the Inglis Station of The Florida Power Corporation when burning a dolomite-treated oil. It is known that test specimens which corrode catastrophically in an oil-fuel atmosphere show no corrosion in an atmosphere formed by the products of combustion of pulverized coal with a 5 to 6 per cent sulphur content and 16 per cent ash composed of oxides of aluminum, silicon, and iron.

The authors wish to thank the discussers for their important contributions to the subject of low-temperature corrosion. It is gratifying to note that the interest shown in this subject is not of the casual type but indicates that others share the authors' viewpoints on the importance of a solution. Further, it points to the fact that this work must be continued.

Influence of Fine Particles on Corrosion of Economizer and Air-Preheater Surfaces by Flue Gases

By PETER HODSON,[1] WELLSVILLE, N. Y.

Fine particles are those less than 10 microns in diameter and are often not detected as single particles by a light microscope. They have a very large relative surface area which tends to accelerate any reaction as well as increasing their ability to adsorb another substance. Flue-gas corrosion is caused by sulphur compounds and water vapor forming sulphuric acid which attacks iron to form ferric and ferrous sulphate. The former is a catalyst in the formation of sulphur trioxide from sulphur dioxide. Sulphur trioxide and ferric sulphate also raise the dew point. Fine particles consist of unburned fuel and ash spheres known as cenospheres or fragments of the latter. They increase the reaction rate as well as the condensation temperature and rate. They can attain a temperature lower than that of the gas stream by radiation and are good condensation nuclei. A qualitative test of the formation temperature, extent, and nature of deposits from cleaned and dirty gas showed that deposits tend to build up in a narrow range and that cleaning the gas greatly decreases the rate of deposit build-up.

The Ancient Problem of Smoke

MANY people think that the problem of "smoke" with its attendant dust and corrosion is a fairly modern topic. Actually smoke is very ancient—in fact, in the Old Testament in Genesis 19:28 Abraham "looked toward Sodom and Gomorrah and toward all the land of the plain, and beheld, and, lo, the smoke of the country went up as the smoke of a furnace." Having seen that vast volume of smoke was associated with furnaces even in the old days, let us proceed to the influence of fine particles in this smoke on the corrosion of economizer and air-preheater surfaces.

The definition of a fine particle is largely a matter of comparison since what would be considered a very small particle to one accustomed to working with articles measured in feet would be considered very large to a person dealing with the fly ash from a boiler. The generally accepted unit for measuring fly-ash particles is the micron which is equal to 0.001 mm or approximately $^1/_{25000}$ in. The particles may be divided into three general classes or sizes depending upon the way they act when suspended in a gaseous medium. The first class is those particles over about 5000 microns which fall with increasing velocity; the second class extends downward to approximately 0.1 micron and these settle with a constant velocity; the third class is those particles less than 0.1 micron which do not settle, since their diameters are less than the mean free path of the gas molecules at normal temperatures and pressure, and the impacts of the gas molecules drive the particles at random in Brownian movement. By fine particles, we mean this latter class plus those particles less than 10 microns in diameter which cannot be seen readily with the naked eye.

Relative Sizes of Various Particles

Fig. 1 shows the relative sizes of a number of dusts as well as the number of particles in 1 cu ft at a loading of 0.0006 grains per cu ft. Notice how rapidly the number of particles and their total surface area increase with decrease in size. For example, 50-micron particles at this loading would give 0.0073 sq in. while 0.005 micron would give 10,000 times as much or 73 sq in.

An example of the small size of many particles associated with smokes is shown in the accompanying photomicrographs made with an electron microscope (1).[2] The first two, Figs. 2 and 3, show two types of carbon both magnified over 100,000 times. The agglomeration of particles less than 0.1 micron in size shows clearly. This agglomeration takes place because small particles in Brownian motion frequently collide and these collisions are inelastic forming chainlike aggregates (2). With standard light microscopes these chains and clumps would be seen as individual particles since they are in many cases smaller than the wave length of the light and, consequently, the interior details do not show up. The next illustrations, Figs. 4 and 5, show this effect more clearly. Both show zinc-oxide pigment. However, the first one is an electron-microscope photograph at ×35,000 while the second is with a special ultraviolet-light microscope at ×4000. The large particles in Fig. 5 turn out to be agglomerations of smaller particles at the higher magnification of Fig. 4. With a common microscope giving ×400 even less detail would be seen.

Properties of Fine Particles

One of the important properties of these fine particles is their enormous aggregate surface area. For example, a solid cube 1 cm long on each side has a surface area of 6 cm; if this cube were divided into smaller ones, each 1 micron on a side, the total surface area of all the cubes would become 60,000 sq cm. If, in addition, it were broken into irregular-shaped or porous pieces, the increase would be even greater. One of the reasons this property of fine particles is important is that the surface of a solid fairly bristles with physical and chemical energy. Aluminum, for example, which is a relatively incombustible substance, when divided into fine particles to expose more surface will burn with explosive violence in contact with air. Other examples are the disastrous dust explosions in flour mills and grain elevators. Another property of fine particles that facilitates the release of energy is their increased solubility.

A most important property of fine particles and one which plays a great part in their action in the promotion of corrosion of the cold end surface of a boiler is their ability to adsorb a ma-

---

[1] The Air Preheater Corporation.

Contributed by the Research Committee on Low Temperature Flue Gas Corrosion and Deposits and presented at the Annual Meeting, New York, N. Y., November 29–December 4, 1953, of The American Society of Mechanical Engineers.

 Manuscript received at ASME Headquarters, November 2, 1953. Paper No. 53—A-232.

[2] Numbers in parentheses refer to the Bibliography at the end of the paper.

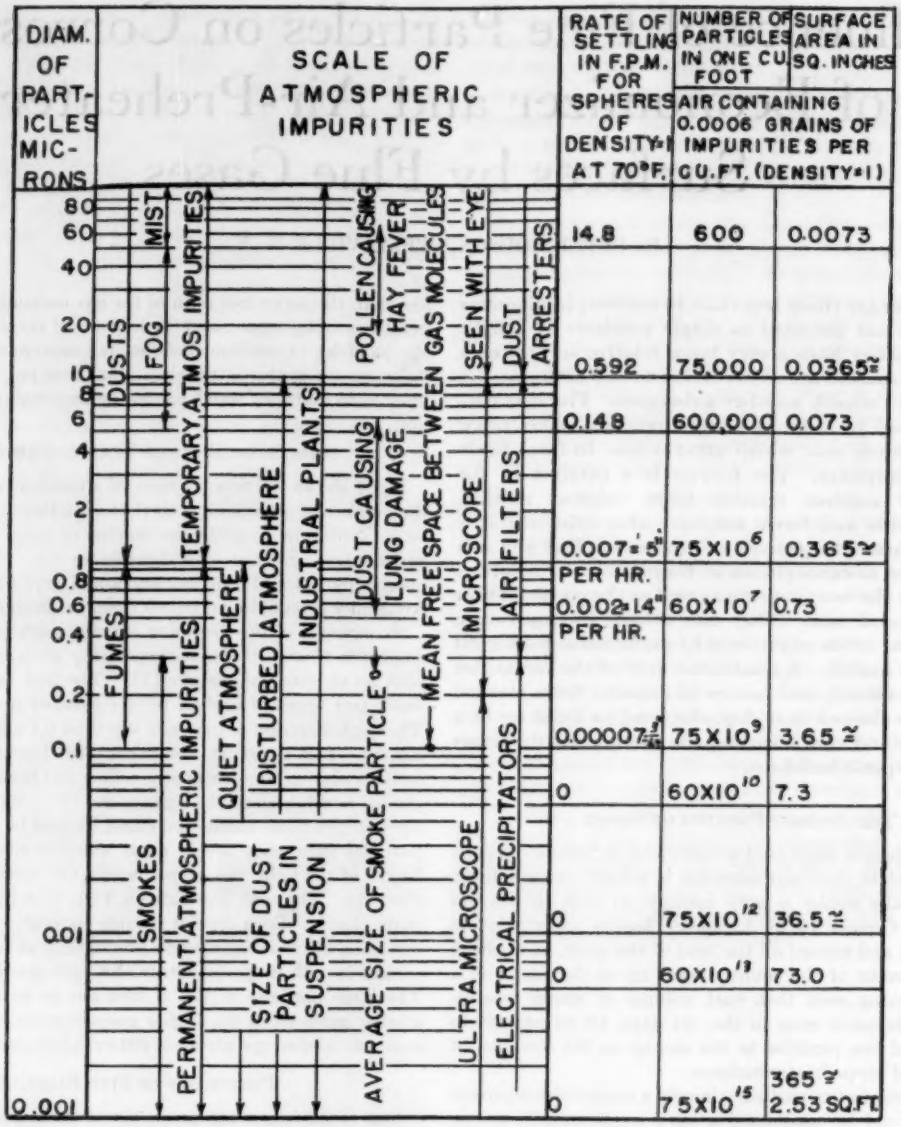

FIG. 1 RATE OF FALL, SIZE, AND DISTRIBUTION OF AIR-BORNE PARTICLES
(Compiled from Stokes' law.)

terial, i.e., make it stick to their surfaces. Fine particles always tend to coat their surfaces with a layer of the substance to which they are exposed, be it gas, liquid, or a finer solid. The surface holds an adsorbed substance with tremendous force—according to some estimates equivalent to 10,000 atm in the case of an adsorbed gas (3). It is obvious from this that water vapor, SO_2, or any other gas or liquid with which a fine particle has once been in contact will be held by that particle even at high temperatures and will be deposited with it if it comes to rest on any surface.

A good example of the increased chemical and physical activity of fine particles can be found in the study of silicosis, an occupational disease caused by the breathing of siliceous particles. Those particles retained by the lungs produce a permanent tissue change called fibrosis and they are probably the most dangerous. The degree of damage to the lungs shows a rapid increase as the particles decrease in size as might be expected. Size seems to be at least as important as chemical composition since particles about 0.2 micron diam, whatever their composition, appear to be the ones that cause fibrosis.

CORROSION ON HEAT-TRANSFER SURFACES

The corrosion of iron and steel in boiler heat-transfer surfaces such as the economizer and air preheater is mainly due to the sulphur originally present in the coal. This sulphur is burned to SO_2 and SO_3 in the boiler furnace and, in the presence of water vapor, the SO_3 is adsorbed to form sulphuric acid. This attacks the iron to form ferrous and ferric sulphate. In addition, the deposit which accumulates on the surface of the metal in the boiler usually contains a large percentage of sulphur, a part of which exists in the form of sulphates of iron. Undoubtedly these are formed from the fly ash itself and are not the result of any action of sulphuric acid on the ash after deposition.

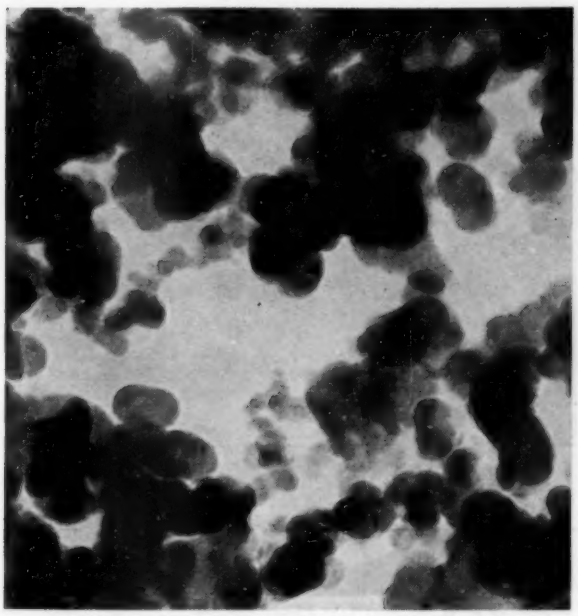

FIG. 2 CARBON BLACK FROM CAMPHOR; ×110,000
(Courtesy RCA Laboratories Division.)

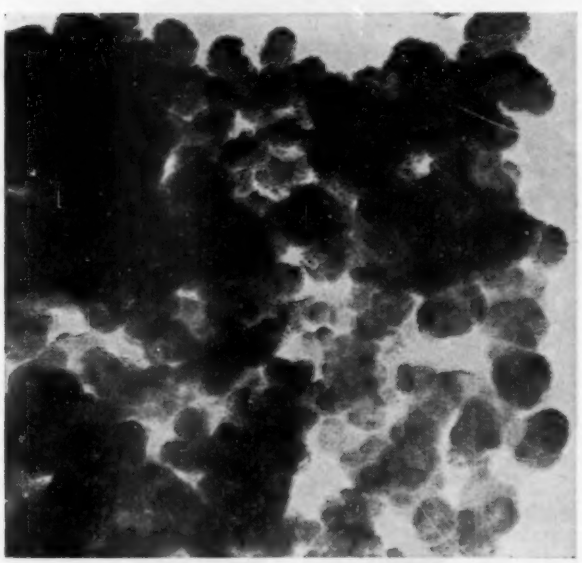

FIG. 3 CHANNEL BLACK LIGHTLY SHADOWED WITH CHROMIUM TO SHOW SURFACE STRUCTURE; ×152,000
(Courtesy RCA Laboratories Division.)

It has been shown that solutions of ferric sulphate act as powerful catalysts for the conversion of sulphur dioxide to sulphuric acid (4), and that a slight oxidation of sulphur dioxide takes place even at high temperatures as a result of the catalytic action of flue dust. However, the greatest oxidation of the dioxide takes place on a surface covered with a moist layer of saturated ferric sulphate, the conversion to sulphuric acid being very rapid so that such a layer must always contain a high concentration of acid.

The action of both sulphuric acid and of solutions of ferric sulphate on iron or steel produces ferrous sulphate which may be converted immediately to ferric sulphate by the action of flue gases containing sulphur dioxide. Sulphur dioxide, which forms the greatest proportion of the combustion products of the sulphur in the coal, plays a part in the corrosion process, therefore, by being converted to sulphuric acid by saturated solutions of hygroscopic ferric sulphate. It has been shown that even the corrosion by a spray of sulphuric acid is small compared to that caused by the combined oxidizing and acidic action of a moist film of ferric sulphate (5).

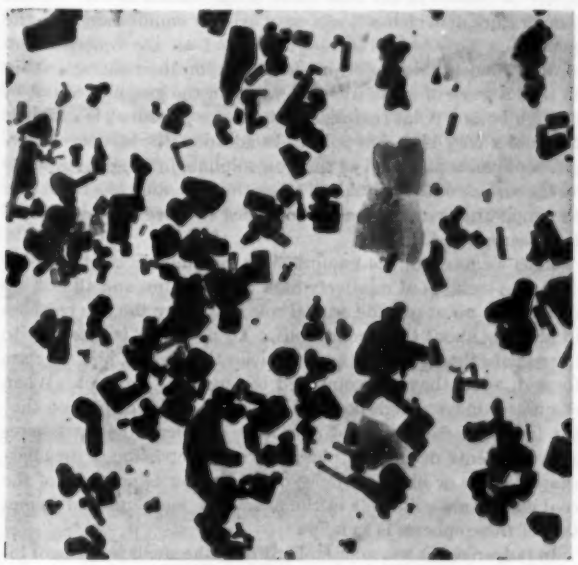

FIG. 4 ZINC-OXIDE PIGMENT; ×35,000
(Courtesy RCA Laboratories Division.)

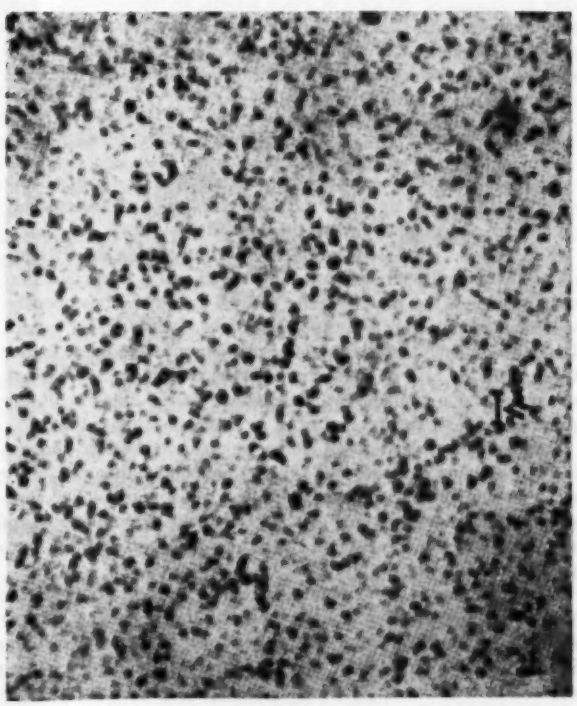

FIG. 5 ZINC-OXIDE PIGMENT; ×4000; ULTRAVIOLET-LIGHT MICROGRAPH

How Fine Particles Promote Corrosion

We have seen that the requirements for the rapid corrosion of cold end surfaces are the presence of sulphur in the fuel and moisture on the surface. What then is the role played by fine particles in the promotion of rapid corrosion even at temperatures well above the normal dew point of the gases? The dew point is usually defined as "the temperature at which a given mixture of air and water vapor is saturated with water vapor" (6). It might better be defined in the case under consideration as the "highest temperature at which a liquid may exist in equilibrium with the gas" (5). This temperature will depend on the concentration of each condensable vapor present and upon their characteristics so that a trace of sulphuric-acid vapor in the gas, on account of its high boiling point (extremely low vapor pressure), is sufficient to cause a very high dew point. In addition, the existence of hygroscopic material, such as the iron sulphate in flue-dust deposits on the surface of the metal, will cause the formation of a moist film at temperatures as much as 50 to 75 deg F above the dew point of the clean gases (5).

Thus we have all the requirements for a highly corrosive condition on surfaces at relatively high temperatures and all that remains is to point out the crucial role played by the fine particles in bringing about these conditions. To do this it is necessary to investigate the nature of these particles themselves, how they are formed, what they are composed of, and how they act. When examined under a high-powered microscope, it will be seen that the fly-ash particles consist of a large number of hollow spheres and fragments of spheres plus a certain proportion of irregular-shaped white or black particles depending on ash content of the coal and combustible left in the ash. The mechanism of formation of these spheres is as follows:

In pulverized or spreader-stoker-firing, the small particles of bituminous coal in suspension are heated rapidly when exposed to the intense heat of the furnace. These particles soften and swell into multicellular bubbles of coke known as cenospheres. The coke is then burned leaving a hollow shell consisting of the noncombustible ash. It is these cenospheres and fragments of cenospheres which we see as a substantial proportion of the ash when examined under the microscope (7).

Nature of Fly Ash

Fig. 6 (12) shows the nature of common fly ash—the first being a light fraction and the other a heavier one. They consist largely of spheres or irregular broken portions of spheres.

Fig. 7 shows more details of coal-ash cenospheres greatly magnified. The multicell structure shows well and it is obvious that such a particle has much greater surface area and, consequently, will react much faster than a solid particle of equal size or weight. It is also evident that this type of particle must be much lighter than a solid sphere of equal diameter and, therefore, that it will act more like a smaller particle when under the influence of any mechanical force, as, for example, in a cyclone-type collector.

As mentioned previously, these particles consist of the unburned carbon from the coal and the noncombustible portion or ash present. They consist of various oxides and sulphur compounds and, as tests have shown, the iron and sulphur contents of the finer portion or fly ash are much higher than that of the composite ash from the ash pit (8).

The part played by these fine particles depends largely on the very great surface area due to their small size as well as their shape. Surface area plays such a great part because any reaction is basically the reaction of the molecules on the surface of one substance or phase with those on the surface of another. Since the surface of fine particles is much greater, the number of molecules of the substance that are at the surface, and therefore

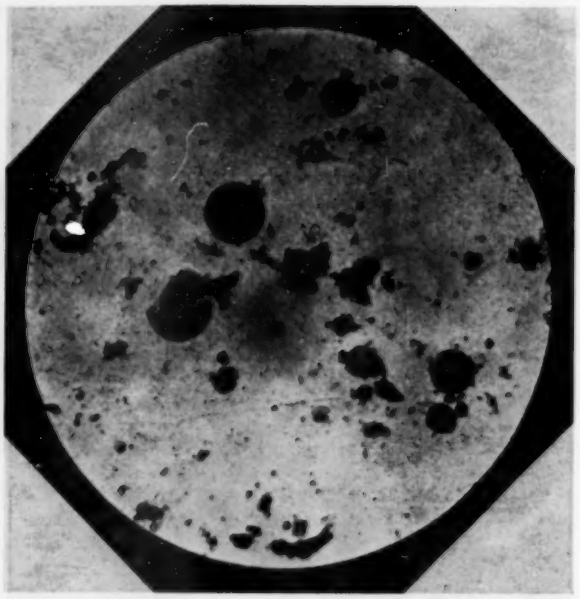

Fig. 6(*a*) Photomicrograph Showing Lighter Flue Dust
(More light unconsolidated ash, fewer and smaller fused spherical particles.)

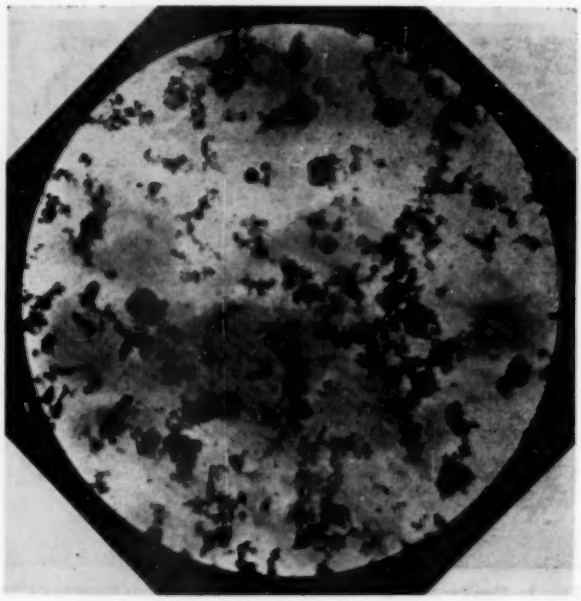

Fig. 6(*b*) Photomicrograph Showing Heavier Flue Dust
[Less light unconsolidated ash, more and larger fused spherical particles Reference (12).]

immediately available for any physical or chemical reaction, will be increased enormously. This increase represents approximately the extent to which the chemical activity of a substance is increased by subdivision into fine particles and the rate at which a reaction takes place will depend on the rate at which the molecules become available, that is, the rate at which they come to the surface. Fine particles then, owing to the enormously increased area of the surface of contact, greatly accelerate physical or chemical reactions such as evaporation and condensation or actual chemical combination once a reaction is initiated (10).

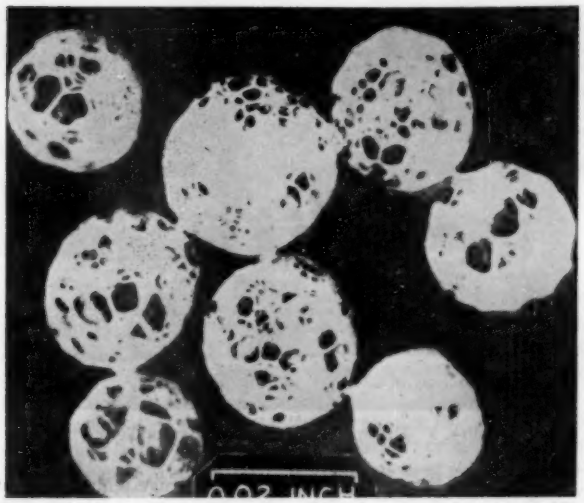

FIG. 7 CENOSPHERES MAGNIFIED TO SHOW STRUCTURE

In the case of the adsorption of some gas by fine particles, we have seen that the molecules of gas or vapor are held to the adsorbing surface by a relatively large attractive force. Consequently, an adsorbed layer of gas or vapor molecules can be formed at a solid or liquid surface at temperatures far above the normal boiling point of the adsorbed substance. Such an adsorbed layer of molecules would re-evaporate only with great difficulty (9).

Fine particles are a vital necessity to any condensation. In a homogeneous system, it is very difficult to induce a change of state unless some point of singularity, some nucleus or free surface is present to act as a center from which the change can spread. A gas then may be cooled until it has become a highly supersaturated vapor and yet not condense to liquid if there are not suitable condensation nuclei present. Such condensation nuclei may be fine dust or smoke particles. In addition, it is possible that condensation can take place at temperatures higher than the normal saturation point if fine particles are present.

For example, when warm humid air containing suspended dust particles drifts along the ground after a warm day, the dust particles lose heat by radiation more rapidly than the surrounding air and become relatively cold so that water vapor condenses upon them to form a mist. This is exactly the condition which exists at boiler heat-transfer surfaces such as the economizer and air preheater.

Gases are very transparent to radiant heat. Dust or smoke particles suspended in a gas diminish its thermal transparency and adsorb the heat radiation. The particles become warmed and communicate their heat by conduction to the gas immediately surrounding them. If the heat rays be intercepted, as in a preheater, the suspended particles quickly cool by radiation and assume a lower temperature than that of the gas. If the gas contains sufficient water vapor to saturate it at the temperature of those cooling particles, some of it will condense upon them (10).

We understand from a private communication by Mr. R. J. Robertson and Mr. W. B. Gurney of the Gulf States Utilities Company, that with refinery gas-firing, dirty flue gas has shown a 75-deg F higher dew point than clean gas along with a fourfold increase in sulphuric-acid concentration. With a combination of acid sludge and natural gas as fuel, the same effect to a lesser extent was observed.

We see, then, that particle size is perhaps the most important single variable since the surface exposed in a given amount of material is greater as the particle size decreases. Catalysis, solubility, and adsorption are all phenomena dependent on surface and smaller particles also permit a more rapid diffusion of heat.

CONDENSATION AFFECTED BY SHAPE OF PARTICLES

Condensation is also affected by the shape and nature of the particles. The vapor pressure of a liquid is affected by the curvature of the surface to which it adheres. Liquid on the convex surface of a particle with extremely small radius of curvature exerts a vapor pressure greater than that on a plane or concave surface. Hence vapor will condense more readily at a given temperature within a concave surface than upon a convex one. For this reason, an irregular or porous particle will condense moisture better than the surface of a smooth sphere with approximately the same diameter. To induce and increase condensation, therefore, it is necessary to introduce suitable nuclei that will reduce the vapor pressure at their surfaces. Such nuclei may be as follows:

1 Small inert particles having many plane surfaces offering larger areas for condensation.

2 Inert particles having porous surfaces such that the radius of curvature of the pores is less than 1 micron. Once a film of vapor molecules has formed on such a surface by adsorption, vapor will condense even above the saturation temperature and as the radius of curvature of the pores is further diminished, it will condense readily even from vapor at pressures below its saturation point.

3 By introducing small particles carrying an electric charge, such as are commonly found as a result of thermal action and friction on small particles.

4 By particles having a strong chemical affinity for the vapor, hygroscopic substances, such as sulphur trioxide, ferric sulphate, and so on, combine with the water vapor and form droplets which have lower vapor pressure upon which more moisture readily condenses.

The effect of fine particles, then, is to increase the rate of any chemical reaction taking place between solid and liquid or gas phases because of their great surface area and porous nature. In addition, a deposited layer of such particles forms even more pores because of the spaces between individual particles. This rate is enhanced further by the Brownian motion of the fine particles which constantly exposes new surface and transfers the reaction throughout the liquid or gas phase in which the particles are contained (10, 11).

MINIMIZING CORROSION

From the foregoing it is evident that the removal of the fine particles will have a triple effect. The first and most obvious is that the less material available for deposit or to cause corrosion, the longer the deposit or corrosion will take to reach dangerous proportions. Also, there is a decrease in the rate of chemical reactions taking place between a metal surface and the deposit as a result of the smaller surface area and thus decreased chemical, physical, and catalytic action of the remaining particles. Finally, there is a lowering of the temperature and rate at which condensation of a liquid from the vapor phase can take place because of the removal of those particles which tend to increase these quantities.

Some rough tests have been run to show qualitatively the effect of removing a large percentage of the dust in the flue gases on the formation temperature, extent, and nature of deposits which might be expected in a tubular-type preheater.

For these tests, two identical test setups, as shown in Fig. 8, were made. They consist of three glass condenser units arranged

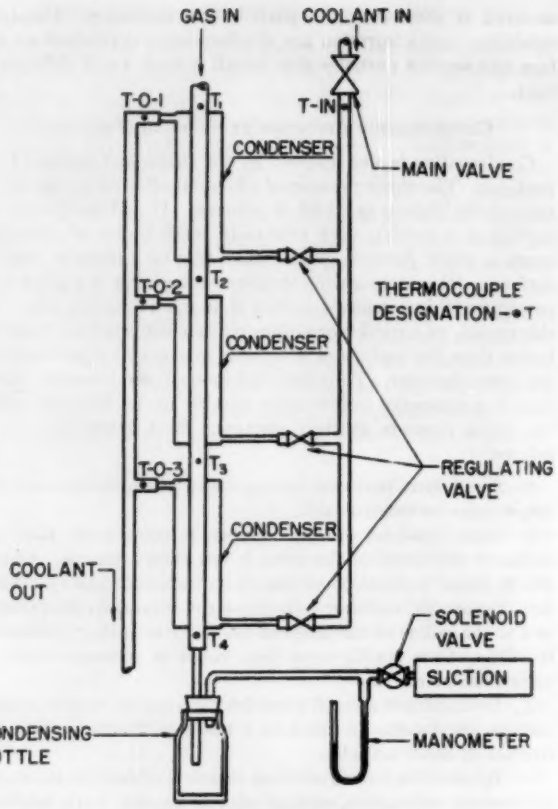

FIG. 8 DEPOSIT TEST RIG

for series gas flow and provided with inlets and outlets for the saturated steam at atmospheric pressure which was used as a cooling medium. This steam was individually regulated to each condenser to give the desired temperature gradient, temperatures being measured by thermocouples, located at the points shown. One such setup was operated on untreated gas from the boiler while the other operated on cleaned gas from an experimental high-temperature precipitator unit operating at an efficiency of 97 to 98 per cent over-all. The gas temperature was regulated by heating the inlet tubing to give a temperature of gas entering each of the first condensers of approximately 320 F. The wet steam gave a constant cooling-medium temperature of 200 to 215 F in all condensers, which allowed the gas temperature to drop from 320 F at the inlet to 210 F at the outlet. In addition, a condensing bottle was located after each setup to reduce the temperature of the leaving gases further.

Continuous observations of the extent of deposits were made during the run and it was noted that deposits started in the middle dirty-gas condenser almost at once. Average gas temperature in this condenser was 255 F. A slight moistening of the clean-gas condensers was noted after about $^1/_2$ hr, but this was a surface film only and never became heavy enough to cause a full wetting of the surface.

The test was continued for 8 hr after which the unit was shut down and examined and the deposits removed. All clean-gas condensers showed only a very small amount of fine light dust while the dirty-gas condensers had a heavy dark deposit along their full length. Fig. 9 shows one of the dirty-gas condensers and the heavy dark deposit shows very well. There was so little deposit in the clean-gas condensers that it was possible to distinguish them from unused units only by very close inspection.

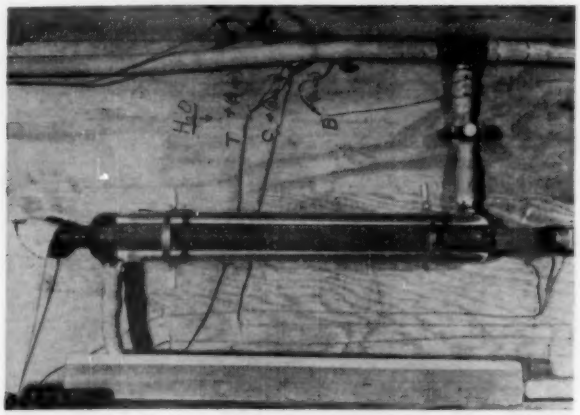

FIG. 9 DIRTY-GAS CONDENSER AFTER TEST

The middle dirty-gas condenser at an average temperature of 255 F showed the heaviest deposit, while the upper one at an average temperature of 290 F had about $^1/_2$ the amount, and the lower one at 230 F had about $^1/_3$ as much.

While these tests were rough and qualitative only, it can be concluded from them that with clean gas the decrease in the extent of deposits with consequent danger of plugging and corrosion will be even greater than the percentage of the dust removed. For this type of setup, the range of greatest deposits occurs in a relatively short range from 235 to 275 F. It also should be noted that this appears to agree with corrosion observed in preheaters which seems to occur in a narrow band a few inches down from the cold end.

CONCLUSION

While our primary interest is in preventing corrosion in preheaters, another very important result of removing the dust will be the alleviation of the curse mentioned by Abraham earlier in the paper, namely, the smoke from the furnaces.

The company with which the author is associated is carrying out a program to determine how effectively these fine particles can be caught at high temperatures and what effect this will have on corrosion and plugging of economizer and/or air-preheater surfaces. The results of this program will be available in the near future.

BIBLIOGRAPHY

1 "The Electron Microscope in the Determination of Particle Size Characteristics," James Hillier, Symposium on New Methods for Particle Size Determination in the Sub-Sieve Range, ASTM Technical Publication No. 51, March 4, 1951.

2 "Handbook on Air Cleaning," by S. K. Friedlander, L. Silverman, P. Drinker, and M. W. First, U. S. Atomic Energy Commission, Washington, D. C., September, 1952.

3 "Fine Particles," by Clyde Orr, Jr., Research Assistant at the State Engineering Experiment Station of the Georgia Institute of Technology, published in *Scientific American*, vol. 183, no. 6, December, 1950, p. 50.

4 "Ferric Sulphate and Sulphuric Acid From Sulphur Dioxide and Air," by E. S. Leaver and R. V. Thurston, Reports of Investigations, serial 2556, Bureau of Mines, 1923.

"The Ferric Sulphate—Sulphuric Acid Process," by O. C. Ralston and C. G. Maier, Bulletin 260, Bureau of Mines, 1927.

5 "Corrosion of Power Plant Equipment by Flue Gases," by H. F. Johnstone, Bulletin No. 228, Engineering Experiment Station, University of Illinois, June 9, 1931.

6 "Principles of Chemical Engineering," by W. H. Walker, et al.; McGraw-Hill Book Company, Inc., New York N, Y., second edition, 1927, p. 442.

7 "Some Fundamentals of the Carbonization of Caking Coals—The Formation of Cenospheres," by F. S. Sinnatt, Proceedings of the

International Congress of Bituminous Coal, vol. 1, 1928, pp. 560–585.
8 "Refractories Service Conditions in a Furnace Burning Pittsburgh Coal on Underfeed Stokers," by R. A. Sherman and W. E. Rice, *Mechanical Engineering*, vol. 49, 1927, pp. 1085–1092.
9 "Chemical Reactions on Surfaces," by Irving Langmuir, Trans. Faraday Society, vol. 17, 1922, pp. 607–620.
10 "Clouds and Smokes," by W. E. Gibbs, J. and A. Churchill, London, England, 1924, pp. 58–62.
11 "Micromeritics," by J. M. DallaValle, Pitman Publishing Company, New York, N. Y., second edition, 1948.
12 Bureau of Mines, Reports of Investigations No. 3472.

Discussion

HILMER KARLSSON.[3] This subject has received very little attention by mechanical engineers although the phenomenon discussed has been well known to the physicists for a long time as it affects our daily lives to a much larger extent than we normally believe.

Our organization became greatly interested in this phenomenon at the time it started a co-operative research program with the U. S. Bureau of Mines in 1946, for the purpose of studying corrosion and its effects on different types of material in an effort to find a material or coating that would permit operation at lower temperatures of economizer and/or air-preheater surface.

Our studies convinced us that the presence of fine particles in a gas stream containing sulphur compounds would result in corrosive attack of economizer and air-preheater surfaces exposed thereto at considerably higher temperatures than if such particles could be eliminated. Our study further covered means for eliminating such particles in a gas stream at high velocity and high temperature permitting removal of such particles ahead of an economizer and/or air-preheater surface.

It was found that none of the conventional equipment used was suitable and in order to accomplish this it would be necessary to devise different methods. In co-operation with the Raytheon Manufacturing Company of Waltham, Mass., a program was developed to investigate the feasibility of the removal of fines from a gas stream at high velocities and temperatures by means conceived by members of our organization. Laboratory testing, on a very small scale, indicated it was possible to remove extremely fine particles from a high-temperature gas stream at high velocity in that we successfully removed up to 95 per cent and better of the solids in a gas stream consisting of dense smoke generated by burning fuel oil in a domestic-type furnace. These results were obtained at temperatures of 800 F and velocities in the gas stream of up to 50 fps.

Through the co-operation of the Consolidated Edison Company of New York, Inc., a small pilot plant was then installed at the Hell Gate Station where flue gases from a boiler burning pulverized coal and oil were utilized in the experiments—the treated volume, however, being limited to 2000 cfm. These experiments also proved that the methods proposed appeared sound in that excellent collecting efficiencies were obtained on both pulverized-coal and oil firing, respectively, at velocities of 40 fps and temperatures up to 750 F.

As a result of these latter experiments, our English associates, Messrs. James Howden & Company of Glasgow and London, became extremely interested in our work and through them the British Electricity Authority also became much interested. The end result of this was that a commercial-sized test plant was designed and is now being installed in conjunction with a 160,000-lb per hr pulverized-coal-fired boiler at the Barking Steam Generating Station of the British Electricity Authority and in which provision has been made to determine the effect on air-preheater surface by the elimination of the fines in the gas stream in comparison with the effects of untreated gas of otherwise identical composition. It is anticipated that this test plant will be commissioned within a few months and that results indicating whether the method is as effective, as anticipated, or not, will be available before the end of another year.

[3] Technical Manager, Air Preheater Corporation, Wellsville, N. Y. Fellow ASME.

E. F. ROTHEMICH.[4] The author has presented a comprehensive analysis of the influence of fine particles of less than 10-micron size on low-temperature flue-gas corrosion.

On conventional coal-fired installations, either stoker-fired or pulverized-coal-fired, the ash particles are never confined to the 10-micron and smaller sizes but include a high percentage of sizes large enough to fall through a gaseous medium with either constant or increasing velocities.

We are familiar with two spreader-stoker-fired installations that have a dust collector ahead of the air heater and these air heaters are subject to plugging. Normally, when the dust collector follows the air heater, the coarse fly-ash particles tend to have a scouring action which apparently eliminates or reduces the plugging difficulties.

It also may be that the larger particles act as nuclei for the condensation and acid formation, but have sufficient mass to flow through a tubular air heater and carry the acid off without being deposited on the metal surface.

We also have noted that the air-heater tubes with lowest gas velocity are most prone to plug with fine particles whereas other tubes in the same air heater which had higher gas velocities and normally a higher percentage of large particles remained clean. These latter tubes naturally had the advantage of higher gas temperature and tube-metal temperature which would assist greatly in preventing condensation and deposits, so the effect of particle size on this type plugging is indeterminate.

One of the previously mentioned spreader-stoker-fired installations was equipped with fly-ash-return system from the dust collector. During initial operation, tests indicated that the carbon content of this fly ash was too low to make it economically advantageous to continue this reinjection. It is with this reduced fly-ash loading through the system that the plugging is occurring. It is unfortunate that we do not have more accurate information from this installation on the effect of particle size on plugging but the indications are that elimination of reinjection increased the plugging.

It would be interesting to learn the effect on air-heater plugging of particle size of fly-ash injection as used in England, and of dolomite injection ahead of the air heater as practiced at Kearny. Both of the practices mentioned were successful in reducing plugging and corrosion but it is not known what percentage of the particles injected was less than 10-micron size. Since the use of dolomite depends to some degree on the chemical reaction to neutralize the acid formed, it would appear that fine particles would be required to assist this chemical mixing and reaction. This might not be the case with fly ash.

An analysis of the effect on plugging and corrosion of the particle sizes normally found in coal and oil-fired installations would be an interesting supplement to this paper.

A. J. TIGGES.[5] This is an excellent thesis in physical chemistry as applied to the phenomenon of flue gases and their activities. It is based on a great deal of research work both documentary and laboratory.

Hygroscopic properties of fine particles seem to be related to surface vapor pressures which, as indicated, are very high. A

[4] Assistant Chief Service Engineer, Riley Stoker Corporation, Worcester, Mass. Mem. ASME.

[5] Jackson & Moreland, Engineers, New York, N. Y. Mem. ASME.

measure of these pressures can be determined from vapor drift from Niagara Falls in zero F temperature. The droplets are in liquid state and are on the order of 50 microns in size. To hold water in liquid state at zero F requires a pressure of not less than 35,000 psi. Smaller particles would have higher pressures but this is offset by higher flue-gas temperatures which reduce the surface-vapor pressure. But it is evident that the effect is that the surface pressures of fine particles are high.

These hygroscopic properties permit fine particles to pick up water vapor from the air at normal condition rather rapidly. For instance, if fly ash containing sulphur compounds is left in metal flues for any length of time after the boiler is shut down, there will be an active attack of the metal. In industrial boiler plants in the 1920's, burning sulphur-bearing fuel oil, and with gas-exit temperature of 500 to 600 F, no corrosion took place in unlined metal flues. But during the depression serious corrosion took place when these plants shut down without cleaning the boiler and flues. Therefore it is evident fly ash can be very corrosive in the presence of water vapor even without the presence of flue gas.

It may be concluded from the foregoing that elimination of a large portion of the fine particles from the flue gas before the temperature drops below 400 to 500 F will reduce materially corrosion and plugging of the air preheater.

In general, conditions in flue gases follow nature in that raindrops, fog, mist, snow, and hail all require a nucleus of fine particles.

Author's Closure

The author wishes to thank Messrs. Karlsson, Rothemich, and Tigges for their kind and helpful discussions of this paper.

Mr. Rothemich has presented some very interesting experiences with plugging of air heaters on spreader-stoker-fired boilers. We have studied a number of pulverized-coal-fired installations with mechanical dust collectors ahead of the air heater without being able to reach any definite conclusion. Of course, this type of collector is relatively inefficient on particles under 10 microns, and as a result it appears likely to have very little effect. The onset of plugging and corrosion appears to commence when the gas temperature measures a certain point dependent on the coal analysis, firing conditions, and a number of other factors as long as fine particles are present. If, as we believe, the size of the particles is the controlling factor, anything short of removal of the majority of the finer particles would be expected to have very little effect and might even lead to the condition described where removal of large particles accelerated deposit formation. While the mechanical action of large particles may reduce deposits in a certain temperature range when fly ash is reinjected and dolomite may be effective through chemical means, it is the author's belief that the deposit and corrosion will still take place if exit-gas temperatures are lowered or at some later point in the system. In addition, it must be remembered that anything added to the system must be deposited somewhere or removed from the stack gases in order to meet air-pollution requirements.

It might be interesting to point out that recent studies of fly ash show that the germanium content of the finer portions is quite a bit higher than that of the larger portions. Since the germanium is volatilized as an oxide at furnace temperatures, this indicates a preferential condensation on the fines similar to that which occurs with sulphur compounds and water vapor.

Mr. Tigges' practical observations of the effect and nature of deposits in promoting condensation and corrosion are a valuable contribution. His reference to the nature of water-vapor particles at subzero temperatures at Niagara Falls tends to confirm the high pressure generally associated with very small particles and droplets. In this connection it has also been reported that hours are required for the evaporation of submicroscopic ice particles as contrasted to their nucleation and growth in a fraction of a second. This would indicate the existence of an energy barrier at the surface dependent on the particle size.[6]

[6] "Airborne Particle Study," Contract N.70 NR.405. Task 1. Project NR.082-013. Reports Nos. 18 to 25. Issued during period from Dec. 31, 1951, to Sept. 30, 1953, New Mexico Institute of Mining and Technology.

Applying Bearing Theory to the Analysis and Design of Pad-Type Bearings

By A. A. RAIMONDI[1] and JOHN BOYD,[2] EAST PITTSBURGH, PA.

A review-type paper which presents charts and tables for the design and analysis of both fixed-pad and pivoted-pad thrust bearings. These data yield theoretical bearing-performance characteristics on the basis of what is generally regarded to be the most usable theory. Typical bearing design examples are included which illustrate the facility with which theoretical calculations can be made.

PART 1 FIXED-PAD BEARINGS

Introduction

In a previous paper under a somewhat similar title,[3] the authors discussed the application of bearing theory to journal bearings. The purpose of the paper was to provide a means whereby designers and others concerned with the operation of journal bearings could more easily determine what their theoretical performance would be under various circumstances without being compelled to make an exhaustive study of the subject. The paper relied upon the use of charts and method-of-solution tables to aid in solving for the quantities usually desired. The present paper on fixed-pad bearings follows the same pattern as the one on journal bearings and the charts and tables contained herein yield the results to be expected for fixed-pad bearings on the basis of what is generally regarded to be the most usable theory. It is not within the scope of this paper to recommend proper bearing proportions, allowable temperature rises, and so on. These must be left to the judgment of the designer to be decided on the basis of experience or test.

Nomenclature

The following nomenclature is used in Part 1 of this paper. Some terms are shown diagrammatically in Figs. 1, 2, and 3:

Nomenclature for Individual Pads:

W = load per pad, lb
U = velocity of sliding surface, ips
B = length of pad in direction of motion, in.
L = length of pad perpendicular to direction of motion, in.
P = load per unit area = W/BL, psi
μ = viscosity in reyns, lb sec/in.^{2}
h_1 = inlet film thickness, in.
h_2 = outlet or minimum film thickness, in.
m = slope of pad surface = $(h_1 - h_2)/B$, dimensionless
f = coefficient of friction, dimensionless
H = power consumed in friction per pad, hp
Q = flow of lubricant drawn into film at inlet, cu in/sec
Q_s = flow of lubricant out both sides of pad, cu in/sec
K_f = bearing characteristic number for fixed pad = $(1/m^2)\mu U/PB$, dimensionless

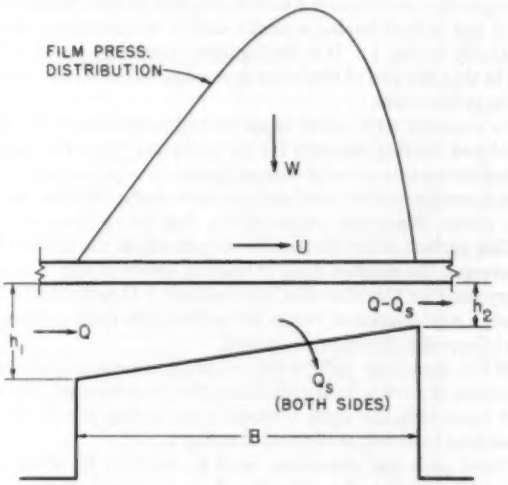

Fig. 1 Diagrammatic Sketch of Fixed-Pad Bearing

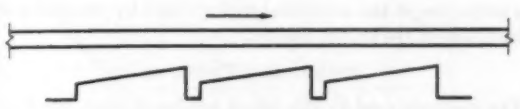

Fig. 2 Diagrammatic Sketch of Multiple Fixed-Pad Bearing

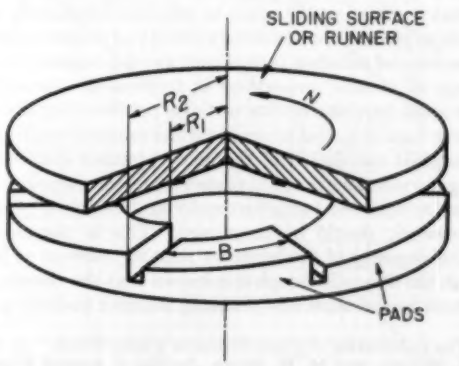

Fig. 3 Diagrammatic Sketch of Fixed-Pad Thrust Bearing

---

[1] Research Engineer, Westinghouse Electric Corporation. Assoc. Mem. ASME.

[2] Manager, Lubrication Section, Westinghouse Electric Corporation. Mem. ASME.

[3] "Applying Bearing Theory to the Analysis and Design of Journal Bearings I and II," by John Boyd and A. A. Raimondi, *Journal of Applied Mechanics*, Trans. ASME, vol. 73, 1951, Part I, p. 298; Part II, p. 310.

Contributed by the Lubrication Activity Division and presented at a joint session of the Lubrication Activity, Applied Mechanics, and Machine Design Divisions, and the American Society of Lubrication Engineers at the Annual Meeting, New York, N. Y., November 29–December 4, 1953, of The American Society of Mechanical Engineers.

Note: Statements and opinions advanced in papers are to be understood as individual expressions of their authors and not those of the Society. Manuscript received at ASME Headquarters, August 7, 1953. Paper No. 53—A-84.

t = temperature, deg F

t_1 = temperature at inlet to pad, deg F

t_2 = temperature at outlet of pad, deg F

Δt = temperature rise = $t_2 - t_1$, deg F

t_a = average film temperature = $t_1 + \Delta t/2$, deg F

Nomenclature for Thrust Bearings:

W_T = total load on bearing, lb

n = number of pads

R_1 = inside radius of pads, in.

R_2 = outside radius of pads, in.

R = average radius of pads = $(R_1 + R_2)/2$, in.

k = proportion of circumference occupied by pads, dimensionless

N = speed of runner, rps (see footnote 6)

Types of Fixed-Pad Bearings

The simplest form of fixed-pad bearing provides only for straight-line motion and consists of a flat surface sliding over a fixed pad or land having a profile similar to that shown diagrammatically in Fig. 1. It is distinguished from a pivoted-pad bearing in that the pad of the latter is constructed so that it can pivot while in operation.

In common with other types of hydrodynamic bearings, the fixed-pad bearing depends for its operation upon the lubricant being drawn into a wedge-shaped space, thus producing pressure which counteracts the load and prevents contact between the sliding parts. Since the wedge action only takes place when the sliding surface moves in the direction in which the lubricant film converges, the simplest form of bearing, shown in Fig. 1, can only carry load for this direction of operation. If reversibility is desired, a combination of two or more pads with their surfaces sloping in opposite direction is required.

While most any pad profile, which gives convergence in the direction of motion to the lubricant film, may be used, this paper will treat only the most common type having a uniform slope from inlet to outlet, as illustrated in Fig. 1.

Fixed pads are sometimes used in multiple for straight-line slider bearings as shown in Fig. 2, and are frequently used in multiple for thrust bearings as shown in Fig. 3. In all cases the calculations are carried through on the basis of a single pad and the properties of the complete bearing found by combining these calculations in the proper manner.

Assumptions Involved

The methods used in this paper are based upon the work of Muskat, Morgan, and Meres[4] who have given solutions for the case of a pad of various proportions. These solutions and the fact that the fixed pad is easier to treat mathematically make it possible to present the curves for various pad proportions without the necessity of side-flow factors such as were required for journal bearings of various proportions in footnote 3. Several of the charts given here are similar to those published by the authors but have been extended to cover a wider range of conditions.

A detailed description of the many premises involved in obtaining the solutions is out of place for present purposes but may be found in reference 4 or in textbooks on the subject. One premise, however, should be mentioned. This is the assumption that the viscosity of the lubricant remains constant as it passes through the film. Although it is known that the viscosity varies with both temperature and pressure, the error made by assuming that it remains constant is usually small especially if the temperature rise is not large.

Since the film shape being considered here is continuously convergent from inlet to outlet, there is no cause for the formation of "negative pressures" similar to those which occur in journal bearings under certain circumstances and which require special methods of analysis.

Conditions

Viscosity of Lubricant. As all of the other quantities involved are given in English units, it is desirable that the viscosity of the lubricant be similarly expressed. The standard unit of viscosity (or absolute viscosity as it is often called) in the English system is the reyn which has the units[5] of lb sec/in^2. Fig. 4, which is a reproduction to a somewhat larger scale of viscosity-temperature Chart 1, see footnote 3, shows the viscosity expressed in reyns plotted against temperature for a series of typical SAE numbered motor oils.

Bearing-Characteristic Number. As was found to be the case for journal bearings, the equations required to solve fixed-pad-bearing problems are cumbersome to work with and calculations are most easily made by the use of bearing performance charts. Although such charts can be presented in many ways, plotting the various performance factors as functions of the bearing-characteristic number is probably the best method. This number is similar to the Sommerfeld number for journal bearings but contains somewhat different variables. The characteristic number for fixed-pad bearings will be referred to as K_f and is defined by the following dimensionless[6] group of variables

$$K_f = \frac{1}{m^2}\,\frac{\mu U}{PB}$$

When once this number has been determined for a given condition of operation, all of the operating characteristics become fixed.

In order to minimize the number of charts required, the various bearing-performance characteristics such as coefficient of friction, power loss, and so on, have been combined in dimensionless groups such as the coefficient-of-friction variable, f/m; the power-loss variable, $10^4H/PBLUm$; and so forth. The manner in which these quantities are used will be illustrated by sample problems.

Coefficient of Friction. Chart 1[7] shows the coefficient-of-friction variable f/m, plotted against K_f for various pad proportions L/B. Also shown are the running positions of the sliding surface and pad which correspond to the given K_f numbers, the quantities B and m being held constant.

As an example of the use of Chart 1, suppose it is desired to determine the coefficient of friction for a pad having the following conditions of operation

W = 3600 lb

U = 1200 ips

B = 3 in.

L = 3 in.

m = 0.001 in/in.

$\mu = 6 \times 10^{-6}$ reyns

[4] "The Lubrication of Plane Sliders of Finite Width," by M. Muskat, F. Morgan, and M. W. Meres, *Journal of Applied Physics*, vol. 11, 1940, p 208.

[5] Formulas for converting between various viscosity units will be found in footnote 3.

[6] In the paper on journal bearings[3] the characteristic number was not strictly dimensionless but had the units of sec/min. While this was done to allow the speed to be expressed in revolutions per minute instead of the less common revolutions per second, it gave rise to confusion. In this paper, speed will be expressed either in inches per second (ips) or in revolutions per second (rps).

[7] The co-ordinates of this plot are proportional to the arc hyperbolic sine.

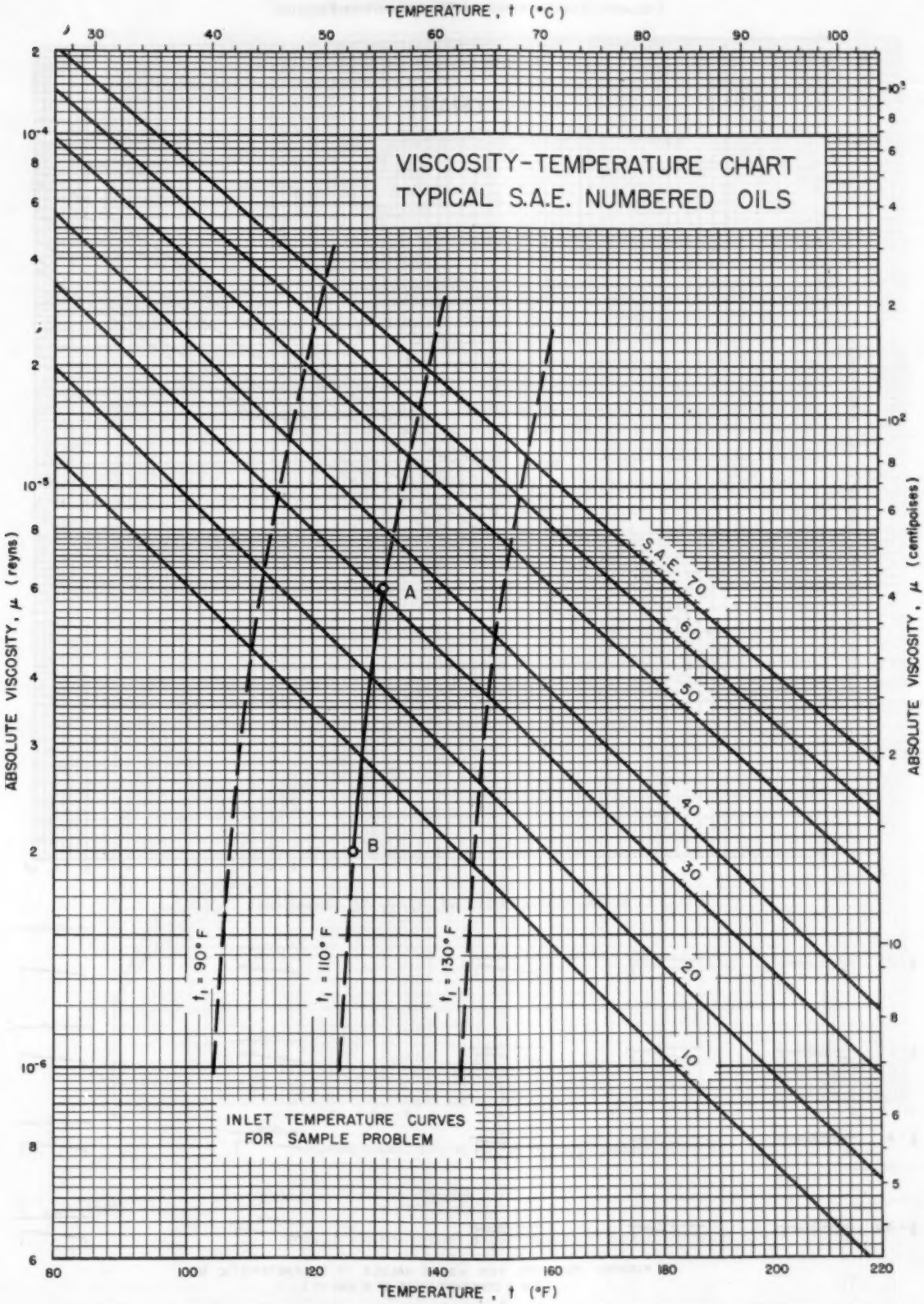

FIG. 4 VISCOSITY-TEMPERATURE CHART OF TYPICAL SAE NUMBERED OILS, SHOWING SOLUTION OF SAMPLE PROBLEM

CHART 1 FOR DETERMINING COEFFICIENT OF FRICTION

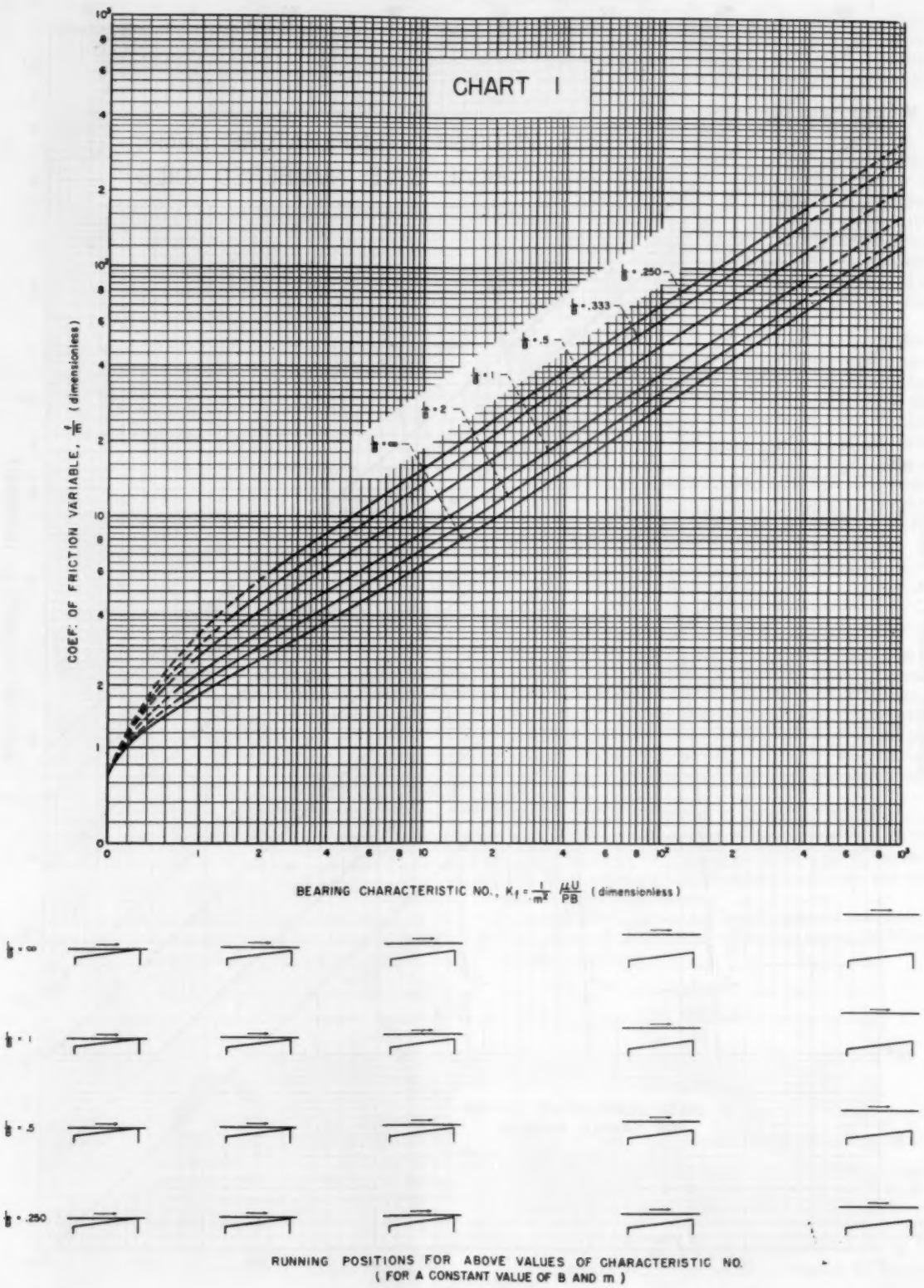

CHART 2 FOR DETERMINING POWER LOSS

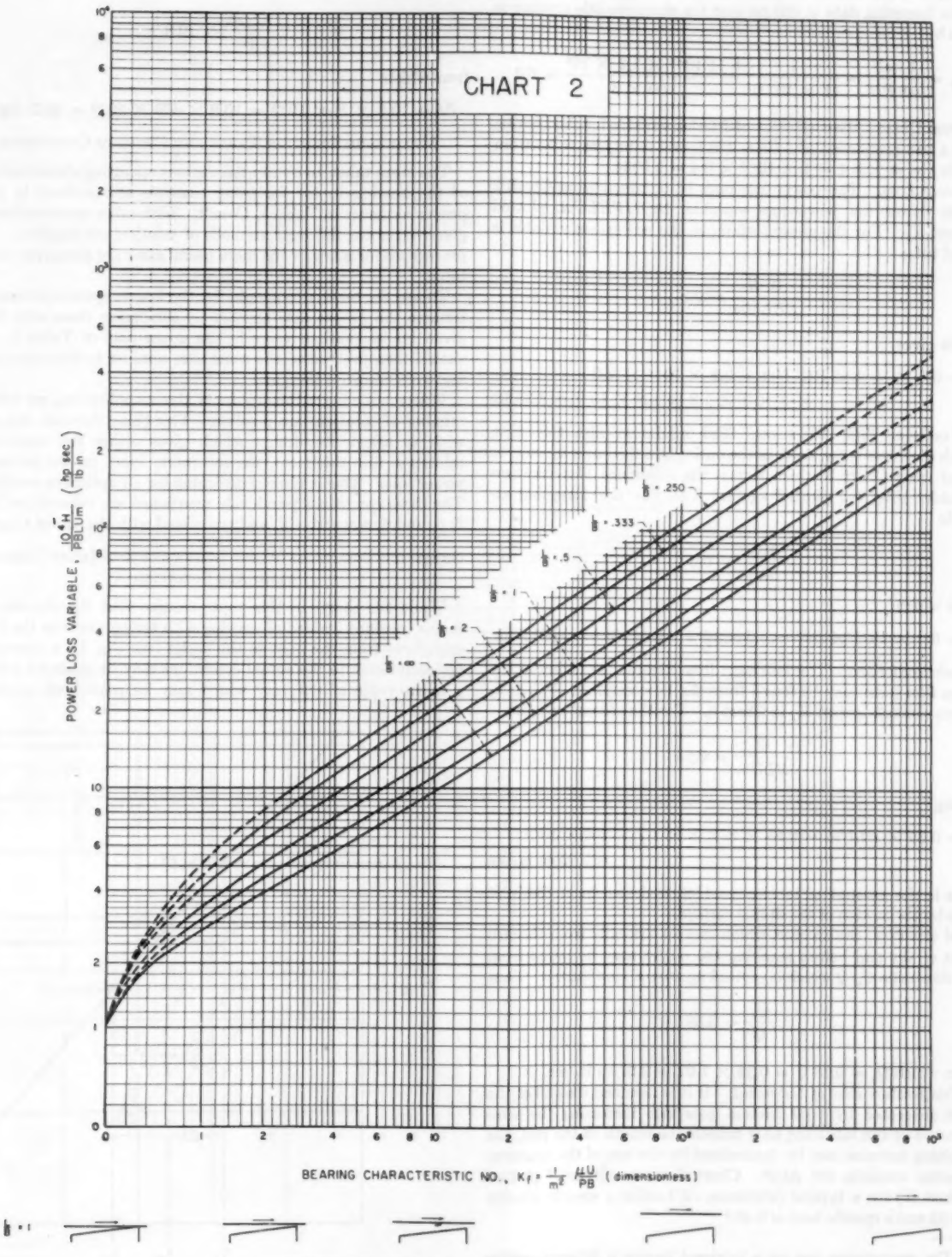

The load per unit of projected area, $P = W/BL$, on the basis of the foregoing data is 400 psi and the characteristic number is given by

$$K_f = \frac{1}{m^2}\frac{\mu U}{PB} = \frac{1}{(1 \times 10^{-3})^2}\frac{6 \times 10^{-6} \times 1.2 \times 10^3}{400 \times 3} = 6.0$$

From Chart 1 the coefficient-of-friction variable for this bearing with a pad proportion of $L/B = 1$ is found to be $f/m = 6.4$ from which $f = m \times 6.4 = 1 \times 10^{-3} \times 6.4 = 0.0064$.

Power Loss. The power loss may be obtained from Chart 2 which shows the power-loss variable, $10^4H/PBLUm$, plotted against K_f. For the present example, the power-loss variable is found to be

$$\frac{10^4H}{PBLUm} = 9.8$$

which gives

$$H = 9.8 \times 10^{-4} \times PBLUm = 9.8 \times 10^{-4} \times 400 \times 3 \times 3 \times 1.2 \times 10^3 \times 10^{-3} = 4.24 \text{ hp}$$

Minimum Film Thickness. The minimum film thickness, which of course is the same as the outlet film thickness h_2, may be found from Chart 3 which shows the minimum film-thickness variable, $10h_2/Bm$, plotted against K_f. For the foregoing example

$$\frac{10h_2}{Bm} = 6.6$$

from which

$$h_2 = 6.6 \times 10^{-1} \times Bm = 6.6 \times 10^{-1} \times 3 \times 10^{-3} = 0.00198 \text{ in.}$$

Lubricant Flow. The lubricant flow required to maintain the given film form may be found from the flow variable, $Q/BLUm$, shown plotted against K_f in Chart 5. For the present problem

$$\frac{Q}{BLUm} = 0.65$$

giving

$$Q = 0.65 \times BLUm = 0.65 \times 3 \times 3 \times 1.2 \times 10^3 \times 10^{-3} = 7.02 \text{ cu in/sec}$$

This is the amount of lubricant which is drawn in at the inlet edge by the motion of the sliding surface.

Of this flow, the amount which escapes laterally from the two sides of the pad before reaching the outlet may be found from the flow ratio Q_s/Q which is plotted against K_f in Chart 4. Thus

$$\frac{Q_s}{Q} = 0.38$$

from which $Q_s = 0.38\,Q = 0.38 \times 7.02 = 2.67$ cu in/sec.

Temperature Rise of Lubricant. If it is assumed that all of the heat generated by fluid friction goes into increasing the temperature of the lubricant as it travels the length of the pad, the resulting increase can be determined by the use of the temperature-rise variable, $10^3\,\Delta t/P$. Chart 6 shows $10^3\,\Delta t/P$ plotted against K_f for a typical petroleum oil having a specific gravity of 0.83 and a specific heat of 0.40.[8]

[8] The temperature rise for a lubricant having a different specific gravity and a different specific heat may be found by multiplying the temperature rise as computed from the chart by

$$\frac{0.332}{\text{Specific gravity} \times \text{specific heat}}$$

For the foregoing example

$$\frac{10^3\,\Delta t}{P} = 10.8$$

from which

$$\Delta t = 10.8 \times P \times 10^{-3} = 10.8 \times 400 \times 10^{-3} = 43.2 \text{ deg F}$$

Method-of-Solution Table and Optimum Conditions

The steps taken to obtain the various operating characteristics of the bearing in the foregoing example are outlined in their proper sequence in Table 1, Case 2. With other combinations of given variables, different methods of solution are required. The procedures for a few of the more useful cases are also given in the table.

To use the table, one should list the known quantities and determine the proper case number by comparing them with those given for the various cases in the upper part of Table 1. He should then proceed to the same case number in the main table and work from left to right.

When designing a bearing for a given application, an infinite number of solutions are possible. This being the case, one may wish to select the design which gives either the maximum-minimum film thickness, the maximum load, or the minimum power loss. This is termed designing for an optimum condition. The three conditions previously mentioned are covered in Cases 7, 5, and 6, respectively, and are solved with the aid of Chart 7.

Obtaining Solutions When Lubricant and Inlet Temperature Are Specified

While the charts in this paper assume that the viscosity remains constant instead of varying with temperature as the lubricant flows from the inlet to the outlet (see Fig. 5), a reasonable approximation to the actual conditions may be made by picking a mean value of viscosity which may be considered constant.

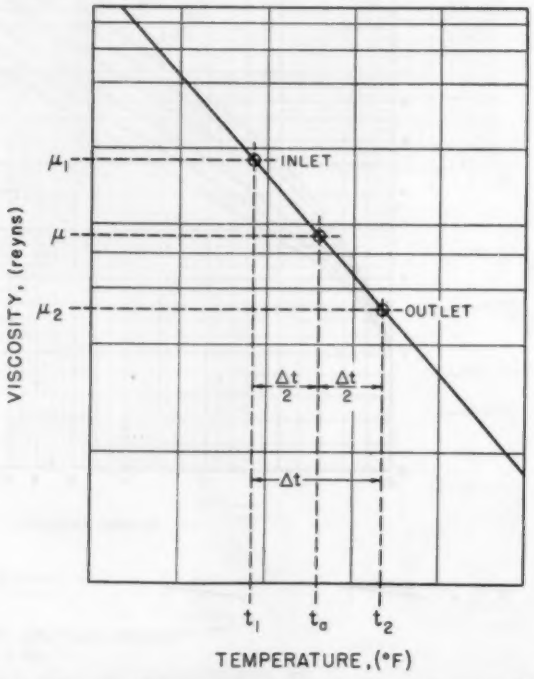

Fig. 5 Viscosity-Temperature Chart Showing Relation Between Viscosity μ and Average Temperature t_a

CHART 3 FOR DETERMINING MINIMUM FILM THICKNESS

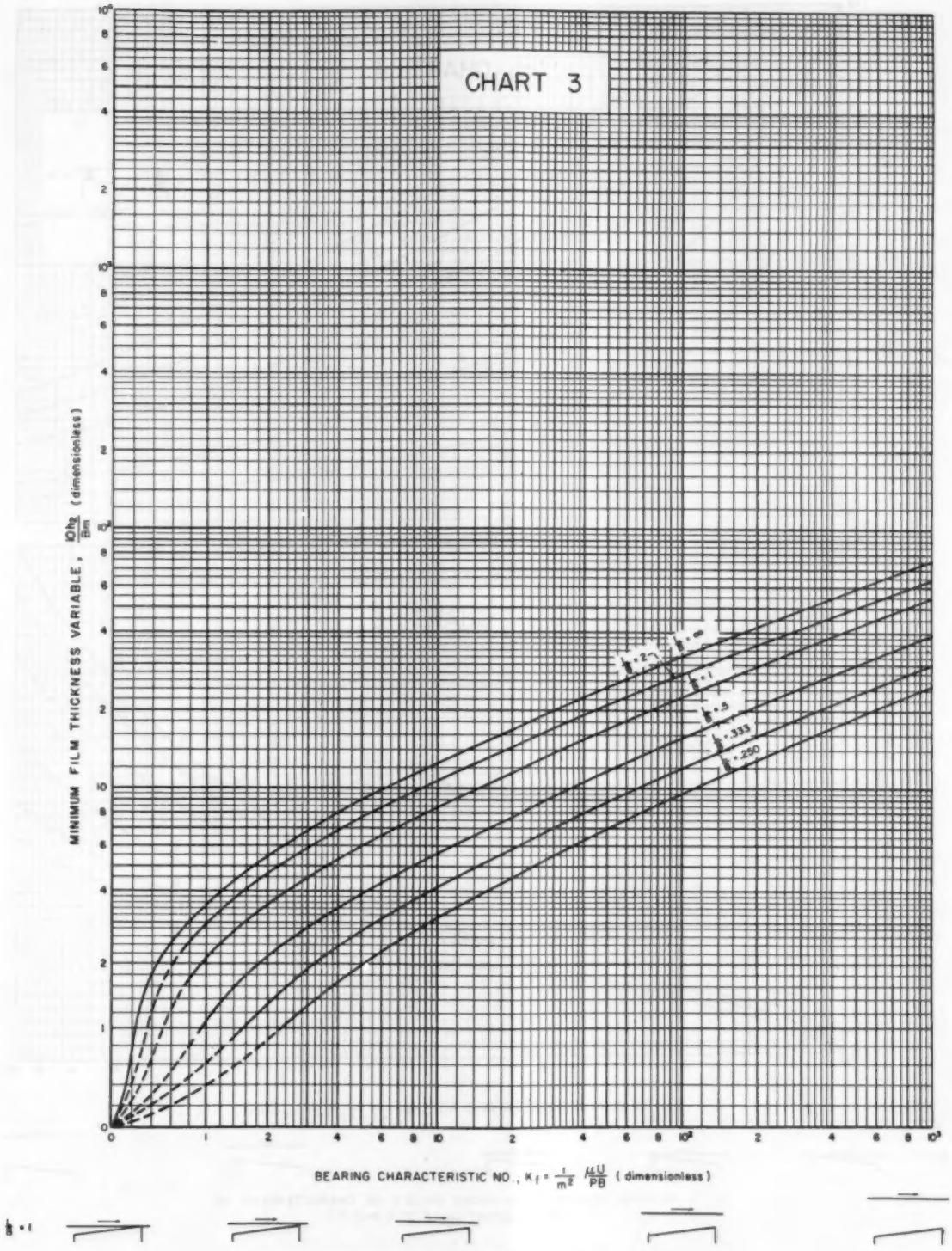

RUNNING POSITIONS FOR ABOVE VALUES OF CHARACTERISTIC NO.
(FOR A CONSTANT VALUE OF B AND m)

CHARTS 4 AND 5 FOR DETERMINING LUBRICANT FLOW

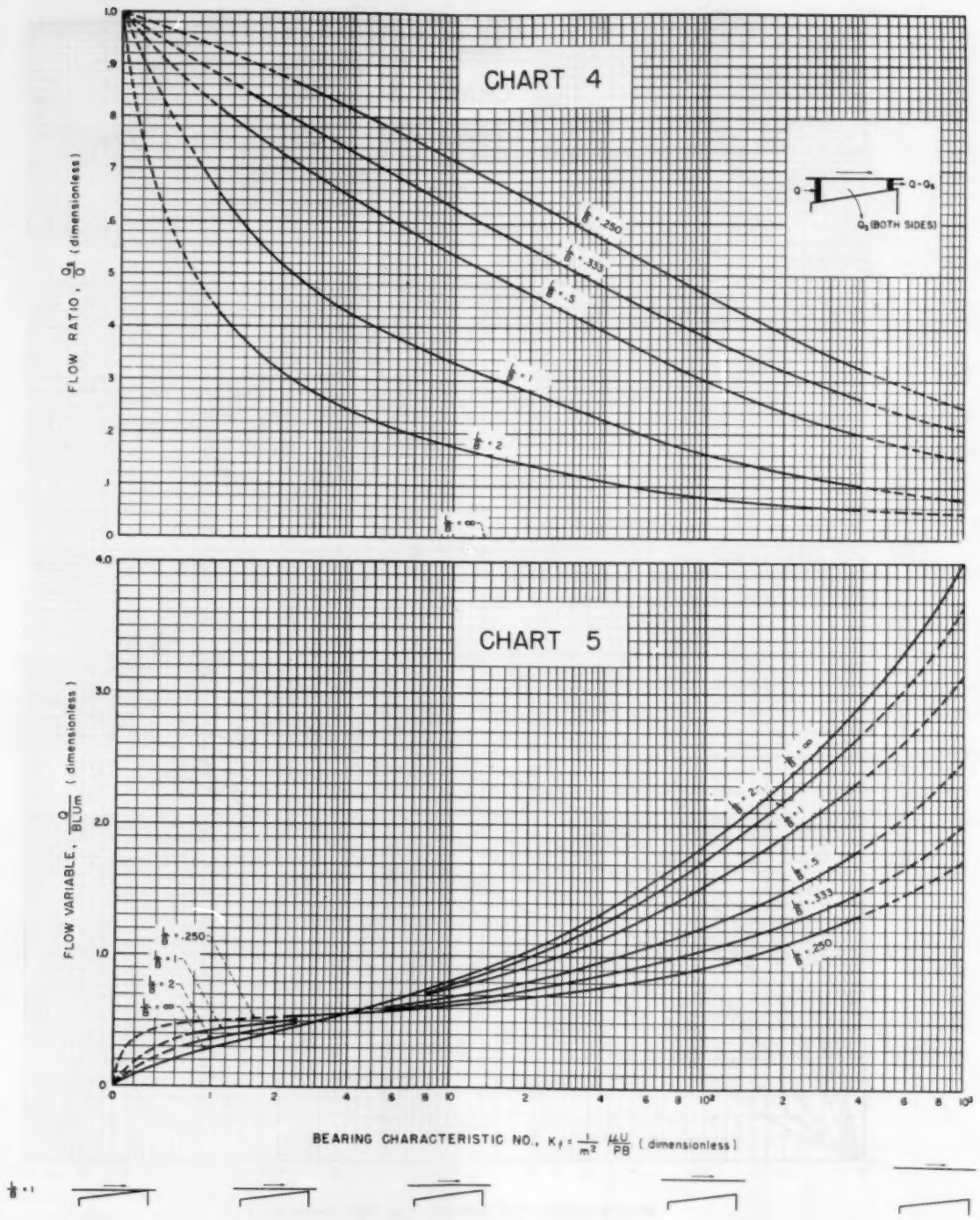

RUNNING POSITIONS FOR ABOVE VALUES OF CHARACTERISTIC NO.
(FOR A CONSTANT VALUE OF B AND m)

CHART 6 FOR DETERMINING FILM-TEMPERATURE RISE

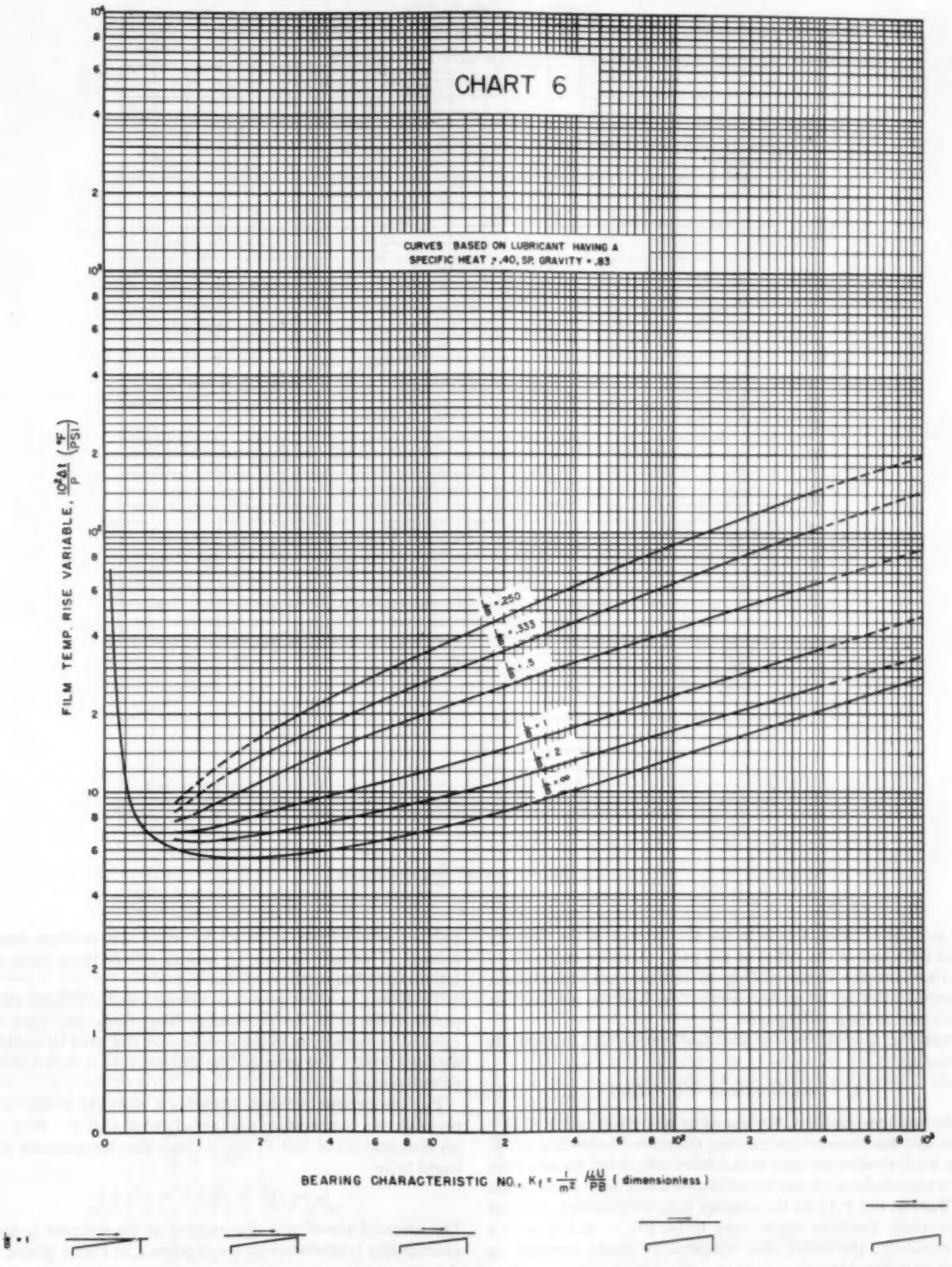

CHART 7 FOR DETERMINING VALUES OF $10h_2/Bm$ CORRESPONDING TO MAXIMUM LOAD, MAXIMUM-MINIMUM FILM THICKNESS, OR MINIMUM POWER LOSS FOR VARIOUS PAD PROPORTIONS

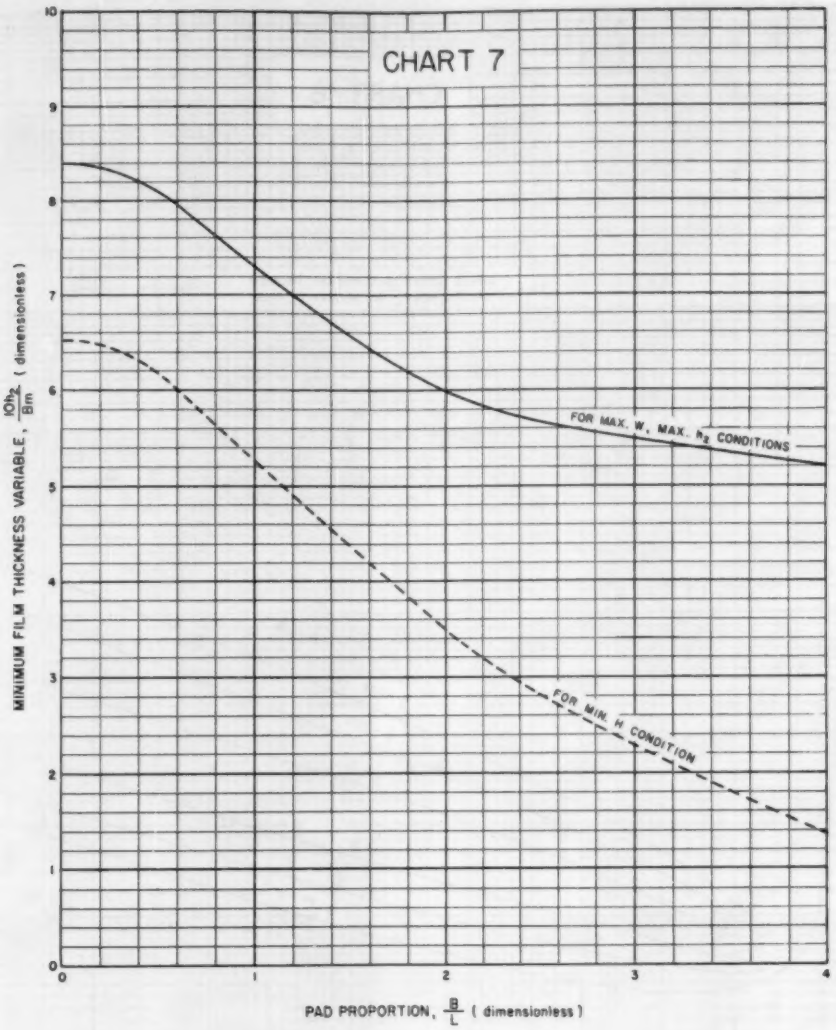

One method of doing this is to use the average of the viscosity at the inlet and at the outlet of the pad. Another method is to use the viscosity corresponding to the average temperature. Since the latter is the more conservative, it is the method that will be used in the present paper.

From Fig. 5 it will be seen that the average film temperature is given by

$$t_a = \text{avg film temp} = t_i + \Delta t/2 \quad [1]$$

In the previous problem, the viscosity was given as 6.0×10^{-6} reyns and the temperature rise was calculated to be 43.2 deg F. If an SAE 10 oil were used as the lubricant, it will be seen from Fig. 4 that such an oil has a viscosity of 6.0×10^{-6} reyns at 100 F. Taking 100 F to be the average film temperature, the inlet temperature therefore would have to be $100 - 43.2/2 = 78.4$ F. Similarly, the outlet film temperature would therefore be $100 + 43.2/2 = 121.6$ F.

If, on the other hand, the viscosity were not given, but it was specified that an SAE 10 oil was to be used and that it would be supplied at an inlet temperature of, say, 110 F, a temperature balance would have to be made before the problem could be solved. This may be done by making two or three check calculations and plotting the results on Fig. 4.

To do this, one first assumes a viscosity and calculates the temperature rise as in the previous problem (only that part of the calculation pertaining to the temperature rise need be carried out at this time). The average film temperature is then calculated from Equation [1].

For the present problem, choosing a viscosity of 6.0×10^{-6} reyns gives a temperature rise (as before) of 43.2 F. With an inlet temperature of 110 F, the average film temperature is then found to be

$$t_a = 110 + 43.2/2 = 131.6 \text{ F}$$

The assumed viscosity is then plotted as the ordinate μ, and the average film temperature as the abscissa t, in Fig. 4, giving point *A*.

Another value of viscosity, say, $\mu = 2.0 \times 10^{-6}$ reyns, is then assumed and the corresponding average film temperature calculated. These values are also plotted on Fig. 4, giving point *B*.

TABLE 1 METHOD OF SOLUTION FOR PROBLEMS ON FIXED-PAD BEARINGS

CASE NO.	GIVEN VARIABLES AND CONDITIONS									
	VARIABLES							CONDITIONS		
	W	U	B	L	m	h_2	μ	MAX. W	MIN. H	MAX. h_2
1	X	X	X	X	X	X		–	–	–
2	X	X	X	X	X		X	–	–	–
3		X	X	X	X	X	X	–	–	–
4	X		X	X	X	X	X	–	–	–
5		X	X	X		X	X	X	–	–
6	X	X	X	X		X		–	X	–
7	X	X	X	X			X	–	–	X

DETERMINE CASE NO. FROM ABOVE, THEN WORK FROM LEFT TO RIGHT IN TABLE BELOW.

CASE NO.	METHOD OF OBTAINING QUANTITIES LISTED BELOW										
	B	L	$\frac{L}{B}$	$\frac{10h_2}{Bm}$	K_f	W	P	m	h_2	μ	U
1	given	given	$\frac{L}{B}$	$\frac{10h_2}{Bm}$	from chart 3	given	$\frac{W}{BL}$	given	given	$\frac{PBm^2K_f}{U}$	given
2	"	"	"	from* chart 3	$\frac{1}{m^2}\frac{\mu U}{PB}$	"	"	"	$\left(\frac{10h_2}{Bm}\right)\frac{Bm}{10}$	given	"
3	"	"	"	$\frac{10h_2}{Bm}$	from chart 3	PBL	$\frac{\mu U}{m^2K_fB}$	"	given	"	"
4	"	"	"	"	"	given	$\frac{W}{BL}$	"	"	"	$\frac{PBm^2K_f}{\mu}$
5	"	"	"	from chart 7	"	PBL	$\frac{\mu U}{m^2K_fB}$ †	$\frac{10h_2}{B} \div \left(\frac{10h_2}{Bm}\right)$	"	"	given
6	"	"	"	"	"	given	$\frac{W}{BL}$	"	"	$\frac{PBm^2K_f}{U}$	"
7	"	"	"	"	"	"	"	$\sqrt{\frac{\mu U}{PBK_f}}$	$\left(\frac{10h_2}{Bm}\right)\frac{Bm}{10}$	given	"

CASE NO.	METHOD OF OBTAINING QUANTITIES LISTED BELOW (CONT'D)								
	$\frac{f}{m}$	f	$\frac{10^6H}{PBLUm}$	H	$\frac{Q}{BLUm}$	Q	Q_s	$\frac{10^2\Delta t}{P}$	Δt
1 to 7 inc.	from chart 1	$\left(\frac{f}{m}\right)\cdot m$	from chart 2	$\left(\frac{10^6H}{PBLUm}\right)\frac{PBLUm}{10^6}$	from chart 5	$\left(\frac{Q}{BLUm}\right)\cdot BLUm$	from chart 4	from chart 6	$\left(\frac{10^2\Delta t}{P}\right)\frac{P}{10^2}$

† Calculate m first

* Calculate K_f before entering chart 3

Drawing a line between points A and B and noting where it crosses the SAE 10 line shows that SAE 10 oil will satisfy the given conditions with a viscosity of 2.8×10^{-6} reyns and an average film temperature of 128.0 F.

Using 2.8×10^{-6} reyns for the viscosity and proceeding as in the previous problem gives the following results for the bearing when supplied with SAE 10 oil at an inlet temperature of 110 F

$$\Delta t = 36.0 \text{ deg F}$$
$$t_a = 128.0 \text{ F}$$
$$t_2 = 146.0 \text{ F}$$
$$\mu(\text{at } t = t_a) = 2.8 \times 10^{-6} \text{ reyns}$$
$$f = 0.0041$$
$$H = 2.72 \text{ hp}$$
$$h_2 = 0.0013 \text{ in.}$$
$$Q = 5.61 \text{ cu in/sec}$$
$$Q_s = 2.58 \text{ cu in/sec}$$

By extending the lines through A-B for additional assumed values of viscosity, operating conditions with other SAE oils are readily obtained. Since the average film temperature t_a for a given viscosity μ is found from Equation [1] by adding the inlet temperature to $\Delta t/2$ (which remains constant for a given μ), curves for various inlet temperatures are easily constructed if desired and appear as in Fig. 4.

The steps used to solve the second problem are outlined in Table 1A, Case 2A, which is seen to be a counterpart of Table 1, Case 2, but with the lubricant and inlet temperature given rather than the viscosity. The other cases of Table 1A are similarly related to those of Table 1.

Fixed-Pad Thrust Bearings

By arranging a series of pads in an annular configuration, one obtains a fixed-pad thrust bearing as shown in Fig. 3. From symmetry of construction, it will be seen that all pads will perform exactly alike and it is evident that the performance of the thrust

TABLE 1A METHOD OF SOLUTION FOR PROBLEMS ON FIXED-PAD BEARINGS WHERE LUBRICANT AND INLET TEMPERATURE ARE AMONG VARIABLES

CASE NO.	GIVEN VARIABLES AND CONDITIONS										
	VARIABLES								CONDITIONS		
	W	U	B	L	m	h_2	t_i	lubricant	MAX. W	MIN. t_i	MAX. h_2
1A	X	X	X	X	X	X	X		—	—	—
2A	X	X	X	X	X		X	X	—	—	—
3A		X	X	X	X	X	X	X	—	—	—
4A	X		X	X	X	X	X	X	—	—	—
5A		X	X	X		X	X	X	X	—	—
6A	X	X	X	X		X	X		—	X	—
7A	X	X	X	X			X	X	—	—	X

DETERMINE CASE NO FROM ABOVE THEN WORK FROM LEFT TO RIGHT IN TABLE BELOW.

CASE NO.	METHOD OF OBTAINING QUANTITIES LISTED BELOW														
	B	L	$\frac{L}{B}$	$\frac{10h_2}{Bm}$	K_f	W	P	m	h_2	$\frac{10^2\Delta t}{P}$	Δt	t_i	lubricant	μ	U
1A	given	given	$\frac{L}{B}$	$\frac{10h_2}{Bm}$	from chart 3	given	$\frac{W}{BL}$	given	given	from chart 6	$\left(\frac{10^2\Delta t}{P}\right)\cdot\frac{P}{10^2}$	given	see † note 1	$\frac{PBm^2K_f}{U}$	given
2A	"	"	"	from * chart 3	see note 2	"	"	"	$\left(\frac{10h_2}{Bm}\right)\cdot\frac{Bm}{10}$	"	"	"	given	see note 2	"
3A	"	"	"	$\frac{10h_2}{Bm}$	from chart 3	PBL	$\frac{\mu U}{Bm^2K_f}$ †	"	given	"	see note 4	"	"	see note 4	"
4A	"	"	"	"	"	given	$\frac{W}{BL}$	"	"	"	$\left(\frac{10^2\Delta t}{P}\right)\cdot\frac{P}{10^2}$	"	"	see note 5	$\frac{PBm^2K_f}{\mu}$
5A	"	"	"	from chart 7	"	PBL	$\frac{\mu U}{Bm^2K_f}$ †	$\frac{10h_2}{B}\div\left(\frac{10h_2}{Bm}\right)$	"	"	see note 4	"	"	see note 4	given
6A	"	"	"	"	"	given	$\frac{W}{BL}$	"	"	"	$\left(\frac{10^2\Delta t}{P}\right)\cdot\frac{P}{10^2}$	"	see † note 1	$\frac{PBm^2K_f}{U}$	"
7A	"	"	"	"	"	"	"	$\sqrt{\frac{\mu U}{PBK_f}}$ †	$\left(\frac{10h_2}{Bm}\right)\cdot\frac{Bm}{10}$	"	"	"	given	see note 5	"

CASE NO	METHOD OF OBTAINING QUANTITIES LISTED BELOW (CONT'D)						
	$\frac{f}{m}$	f	$\frac{10^4H}{PBLUm}$	H	$\frac{Q}{BLUm}$	Q	Q_s
1A to 7A inc.	from chart 1	$\left(\frac{f}{m}\right)\cdot m$	from chart 2	$\left(\frac{10^4H}{PBLUm}\right)\cdot\frac{PBLUm}{10^4}$	from chart 5	$\left(\frac{Q}{BLUm}\right)\cdot BLUm$	from chart 4

† Obtain Δt and μ first. * Obtained by entering chart 3 with K_f. † Obtain m first, then get μ by applying note 4.

Note 1: The proper lubricant is the one whose viscosity-temperature curve passes through the point given by μ and t on a visc.-temp. chart (such as Fig. 4) where the temp., t, equals $t_a = t_i + \Delta t/2$

Note 2: Assume a trial value of μ, calculate K_f where $K_f = \frac{1}{m^2}\frac{\mu U}{PB}$ Obtain $\left(\frac{10^2\Delta t}{P}\right)$ from chart 6, calculate Δt. Then follow procedure given in note 3 below to obtain correct μ Using correct μ, calculate K_f and complete solution of problem.

Note 3: Using a visc.-temp. chart, plot trial μ against temperature, t, where $t = t_a = t_i + \Delta t/2$. Several trial viscosities, (see, for example, points A and B, Fig. 4), may be necessary to arrive at the correct viscosity which is given by the intersection of the visc.-temp. curve for the given lubricant with the curve compromising the locus of the trial viscosities.

Note 4: Enter chart 6 with K_f, obtain $\left(\frac{10^2\Delta t}{P}\right)$. Assume a trial value of μ, calculate Δt from equation, $\Delta t = \frac{\mu U}{10^2Bm^2K_f}\cdot\left(\frac{10^2\Delta t}{P}\right)$. Then follow procedure given in note 3 above to obtain correct μ Using correct μ, calculate P from equation $P = \mu U/Bm^2K_f$.

Note 5: The viscosity, μ, is obtained from a visc.-temp. chart for the given lubricant. Enter the chart with the temperature, t, equal to t_a where $t_a = t_i + \Delta t/2$

bearing as a unit can be determined from an analysis of any individual pad. Although the pads employed on thrust bearings are usually sector-shaped, and although the motion of the runner is rotational, the only complete solutions which are presently available are those given, herewith, for rectangular pads with straight-line sliding motion.

In the absence of a more exact analysis, therefore, it will be assumed that the solutions for sector-shaped thrust-bearing pads can be approximated by those for rectangular pads with the speed, slope, and pad length B being measured at the average radius of the pads.

To relate the individual pads to the complete bearing, the following equations are necessary

$$W = \frac{W_T}{n} \quad [2]$$

$$L = R_2 - R_1 \quad [3]$$

$$B = \frac{\pi(R_1 + R_2)k}{n} \quad [4]$$

$$P = \frac{W}{BL} \quad [5]$$

$$k = \frac{n(R_2 - R_1)}{\pi(L/B)(R_1 + R_2)} \quad [6]$$

$$U = \pi(R_1 + R_2)N \quad [7]$$

where W_T is the total load, W the load per pad, n the number of pads, and k the proportion of the circumference occupied by pads.

To illustrate the manner in which the calculations are carried out, let it be required to design the bearing with the following information given, for the optimum condition of maximum-minimum film thickness

$W_T = 12{,}000$ lb
$R_1 = 2$ in.
$R_2 = 4$ in.
$N = 30$ rps (1800 rpm)
$n = 6$
$L/B = 1$
SAE 10 oil
$t_1 = 100$ F

Substituting in Equations [2], [3], [5], [7] gives the following values: $W = 2000$ lb; $L = 2$ in. $= B$; $P = 500$ psi, and $U = 180\pi$ ips. The problem can now be treated on the basis of a single pad, using Case 7A of Table 1A. Proceeding as outlined in the table gives the following results for each pad

$10\,h_2/Bm = 7.3$	$h_2 = 6.65 \times 10^{-4}$ in.
$K_f = 7.5$	$f = 3.33 \times 10^{-3}$
$\Delta t = 57.5$ F	$H = 0.578$ hp
$t_a = 128.8$ F	$Q = 0.710$ cu in/sec
μ(at $t = t_a$) $= 2.75 \times 10^{-6}$ reyns	$Q_s = 0.254$ cu in/sec
$m = 4.56 \times 10^{-4}$ in/in.	

The corresponding values for the complete bearing are exactly the same as those for the individual pads except for the power loss and the flow. Thus the power loss for the complete bearing is given by

$$H(\text{complete bearing}) = nH(\text{pad}) = 6 \times 0.578 = 3.47 \text{ hp}$$

The flow for the complete bearing may or may not have any clear meaning depending upon the construction of the bearing. For example, if all of the inlet spaces are supplied in parallel from the same source, and if the flow from the outlet spaces is carried away without being drawn into the adjacent inlets, the total flow through the bearing will be given by

$$Q(\text{complete bearing}) = nQ(\text{pad}) = 6 \times 0.710 = 4.26 \text{ cu in/sec}$$

If the bearing is not designed so that the flow is controlled as in the previous example, considerable recirculation between the different pads will take place and little meaning can be attached to the concept of flow for the complete bearing. At the same time, the temperatures throughout the bearing may be greatly upset, thus introducing considerable error into the calculations.

Agreement Between Theory and Test

While many tests have been published on fixed-pad thrust bearings, much of the information is either too incomplete or too inaccurate to enable satisfactory comparisons to be made with theoretical predictions. Most of the data are concerned with the coefficient of friction or the power loss and the authors were unable to find any usable published results on film thicknesses. Fig. 6 shows the power-loss variable computed from the experimental data given by Linn and Sheppard[9] compared with the theoretical power-loss variable as calculated by the methods given here.

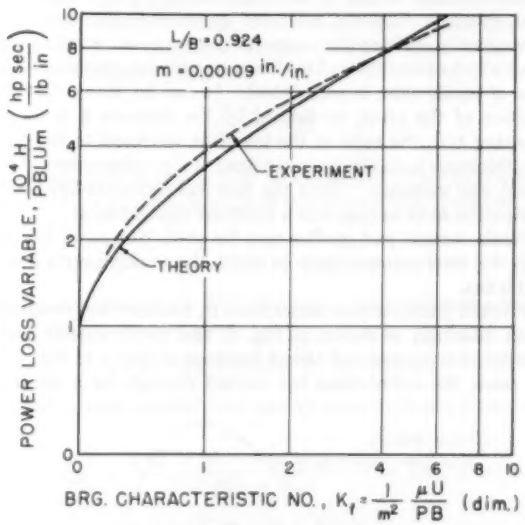

Fig. 6 Comparison Between Theoretical and Experimental Power-Loss Variables for Fixed-Pad Bearing

While better agreement could probably have been obtained if more accurate temperature data had been available, a comparison of the curves shows a satisfactory correlation between theory and experiment, in so far as the power loss is concerned. A better check, however, also would include a comparison of the minimum film thicknesses.

PART 2 PIVOTED-PAD BEARINGS

Introduction

Most of the introductory remarks on fixed-pad bearings, in Part 1, are equally applicable to pivoted-pad bearings. In fact, both types of bearings can be treated by the same analysis, but this is done at the expense of additional complication in the case of bearings of the pivoted-pad type. The latter are more con-

[9] "Thrust Bearings," by F. C. Linn and R. Sheppard, Trans. ASME, vol. 60, 1938, p. 245.

veniently handled by the analysis about to be described rather than by that already discussed for fixed-pad bearings. The present treatment also employs charts and method-of-solution tables and those that are presented here yield the results to be expected on the basis of what is generally regarded to be the most usable theory.

Nomenclature

In addition to the nomenclature which was given in Part 1, the following quantities will be used in the discussion on pivoted-pad bearings (see also Fig. 7):

$\mathfrak{x}$ = distance from inlet edge of pad to pivot, in.
K = performance number = $\mu U/PB$, dimensionless

Types of Pivoted-Pad Bearings

The simplest form of pivoted-pad bearing provides only for straight-line motion and consists of a flat surface sliding over a pivoted pad as shown diagrammatically in Fig. 7. If the pad is assumed to be in equilibrium under a given set of operating conditions, any change in these conditions, such as a change in load, speed, or viscosity, will alter the pressure distribution, thus momentarily shifting the center of pressure and creating a moment which causes the pad to change its inclination until a new position of equilibrium is established. It can be shown that if the position of the pivot, as defined by the distance $\mathfrak{x}$, is fixed by choosing $\mathfrak{x}/B$, the ratio of the inlet-film thickness to the outlet-film thickness h_1/h_2 also becomes fixed and is independent of load, speed, and viscosity. Thus the pad will automatically alter its inclination so as to maintain a constant value of h_1/h_2.

While various pad profiles may be used, this paper will treat only the most common type in which the working surface of the pad is flat.

Pivoted pads are sometimes used in multiple for straight-line slider bearings, as shown in Fig. 8, and are frequently used in multiple for pivoted-pad thrust bearings as shown in Fig. 9. In all cases, the calculations are carried through for a single pad

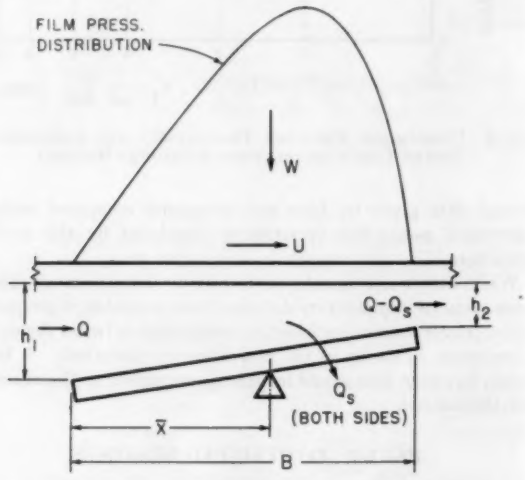

Fig. 7 Diagrammatic Sketch of Pivoted-Pad Bearing

Fig. 8 Diagrammatic Sketch of Multiple Pivoted-Pad Bearing

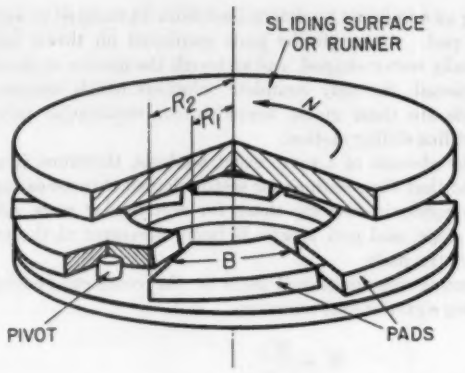

Fig. 9 Diagrammatic Sketch of Pivoted-Pad Thrust Bearing

and the properties for the complete bearing found by combining these calculations in the proper manner.

Normally, a pivoted pad will only carry load if the pivot is placed somewhere between the center of the pad and the outlet edge (i.e., $\mathfrak{x}/B$ is between 0.5 and 1.0). With the pivot so placed, the pad therefore can only carry load for one direction of rotation. More will be said on this point later.

Assumptions Involved

The methods used in this paper are based on the solutions given by Muskat, Morgan, and Meres[4] for the case of a rectangular pivoted pad of various proportions. Since the solutions permit pads of various L/B ratios (length perpendicular to motion/length parallel to motion) to be treated directly, side-flow factors such as were used in footnote 3 for journal bearings are not required.

The remaining assumptions, which are important in interpreting the results of calculations, are the same as those for the fixed-pad bearing and are discussed in Part 1. However, more will be mentioned later in connection with the effect of variation of viscosity in the pivoted-pad bearing.

Viscosity of Lubricant. See similar topic under Part 1.

Bearing-Performance Number

The equations, upon which the analysis of pivoted-pad bearings is based, are the same as those for fixed-pad bearings with the exception that a relation, which takes account of moments about the pivot, must be added. This prevents the choice of a convenient bearing (characteristic) number. However, if one prescribes the position of the pivot (i.e., prescribes $\mathfrak{x}/B$) or if the position of the pivot is known in advance, the various bearing-performance characteristics can be determined from a series of performance variables which become fixed once the pivot position is established.

The performance variables for pivoted pads are similar to the coefficient-of-friction variable, the power-loss variable, the minimum-film-thickness variable, and the flow variable for fixed-pad bearings, except that they contain the quantity $\sqrt{K}$, in place of the slope m, and are plotted against the pivot position factor $\mathfrak{x}/B$. The flow-ratio and the temperature-rise variables are also plotted against $\mathfrak{x}/B$ but do not contain $\sqrt{K}$.

The letter K, which has been chosen in honor of the pivoted-pad-bearing pioneer, Albert Kingsbury, represents the group of variables, $\mu U/PB$, and will be referred to as the bearing-performance number. The characteristic number for fixed-pad bearings K_f is thus seen to be related to the performance number K, by the expression $K_f = (1/m^2)\mu U/PB = K/m^2$.

Since the variables for coefficient of friction, power loss, mini-

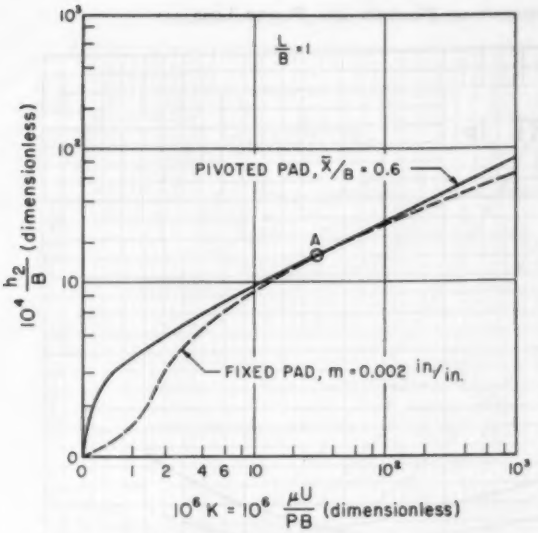

FIG. 10 COMPARISON BETWEEN FIXED-PAD AND PIVOTED-PAD BEARINGS ON BASIS OF MINIMUM FILM THICKNESS

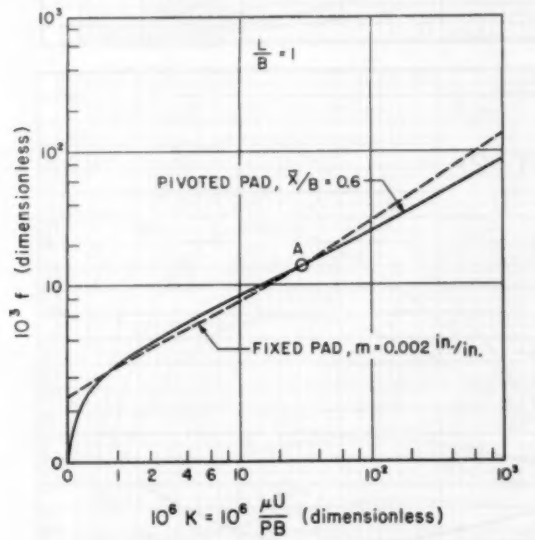

FIG. 11 COMPARISON BETWEEN FIXED-PAD AND PIVOTED-PAD BEARINGS ON BASIS OF COEFFICIENT OF FRICTION

mum film thickness, slope, and flow all become fixed as soon as the pivot position is established, and since each contains the quantity $\sqrt{\bar{K}}$, new variables containing the coefficient of friction, the power loss, the minimum film thickness, the slope, and the flow can all be expressed in terms of the performance number K. (As an example, see Figs. 10 and 11 where $10^3 f$ and $10^4 h_2/B$ are plotted against $10^6 K$ for a pivoted-pad bearing.)

Since the temperature-rise variable does not contain K (the same is true for Q_s/Q), the temperature rise depends only on the pivot position and the unit pressure P. This is a rather unique and useful relation.

ILLUSTRATIVE PROBLEM

As was pointed out in Part 1, two general classes of problems are possible. These differ only in the manner in which the data relative to the lubricant are given. In one case it is the viscosity which is either given or to be found and in the other case it is the lubricant and its inlet temperature. The former case, which is the simpler, is primarily of academic interest and is useful for study and instructional purposes. The latter case is the one usually encountered in practice. The following problem will be of this type.

To illustrate the method by which the charts are used, let it be required to determine the operating characteristics for a pivoted pad having the following information given

$$W = 36{,}000 \text{ lb}$$
$$U = 1200 \text{ in/sec}$$
$$B = 3 \text{ in.}$$
$$L = 3 \text{ in.}$$
$$\bar{x}/B = 0.55$$
$$t_1 = 110 \text{ F}$$
$$\text{Lubricant} = \text{SAE 10 oil}$$

From inspection, $L/B = 1$ and $P = W/BL = 36{,}000/3 \times 3 = 400$ psi. Entering Chart 7P, which shows the temperature-rise variable $\Delta t/P$, plotted against the pivot position $\bar{x}/B$, with $\bar{x}/B = 0.55$ and $L/B = 1$ gives

$$\frac{\Delta t}{P} = 0.22$$

from which $\Delta t = 0.22P = 0.22 \times 400 = 88.0$ F (see footnote 8).

The average film temperature is then found from Equation [1], Part 1, to be

$$t_a = t_1 + \Delta t/2 = 110 + 88.0/2 = 154.0 \text{ F}$$

The viscosity which SAE 10 oil has at this temperature is now obtained from Fig. 4 which gives

$$\mu \text{ (at } t = t_a) = 1.65 \times 10^{-6} \text{ reyns}$$

The performance number may now be computed and is found to be

$$K = \frac{\mu U}{PB} = \frac{1.65 \times 10^{-6} \times 1.20 \times 10^3}{400 \times 3} = 1.65 \times 10^{-6}$$

and

$$\sqrt{\bar{K}} = 1.29 \times 10^{-3}$$

The minimum film thickness can now be obtained from Chart 4P which shows the minimum film-thickness variable $h_2/B\sqrt{\bar{K}}$, plotted against $\bar{x}/B$. For the present problem

$$\frac{h_2}{B\sqrt{\bar{K}}} = 0.240$$

from which

$$h_2 = 0.240 \times B\sqrt{\bar{K}} = 0.240 \times 3 \times 1.29 \times 10^{-3} = 0.00093 \text{ in.}$$

The coefficient of friction can next be found from Chart 1P which shows the coefficient of friction variable $f/\sqrt{\bar{K}}$, plotted against $\bar{x}/B$. This gives

$$\frac{f}{\sqrt{\bar{K}}} = 3.5$$

which yields

$$f = 3.5\sqrt{\bar{K}} = 3.5 \times 1.29 \times 10^{-3} = 0.0045$$

To get the power loss, Chart 2P, which shows the power-loss variable, $10^4 H/PBLU\sqrt{\bar{K}}$, plotted against $\bar{x}/B$, is used. For the problem being solved

$$\frac{10^4 H}{PBLU\sqrt{\bar{K}}} = 5.4$$

CHARTS 1P AND 2P FOR DETERMINING COEFFICIENT OF FRICTION AND POWER LOSS

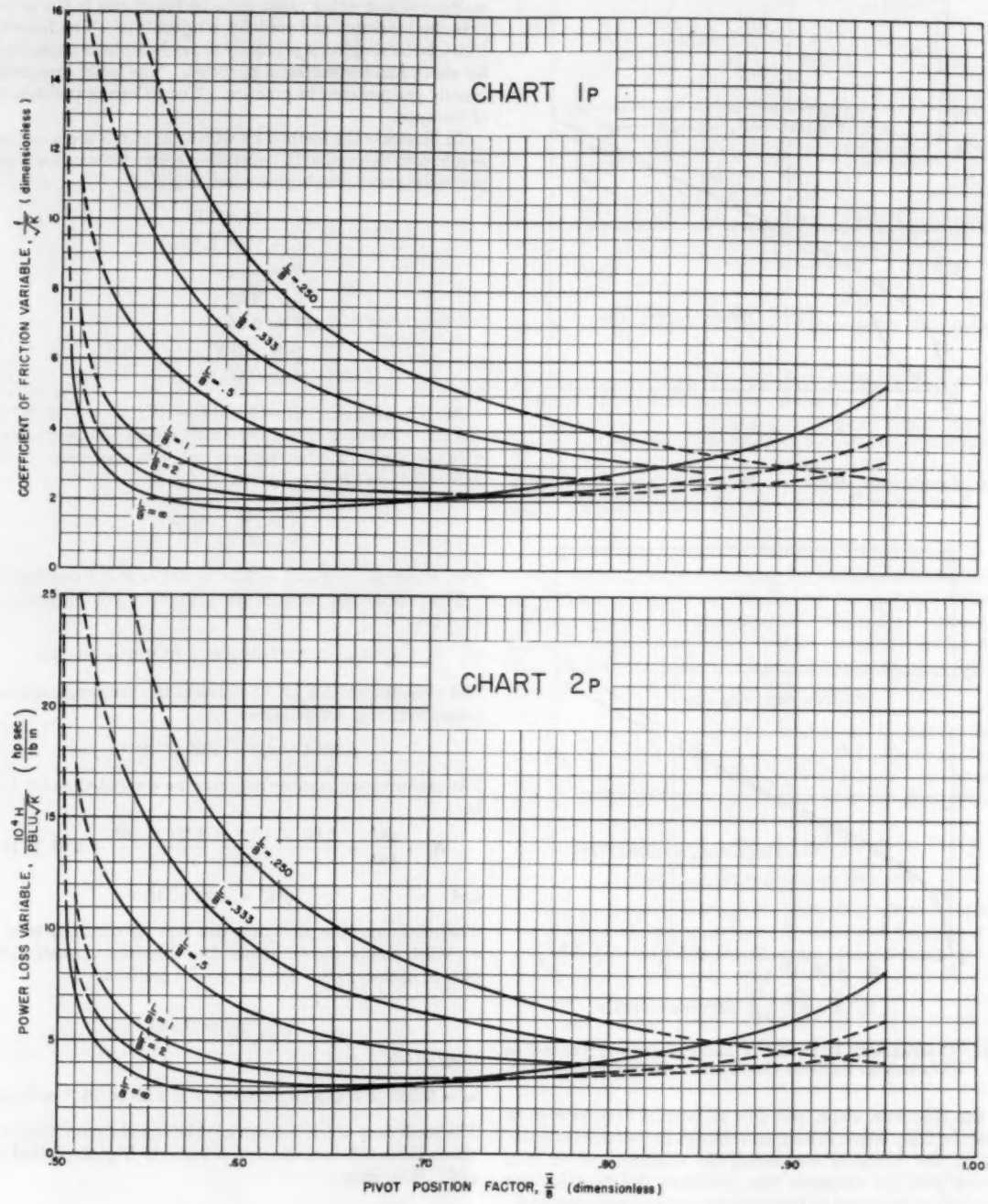

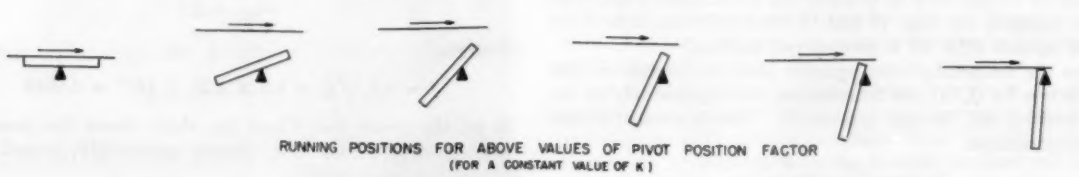

RUNNING POSITIONS FOR ABOVE VALUES OF PIVOT POSITION FACTOR
(FOR A CONSTANT VALUE OF K)

CHARTS 3P AND 4P FOR DETERMINING SLOPE OF TILTING PAD AND MINIMUM FILM THICKNESS

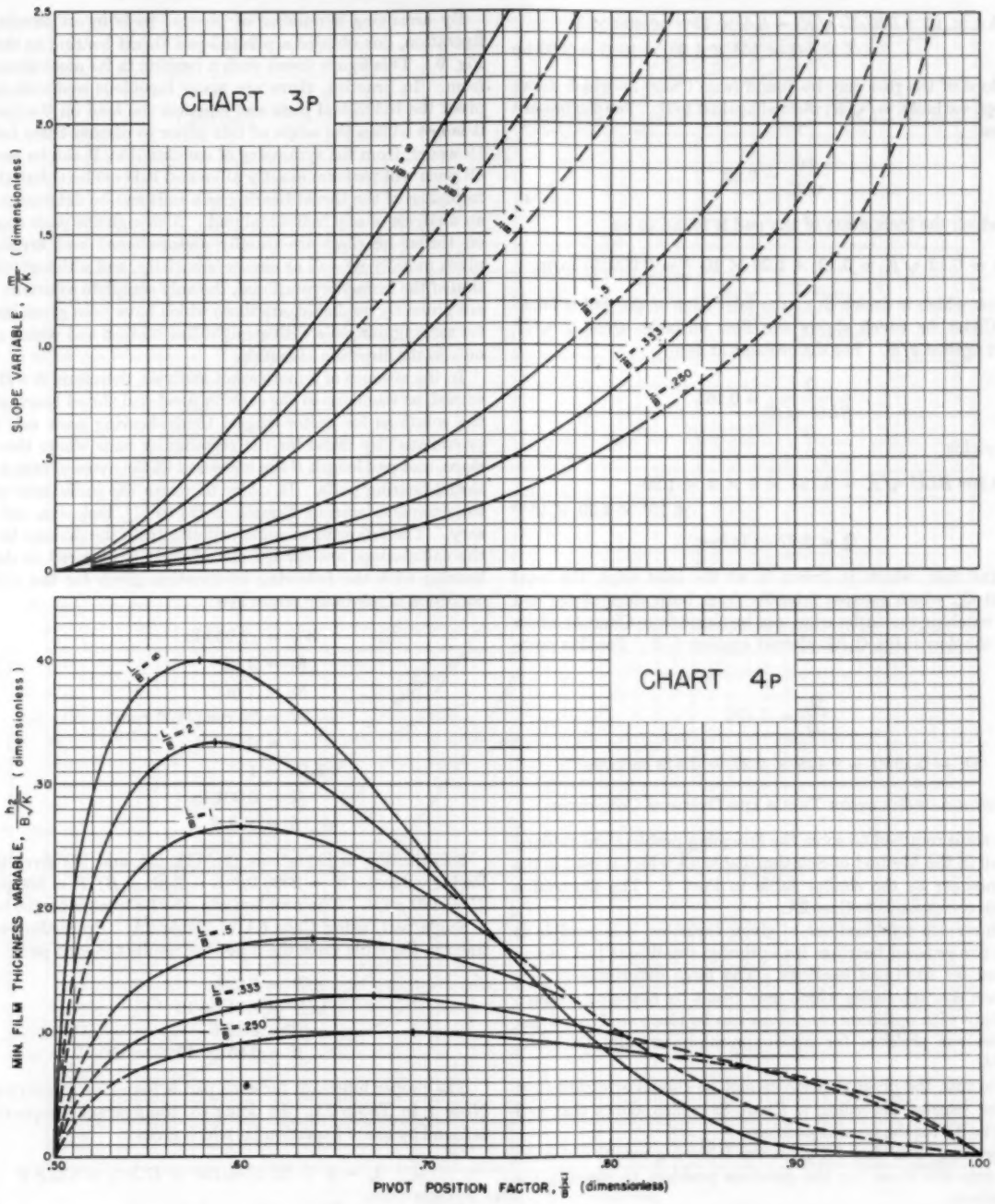

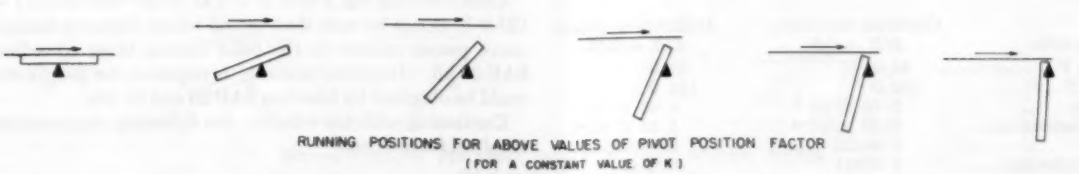

RUNNING POSITIONS FOR ABOVE VALUES OF PIVOT POSITION FACTOR
(FOR A CONSTANT VALUE OF K)

which may be solved to give

$$H = 5.4 \times 10^{-4}\, PBLU\sqrt{K} = 5.4 \times 10^{-4} \times 400 \times 3 \times 3 \times 1.2 \times 10^{3} \times 1.29 \times 10^{-3} = 3.00 \text{ hp}$$

The slope of the pad may be found from Chart 3P which shows the slope variable, $m/\sqrt{K}$, plotted against x/B. For the present problem

$$\frac{m}{\sqrt{K}} = 0.12$$

from which the inclination of the pad is found to be

$$m = 0.12\sqrt{K} = 0.12 \times 1.29 \times 10^{-3} = 0.000154 \text{ in/in.}$$

The flow which is drawn in at the inlet edge of the pad is found from Chart 6P which shows the flow variable, $Q/BLU\sqrt{K}$, plotted against x/B. For the problem at hand

$$\frac{Q}{BLU\sqrt{K}} = 0.164$$

which yields

$$Q = 0.164\, BLU\sqrt{K} = 0.164 \times 3 \times 3 \times 1.20 \times 10^{3} \times 1.29 \times 10^{-3}$$

or

$$Q = 2.27 \text{ cu in/sec}$$

Of the flow, which is drawn in at the inlet edge, the total amount Q_s, which escapes laterally from both sides of the pad before reaching the outlet edge, can be found from Chart 5P which shows the flow ratio, Q_s/Q, plotted against x/B. For this problem

$$\frac{Q_s}{Q} = 0.195$$

and

$$Q_s = 0.195Q = 0.195 \times 2.27 = 0.442 \text{ cu in/sec}$$

Method-of-Solution Table and Optimum Conditions

The steps required to solve the foregoing problem are outlined in detail in the Method-of-Solution Table 2A which is used in the same manner as the similar table in Part 1. The illustrative problem corresponds to Case 2A.

With certain combinations of given variables, it is possible to design pivoted-pad bearings for optimum conditions just as was the case for fixed-pad bearings. The large differences in performance characteristics which may result by changing a design to comply with optimum conditions can be illustrated by solving the previous problem for maximum-minimum film thickness, Case 7A.

To do this, the pivot position cannot be chosen arbitrarily but must be selected according to Chart 8P which shows that x/B should be 0.6 for the present problem.

Proceeding as in Case 7A gives the following results which are listed opposite those for the previous problem to simplify the comparison:

Variable	Optimum condition $x/B = 0.6$	Arbitrary condition $x/B = 0.55$
Δt, deg F	44.0	88.0
t_a, deg F	132.0	154.0
μ, reyns	2.60×10^{-6}	1.65×10^{-6}
K, dimensionless	2.60×10^{-6}	1.65×10^{-6}
h_2, in.	0.00128	0.000925
f, dimensionless	0.00411	0.0045
H, hp	2.71	3.00
m, in. per in.	0.000564	0.000154
Q, cu in/sec	4.46	2.27
Q_s, cu in/sec	1.59	0.442

Pivoted-Pad Thrust Bearings

By arranging a number of pivoted pads in an annular configuration, one obtains a pivoted-pad thrust bearing as shown in Fig. 9. This figure shows such a bearing in its most elementary form. In practice, there are many ingenious methods used to pivot the individual pads and equalize the load on the pads but it is not within the scope of this paper to discuss these features. However, from the symmetry of construction, it can be seen that all pads will perform exactly alike and it is evident that the performance of the thrust bearing as a unit can be determined from an analysis of any individual pad. Although the pads employed on thrust bearings are usually sector-shaped and arranged to pivot radially as well as circumferentially, and although the motion of the runner is rotational, the only complete solutions, which are presently available, are those which have been given herewith for rectangular pads with straight-line motion and which can tilt only in the direction of motion.

In the absence of a more exact analysis, therefore, it will be assumed, as was done in the case for fixed-pad thrust bearings, that the solutions for sector-shaped thrust-bearing pads can be approximated by those for the rectangular pads where the speed, slope, and pad length B are measured at the average radius of the thrust-bearing pads. In order to relate the individual pads to the complete bearing, Equations [2] to [7], inclusive, are necessary. The following example will illustrate the manner in which the calculations are carried out when it is required to design a bearing with the following information given for the optimum condition of minimum power loss

$$W_T = 12{,}000 \text{ lb}$$
$$R_1 = 2 \text{ in.}$$
$$R_2 = 4 \text{ in.}$$
$$N = 30 \text{ rps (1800 rpm)}$$
$$n = 6$$
$$L/B = 1$$
$$h_2 = 0.001 \text{ in.}$$
$$t_1 = 100 \text{ F}$$

Substituting in Equations [2], [3], [5], and [7] gives the following values: $W = 2000$ lb; $L = 2$ in. $= B$; $P = 500$ psi, and $U = 180\pi$ ips. The problem can now be treated on the basis of a single pad, using Case 6A of Table 2A. Proceeding as outlined in the table gives the following results for each pad

$$x/B = 0.622$$
$$\sqrt{K} = 1.91 \times 10^{-3}$$
$$\Delta t = 47.5 \text{ F}$$
$$\mu = 6.45 \times 10^{-6} \text{ reyns}$$

The proper lubricant for each pad is found by complying with Note 1 in Table 2A. In doing so, the average temperature t_a is found by use of Equation [1] which gives

$$t_a = t_1 + \Delta t/2 = 100 + 47.5/2 = 123.8 \text{ F}$$

Upon entering Fig. 4 with $\mu = 6.45 \times 10^{-6}$ reyns and $t = t_a = 123.8$ F, it can be seen that the oil whose viscosity-temperature curve passes nearest to the point having those co-ordinates is SAE 30 oil. If greater accuracy is required, the proper viscosity could be obtained by blending SAE 20 and 30 oils.

Continuing with the solution, the following characteristics are obtained for each pad

$$f = 0.00458$$
$$H = 0.786 \text{ hp}$$
$$m = 0.936 \times 10^{-3} \text{ in/in.}$$

CHARTS 5P AND 6P FOR DETERMINING LUBRICANT FLOW

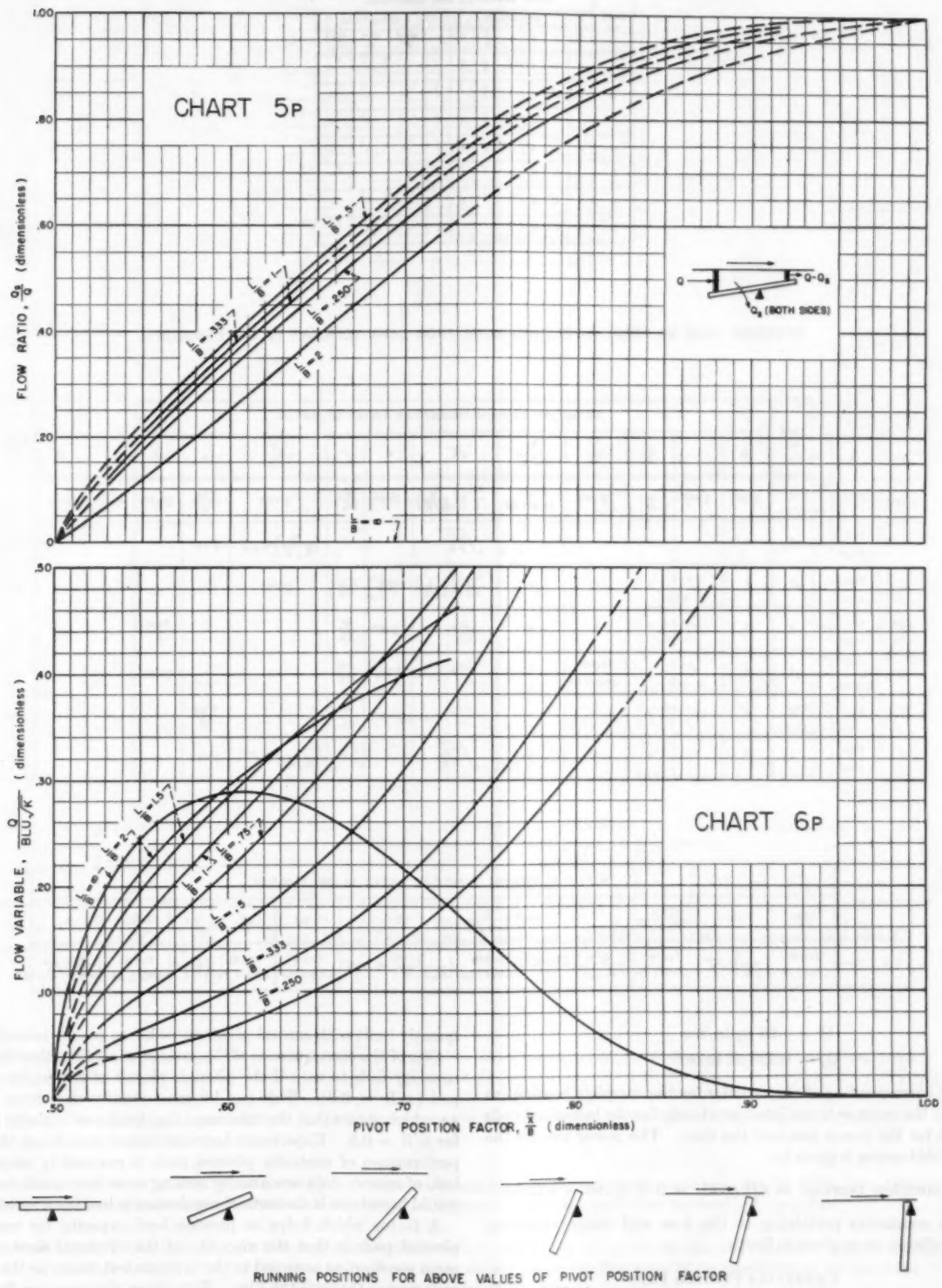

RUNNING POSITIONS FOR ABOVE VALUES OF PIVOT POSITION FACTOR
(FOR A CONSTANT VALUE OF K)

TABLE 2 METHOD OF SOLUTION FOR PROBLEMS ON PIVOTED-PAD BEARINGS

CASE NO.	GIVEN VARIABLES AND CONDITIONS									
	VARIABLES							CONDITIONS		
	W	U	B'	L	$\frac{\bar{x}}{B}$	h_2	μ	MAX. W	MIN. H	MAX. h_2
1	X	X	X	X	X	X		–	–	–
2	X	X	X	X	X		X	–	–	–
3		X	X	X	X	X	X	–	–	–
4	X		X	X	X	X	X	–	–	–
5		X	X	X		X	X	X	–	–
6	X	X	X	X		X		–	X	–
7	X	X	X	X			X	–	–	X

DETERMINE CASE NO. FROM ABOVE. THEN WORK FROM LEFT TO RIGHT IN TABLE BELOW

CASE NO.	METHOD OF OBTAINING QUANTITIES LISTED BELOW										
	B	L	$\frac{L}{B}$	$\frac{\bar{x}}{B}$	$\frac{h_2}{B\sqrt{K}}$	$\sqrt{K}$	W	P	h_2	μ	U
1	given	given	$\frac{L}{B}$	given	from chart 4P	$\frac{h_2}{B} \div \left(\frac{h_2}{B\sqrt{K}}\right)$	given	$\frac{W}{BL}$	given	$\frac{PBK}{U}$	given
2	"	"	"	"	"	$\sqrt{\frac{\mu U}{PB}}$	"	"	$\left(\frac{h_2}{B\sqrt{K}}\right) \cdot B\sqrt{K}$	given	"
3	"	"	"	"	"	$\frac{h_2}{B} \div \left(\frac{h_2}{B\sqrt{K}}\right)$	PBL	$\frac{\mu U}{KB}$	given	"	"
4	"	"	"	"	"	"	given	$\frac{W}{BL}$	"	"	$\frac{PBK}{\mu}$
5	"	"	"	from chart 8P	"	"	PBL	$\frac{\mu U}{KB}$	"	"	given
6	"	"	"	"	"	"	given	$\frac{W}{BL}$	"	$\frac{PBK}{U}$	"
7	"	"	"	"	"	$\sqrt{\frac{\mu U}{PB}}$	"	"	$\left(\frac{h_2}{B\sqrt{K}}\right) \cdot B\sqrt{K}$	given	"

CASE NO	METHOD OF OBTAINING QUANTITIES LISTED BELOW (CONT'D)										
	$\frac{f}{\sqrt{K}}$	f	$\frac{10^4 H}{PBLU\sqrt{K}}$	H	$\frac{Q}{BLU\sqrt{K}}$	Q	Q_s	$\frac{\Delta t}{P}$	Δt	$\frac{m}{\sqrt{K}}$	m
1 to 7 inc.	from chart 1P	$\left(\frac{f}{\sqrt{K}}\right) \cdot \sqrt{K}$	from chart 2P	$\left(\frac{10^4 H}{PBLU\sqrt{K}}\right) \frac{PBLU\sqrt{K}}{10^4}$	from chart 6P	$\left(\frac{Q}{BLU\sqrt{K}}\right) \cdot BLU\sqrt{K}$	from chart 5P	from chart 7P	$\left(\frac{\Delta t}{P}\right) \cdot P$	from chart 3P	$\left(\frac{m}{\sqrt{K}}\right) \cdot \sqrt{K}$

$$Q = 1.26 \text{ cu in/sec}$$

$$Q_s = 0.529 \text{ cu in/sec}$$

The corresponding characteristics for the complete bearing are exactly the same as those listed previously for the individual pads except for the power loss and the flow. The power loss for the complete bearing is given by

$$H \text{ (complete bearing)} = nH \text{ (pad)} = 6 \times 0.786 = 4.72 \text{ hp}$$

The comments pertaining to the flow and temperature rise are similar to those given in Part 1.

Centrally Pivoted Pads

Since a pad with an offset pivot ($\bar{x}/B$ between 0.5 and 1) is normally suitable for operation in one direction only, pads are frequently built with central pivots in order to secure reversibility.

One of the consequences of the present analysis is that the load capacity falls to zero if the pivot is placed at the center of the pad ($\bar{x}/B = 0.5$). This can be most readily seen from Chart 4P, which shows that the minimum film-thickness variable is zero for $\bar{x}/B = 0.5$. Experience, however, seems to indicate that the performance of centrally pivoted pads is reasonably successful, but, of course, data are usually lacking as to how much better it would have been if theoretical requirements had been satisfied.

A factor which helps to provide load capacity for centrally pivoted pads is that the viscosity of the lubricant does not remain constant as assumed in the analysis but varies as the lubricant passes through the film. This alters the pressure distribution sufficiently to permit the resultant pressure to fall in the center of the pad, making it possible to carry load. The calcu-

TABLE 2A METHOD OF SOLUTION FOR PROBLEMS ON PIVOTED-PAD BEARINGS WHERE LUBRICANT AND INLET TEMPERATURE ARE AMONG VARIABLES

CASE NO.	GIVEN VARIABLES AND CONDITIONS										
	VARIABLES								CONDITIONS		
	W	U	B	L	$\frac{\bar{x}}{B}$	h_2	t_i	lubricant	MAX W	MIN H	MAX h_2
1A	X	X	X	X	X	X	X		—	—	—
2A	X	X	X	X	X		X	X	—	—	—
3A		X	X	X	X	X	X	X	—	—	—
4A	X		X	X	X	X	X	X	—	—	—
5A		X	X	X		X	X	X	X	—	—
6A	X	X	X	X		X	X		—	X	—
7A	X	X	X	X			X	X	—	—	X

DETERMINE CASE NO FROM ABOVE THEN WORK FROM LEFT TO RIGHT IN TABLE BELOW

CASE NO.	METHOD OF OBTAINING QUANTITIES LISTED BELOW														
	B	L	$\frac{L}{B}$	$\frac{\bar{x}}{B}$	$\frac{h_2}{B\sqrt{K}}$	$\sqrt{K}$	W	P	h_2	$\frac{\Delta t}{P}$	Δt	t_i	lubricant	μ	U
1A	given	given	$\frac{L}{B}$	given	from chart 4▸	$\frac{h_2}{B} \div \left(\frac{h_2}{B\sqrt{K}}\right)$	given	$\frac{W}{BL}$	given	from chart 7▸	$\left(\frac{\Delta t}{P}\right) \cdot P$	given	see note 1 *	$\frac{PBK}{U}$	given
2A	"	"	"	"	"	$\sqrt{\frac{\mu U}{PB}}$ *	"	"	$\left(\frac{h_2}{B\sqrt{K}}\right) \cdot B\sqrt{K}$	"	"	"	given	see note 2	"
3A	"	"	"	"	"	$\frac{h_2}{B} \div \left(\frac{h_2}{B\sqrt{K}}\right)$	PBL	$\frac{\mu U}{KB}$ *	given	"	see note 3	"	"	see note 3	"
4A	"	"	"	"	"	"	given	$\frac{W}{BL}$	"	"	$\left(\frac{\Delta t}{P}\right) \cdot P$	"	"	see note 2	$\frac{PBK}{\mu}$
5A	"	"	"	from chart 8▸	"	"	PBL	$\frac{\mu U}{KB}$ *	"	"	see note 3	"	"	see note 3	given
6A	"	"	"	"	"	"	given	$\frac{W}{BL}$	"	"	$\left(\frac{\Delta t}{P}\right) \cdot P$	"	see note 1 *	$\frac{PBK}{U}$	"
7A	"	"	"	"	"	$\sqrt{\frac{\mu U}{PB}}$ *	"	"	$\left(\frac{h_2}{B\sqrt{K}}\right) \cdot B\sqrt{K}$	"	"	"	given	see note 2	"

CASE NO.	METHOD OF OBTAINING QUANTITIES LISTED BELOW (CONT'D)								
	$\frac{t}{\sqrt{K}}$	t	$\frac{10^4 H}{PBLU\sqrt{K}}$	H	$\frac{Q}{BLU\sqrt{K}}$	Q	Q_s	$\frac{m}{\sqrt{K}}$	m
1A to 7A inc.	from chart 1▸	$\left(\frac{t}{\sqrt{K}}\right) \cdot \sqrt{K}$	from chart 2▸	$\left(\frac{10^4 H}{PBLU\sqrt{K}}\right) \cdot \frac{PBLU\sqrt{K}}{10^4}$	from chart 6▸	$\left(\frac{Q}{BLU\sqrt{K}}\right) BLU\sqrt{K}$	from chart 5▸	from chart 3▸	$\left(\frac{m}{\sqrt{K}}\right) \cdot \sqrt{K}$

* Obtain Δt and μ first.

Note 1: The proper lubricant is the one whose viscosity-temperature curve passes through the point given by μ and t on a visc.-temp. chart (such as Fig. 4) where the temp., t, equals $t_a = t_i + \Delta t/2$.

Note 2: The viscosity, μ, is obtained from a visc.-temp. chart for the given lubricant. Enter the chart with the temperature, t, equal to t_a where $t_a = t_i + \Delta t/2$.

Note 3: Enter chart 7▸ with $\frac{\bar{x}}{B}$ and obtain $\left(\frac{\Delta t}{P}\right)$. Assume a trial value of μ, calculate Δt from equation, $\Delta t = \frac{\mu U}{KB} \cdot \left(\frac{\Delta t}{P}\right)$. Then follow procedure given in note 4 below to obtain correct μ. Using correct μ, calculate P from equation, $P = \mu U/KB$.

Note 4: Using a visc.-temp. chart, plot trial μ against temperature, t, where $t = t_a = t_i + \Delta t/2$. Several trial viscosities, (see, for example, points A and B, Fig. 4), may be necessary to arrive at the correct viscosity which is given by the intersection of the visc.-temp. curve for the given lubricant with the curve compromising the locus of the trial viscosities.

CHART 7P FOR DETERMINING FILM-TEMPERATURE RISE

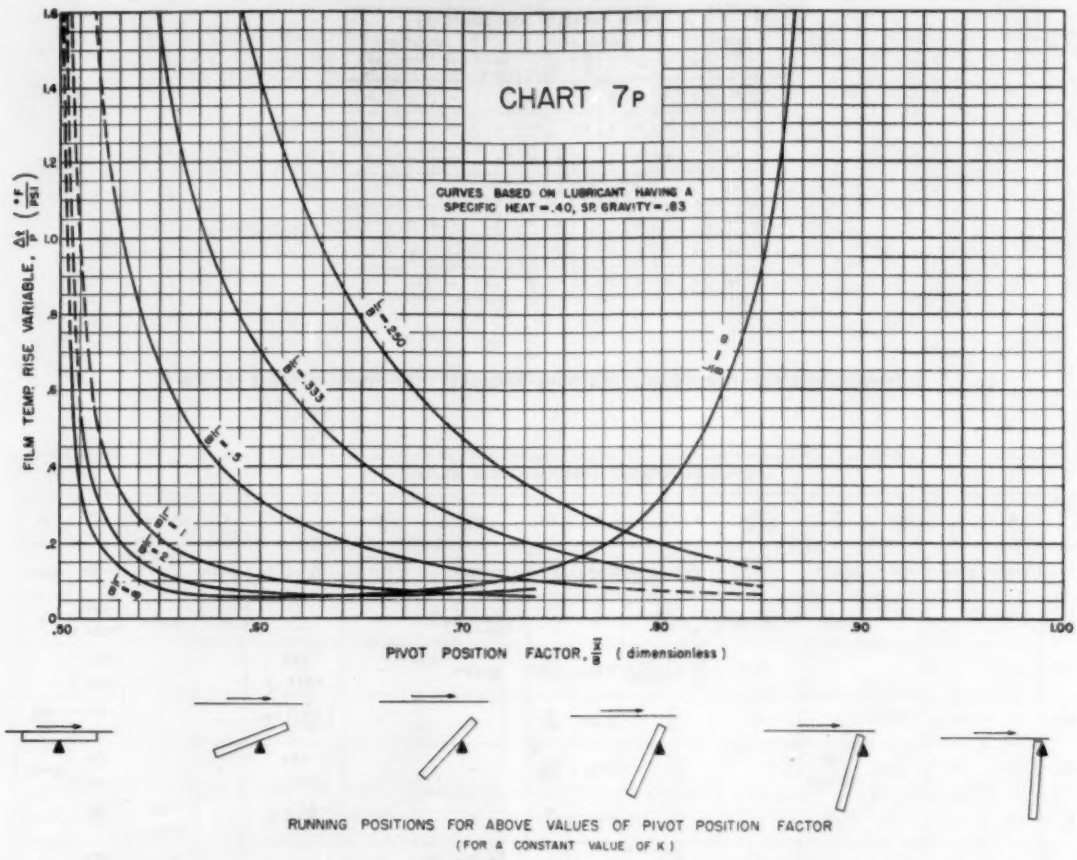

lated value of this load is considerably less than for a pad with a more favorably placed pivot, see Fig. 10, footnote 10.

Since the position of the resultant pressure does not affect the film form, and hence the load capacity, of fixed-pad bearings as it does for pivoted-pad bearings, the influence of variable viscosity is usually not considered so important in bearings of the former type. It should be noted, however, that the adjustment of the viscosity to conform to the average temperature, as discussed in this paper, has no influence on the position of the resultant since the viscosity is still considered to be constant at the adjusted value. The adjustment merely corrects the viscosity for the average temperature.

The case of the centrally pivoted pad was discussed in some detail by the present authors in footnote 10. It was found that such pads could be made to carry loads comparable with those carried by pads with optimumly placed pivots if the pad surface was very slightly convex. The proper amount of convexity is about one half the minimum film thickness but lesser amounts have a very significant effect. It is possible and, indeed, quite probable that convexity of this order, resulting from machining techniques, temperature, and pressure distortions, and so forth, is present in many of the supposedly flat pads which are in service.

Owing to the lack of more complete data on the treatment of centrally pivoted pads, the designer must either assign safety factors to the values obtained from the analysis given in this paper for pads with more favorably placed pivots or should employ crowned pads. Relieving the inlet and/or the outlet edge for an appreciable distance (say, 10 per cent of B) has been shown to be helpful but the amount of material removed should be small (of the order of the film thickness).

[10] "The Influence of Surface Profile on the Load Capacity of Thrust Bearings With Centrally Pivoted Pads," by A. A. Raimondi and J. Boyd, published in this issue, pp. 321–330.

Comparison Between Fixed and Pivoted-Pad Bearings

Because of the different variables involved, fixed-pad bearings and pivoted-pad bearings cannot be compared readily unless the slope of the former and the pivot position of the latter are fixed. When this has been done both bearings can be compared on the basis of the performance number K.

Fig. 10 shows the quantity, $10^4 h_2/B$, plotted against $10^4 K$ for the two types of bearings. In constructing the figure, both bearings were considered to have $L/B = 1$. The slope of the fixed-pad bearing was taken as 2×10^{-3} in/in. and the pivot position of the pivoted-pad bearing was chosen for maximum-minimum film thickness, giving $x/B = 0.6$. The curves show that, with the exception of the common point A, the film thickness of the pivoted-pad bearing is always greater than that of the fixed-pad bearing. This is a consequence of the pad automatically adjusting itself to maintain an optimum value of h_1/h_2.[11] The fixed-pad

[11] If it is desired to calculate the value of h_1/h_2 for a given pivoted-pad bearing the following equation may be used:
$h_1/h_2 = 1 +$ slope var/min film thick var $= 1 + (m/\sqrt{K})/(h_2/B\sqrt{K})$; similarly for the fixed-pad bearing
$h_1/h_2 = 1 +$ 1/min film thick var $= 1 + 1/(h_2/Bm)$

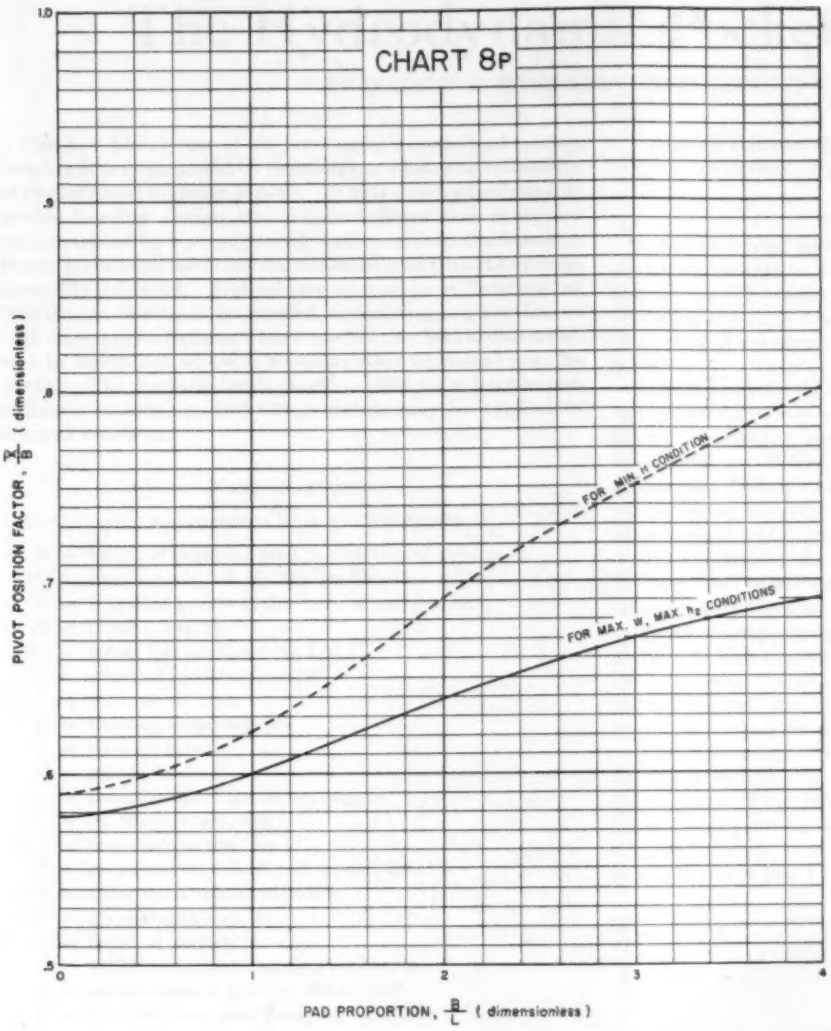

CHART 8P FOR DETERMINING VALUES OF $\bar{x}/B$ CORRESPONDING TO MAXIMUM LOAD, MAXIMUM-MINIMUM FILM THICKNESS, OR MINIMUM POWER LOSS FOR VARIOUS PAD PROPORTIONS

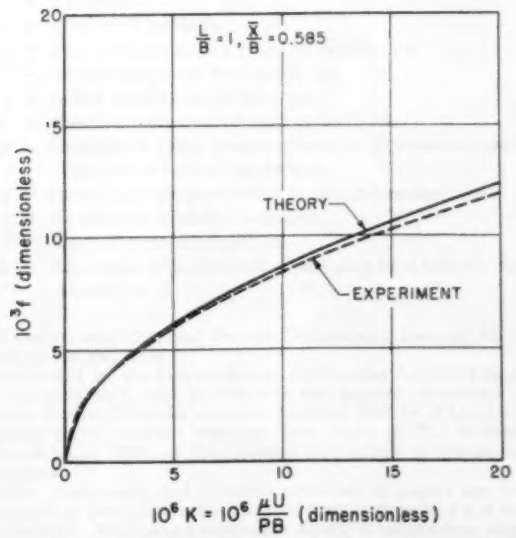

FIG. 12 COMPARISON BETWEEN THEORETICAL AND EXPERIMENTAL COEFFICIENTS OF FRICTION FOR PIVOTED-PAD BEARING

bearing only attains optimum conditions at one point, in this instance, point A, (same h_1/h_2) which corresponds to the solution which would be obtained from Table 1, Case 7.

Fig. 11 shows the quantity, $10^3 f$, plotted against $10^6 K$ for the same bearings. It will be noted that the friction coefficients do not differ to the same extent as the minimum film thicknesses. The two sets of curves illustrate the fallacy of making bearing comparisons on the basis of friction coefficient alone.

AGREEMENT BETWEEN THEORY AND TEST

While a great deal of experimental data have been published on pivoted-pad bearings, the authors have been unable to find any which was complete enough to permit a check on quantities other than the coefficient of friction.

Fig. 12 shows the coefficient-of-friction data published by Morgan, Muskat, and Reed[12] compared with theoretical predictions. Although better agreement might have been obtained if the test pads had been larger (pads were 1 cm square), a comparison of the curves shows a satisfactory correlation with experiment in so far as coefficient of friction is concerned. As with fixed-pad bearings, however, a better check would also include a comparison of the minimum film thicknesses.

[12] "Lubrication of Plane Sliders," by F. Morgan, M. Muskat, and D. W. Reed, *Journal of Applied Physics*, vol. 11, 1940, p. 541.

The Hydrodynamic Pocket Bearing

By DONALD F. WILCOCK,[1] SCHENECTADY, N. Y.

The low power loss of an externally pressurized pocket bearing is accompanied by dependence upon the reliability of the external pressure source. In this new hydrodynamic pocket-bearing design the required flows and pressures are generated by hydrodynamic action within the bearing. Power loss about half that for conventional thrust bearings is readily achieved. Preliminary operation on bearings of this design has been successful, indicating application in high-speed installations where low bearing loss is desirable, and in machines where a measurement of thrust may be useful. The bearing lends itself readily to a frictionless ball-seat mounting, and the principle may be applied to journal bearings.

Nomenclature

The following nomenclature is used in the paper:

B = length of pumping land in direction of motion, in.
C_p = heat capacity of oil, Btu/gal/deg C
E = length of pocket in direction of motion, in.
H = bearing loss, hp
H_p = power loss over pockets, hp
L = width of pumping land, in.
N = shaft speed, rpm
P = pressure in pocket, psi
Q = oil flow, gpm
R = radius, in.
R_m = mean radius of thrust bearing, in
T = oil temperature, deg C
ΔT = temperature rise, deg C
U = mean surface velocity of runner, ips
dV = differential volume element
W = gross thrust load, lb
a = depth of pocket, in.
b = width of land surrounding pocket, in.
g = acceleration of gravity, 386 in/sec^2
h = film thickness over pumping land, in.
k = a constant
n = number of pockets
p = unit pressure at any point in oil film, psi
t = oil-film thickness over lands, in.
v = radial velocity in oil film, ips
w = effective perimeter of leakage land, in.
x = co-ordinate along pumping land in direction of motion, measured from oil groove, in.
y = co-ordinate perpendicular to thrust-bearing face
z = co-ordinate in radial direction
δ = taper of pumping land, in.
Δ = depression of pocket end of pumping land below leakage lands, in.
μ = oil viscosity, lb sec/in^2 (reyns)
ρ = oil density, lb per cu in.

Introduction

Tapered-land and pivoted-shoe thrust bearings have high rates of power consumption when they must be operated at high surface speeds. This is the result of a high rate of shear in oil films extending over large areas. Correspondingly large quantities of lubricating oil are required in order to maintain a reasonable temperature.

At least partly for these reasons, hydrodynamic thrust bearings have found little favor with aircraft-engine designers despite the limited life of highly loaded, high-speed-rolling-element bearings. Both the larger oil flow, with its attendant large lubricating-oil system, and the larger cooling system required to handle the heat rejection from the hydrodynamic bearings penalize the user with added weight and decreased efficiency. If these disadvantages could be minimized, the inherent simplicity and long life of these bearings could be utilized in aircraft applications; and their usefulness in land-based and marine equipment would be enhanced.

Thrust bearings consisting of pockets into which lubricant is pumped at high pressure confine the area of high shear to the lands enclosing the pockets. The power consumption is then much lower than in a conventional bearing, but of course some additional power is required to pump the oil.

The most serious disadvantage of the externally pressurized bearing is its complete dependence upon the high-pressure external pump. If the pump could be made an integral part of the pocket bearing, its reliability would be equal to that of the conventional bearing. A new bearing configuration which meets this goal is shown in Fig. 1. This particular bearing successfully replaced a tapered-land bearing in a 500-kw steam turbine in extensive tests to full power. The rotation of the runner was counterclockwise. The three pump sections are located between each oil groove and its following pocket.

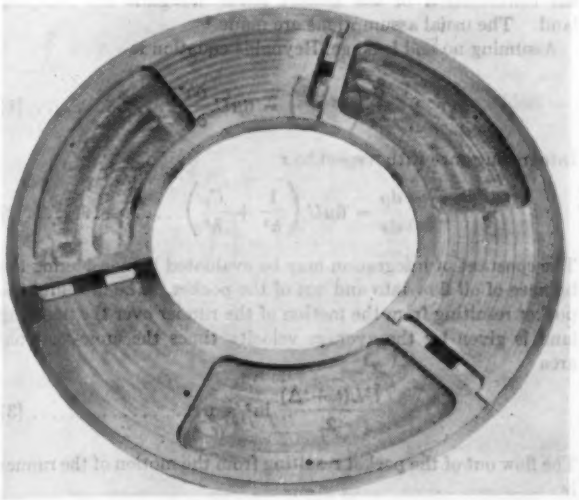

Fig. 1 4 1/4-In. × 8 1/2-In. Hydrodynamic Pocket Thrust Bearing for Test in 500-Kw Turbine

[1] Materials and Chemical Process Department, General Electric Company. Mem. ASME.

Contributed by the Design Group, Lubrication Activity Division, and presented at a joint session with the Applied Mechanics and Machine Design Divisions, and the American Society of Lubrication Engineers at the Annual Meeting, New York, N. Y., November 29–December 4, 1953, of The American Society of Mechanical Engineers.

Note: Statements and opinions advanced in papers are to be understood as individual expressions of their authors and not those of the Society. Manuscript received at ASME Headquarters, August 10, 1953. Paper No. 53—A-83.

The principle of construction is more readily understood from the circumferential section and plan view in Fig. 2. Oil is dragged by the motion of the runner out of the oil groove, over the pumping land, and into the pocket. Oil leaks out of the pocket through the clearance between the lands and the runner, and this clearance must adjust itself until the oil flows into and out of the pocket are equal, at which point the pocket pressure is sufficient to support the external load.

Hydrodynamic Relations

The pumping land is indicated, in Fig. 2, to lie a distance Δ below the lands surrounding the pocket. It also is indicated to have a slope δ/B in the direction of motion. The differential equation governing flow and oil pressure over the pumping land is Reynolds equation, but solution must be obtained for the unique boundary condition in which the pressure at the end of the land is not zero, but is equal to the pocket pressure. End leakage is restricted by the continuation of the pocket lands alongside the pumping land. The usual assumptions are made.[3]

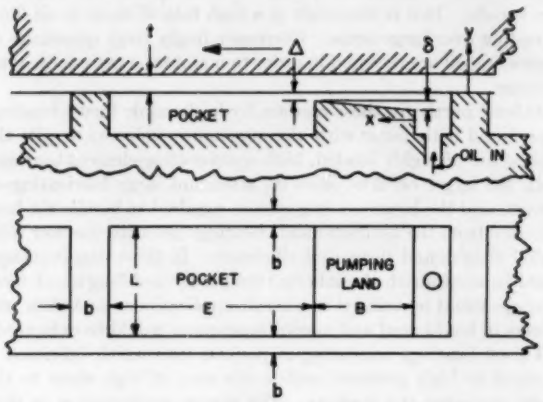

Fig. 2 Section and Plan View of One Sector of Hydrodynamic Pocket Thrust Bearing

Assuming no end leakage, Reynolds equation is

$$\frac{\partial}{\partial x}\left(h^3\frac{\partial p}{\partial x}\right) = 6\mu U\frac{\partial h}{\partial x} \quad \ldots\ldots [1]$$

Integrating once with respect to x

$$\frac{dp}{dx} = 6\mu U\left(\frac{1}{h^2} + \frac{C_1}{h^3}\right) \quad \ldots\ldots [2]$$

The constant of integration may be evaluated by considering the balance of oil flow into and out of the pocket. The flow into the pocket resulting from the motion of the runner over the pumping land is given by the average velocity times the cross-sectional area

$$\frac{UL(t+\Delta)}{2} \text{ in}^3/\text{sec} \quad \ldots\ldots [3]$$

The flow out of the pocket resulting from the motion of the runner is

$$\frac{ULt}{2} \text{ in}^3/\text{sec} \quad \ldots\ldots [4]$$

The outflow due to the pressure P in the pocket is

$$\frac{wPt^3}{12\mu b} + \frac{L(t+\Delta)^3}{12\mu}\left(\frac{dp}{dx}\right)_B \quad \ldots\ldots [5]$$

The effective leakage perimeter w is given approximately by

$$w = 2E + 2b + L + B \quad \ldots\ldots [6]$$

half the length of the pumping land being included since the average pressure will be about half the pocket pressure.

Equating [3] to [4] plus [5] and rearranging

$$\left(\frac{dp}{dx}\right)_B = 6\mu U\left[\frac{1}{(t+\Delta)^2} - \frac{1}{(t+\Delta)^3}\left(t + \frac{wPt^3}{6\mu UbL}\right)\right] \quad \ldots\ldots [7]$$

Since $h = t + \Delta$ when $x = B$, the constant C_1 in Equation [2] is seen by comparison to be

$$C_1 = t + \frac{wPt^3}{6\mu UbL} \quad \ldots\ldots [8]$$

and

$$\frac{dp}{dx} = 6\mu U\left[\frac{1}{h^2} - \frac{1}{h^3}\left(t + \frac{wPt^3}{6\mu UbL}\right)\right] \quad \ldots\ldots [9]$$

Note that h is a function of x, namely

$$h = t + \Delta + \delta\left(1 - \frac{x}{B}\right) \quad \ldots\ldots [10]$$

so that

$$\frac{dp}{dx} = \frac{dp}{dh}\frac{dh}{dx} = -\frac{\delta}{B}\frac{dp}{dh} \quad \ldots\ldots [11]$$

Substituting Equation [11] in [9] and integrating

$$p = \frac{6\mu UB}{\delta}\left[\frac{1}{h} - \frac{1}{2h^2}\left(t + \frac{wPt^3}{6\mu UbL}\right)\right] + C_2 \quad \ldots\ldots [12]$$

C_2 is determined by noting that $p = 0$ when $h = t + \Delta + \delta$, so that

$$p = \frac{6\mu UB}{\delta}\left[\frac{t + \Delta + \delta - h}{h(t + \Delta + \delta)} - \frac{(t + \Delta + \delta)^2 - h^2}{2h^2(t + \Delta + \delta)^2}\left(t + \frac{wPt^3}{6\mu UbL}\right)\right] \quad \ldots\ldots [13]$$

gives the pressure along the pumping land. When $h = t + \Delta$, $p = P$, and Equation [13] becomes

$$P = 6\mu UB\left[\frac{1}{(t+\Delta)(t+\Delta+\delta)} - \frac{2t + 2\Delta + \delta}{2(t+\Delta)^2(t+\Delta+\delta)^2}\left(t + \frac{wPt^3}{6\mu UbL}\right)\right] \quad \ldots\ldots [14]$$

For given bearing dimensions and pocket pressure P, Equation [14] is an equation determining the film thickness t. In order to determine the values of Δ and δ which will maximize t, set $\partial t/\partial\Delta = 0$ and $\partial t/\partial\delta = 0$. After much simplification this results in

$$\delta(1 + t + \Delta) = 0 \quad \ldots\ldots [15]$$

Since $t + \Delta = -1$ is physically impossible, $\delta = 0$ satisfies Equation [15] for all values of t and Δ. The corresponding value of Δ, for maximum film thickness, is

$$\Delta = \sqrt{\frac{2\mu UB}{P}} - t' \quad \ldots\ldots [16]$$

where t' denotes the maximum value of t. Substituting $\delta = 0$, and the Relation [16] in Equation [14]

$$\frac{wP}{12bLU\mu}t'^3 + \frac{t'}{2} = \frac{1}{3}\sqrt{\frac{2\mu UB}{P}} \quad \ldots\ldots [17]$$

[3] "Analysis and Lubrication of Bearings," by M. C. Shaw and E. F. Macks, McGraw-Hill Book Company, Inc., New York, N. Y., 1949, pp. 160–166.

The design dimension Δ may be determined by solving Equation [17] for t' and substituting this value in Equation [16].

The general equation for t is obtained by setting $\delta = 0$ in Equation [14] and rearranging

$$(t + \Delta)^3 + \frac{wB}{bL} t^3 = \frac{6\mu UB\Delta}{P} \quad [18]$$

For the maximum film thickness at a given speed and load, the taper of the pumping land must be zero. In a conventional tapered land or Kingsbury bearing there must be a taper to produce load-carrying pressures in the oil film. However, in the hydrodynamic pocket bearing the restriction normally afforded by the taper is provided by the restricted outflow from the pocket. Mathematically, this restriction is introduced in the determination of the constant of integration, C_1.

The zero taper desired for the pumping land of the hydrodynamic pocket bearing greatly simplifies its machining, the only critical dimension being the depression Δ, of the pumping land below the surface lands.

Performance Variables

Power loss results from shearing of oil over the lands from motion of the runner and from the shearing force on the runner created by the outflow from the pocket due to the pocket pressure. For each pocket the latter force is the sum of a retarding force

$$\frac{PL(t + \Delta)}{2}$$

and an accelerating force

$$\frac{PLt}{2}$$

so that the net force per land is

$$\frac{PL\Delta}{2}$$

and the power loss from this cause is

$$\frac{PLR_mN\Delta}{126{,}000}$$

The total power loss is

$$H = \frac{N^2b\mu}{95{,}900t}\left[\left(R_m - \frac{1}{2}(L + b)\right)^3 + \left(R_m + \frac{1}{2}(L + b)\right)^3\right] + \frac{nN^2R_m^2L\mu}{601{,}000}\left[\frac{b}{t} + \frac{B}{t + \Delta}\right] + \frac{nNR_mLP\Delta}{126{,}000} \quad [19]$$

Equation [19] does not contain a term for power loss over the pocket, since the pocket may be made deep, e.g., $50t$ to $100t$, and the power loss under laminar flow is then negligible. Undoubtedly, some loss will occur under turbulent conditions. Determination of this loss and of optimum pocket depth has not been made, but initial tests indicate that the pocket loss is small except at high speed.

The net oil flow through the bearing is

$$Q = \frac{60n}{231}\left[\frac{UL(t + \Delta)}{2}\right] - \frac{L(t + \Delta)^3P}{12\mu B} \quad [20]$$

The temperature rise is

$$\Delta T = \frac{42.4H}{QC_p} \quad [21]$$

The total load carried is

$$W = \frac{nP}{2}\left[(L + b)(2E + B + b) + b^2\right] \quad [22]$$

Centrifugal Effect

Centrifugal force, acting on each particle of oil between the runner and the leakage lands, is an additional cause of oil flow from the bearing. It was not included in the general treatment because its effect is small except at high speeds and low loads. Centrifugal force will increase the flow from the outer land and decrease the flow from the inner land.

An approximate solution is obtained by considering the centrifugal flow to occur in laminae parallel to the bearing surface and thrust runner. It is assumed further that the circumferential velocity, dx/dt, is given by

$$\frac{dx}{dt} = \frac{2\pi RN}{60}\frac{y}{t} \text{ ips} \quad [23]$$

The centrifugal acceleration force on an elemental volume dV is

$$dF = \frac{\rho dV}{gR}\left(\frac{dx}{dt}\right)^2 = \frac{1.10 \times 10^{-3}\rho RN^2}{gt^2} y^2dV = ky^2dV \quad [24]$$

The opposing viscous force, for a shearing stress τ, is

$$dF = \left(\frac{\partial\tau}{\partial y}dy\right)dx\,dz = \frac{\partial}{\partial y}\left(\mu\frac{\partial v}{\partial y}\right)dV = \mu\frac{\partial^2 v}{\partial y^2}dV \quad [25]$$

Equating forces gives the differential equation

$$\mu\frac{d^2v}{dy^2} = -ky^2 \quad [26]$$

Integrating twice and noting that $v = 0$ when $y = 0$ and $y = t$

$$v = \frac{ky}{12\mu}(t^2 - y^2) \quad [27]$$

The flow per unit length of perimeter is

$$\int_0^t v\,dy = \frac{kt^3}{40\mu} = \frac{8.50 \times 10^{-4}\rho RN^2t^3}{12\mu} \text{ in}^2/\text{sec/in.} \quad [28]$$

The net outflow resulting from centrifugal effect to be added to Equation [5] is therefore

$$\frac{8.50 \times 10^{-4}\rho N^2t^3}{12\mu}\left[\frac{2\pi}{n}\left(R_m + \frac{L + b}{2}\right)^2 - \frac{2\pi}{n}\left(R_m - \frac{L + b}{2}\right)^2\right] = \frac{1.07 \times 10^{-4}\rho N^2t^3R_m(L + b)}{12\mu n} \text{ in}^3/\text{sec} \quad [29]$$

Equation [18] for t now becomes

$$(t + \Delta)^3 + \frac{wB}{bL}t^3 + \frac{1.07 \times 10^{-4}\rho N^2R_m(L + b)B}{nPL}t^3 = \frac{6\mu UB\Delta}{P} \quad [30]$$

in which the third term represents the approximate influence of centrifugal force. When the coefficient of t^3 in the third term of Equation [30] becomes appreciable with respect to the coefficient of the second term, the centrifugal effect should be included in the analysis.

Bearing Proportions

A design study of the influence of bearing proportions upon the

performance of a hydrodynamic pocket thrust bearing illustrates the relative importance of each. For simplicity, a constant value of oil viscosity is assumed

$$\mu = 2.6 \times 10^{-6} \text{ lb sec/in}^2 \text{ (reyns)}$$

Consider a bearing having an outer diameter of 13 in., an inner diameter of 7 in., three pockets, and operating at 6000 rpm. For this bearing $U = 3140$ in/sec, $E + B + b = 10.00$ in., $L + 2b = 3.00$ in. and $R_m = 5.00$ in. It is assumed that $C_p = 6.3$. Within these limitations the influence of the $E/(E + B)$ and $2b/(L + 2b)$ ratios and of film thickness t on the pocket pressure P, total load capacity W, power loss H, oil flow Q, and temperature rise ΔT has been determined. For each set of t, $E/(E + B)$, $2b/(L + 2b)$ values, the pumping land depression Δ for maximum pocket pressure, was first computed. From Equation [18], setting $\partial p/\partial \Delta = 0$, one obtains

$$(t + \Delta)^3 - \frac{3t}{2}(t + \Delta)^2 - \frac{Bwt^3}{2Lb} = 0 \quad \ldots\ldots [31]$$

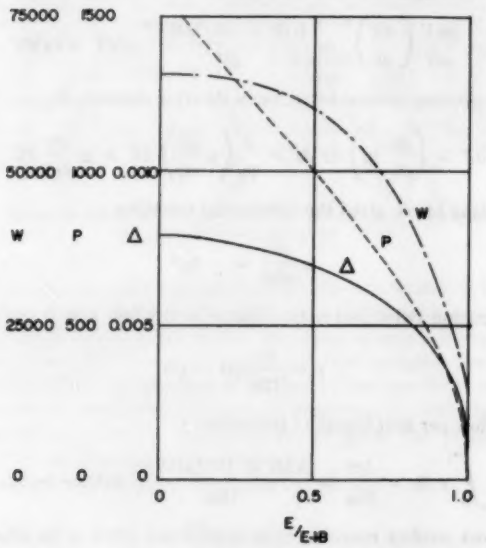

FIG. 3 OPTIMUM LAND DEPRESSION Δ, POCKET PRESSURE p, AND GROSS LOAD W, AS A FUNCTION OF POCKET-LENGTH RATIO $E/(E + B)$ FOR CONSTANT FILM THICKNESS $t = 0.002$ IN. AND LAND WIDTH $b = 0.300$ IN.

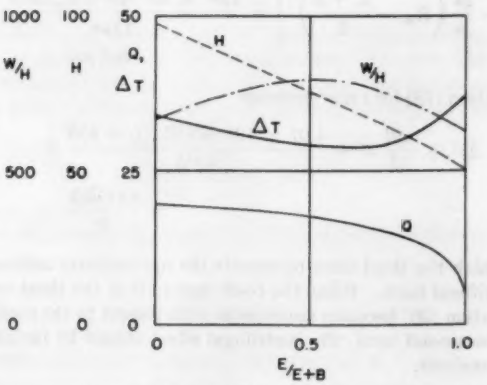

FIG. 4 POWER LOSS H, OIL FLOW Q, TEMPERATURE RISE ΔT, AND LOAD-CARRYING EFFICIENCY W/H, AS A FUNCTION OF POCKET-LENGTH RATIO $E/(E + B)$ FOR $t = 0.002$ IN., $b = 0.300$ IN.

from which the optimum value of Δ may be determined.

The influence of the $E/(E + B)$ ratio is shown in Figs. 3 and 4 for $b = 0.3$ in., $t = 0.002$ in. As the relative pocket length is increased, the optimum land depression Δ, decreases, at first slowly, then rapidly. The pocket pressure generated is nearly inversely proportional to pocket length, but the gross load carried by the bearing is not reduced appreciably by pocket-length ratios up to 0.5. The power loss decreases rapidly as the pocket-length ratio is increased, but the efficiency of load-carrying W/H, reaches a maximum at a pocket-length ratio of 0.5. The temperature rise is near a minimum at this point also.

The influence of the $2b/(L + 2b)$ ratio is indicated in Figs. 5 and 6 for the same film thickness, $t = 0.002$ in., and for $E = 3.0$ in. As would be expected, the power loss and temperature rise increase rapidly as the leakage-land width is increased. The gross load capacity reaches a maximum when $2b/(L + 2b) = 0.3$. The load-carrying efficiency, pounds per horsepower, is largest at small values of b.

It is apparent that for a desired minimum film thickness the optimum design must be a compromise. In the particular case under discussion, the best values might be $3 < E < 7$ and $0.1 < b < 0.5$. Fig. 7 shows curves of constant W and constant W/H as a

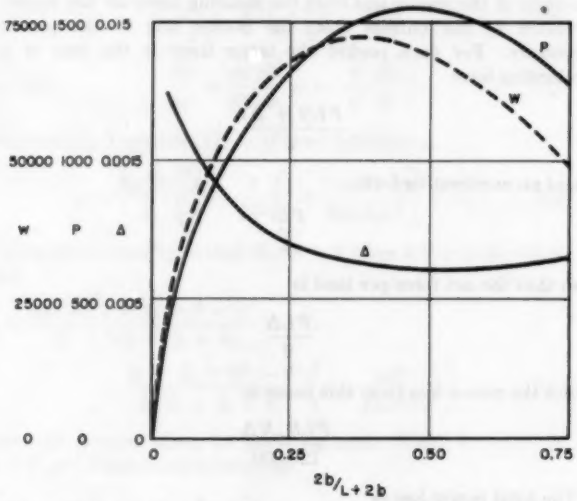

FIG. 5 OPTIMUM LAND DEPRESSION Δ, POCKET PRESSURE p, AND GROSS LOAD W, AS A FUNCTION OF LAND WIDTH RATIO $2b/L + 2b$ FOR $t = 0.002$ IN., $E = 3.0$ IN.

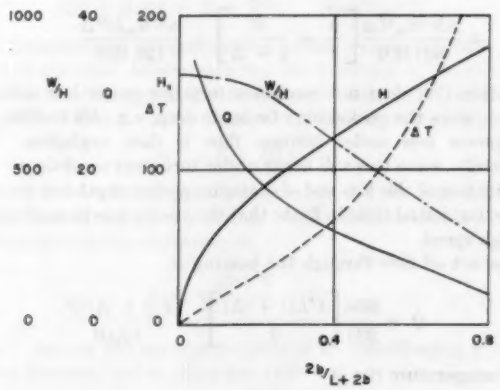

FIG. 6 POWER LOSS H, OIL FLOW Q, TEMPERATURE RISE ΔT, AND LOAD-CARRYING EFFICIENCY W/H, AS A FUNCTION OF LAND WIDTH RATIO $2b/L + 2b$, FOR $t = 0.002$ IN., $E = 3.0$ IN.

function of E and b. From these the values of E and b for maximum efficiency at any load may be determined.

Fig. 8 shows the influence of film thickness at $E = 3.0$ in., $b = 0.3$ in. Both the gross load capacity and the temperature rise increase rapidly as the film thickness is decreased. The load-carrying efficiency also increases rapidly.

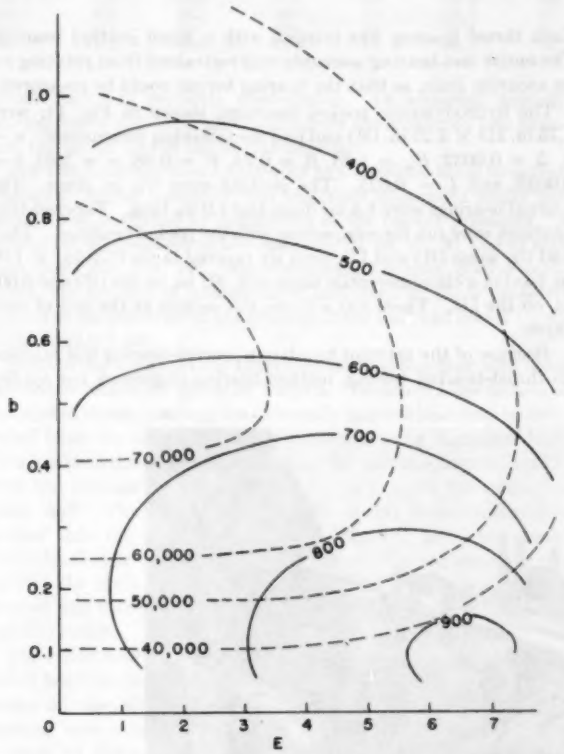

Fig. 7 Plot Showing Lines of Constant Load Capacity W (Dotted Lines) and Constant Load-Carrying Efficiency W/H (Solid Lines) as a Function of b and E for $t = 0.002$ In.

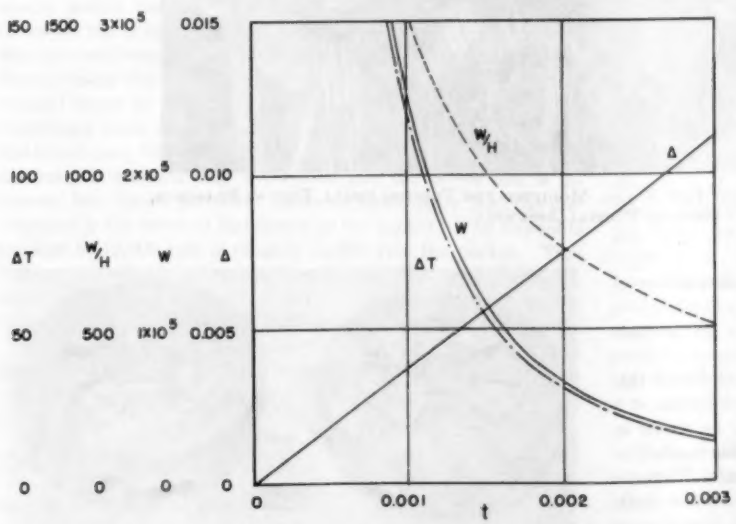

Fig. 8 Optimum Land Depression Δ, Gross Load W, Load-Carrying Efficiency W/H, and Temperature Rise ΔT, as a Function of Film Thickness t for $E = 3.0$, $b = 0.3$

Comparison With Tapered-Land Bearing

Comparison of the hydrodynamic pocket thrust bearing with a tapered-land bearing of similar over-all dimensions at equal oil-film viscosity shows the lower power loss of the pocket bearing. The bearing studied in the foregoing, with an OD of 13 in., an ID of 7 in., and with $n = 3$, $b = 0.3$ in., $E = 5.0$ in., $B = 4.7$ in., and $\mu = 2.6 \times 10^{-6}$ reyns, is selected as near the optimum proportions. It is compared with a tapered-land bearing having nine 3×3-in. lands, each with a compound taper of 0.004 in. on the OD and 0.007 in. on the ID.

For the pocket bearing, reference to Fig. 3 shows that for $b = 0.3$ and $E/(E + B) = 0.52$, $\Delta = 0.0069$ and $W = 59{,}500$ lb at $N = 6000$ and $t = 0.002$. The film thickness for other loads and speeds is then computed using Equation [18]. The results are plotted in Fig. 9, curve (1), showing t as a function of the dimensionless number, $\mu N/60P$. Note that the film thickness drops off rapidly below $\mu N/60P = 80$. At values of $\mu N/60P$ below that at

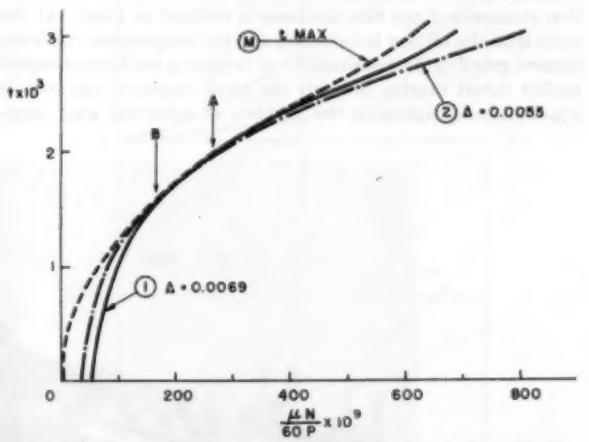

Fig. 9 Film Thickness t as a Function of Dimensionless Quantity $(\mu N/_{60}P)$ for 7-In. $\times$ 13-In. Bearings With $n = 0.3$, $b = 0.3$, $E = 5.0$, $B = 4.7$ and $\mu = 2.6 \times 10^{-6}$

(Curve M, maximum t from Equation [17]; curve 1, working curve for $\Delta = 0.0069$, from Equation [18] tangent to M at A; curve 2, working curve for $\Delta = 0.0055$, tangent to M at B.)

which $t = 0$, the pocket pressure is proportional to μN

$$P = \frac{\pi B R_m \mu N}{5\Delta^2} \quad \ldots\ldots\ldots [32]$$

and the balance of the external load must be carried directly by the leakage lands.

Curve M in Fig. 9 shows the maximum possible value of film thickness, as calculated from Equation [17]. Curve (1) is tangent to M at point A where $t = 0.002$, as calculated in the previous section. For any value of Δ, a curve will be obtained tangent to M at the optimum design point. Smaller values of Δ give larger film thickness at values of $\mu N/60P$ below the design point, and smaller film thickness above the design point.

For a gross average load of 1000 psi, the total load is $W = 94{,}000$ lb, and the design point is B in Fig. 9 with $\Delta = 0.0055$. However, if the original value of $\Delta = 0.0069$ is retained the film thickness at the higher load is reduced only from the maximum value of 0.00159 to 0.00154,

TABLE 1 PERFORMANCE COMPARISON OF 7-IN. × 13-IN. HYDRODYNAMIC POCKET BEARING WITH 7-IN. × 13-IN. TAPERED-LAND BEARING

		Power loss, hp		Film thickness, mils	
N	W	HP brg	TL brg	HP brg	TL brg
6000	94000	97	200	1.54	1.40
4900	94000	58	105	1.12	1.05
3000	47000	24	47	1.54	1.42

or 3 per cent. Therefore the comparison with the tapered-land bearing is made on the basis of design point A, $\Delta = 0.0069$, in Table 1. For the proportions chosen, the power loss of the pocket bearing is about half that of the comparable tapered-land bearing, while the minimum film thickness is appreciably greater. This is close to the maximum film thickness attainable, for, as Fig. 7 shows, a gross load much over 70,000 lb is not attainable at $t = 0.002$.

If a smaller film thickness can be tolerated, the land width b can be reduced for the same gross load, and the power loss of the bearing will be considerably reduced. Table 2 shows the reduction attainable if the film thickness is reduced to 1 mil. At the same time the oil flow is increased and the temperature rise is decreased greatly. The desirability of designing the hydrodynamic pocket thrust bearing properly for small clearance operation is apparent, and highlights the problem of achieving good alignment of bearing and runner during operation. A simple way of accomplishing this is described in a later section.

TABLE 2 EFFECT OF FILM THICKNESS ON PERFORMANCE OF 7-IN. × 13-IN. HYDRODYNAMIC POCKET BEARING CARRYING 94,000 LB AT 6000 RPM

Film thickness, in.	0.00154	0.00103
Pumping land depression, in.	0.0069	0.0063
Land width, b, in.	0.300	0.063
Pocket pressure, psi	1545	1445
Power loss, hp	97	61
Oil flow, gpm	13.9	17.0
Temperature rise, deg C	47	24

Developmental Confirmation

Some tests have been run to demonstrate the validity of this new design principle. The tests were run in a modification of a previously described[3] journal-bearing test stand, as shown in Fig. 10. A pair of bearings was used, the load being applied by compression of the heavy spring surrounding the shaft. Thus the bearings were forced apart against the shoulders on the shaft. Each thrust bearing was integral with a small journal bearing. The entire test-bearing assembly was restrained from rotating by an accurate scale, so that the bearing torque could be measured.

The hydrodynamic pocket bearings, shown in Fig. 11, were 1.75 in. ID × 3.25 in. OD and had the following dimensions: $n = 4$, $\Delta = 0.0032$, $R_m = 1.25$, $B = 0.74$, $E = 0.98$, $w = 3.63$, $b = 0.0625$, and $L = 0.625$. The pockets were $^3/_{16}$ in. deep. The journal bearings were 1.5 in. diam and 1.0 in. long. Tapered-land bearings were run for comparison with the pocket bearings. They had the same OD and ID, with six tapered lands 0.75 in. × 1.06 in. having a circumferential taper of 0.001 in. on the OD and 0.002 in. on the ID. There was a $^1/_8$-in. flat section at the end of each taper.

Because of the attempt to adapt a journal-bearing test machine to thrust-bearing testing, neither bearing alignment nor applied

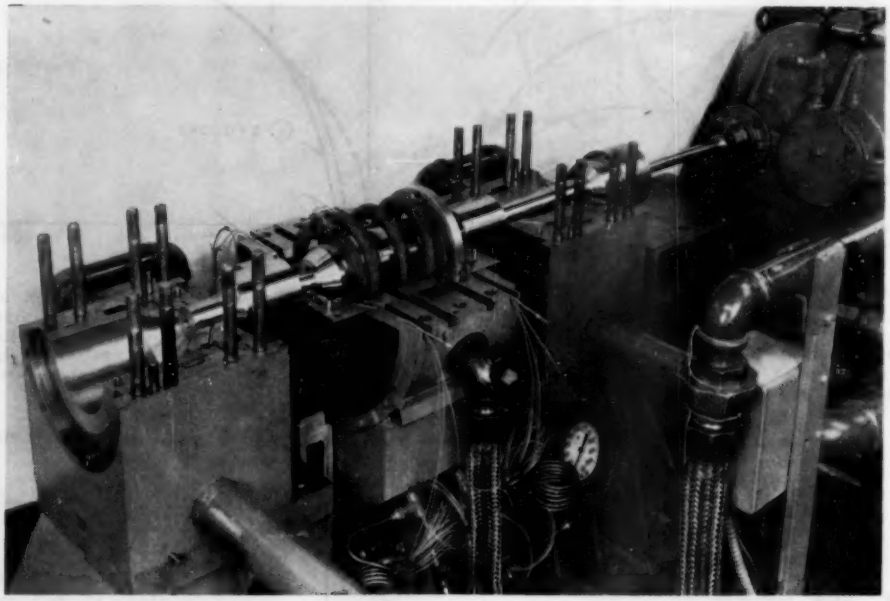

Fig. 10 View of Journal-Bearing Test Stand, Modified for Testing Small Thrust Bearings, Showing Partial Assembly

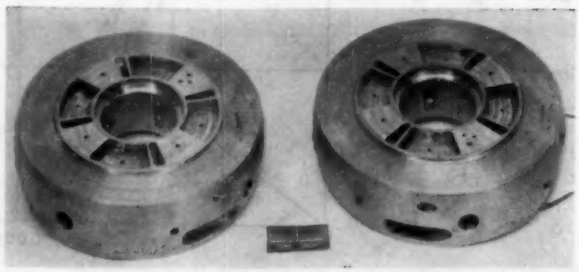

Fig. 11 $1^3/_8$-In. × $3^1/_8$-In. Hydrodynamic Pocket Thrust Bearings for Experimental Runs

[3] "Oil Flow, Key Factor in Sleeve Bearing Performance," by D. F. Wilcock and Murray Rosenblatt, Trans. ASME, vol. 74, 1952, p. 849.

TABLE 3 SUMMARY OF TEST RUNS ON 1¹/₄-IN. × 3¹/₄-IN. HYDRODYNAMIC POCKET THRUST BEARINGS

(Test Oil—29.2 cp at 100 F; 4.7 cp at 210 F)

	W (lb)			Inlet oil			Average oil,	Power loss per bearing (hp)				
N	Fwd	Rear	Avg	Psi	Deg C	Outlet oil, Deg C	viscosity, centipoises	Measured	Radial only	Thrust only	Cal, thrust	Cal. film thickness, mils
6000	172	208	190	22	55.0	55.6	14.4	0.63	0.31	0.32	0.25	1.72
11970	188	214	201	22	55.0	58.9	13.5	2.08	1.08	1.00	0.77	2.13
18090	214	216	215	22	55.0	66.4	11.9	4.62	1.93	2.69	1.43	2.31
24150	226	247	236	18	54.9	70.8	11.1	7.96	3.05	4.91	2.29	2.41
5970	920	926	923	23	54.9	58.2	13.8	0.91	0.28	0.63	0.53	0.75
12020	879	895	887	23	55.3	62.2	12.7	2.53	0.97	1.56	1.35	1.12
18030	921	931	926	23	55.1	67.9	11.6	5.48	1.84	3.64	2.45	1.27
24050	1070	1090	1080	19	55.2	75.0	10.3	9.42	2.62	6.80	3.83	1.28

thrust load was perfectly controllable. In addition, journal-bearing losses had to be subtracted from the measured loss to obtain the power loss of the thrust bearing.

The test bearings were ball-seated at a 5.000-in. diam to permit alignment during assembly, but imperfect alignment under test usually was indicated by differences in the pocket pressures. A typical set of pressures at low load was 70, 80, 45, 30, and at high load, 220, 280, 275, 193. By computing for each pocket separately, the amount of misalignment indicated by these pressures is 1 mil in the diameter of the bearing at low load and about ½ mil at the higher load.

Some of the results of the experimental runs together with some calculated values are given in Table 3. Because of the nature of the pocket thrust bearing, the externally applied load may be computed from the observed pocket pressures using Equation [22]. This has been done for each bearing in the pair in columns 2 and 3, with the average given in column 4. In general, the two agree quite well. The load applied by the spring was considerably greater than the computed load, the difference being accounted for by friction or cocking of the sliding front-bearing mount in the bore of the main housing. Load was applied after rotation was started, and there was no evidence of contact between the bearing and the runner.

The radial bearing losses were computed from tests on a pair of radial bearings only, having the same dimensions, for the same outlet oil viscosity. The calculated power loss for the pocket bearing was obtained from the average gross load W, the average oil viscosity, and the dimensions of the bearing, using Equations [22], [18], and [19].

The power-loss results are plotted versus speed in Fig. 12, which shows the considerably lower power loss of the hydrodynamic pocket bearing. The dotted lines show the calculated losses for the pocket bearing. These are in good agreement with the observed losses up to 12,000 rpm, but at higher speeds the observed losses are much higher than the calculated. These increased losses at high speeds might be due to the influence of centrifugal force as expressed in Equation [30]. However, when the worst case, for low load at 24,000 rpm, is calculated the film thickness is reduced only 4 per cent and the power loss is increased less than 3 per cent. It seems more likely that the discrepancy is the result of turbulence in the pocket. The Reynolds number at 12,000 rpm is roughly 13,000 over the pocket. Turbulence is probably present at speeds over 2000 rpm, therefore, since a Reynolds number of 2000 is usually accepted as the boundary condition between laminar and turbulent conditions.

The method of plotting employed in an earlier study of turbulence in journal bearings[4] may be applied to this case. The equation for power loss over the pockets, assuming laminar flow

$$H_p = \frac{nEL(2\pi R_m)^2}{6050a}\,\mu\left(\frac{N}{60}\right)^2 \qquad [33]$$

may be rearranged to give

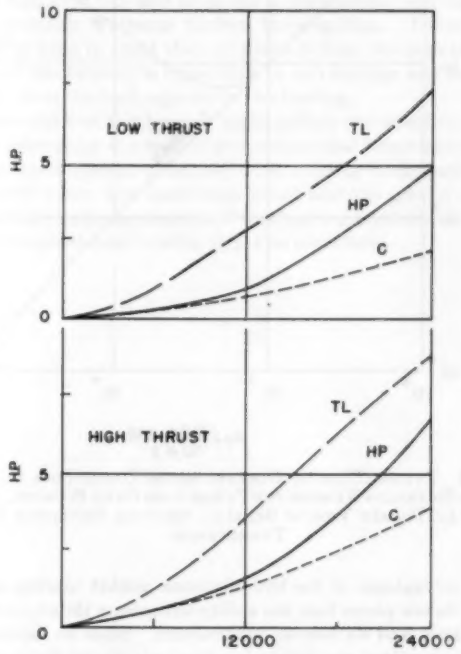

FIG. 12 POWER LOSS AS A FUNCTION OF SPEED
(Curve TL, tapered-land bearing; curve HP, hydrodynamic pocket bearing; curve C, calculated for HP bearing.)

$$\left(\frac{2\pi R_m N a\rho}{60\mu g}\right)\left(\frac{2.78\times 10^{10} H_p}{nELR_m{}^3N^3\rho}\right) = 1 \qquad [34]$$

in which the two quantities in parentheses are dimensionless, the first being Reynolds number. Equation [34] gives the straight line for laminar flow shown in Fig. 13, in which Reynolds number is the abscissa, and the second dimensionless quantity is the ordinate. If H_p is assumed to be the discrepancies between experimental and calculated pocket-bearing losses, the points shown in Fig. 13 are obtained for the high-speed runs at 12,000, 18,000, and 24,000 rpm. The marked deviation from laminar behavior is apparent, indicating that under high-speed conditions a smaller pocket depth might be desirable for minimum loss. In this simple analysis, no account has been taken of the circulation which probably occurs within each pocket even under low-speed laminar conditions.

APPLICATION

The application of the hydrodynamic pocket thrust bearing will depend in large measure upon its advantages and disadvantages relative to thrust bearings of other designs. These are the tapered-land bearing, the spring-supported plate bearing, and the pivoted-shoe or Kingsbury bearing, of the oil-film type, and ball and tapered-roller thrust bearings of the rolling-element type.

[4] "Turbulence in High-Speed Journal Bearings," by D. F. Wilcock, Trans. ASME, vol. 72, 1950, pp. 825–834.

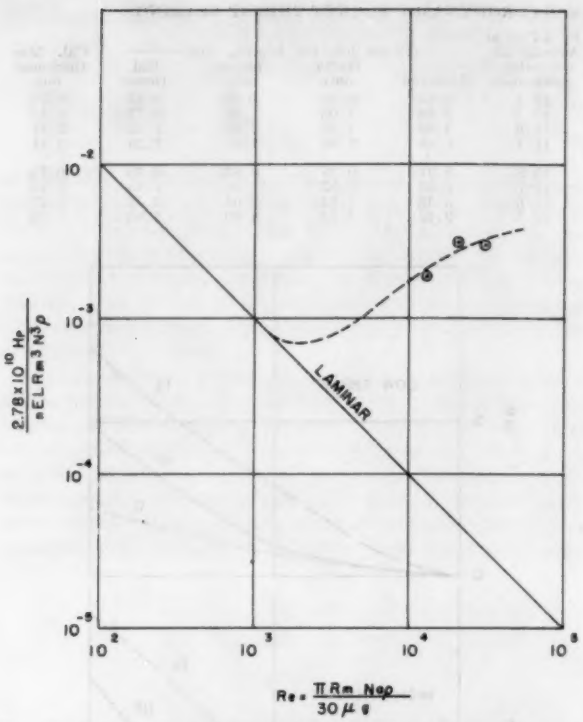

FIG. 13 TAYLOR PLOT OF DIMENSIONLESS POWER-LOSS FUNCTION VERSUS REYNOLDS NUMBER FOR POWER LOSS OVER POCKETS, 1³/₄-IN. × 3¹/₄-IN. POCKET THRUST BEARING, SHOWING DEVIATION DUE TO TURBULENCE

The advantages of the hydrodynamic pocket bearing are primarily its low power loss, the ability to measure thrust, its ease of lubrication, and its ease of manufacture. Since no tapered surfaces are required, machining involves only straightforward milling and turning operations. Because the bearing has enclosed oil grooves, oil feed is straightforward, simple, and may be at low pressure. Thrust is readily measured by connecting each pocket with a pressure gage. The low power loss has been amply demonstrated, both theoretically and experimentally, at film thicknesses more than equivalent to other oil-film bearings.

The disadvantages of the hydrodynamic pocket bearing lie in its zero film thickness below a limiting value of $\mu N/W$, in its limited flat land area for carrying load at low speed, and in its sensitivity to misalignment. It shares these disadvantages with the tapered-land bearing. Its proportion of flat land area to gross area is usually roughly equivalent to that provided in tapered-land bearings. It has a unique compensating virtue, however, in that high-pressure oil may be fed to the bearing at low speed, if high loads must be carried, so that it operates as a hydrostatic bearing under these conditions. In many applications the thrust load increases with speed, so that low-speed loadings are nominal.

Misalignment is potentially dangerous to any bearing which cannot adjust itself under running conditions. The friction in a conventional ball seat is too great to permit this readjustment under load. However, the ready availability of a source of high-pressure oil in the hydrodynamic pocket bearing permits one to build the ball seat as a hydrostatic bearing, with applied pressure proportional to load. One version of such a design is shown schematically in Fig. 14. Flow-limiting orifices are placed between the pockets of the thrust bearing and the corresponding connected pocket of the ball seat. The lands of the ball-seat pockets may be made broad so that little flow is required to maintain

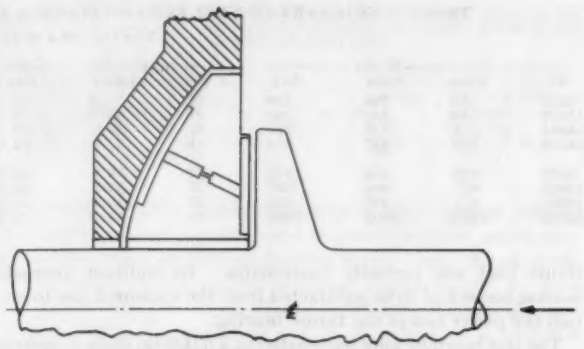

FIG. 14 SKETCH OF HYDRODYNAMIC POCKET THRUST BEARING WITH INTEGRAL PRESSURIZED BALL SEAT

an adequate separation between ball and seat; and this flow is readily made so small that the reduction in film thickness of the thrust bearing due to this additional flow is less than 10 per cent. The pockets of the ball seat should have a total projected area (in an axial direction) at least equal to the net effective area of the thrust bearing, W/P. A stop should be provided to prevent rotation of the thrust bearing.

With a pressurized frictionless ball seat combined with the hydrodynamic pocket thrust bearing, it becomes feasible to consider operating at smaller film thicknesses. In this way, power losses may be reduced still further by decreasing the land width b, or load capacity may be increased considerably. One problem which the reader might consider is what bearing dimensions and oil viscosity are desirable in order to operate with the lowest power loss while carrying a given load W, at a given speed N, with a minimum fixed value of film thickness t, a maximum fixed value of temperature rise ΔT, and a fixed inner bearing diameter. Because of the complex interrelationships between the variables, a numerical example will be found informative.

Under ultra-high-speed conditions, it is apparent that the centrifugal effect upon oil outflow from the bearing should be studied more rigorously. Similarly, the effects of turbulence in the pockets will become pronounced; and experimental studies designed to determine the optimum pocket depth appear desirable.

The principles of the hydrodynamic pocket bearing obviously are applicable to journal bearings, and similar equations have been derived for the journal-bearing design. The analysis is complicated by the fact that the film thickness controlling outflow from each pocket is no longer a constant but is a function of angular position and shaft eccentricity.

CONCLUSION

The mathematical relations governing the performance of a pocket thrust bearing, in which the pocket oil pressures are generated internally by motion of the runner over a depressed circumferential pumping land, have been derived. Operation in a bearing test rig and in a 500-kw steam turbine have demonstrated the practicability of this new principle of bearing design. The advantages of its application have been shown to be low power loss, high load capacity, the ability to measure applied thrust, and, in conjunction with an integrally designed self-pressurized ball seat, the ability to maintain alignment under operating conditions.

ACKNOWLEDGMENT

The helpfulness and assistance of Oscar Pinkus and Ray Ostrowski in conducting the experimental measurements are appreciated sincerely.

Discussion

JOHN A. MEYER.[5] The author presents here a hydrodynamic configuration with less power loss than that for a tapered-land bearing and without the losses and inevitable failure found in a rolling-contact bearing.

Although a close physical resemblance to an externally pressurized bearing is observed, it should be noted that externally pressurized bearings have a feedback feature associated with external resistances that give such bearings an unusually strong tendency to resist motion under applied load. The author's bearing does not incorporate this feature.

The author's solution of Reynold's equation is interesting due to the unusual boundary conditions imposed by the bearing configuration. His assumptions are generally valid, with the possible exception of the assumption of laminar flow, and here the approximation is probably good for moderate speeds. If more detail concerning his calculations in proceeding from Equation [14] to Equation [15] could be given in the closure it would be much easier to evaluate the reliability of this phase of the analysis.

It is probable that the measured power loss in this bearing exceeds that calculated due principally to the turbulence in the pockets as the author suggests. To reduce this loss, the pocket must be made more shallow. This implies a definite design consideration, namely, that there is a best depth for the pocket, at which the sum of shear losses and turbulent losses is a minimum. This value must now be determined experimentally in arriving at an optimum design.

The suggested ball seat as an aid in maintaining bearing alignment certainly warrants further investigation. However, it should be kept in mind that oil drained from the high-pressure region of the bearing is equivalent to end leakage and may adversely affect the load capacity of the bearing.

Future work on this bearing might include the establishment of design criteria for the several proportions and investigation of a pressurization system to be used when starting under load. The low power losses that have been found and the greater ease of manufacture make application of this bearing attractive in places where a tapered-land bearing might be considered.

[5] Teaching Assistant, Massachusetts Institute of Technology, Cambridge, Mass.

The Influence of Surface Profile on the Load Capacity of Thrust Bearings With Centrally Pivoted Pads

By A. A. RAIMONDI[1] and JOHN BOYD,[2] EAST PITTSBURGH, PA.

This paper describes an analysis which reveals the significance of surface profile and its contribution to the load capacity of centrally pivoted pads. Experiments supporting the authors' analysis are described. In addition, variable viscosity and variable density are evaluated and their effect on load capacity is noted.

Nomenclature

The following nomenclature is used in the paper:

B = length of pad in direction of motion, in.
L = length of pad perpendicular to direction of motion, in.
W = total load on pad, lb
P = unit load on pad = W/BL, psi
U = velocity of sliding surface, in/sec
μ = average viscosity in film in reyns, lb sec/sq in.
$\bar{x}$ = distance from inlet edge of pad to pivot, in.
x = co-ordinate in direction of motion, in.
y = co-ordinate perpendicular to sliding surface, in.
h = film thickness at x, in.
h_1 = film thickness at inlet, in.
h_2 = film thickness at outlet, in.
h_{min} = minimum film thickness, in.
h' = minimum film thickness for flat pad with optimum pivot, in.
h_0 = minimum film thickness for convex pad, in.
p = pressure at x, psi
δ = crown of convex pad, in.
R = radius of curvature of convex pad, in.
t_1 = temperature at inlet, deg F
t_2 = temperature at outlet, deg F
Δt = temperature rise = $t_2 - t_1$, deg F
γ = weight per unit volume of lubricant, lb/in.^{3}
c = specific heat, Btu/lb deg F

Introduction

In designing pivoted-pad thrust bearings, the designer usually employs the familiar analysis of Kingsbury (1)[3] and Michell (2) and long experience has inspired confidence in the adequacy of this treatment. There appears, however, to be a disturbing paradox associated with the analysis which seems to indicate that some important factor has been omitted. Several additions or modifications have been suggested, but while these have helped to remove some of the discrepancies, they are not of sufficient magnitude to actually eliminate the difficulty in all cases. This paper will attempt to show that, in reality, a paradox does not exist and that the discrepancies, which have been thought to be present, are a result of theoretical conditions not being realized in practice. The manner in which the findings, which are to be described, can be used to improve the design of pivoted-pad thrust bearings also will be brought out.

The paradox referred to consists in accounting for the observed load-carrying capacity of pivoted-pad thrust bearings when the pivots are located in the centers of the pads. If the pivots are not located at the center of each pad but at a point downstream from the center, no difficulty in calculating appreciable load capacity is encountered. If the pivot is placed at the center, as is frequently done to secure reversibility, the simple theory, assuming uniform viscosity throughout the film, predicts that the load-carrying capacity should be zero.

By refining the assumptions so as to take account of the change in viscosity which takes place when the lubricant heats up because of the work done upon it as it passes through the film, a finite load capacity can be calculated, provided the viscosity decreases with temperature, as is generally true for liquids. If the viscosity increases with temperature, as is the case for gases, it is not possible to ascribe any finite load capacity to gaseous-operated bearings on the basis of variation of viscosity with temperature. As it is well known that a thrust bearing with centrally pivoted pads can be made to operate on air or other gases, it is clear that while taking account of viscosity variations operates in the right direction in the case of liquid lubricants, it is obviously not the complete answer since it does not apply for gases.

Two other effects, the increase in viscosity of the lubricant with pressure and its decrease in density with temperature conceivably might operate in the proper direction to enhance load capacity, but it is difficult to see, as will be shown later, how the former can provide any plausible explanation and how the latter can be of more than minor importance.

What appears to be a factor of far more practical significance in contributing to the load capacity of centrally pivoted pads is the matter of surface profile. In a restricted sense, surface profile, as used here, may be looked upon as departure from flatness.[4] The following analysis shows that a centrally pivoted pad with a slightly convex surface which would be considered "flat" by many standards is capable of carrying a load which is within a few per cent of that carried by an ideally flat pad with the pivot located eccentrically in the position which gives the greatest load capacity. Experiments, to be described, qualitatively confirm the results of this analysis.

The analysis also indicates that surface profile is extremely important in determining performance characteristics and that

[1] Research Engineer, Research Laboratories, Westinghouse Electric Corporation. Assoc. Mem. ASME.
[2] Manager, Lubrication Section, Research Laboratories, Westinghouse Electric Corporation. Mem. ASME.
[3] Numbers in parentheses refer to the Bibliography at the end of the paper.
Contributed by the Special Research Committee on Lubrication and presented at a joint session with the Applied Mechanics and Machine Design Divisions and the American Society of Lubrication Engineers at the Annual Meeting, New York, N. Y., November 29–December 4, 1953, of The American Society of Mechanical Engineers.
Note: Statements and opinions advanced in papers are to be understood as individual expressions of their authors and not those of the Society. Manuscript received at ASME Headquarters, August 17, 1953. Paper No. 53—A-166.
[4] In a broader sense and using the term in a relative manner, it may be defined as the difference in configuration between the surface of the pad and the surface of the runner against which it operates.

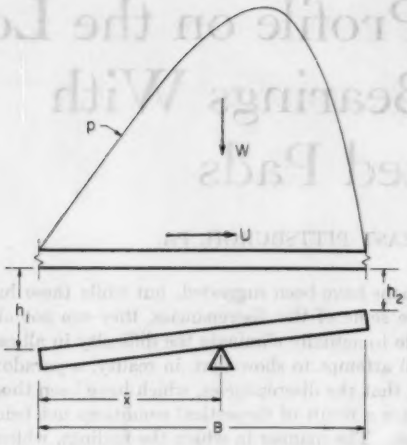

FIG. 1 TYPICAL PRESSURE DISTRIBUTION AND INCLINATION OF FLAT PAD WITH ECCENTRIC PIVOT AND CONSTANT VISCOSITY

convex surfaces with certain degrees of curvature may offer important operational advantages.

In the discussion which follows, the relative contribution of variable viscosity, variable density, and surface profile to the load capacity of centrally pivoted pads will be evaluated separately.

FLAT PIVOTED PAD WITH PIVOT LOCATED FOR MAXIMUM LOAD

Case. 1. Fig. 1 shows a flat pivoted pad with inlet and outlet film thickness h_1 and h_2, respectively. For this assumed film shape and with the viscosity throughout the film considered to be constant and equal to the average of the viscosities at the inlet and at the outlet temperatures, the pressure distribution may be determined and will appear as shown in Fig. 1. In this analysis and that which follows, it will be assumed that there is no side flow, i.e., no flow perpendicular to U. This has been done since solutions which take into account side flow (i.e., which consider bearings of finite length) are available only for the case where the viscosity is considered constant. Since all of the comparisons in this paper will be made on the same basis (no side flow) it is felt that this assumption will not influence qualitatively the results.

Since the pressure distribution is not symmetrical, the resultant of the fluid pressure along the pad does not pass through the center of the pad but is at some point downstream from the center. If the pad is pivoted so that it may tip freely, it can be shown that the pivot must be placed at the position of the resultant if equilibrium is to be obtained with the given film form. If the pivot is not placed at this point, then a new pressure distribution will have to be developed within the film in order that the new resultant will pass through the pivot. This will mean that the pad will have to take on a new position having different values of h_1 and h_2.

It can be shown that if the pivot position, as defined by the distance $\bar{x}$, is fixed by choosing $\bar{x}/B$, then the ratio of the inlet film thickness over the outlet film thickness, h_1/h_2, also becomes fixed and is independent of load, speed, and viscosity. The manner in which h_1/h_2, called the inclination variable, varies with $\bar{x}/B$ is shown in Fig. 2 for the case of no side flow which is equivalent to a pad which is very long in the direction perpendicular to the direction of motion (i.e., $L/B = \infty$).

The unit load, P, which may be carried, and which for given values of the viscosity, μ, and of h_2, U, and B is proportional to

$$\frac{Ph_2^2}{\mu UB}$$

called the load variable, is also plotted against $\bar{x}/B$ in Fig. 2 and can be deduced from the treatment in Norton (3). The relative film shapes corresponding to the different values of $\bar{x}/B$ are shown along the abscissa. A study of Fig. 2 shows that in order to carry maximum load the pivot must be placed in a particular position, namely, $\bar{x}/B$ equal to approximately 0.58. This pad, with $\bar{x}/B = 0.58$, will be used as a standard of comparison in the discussion which follows and will be referred to as the flat pad with optimum pivot.

It also is seen from Fig. 2 that if $\bar{x}/B$ is made equal to 0.5 (i.e., the pivot is placed in the center) the load capacity will be zero.

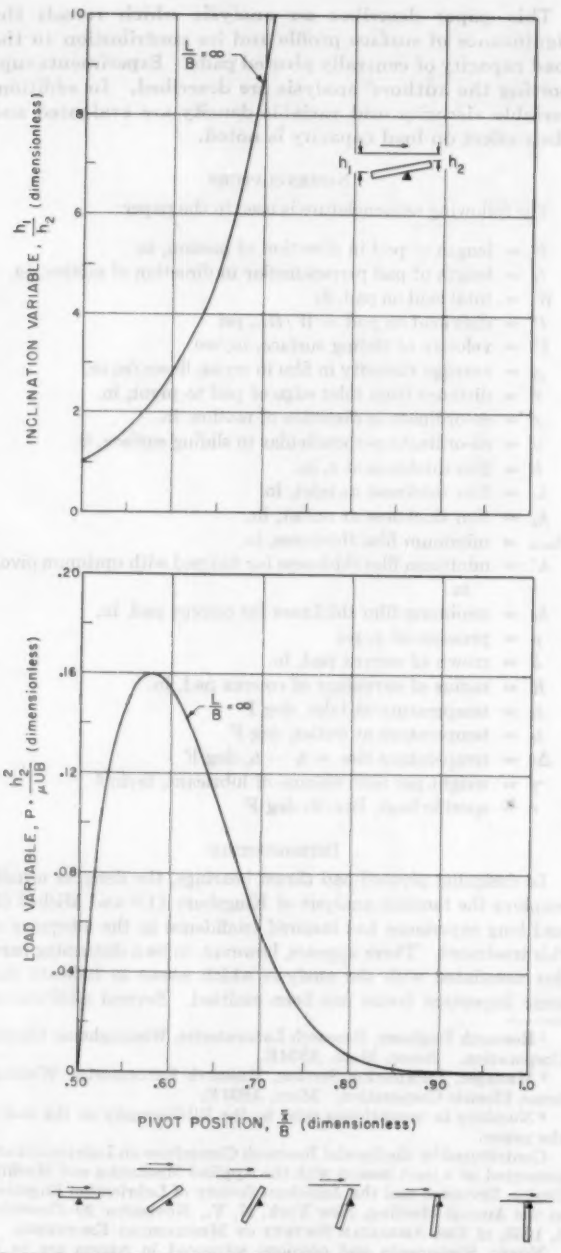

FIG. 2 LOAD VARIABLE AND INCLINATION VARIABLE VERSUS PIVOT POSITION FOR FLAT PAD WITH CONSTANT VISCOSITY

This is because the ratio, h_1/h_2, must fall to 1 in order to get a symmetrical load distribution with the resultant in the center coincident with the pivot. This implies a parallel film which, if the density is considered constant, has zero load capacity.

Since the relative magnitude of the film thickness and the temperature rise are determined by the lubricant used as well as by the loads, speeds, and so forth, Fig. 3 has been drawn to show the operating condition using an SAE 20 oil with an inlet temperature of 100 F and with a unit load of 200 psi; viscosity-

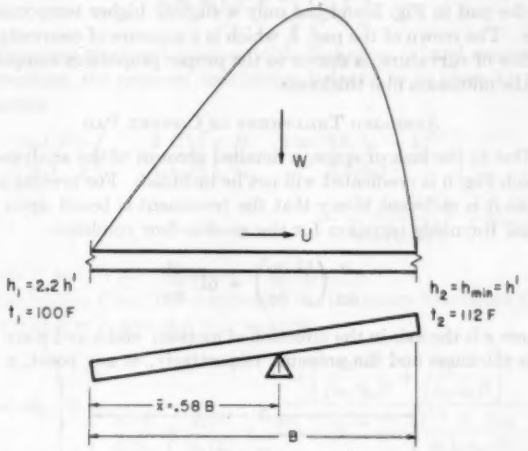

FIG. 3 OPERATING CHARACTERISTICS OF FLAT PAD WITH OPTIMUM PIVOT AND CONSTANT VISCOSITY
(SAE 20 oil, t_1 = 100 F, P = 200 psi.)

temperature properties of the oil are those shown in the Viscosity-Temperature Chart 1 of reference (4). The pivot position has been chosen for maximum load capacity ($\bar{x}/B = 0.58$) and the film shape shows the degree of convergence necessary to carry the resultant load. If the minimum film thickness for this case, h_{min}, is called h', the film thicknesses for the cases yet to be considered can be expressed in terms of h'.

FLAT PIVOTED PAD WITH CENTRAL PIVOT AND VARIABLE VISCOSITY

Case 2. If the viscosity, instead of being considered constant throughout the film, is assumed to change linearly from inlet to outlet, the pressure distribution for a centrally placed pivot is as shown in Fig. 4 when the unit load is again taken to be P and is equal to 200 psi. The calculations are based on the equations given by Norton (5).

It is apparent that the film thickness, both at the exit and at the inlet, has been reduced appreciably from the previous case and thus represents a more dangerous condition of operation. The film-temperature rise, Δt, once again based on SAE 20 oil with an inlet temperature of 100 F, is shown to be twice that obtained for the previous case.

FLAT PARALLEL SURFACES WITH VARIABLE DENSITY

Case 3. If one takes the decrease in fluid density which accompanies the rise in film temperature into account, it is equivalent to adding convergence in the direction of motion to the film, thus permitting a finite load to be calculated for parallel surfaces which ordinarily will not support any load. Although it is not necessary that surfaces be parallel to take advantage of any load-carrying capacity which depends upon variable density, an analysis based upon parallel surfaces enables one to isolate and to evaluate the relative magnitude of the effect. The magnitude

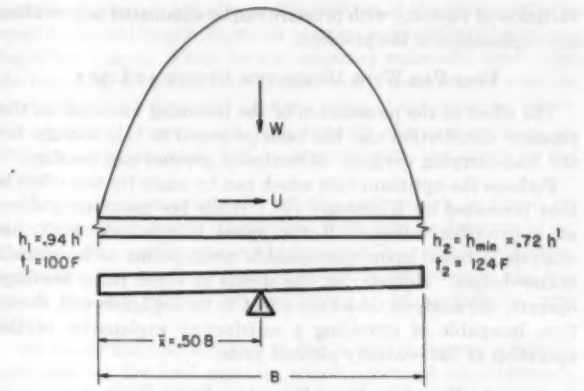

FIG. 4 OPERATING CHARACTERISTICS OF FLAT PAD WITH CENTRAL PIVOT AND VARIABLE VISCOSITY
(SAE 20 oil, t_1 = 100 F, P = 200 psi.)

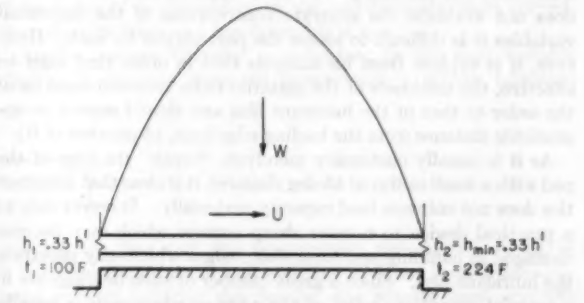

FIG. 5 OPERATING CHARACTERISTICS OF PARALLEL SURFACES WITH VARIABLE DENSITY
(SAE 20 oil, t_1 = 100 F, P = 200 psi.)

depends on the density-temperature relation for the lubricant. Fig. 5 shows the relative operating characteristics of two parallel surfaces with a unit load of 200 psi, an SAE 20 oil, and an inlet temperature of 100 F. [The calculations for this case were based on the formulas given by Shaw (6). Since Shaw neglects the accompanying viscosity change, his treatment, as shown by Cope (7), represents a much more favorable case for variable density than actually exists.] It will be noted in Fig. 5 that the film thickness is only about one third as large as that of the flat pad with optimum pivot (Case 1). At the same time, the temperature rise is found to be about ten times that for Case 1.

Thus the calculations show that parallel surfaces will sustain the same load as the flat pad with optimum pivot, but this is done at the expense of a greatly reduced film thickness and an enormous temperature rise. Since many of the bearings in service appear to operate with thicker films and at lower temperatures than those required to derive any benefit from the effect of variable density, it is felt that this effect is of minor importance in accounting for or in helping to account for the load-carrying capacity of centrally pivoted pad bearings.

FLAT PAD WITH VISCOSITY CHANGING WITH PRESSURE

Case 4. While the effect of pressure on viscosity is usually quite small for the pressures ordinarily encountered, it might be felt that the correction would be important at high pressures. While this is quite true in so far as the load which may be carried for a given film shape is concerned, Charnes and Saibel (8) have shown that the correction moves the resultant pressure, not closer to the center, as would be necessary to account for the load capacity of centrally pivoted pads, but farther away from it. Thus the

variation of viscosity with pressure can be eliminated as providing any explanation to the problem.

Flat Pad With Momentum Effect at Inlet

The effect of the momentum of the incoming lubricant on the pressure distribution also has been proposed to help account for the load-carrying capacity of centrally pivoted pad bearings.

Perhaps the optimum case which can be made for this effect is that presented by Kingsbury (9). While his calculations show an appreciable influence if the speed is relatively high, his analysis is based upon questionable assumptions as he himself acknowledges. However, at the speeds at which many bearings operate, the analysis shows the effect to be negligible and, therefore, incapable of providing a satisfactory explanation of the operation of flat centrally pivoted pads.

Flat Pad With Relieved Inlet Edge

Boswall (10) has shown that by both relieving the inlet edge and taking account of variable viscosity, it is possible theoretically for a flat centrally pivoted pad to carry appreciable load. Since he does not evaluate the separate contribution of the individual variables it is difficult to assess the part played by each. However, it is evident from his analysis that in order that relief be effective, the thickness of the material to be removed must be of the order of that of the lubricant film and should extend an appreciable distance from the leading edge (say, 15 per cent of B).

As it is usually customary merely to "break" the edge of the pad with a small radius of 45-deg chamfer, it is clear that this practice does not enhance load capacity materially. It serves only as a practical device to remove sharp corners which may become damaged in handling and form sharp edges which may penetrate the lubricant film. Since a great number of such bearings are in successful operation, relief of the edge or edges as it is usually carried out does not provide a satisfactory explanation of the facts at hand.

Convex Pad With Central Pivot

Case 5. Since the pressure distribution along the pad depends upon the film shape, it is possible to alter the shape so that the resultant pressure will occur at the center. While the choice of surface profiles by which this may be accomplished is unlimited, the convex profile with a constant radius of curvature will be discussed here because it is a shape that readily is attainable in practice and because it possesses the symmetry required for reversibility. It is especially interesting to find that relatively small changes from perfect flatness are quite important and may explain readily the load-carrying capacity of centrally pivoted pads.

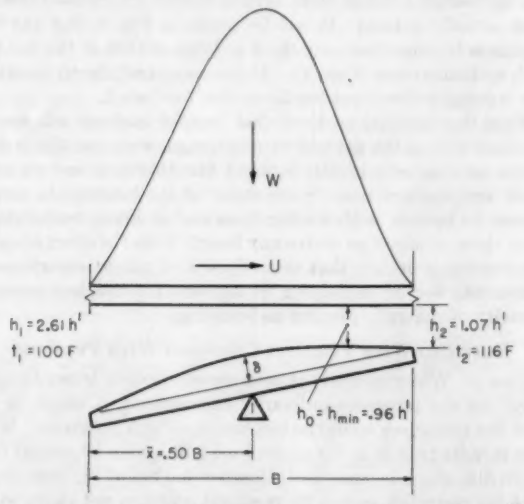

Fig. 6 Operating Characteristics of Convex Pad With Central Pivot
(SAE 20 oil, $t_1 = 100$ F, $P = 200$ psi.)

Fig. 6 shows a convex pad loaded with the same load and supplied with the same oil as the flat pad with optimum pivot, Case 1. Although the pivot for the pad in Fig. 6 is located in the center, it will be seen that it is operating at almost the same film thickness as the pad in Fig. 3 and has only a slightly higher temperature rise. The crown of the pad, δ, which is a measure of convexity or radius of curvature, is drawn to the proper proportion compared to the minimum film thickness.

Abridged Treatment of Convex Pad

Due to the lack of space, a detailed account of the analysis on which Fig. 6 is predicated will not be included. For present purposes it is sufficient to say that the treatment is based upon the usual Reynolds equation for the no-side-flow condition

$$\frac{\partial}{\partial x}\left(\frac{h^3}{\mu}\frac{\partial p}{\partial x}\right) = 6U\frac{\partial h}{\partial x} \quad \ldots\ldots\ldots\ldots\ldots\ldots [1]$$

where x is the axis in the direction of motion; and h and p are the film thickness and the pressure, respectively, at any point, x.

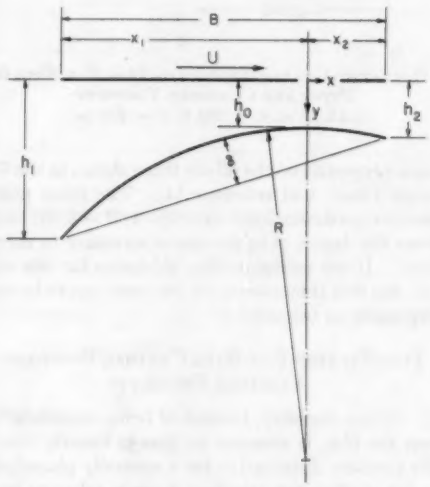

Fig. 7 Nomenclature for Convex Pad

To solve for the pressure, it is necessary to express the film thickness in terms of x. This was done in the present case by assuming the surface of the pad to be a portion of a parabolic cylinder, see Fig. 7. The equation for h then can be expressed in the form

$$h = h_0 + kx^2 \quad \ldots\ldots\ldots\ldots\ldots\ldots [2]$$

where k is the reciprocal of the latus rectum and may be shown to be related to the radius of curvature, R, at the vertex by the relation $k = 1/2R$.

Since the only pad profiles of practical importance are those which do not deviate greatly from a flat surface, the radius of curvature of such pads will be necessarily very large in comparison to the pad length, B. Therefore, although the foregoing equations pertain to pads having a parabolic profile, the variation of the radius of curvature along the pad length will be negligible. Thus, assuming the radius of curvature to be constant and equal to the

value at the vertex, the crown δ may be expressed in terms of B and R by the following equation

$$\delta = \frac{B^2}{8R} \quad \ldots\ldots [3]$$

Using the relation $k = 1/2R$ and substituting Equation [3] into Equation [2] gives a new expression for the film thickness in terms of the crown

$$h = h_0\left[1 + \frac{4\delta}{h_0}\left(\frac{x}{B}\right)^2\right] \quad \ldots\ldots [4]$$

Upon substituting Equation [4] in Equation [1] and assuming μ constant, the pressure distribution is found to be given by the equation

$$p = \frac{3\mu UB}{h_0^2}\left\{\left(1 - \frac{3}{4}\frac{C}{h_0}\right)\left[\frac{x/B}{h/h_0} + \frac{\tan^{-1}(h/h_0 - 1)^{1/2}}{2(\delta/h_0)^{1/2}}\right] - \frac{C}{h_0}\frac{x/B}{2(h/h_0)^2}\right\} + C_1 \ldots [5]$$

where C and C_1 are constants of integration.

Evaluating C and C_1 by imposing the boundary conditions that $p = 0$ at $x = x_2$ and at $x = -x_1$ gives

$$C = 4h_0\left\{3 + \frac{2\left[\frac{x_2/B}{(h_2/h_0)^2} + \frac{x_1/B}{(h_1/h_0)^2}\right]}{\frac{x_2/B}{h_2/h_0} + \frac{x_1/B}{h_1/h_0} + \frac{\tan^{-1}(h_2/h_0 - 1)^{1/2} + \tan^{-1}(h_1/h_0 - 1)^{1/2}}{2(\delta/h_0)^{1/2}}}\right\}^{-1} \quad \ldots\ldots [6]$$

and

$$C_1 = -\frac{3\mu UB}{h_0^2}\left\{\left(1 - \frac{3}{4}\frac{C}{h_0}\right)\left[\frac{x_2/B}{h_2/h_0} + \frac{\tan^{-1}(h_2/h_0 - 1)^{1/2}}{2(\delta/h_0)^{1/2}}\right] - \frac{C}{h_0}\frac{x_2/B}{2(h_2/h_0)^2}\right\} \ldots [7]$$

If μ, U, B, and h_0 are fixed, the shape of the pressure-distribution curve given by Equation [5] will depend not only upon the amount of crown δ, but also on the position of the vertex with respect to the pad length, B, which position is determined by selecting either x_1 or x_2. Thus, for any arbitrary value of δ which fixes the ratio δ/h_0, the position of the resultant pressure varies with the choice of x_2 and there will be some value of the latter for which the resultant pressure will pass through the mid-point of B, thereby permitting the pad to operate with the pivot in the center.

The load-carrying capacity of the pad, which is found by integrating the pressure distribution, then may be determined for the particular configurations which permit the pivot to be located centrally. The results of these calculations are shown in Fig. 8 in which the load variable $Ph_0^2/\mu UB$ is plotted against the ratio δ/h_0.

An interesting result, shown in Fig. 8, is that there is a definite optimum for the load capacity which occurs at approximately $\delta/h_0 = 0.45$. Below 0.45 the load which may be carried for a given value of h_0 falls off as the pad becomes less crowned, thus approaching the flat centrally pivoted pad for which the load capacity is zero. Above 0.45 the load which may be carried for a given value of h_0 diminishes as the pad becomes more curved, since the film takes on a less favorable shape.

As the average viscosity μ, contained in the load variable $Ph_0^2/\mu UB$, depends upon the temperature t_1 of the lubricant entering the film and the temperature rise Δt (where $\Delta t = t_2 - t_1$), specific values of load and film thickness cannot be calculated without knowing the density, the specific heat, and the viscosity-temperature properties of the lubricant being used. On the assumption that all of the friction work goes into raising the lubricant temperature, the temperature-rise variable, $10^4\,\Delta t\gamma c/P$, where γ is the weight per unit volume and c is the specific heat, may be plotted against δ/h_0 as shown in Fig. 9. The vis-

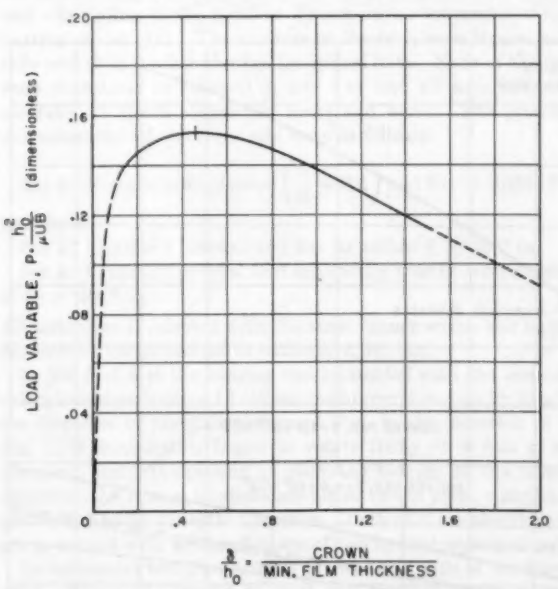

FIG. 8 LOAD VARIABLE VERSUS CROWN TO MINIMUM FILM-THICKNESS RATIO FOR CONVEX PAD

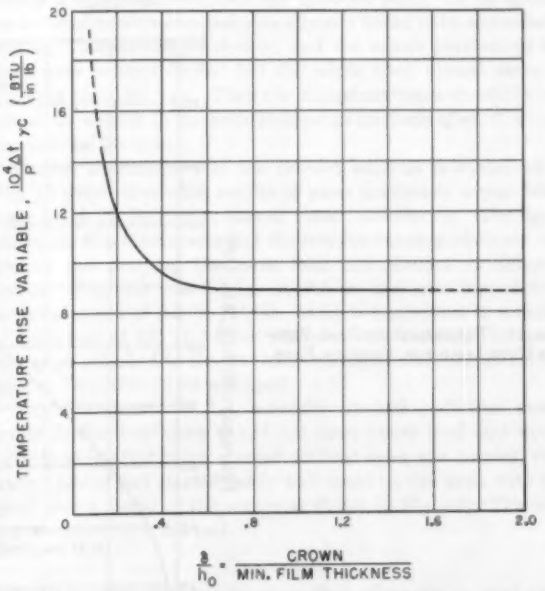

FIG. 9 TEMPERATURE RISE VARIABLE VERSUS CROWN TO MINIMUM FILM-THICKNESS RATIO FOR CONVEX PAD

cosity-temperature properties of the lubricant may be obtained from a conventional plot such as the Viscosity Temperature Chart in reference (4).

Comparison on Basis of Film Thickness Versus Load

While the foregoing cases have been compared pictorially in Figs. 3 to 6 for one given unit load, a better and more general method of comparison is given in Fig. 10 which shows the minimum-film-thickness variable, $10^3 h_{min}/\sqrt{UB}$, plotted against the unit load for each case. An SAE 20 oil with an inlet temperature of 100 F is used throughout. Thus, if the speed and size are known, the film thickness can be determined for any value of the unit load.

Another useful comparison is a plot of the temperature rise versus the unit load as shown in Fig. 11, which again assumes the same lubricant.

Reverting to Fig. 10, the curves show that the film thickness with central pivot and variable viscosity (Case 2) is about 0.7 of that for the flat pad with optimum pivot (Case 1) when compared at the same load of 200 psi. However, when compared at the same minimum film thickness ($10^3 h_{min}/\sqrt{UB} = 0.08$), which is the better criterion, the flat pad with central pivot and variable

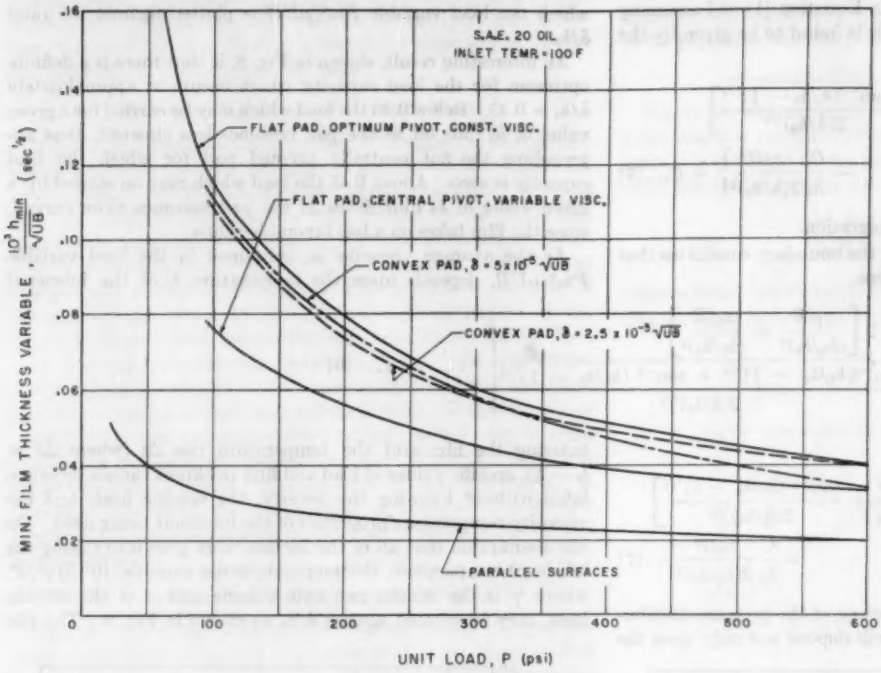

Fig. 10 Minimum Film-Thickness Variable Versus Unit Load for Various Pads

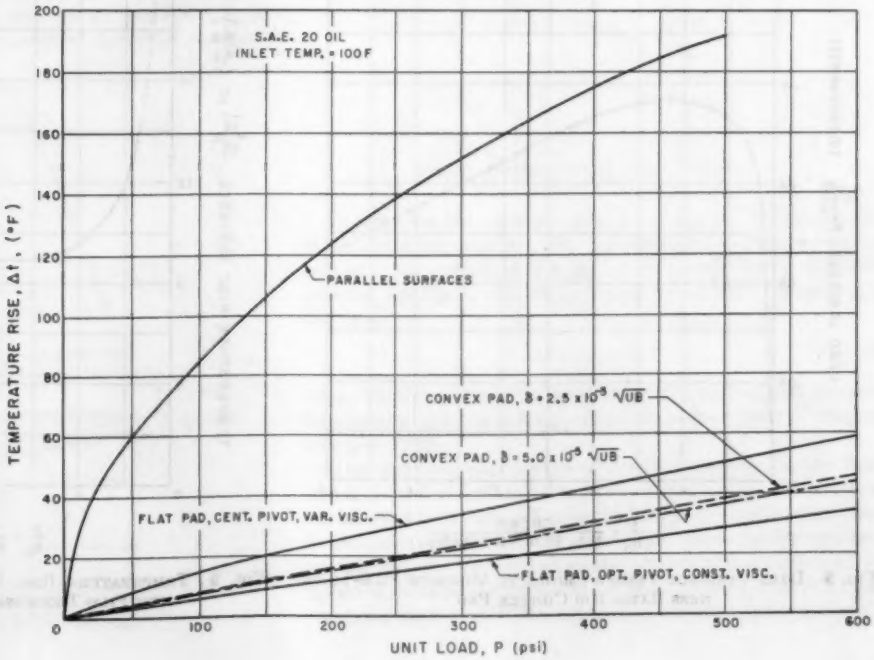

Fig. 11 Temperature Rise Versus Unit Load for Various Pads

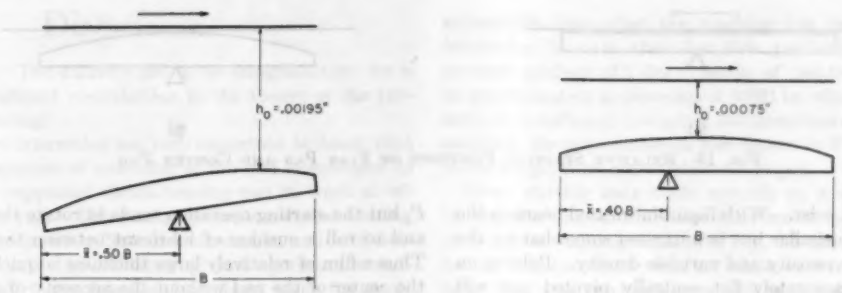

FIG. 12 RELATIVE OPERATING POSITIONS OF CONVEX PAD WITH CENTRAL PIVOT AND PIVOT AHEAD OF CENTER

viscosity will carry only about 0.4 as much load as the flat pad with optimum pivot.

Similarly compared, the parallel-surface pad, Case 3, is much inferior to the flat pad with optimum pivot. In addition, as shown in Fig. 11, the parallel surface gives a much greater temperature rise as has been stated previously.

The curves for the convex pad with central pivot, Case 5, in Figs. 10 and 11 show that this design is practically the equivalent of the flat pad with optimum pivot with regard to load capacity for the same minimum film thickness and that it has only a slightly higher temperature rise.

The same figures show curves for convex pads of two different crowns. Along each of these curves the crown is constant and equal to the value in terms of U and B which is stated in the figure. It will be noted that a smaller amount of crown is required at high load than at low load to give film thicknesses of the order of those for the flat pad with optimum pivot. This is because the film thickness, h_0, decreases with load while the ratio δ/h_0 must remain constant in order to give the greatest minimum film thickness.

EXPERIMENTAL CONFIRMATION

The analysis just presented was confirmed qualitatively by the use of a bearing provided with three interchangeable sets of pads and was similar to the familiar Kingsbury air-lubricated thrust-bearing model (11). The surfaces of the pads were lapped carefully and their profiles checked by optical flats. None of the pads were chamfered or relieved in any way and all were inspected carefully to insure absence of nicks and burrs. The principal characteristics of the three sets were as follows:

Set 1: Eccentrically pivoted $\left(\frac{\bar{x}}{B} = 0.6\right)$ and flat to within 5×10^{-6} in.

Set 2: Centrally pivoted and flat to within 5×10^{-6} in.

Set 3: Centrally pivoted and spherically convex with a crown of 50×10^{-6} in.

All tests were conducted with the same runner which was lapped flat over its entire surface to within 5×10^{-6} in.

In the first test the bearing was assembled with the eccentrically pivoted pads of set 1.[5] When the runner was spun by hand in the direction of pivot displacement (i.e., in the direction of U, Fig. 1) it immediately began to rotate freely on a film of air. However, upon attempting to start the bearing in the reverse direction, the runner immediately stuck to the pads, completely preventing hydrodynamic operation. Both of these observations are in accord with the predictions of the hydrodynamic theory.

In the second test the centrally pivoted flat pads of set 2 were used. Repeated attempt to start this bearing in the manner previously described failed to produce a hydrodynamic film in air for either direction of rotation. Therefore it can be concluded that a pad with a surface which closely approaches perfect flatness will not operate with a hydrodynamic film when the pivot is located in the center and air is used as the lubricant. This also is in accord with the predictions of the hydrodynamic theory but may appear to contradict experience. More will be said of this apparent contradiction later.

In the third test the spherically convex centrally pivoted pads of set 3 were employed. It was found that this bearing started easily in either direction in air and rotated freely on a hydrodynamic film. Again, this is in agreement with the predictions of the hydrodynamic theory as previously outlined for the convex pad.

All of the previous tests were repeated using carbon tetrachloride as the lubricant and were found to give the same results as in air. Carbon tetrachloride was chosen because of its low viscosity and also because it was desired to determine if an incompressible lubricant would perform the same as air.

As the second test, which showed that centrally pivoted pads of a high degree of flatness would not operate in air with a central pivot, appeared to be contradictory to the known satisfactory operation of the original Kingsbury air-lubricated bearing which also was equipped with centrally pivoted pads, the Kingsbury pads therefore were checked optically and found to be appreciably convex. Measurements showed that the center portions of the pads were reasonably flat but the edges were turned down as much as 75×10^{-6} in. Thus the Kingsbury pads should be expected to perform in the same manner as the pads of set 3, as was found to be the case.

Further confirmation of the present analysis is contained in Fig. 12 which shows the results of some previously unpublished tests by H. N. Kaufman, also of these laboratories. The figure shows the film thicknesses and the relative running positions of a convex pad carrying the same load but pivoted at different points. The pad was 3.4 in. $\times$ 2.6 in. and was lapped to a spherical crown of 2.3×10^{-4} in. which is equivalent to a radius of curvature of 525 ft. Film thickness was measured by small dial gages attached to the pad and bearing directly on the runner surface. An SAE 10 oil was used.

Although accurately flat, centrally pivoted pads also tested under similar conditions would not start under load and would seize quickly after being started without load, the convex, centrally pivoted pad started easily and could be run even with the pivot placed ahead of the center as shown in Fig. 12. This was not possible with a flat pad.

DISCUSSION

The preceding paragraphs show that when air is used as a lubricant the observed facts are not in disagreement with the predictions of the hydrodynamic theory and the paradox referred to

[5] This test and the two which follow were demonstrated during the presentation.

(a) (b)

FIG. 13 RELATIVE STARTING POSITIONS OF FLAT PAD AND CONVEX PAD

at the outset does not exist. With liquid-lubricated bearings the situation is also quite similar but is mitigated somewhat by the influence of variable viscosity and variable density. Relying on these influences, an accurately flat centrally pivoted pad will carry load with liquid lubricants. However, a convex pad relying on a more favorable film shape, is superior in that it can carry an appreciably greater load at the same minimum film thickness.

Although a high degree of flatness usually is striven for when manufacturing bearing pads, true flatness is a degree of perfection which is, of course, unattainable. A little reflection, however, will reveal that the usual lapping or scraping techniques will produce pads in which the departures from flatness usually will be in the direction of making the pad surface convex.

Again, even if a pad is perfectly flat before assembly, the deflections due to load and to temperature gradient are such as to make the surfaces of the pad convex while in actual operation. Here then are three, for the most part unsolicited, sources of convexity which contribute to the performance of centrally pivoted pads and which possibly explain the successful operation of such bearings in practice. It is the authors' belief that the successful performance of many supposedly flat pads with central pivots is due more to the pads actually being of a convex nature instead of flat, rather than the influence of variable viscosity and variable density.

The importance of convexity becomes greater as less-viscous fluids are used and as the film thicknesses become smaller. Under these conditions it is easily possible to make centrally pivoted pads "too flat" in which case it may be impossible to start a pad under load or to load it after having been started under no load. By incorporating the right amount of crown, such pads can be made to carry loads almost as large as flat pads with optimum pivots.

An important result of the present analysis is that it predicts the order of convexity required for best performance. Although optimum conditions are obtained when the crown is about one half the minimum film thickness, reasonably good results should be expected with crowns from one fourth to one times the minimum film thickness as may be inferred from Fig. 8. Since these values were obtained on the basis of no side flow, they can serve only as guides, especially if, for practical purposes, it is desirable to make the convex surface spherical rather than cylindrical.

The manner in which the proper crown is obtained is not particularly important, whether it be by machining or by load or temperature deflections. It is possible, therefore, to design so as to take advantage of any or all of these effects.

While crowning permits operation in either direction with a centrally placed pivot, it also aids considerably in starting under load if the load is not great enough to deform appreciably the surfaces elastically and/or plastically, see Figs. 13 (*a* and *b*). When a flat pad has been stopped under load as in Fig. 13(*a*), the film is squeezed down to a small thickness. As the force F, necessary to shear this film upon starting, is given by $F = \mu UBL/h$, the force required to slide the pad may be quite large since h can be very small; in fact, it can exceed easily the value for dry surfaces.

If, however, the pad is convex, not only is the average film thickness greater across the film, thus yielding a smaller value of F, but the starting operation tends to rotate the pad on its pivot and to roll a cushion of lubricant between the sliding surfaces. Thus a film of relatively large thickness is quickly available near the center of the pad without the necessity of dragging in lubricant from the leading edge. Such a bearing therefore should be less apt to wipe on starting.

CONCLUSIONS

The results of the present analysis and tests may be summarized as follows:

1 When operating in air, the load capacity of a truly flat centrally pivoted pad is theoretically zero. Experiments on pads approximately $1^1/_2$ in. $\times$ $1^1/_2$ in. and flat to within 5×10^{-6} in. confirm this prediction.

2 The variation of viscosity of a liquid with temperature accounts for part of the observed load capacity of flat centrally pivoted pads operating with liquid lubricants.

3 The variation of the density of a liquid with temperature accounts for only a small part of the load capacity of flat centrally pivoted pads operating with liquid lubricants.

4 Convexity, inadvertently obtained in machining and by load and temperature deflections in service, probably accounts for a large part of the observed load capacity of centrally pivoted pads.

5 Convexity is an important factor in establishing the load capacity of centrally pivoted pads. By controlling convexity, the load capacity of such bearings, in some cases, may be increased appreciably.

6 The optimum amount of crown (or degree of convexity) is about one half the minimum film thickness. Under these conditions a centrally pivoted convex pad is almost equivalent to a flat pad with the pivot located for maximum load capacity.

7 For light loads where elastic and/or plastic deformations of the surface are negligible, a convex pad has an important advantage over a flat pad in being able to start more easily.

BIBLIOGRAPHY

1 "Optimum Conditions in Journal Bearings," by A. Kingsbury, Trans. ASME, vol. 54, 1932, pp. 123–148.

2 "The Lubrication of Plane Surfaces," by A. G. M. Michell, *Zeitschrift für Mathematik und Physik*, vol. 52, 1905, pp. 123–137.

3 "Lubrication," by A. E. Norton, McGraw Hill Book Company, Inc., New York, N. Y., 1942, p. 77.

4 "Applying Bearing Theory to the Analysis and Design of Journal Bearings," by J. Boyd and A. A. Raimondi, Parts 1 and 2, *Journal of Applied Mechanics*, Trans. ASME, vol. 73, 1951, pp. 298–316.

5 Reference (3), chapter 6.

6 "An Analysis of the Parallel-Surface Thrust Bearing," by M. C. Shaw, Trans. ASME, vol. 69, 1947, p. 387.

7 "The Hydrodynamical Theory of Film Lubrication," by W. F. Cope, Proceedings of the Royal Society of London, England, series A, vol. 197, 1949, p. 201.

8 "On the Solution of the Reynolds Equation for Slider-Bearing Lubrication—II," by A. Charnes and E. Saibel, Trans. ASME, vol. 75, 1953, pp. 269–272.

9 "On Problems in the Theory of Fluid-Film Lubrication, With an Experimental Method of Solution," by A. Kingsbury, Trans. ASME, vol. 53, paper APM—53-5, 1931.

10 "The Theory of Film Lubrication," by R. O. Boswall, Longmans, Green & Company, London, England, 1928, chapter 4.

11 Reference (3), Fig. 4

Discussion

R. A. Baudry.[6] The authors are to be congratulated for a very clear and significant contribution to the theory of the pivoted-pad thrust bearing.

It is not only very interesting but very important to know that a relatively small amount of crowning of the pad is sufficient to permit a centrally supported thrust-bearing pad to work as efficiently as an offset pad. This feature permits a thrust bearing to operate efficiently in either direction of rotation and is of consequence from both the manufacturing and operating standpoints. Pivoted-pad thrust bearings have been made for many years with a central pivot. Recent tests on such a large thrust bearing as shown in Fig. 14, herewith, indicate that a thick tapered oil film is established very rapidly and remains an appreciable time after the machine has been stopped. It is interesting to note that for this particular bearing a temperature gradient of 1 deg C per in. of pad thickness corresponds to approximately a crowning of 0.001 in. which, according to the authors, is sufficient to explain the formation of the oil film. After stopping, the appreciable oil film shown in Fig. 14 is due in part to the temperature deformation of the pad.

[6] Manager, Mechanical Development Section, T&G Engineering Dept., 5-N-So., Westinghouse Electric Corporation, East Pittsburgh, Pa. Mem. ASME.

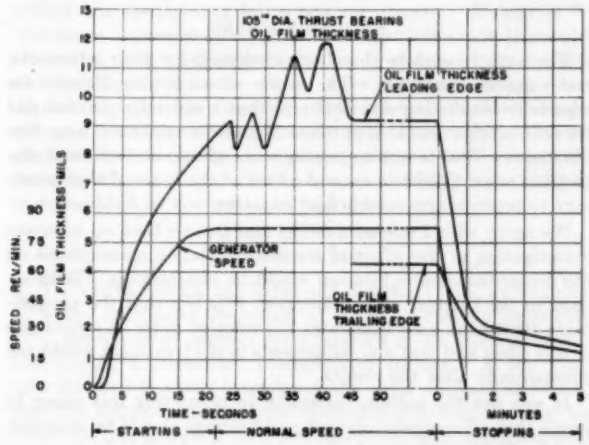

Fig. 14 Test Results on Pivoted-Pad Thrust Bearings

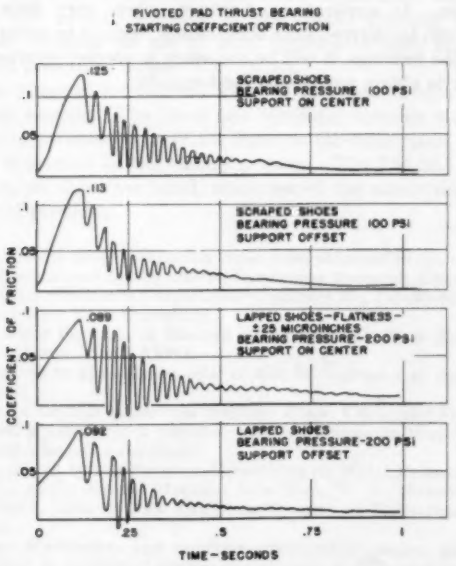

Fig. 15 Starting Coefficient of Friction for Pivoted-Pad Thrust Bearing

Other starting tests made recently on a small thrust-bearing testing machine indicate also that centrally and offset pivoted pads operate equally well. In Fig. 15 are shown four typical tests. The two upper ones are made with pads scraped to a surface plate; the two lower ones with pads having a lapped surface and having a crown smaller than 50 microin. as measured with an optical flat.

The pad with a lapped surface had a slightly smaller starting coefficient of friction but showed larger torque oscillations. These oscillations are self-induced and usually are present when starting a thrust bearing.

The starting period of a thrust bearing starting under load is the most critical interval of all operation on account of the solid and boundary friction and, therefore, there is a limit to the amount of crowning that should be given to the pads of such machines. Apparently, experience indicates that the normal manufacturing variations, temperature gradients, temperature and viscosity effects of the oil are sufficient to permit satisfactory operation of centrally pivoted thrust bearings.

F. Osterle[7] and E. Saibel.[8] As was pointed out in this paper, if adiabatic lubricant flow is assumed for the slider-bearing problem, it becomes necessary to take the variation of viscosity and density with temperature into account. There are several ways of doing this available in the literature. These involve varying degrees of computational difficulty.

The simplest technique is to consider the viscosity and density constant at values corresponding to the average of the inlet and outlet lubricant temperatures. The authors presumably employed this technique with the convex pad. A better approximation is to assume the viscosity to vary linearly with distance along the slider, the linearity constant being adjusted so as to satisfy the energy equation for adiabatic flow. The authors discuss this method in connection with the flat slider case. Recently the writers[9,10] developed a method for taking viscosity variation into account for convex pads of exponential form which is exact to the extent to which the viscosity variation with temperature is representable by an exponential.

Experience has shown that even the rough approximation afforded by the first method (constant viscosity at an average value) yields reasonably accurate results for the load capacity. However, such is not the case with the location of the center of pressure. The predicted location of this point is rather sensitive to the degree of approximation employed in taking the viscosity variation into account.

As an illustration of this, consider the authors' result that by imposing the condition that the center of pressure be at the midpoint of the pad and computing the load by the constant-viscos-

[7] Assistant Professor, Department of Mechanical Engineering, Carnegie Institute of Technology, Pittsburgh, Pa. Assoc. Mem. ASME.

[8] Professor, Department of Mathematics, Carnegie Institute of Technology. Mem. ASME.

[9] "On the Solution of the Reynolds Equation for Slider-Bearing Lubrication—IV: Effect of Temperature on the Viscosity," by F. Osterle, A. Charnes, and E. Saibel, Trans. ASME, vol. 75, 1953, pp. 1117–1123.

[10] "On the Solution of the Reynolds Equation for Slider-Bearing Lubrication—VI: The Parallel-Surface Slider Bearing Without Side Leakage," by F. Osterle, A. Charnes, and E. Saibel, Trans. ASME, vol. 75, 1953, pp. 1133–1136.

ity technique zero load is predicted while the linearly varying viscosity technique predicts an appreciable load.

As a further example, the authors' linearly varying viscosity treatment of the parallel-surface slider predicts a center of pressure very nearly at the mid-point of the pad, Fig. 5 of the paper. This fact figures in the authors' conclusion that density variation alone is incapable of accounting for the load capacity of centrally pivoted pads.

Our exact treatment of the parallel-surface slider bearing, taking account of both density and viscosity variations, predicts a center of pressure considerably upstream of the mid-point of the pad (see Fig. 1[10]), which presents a slightly better case for the "density wedge" as being, partially at least, responsible for the load capacity of centrally pivoted pads.

In the light of the foregoing discussion we think that an interesting investigation would be the determination of the sensitivity of center-of-pressure determinations to the way in which viscosity variations are taken into account.

R. B. Thicke.[11] The authors are to be complimented on this original and interesting paper. It will, no doubt, interest engineers throughout the country who are involved in thrust-bearing design.

Our assumptions for purposes of calculation are that the inclination of the shoe is determined by variation of viscosity and location of support. We assume that load capacity depends on inclination of the shoe, speed, average viscosity, and side leakage. These can be translated into a chart which provides rapid calculation on a trial-and-error basis and gives results which are not much different from those of Norton's "no side-leakage" method or Kingsbury's optimum-conditions method.

Our experience has shown that a shoe with a support over a small area near the center will become convex in operation, although probably to a greater extent than the authors propose. Evidently this explains why a shoe with a central support works nearly as well as one with a support at the optimum position.

Because pressure is higher at the center of the shoe, the shoe will become concave if supported over a large area provided the shoe is of such dimensions as to allow the pressure to overcome temperature distortion. Mr. Gynt[12] found that the operation of spring-mounted bearings was improved by concentrating the supporting springs toward the center of the shoe to eliminate concavity. The authors' paper helps to explain Mr. Gynt's findings.

One point which the writer feels should be stressed is the danger of application of the authors' theory to bearings such as vertical water-wheel-generator thrust bearings which must start under load. As static load on a bearing with shoes of a convex profile probably would be concentrated over a small area, the danger of a wipe would be increased at the instant of start-up even though the tendency of the shoes to roll would build up an oil film rapidly. The writer believes further experiments are necessary before a convex-profiled shoe should be used in such an application.

However, because of the cost, the possibility of controlling the profile during manufacture seems remote even though theoretically a considerable improvement in operation will result. This leaves the design engineer with the interesting problem of flexibilities and temperature distortion if an attempt is made to control the profile during operation.

Authors' Closure

The authors wish to thank the discussers for their interesting and valuable comments. The curves shown by Mr. Baudry are especially interesting and illustrate that a centrally pivoted pad thrust bearing is capable of operating with a relatively large film thickness. This is not surprising since elastic and thermal distortions are sufficient to cause a crown of the order of that necessary to produce appreciable load capacity.

We agree with Professors Saibel and Osterle that an accurate investigation of the effect of viscosity-variation assumptions on the center-of-pressure location would be enlightening. With regard to the thermal wedge, however, it is felt that the approximate treatment used illustrates the relative order of magnitude of this effect and that any refinements in the treatment would not substantially alter the results.

It was not the authors' intention in presenting this paper to imply that all centrally pivoted pad bearings should be crowned. As Mr. Thicke points out, this may not be feasible in some applications. The beneficial effects of variable viscosity and variable density will in many cases be sufficient to permit successful operation. In applications, however, where very little or no benefit can be derived from these effects, such as in water or air-lubricated bearings, it will be necessary to employ crowned pads in order to obtain appreciable load capacity.

[11] Engineer, Product Design Section, Canadian Westinghouse Company, Ltd., Hamilton, Ontario.

[12] "Recent Development of Bearings and Lubrication Systems for Vertical Generators," by S. Gynt, *ASEA Journal*, vol. 20, 1947, pp. 72–87.

The Mechanics of the Simple Shearing Process During Orthogonal Machining[1]

By BERNARD W. SHAFFER,[2] NEW YORK, N. Y.

In the orthogonal machining operation, a continuous chip is often produced by the simple shearing process, which is characterized by the existence of a shear line extending from the tip of the tool to the intersection of the free surfaces of the workpiece and chip. Chip formation by this process is analyzed, and analytical expressions are developed for the force required to machine a given material with a tool having a prescribed coefficient of friction. It is found that when the friction angle is less than the rake angle, the solution is obtained by seeking the condition for which the machining force is a minimum. However, for the more common case, when the friction angle is greater than the rake angle, the solution is obtained by seeking the machining force for which there exists a limiting stress distribution within the chip. Both these solutions are developed from a common foundation. Expressions also are derived for the chip-thickness ratio, as well as for the deformation to be expected when an initially squared grid is embedded in the material being cut.

Introduction

SEVERAL years ago Ernst and Merchant (1, 2, 3)[3] analyzed the machining operation in order to find an expression for the force required to machine a given material with a tool having a prescribed coefficient of friction. A few years later Lee and Shaffer (4) analyzed the same problem and found that the influence of the stress distribution within the chip, between the tool and shear line, previously had been neglected, even though it had a marked influence on the final solution to the problem. Consequently, they proceeded to find a new expression which also took into account the stress distribution within the chip. The over-all solution to the simple shearing process, however, requires the use of both expressions, each applicable within a prescribed range.[4]

Each phase of the over-all solution had been developed in a different manner. The Ernst and Merchant solution was based on finding extreme values of the stress on the shear plane, and the power consumed in the cutting process. The Lee and Shaffer solution, on the other hand, made use of the newly developed theory of plasticity.

It is the purpose of this paper to re-examine the problem in order to show how the afore-mentioned solutions may also be obtained by starting from a common foundation and proceeding along similar lines of reasoning.

Basic Considerations

In this paper the cutting process will be analyzed when a continuous chip is formed by simple shearing action, as a tool moves parallel to the surface of the workpiece. The simple shearing process is characterized by the appearance of a single line of demarcation between the uncut material and the chip being formed, going from the tip of the tool to the intersection of the free surface of the workpiece and chip. This line, known as the shear line, can be seen by looking at photomicrographs taken while the chip is being formed (1, 6).

The face of the tool is assumed plane, meeting the noncutting surface in a straight line which is parallel to the undisturbed surface of the workpiece. The surface of the newly formed chip is also parallel to this line. Such a cutting process is usually referred to as orthogonal machining.

In machining practice it is common for the depth of cut to be small compared with the width of the tool. Therefore it is reasonable to assume that aside from end conditions, the stress distribution in every section taken perpendicular to the width of the tool is the same as in every other section. This means, of course, that the cutting process may be analyzed as a problem of plane strain.

A continuous chip usually is formed when a ductile material is being cut because only a ductile material could undergo the required deformation and still maintain continuity with the uncut portion. Every particle within the material undergoing this deformation does so at a relatively high rate of strain. It has been observed (7, 8, 9) that the rate of strain has a marked influence on the stress-strain law of ductile materials. In particular, as the rate of strain increases, the yield point increases, and the stress-strain curve in the plastic range flattens out and approaches a line parallel to the strain axis. This influence will be taken into consideration by using in the analysis a non-work-hardening stress-strain law. Even lead, which is known to have a rounded stress-strain law, was observed (10) to conform closely to the theory based on a non-work-hardening law, when stressed up to the yield point at a reasonably high rate of strain. Therefore the formulas to be developed can be expected to give good results even when materials other than steel are to be cut.

Since the order of magnitude of the shearing strain which occurs during the machining process is much greater than the order of magnitude of the shearing strain which occurs during elastic deformation, it is permissible to neglect all elastic strains in the analysis. This essentially means that if an area of the chip or work is one in which there is also no plastic flow occurring then it can be treated as a rigid region.

The analysis of the simple shearing process in machining, therefore, reduces to the study of a plane-strain problem in which a chip is formed by the shearing action of a non-work-hardening material. Two types of regions may exist, a rigid region, and a region in which plastic flow occurs.

The stress components on an element in either one of these re-

---

[1] The results presented in this paper were obtained in the course of research sponsored by the Office of Ordnance Research, Department of the Army (Ordnance Corps) under Contract No. DA-30-069-ORD-609, with New York University.

[2] Associate Professor of Mechanical Engineering, New York University. Assoc. Mem. ASME.

[3] Numbers in parentheses refer to the Bibliography at the end of the paper.

[4] Soon after this paper was written, Shaw, Cook, and Finnie (5) published a paper which together with the discussion that followed may be of interest to the reader.

Contributed by the Research Committee on Metal Processing and presented at the Annual Meeting, New York, N. Y., November 29–December 4, 1953, of The American Society of Mechanical Engineers.

Note: Statements and opinions advanced in papers are to be understood as individual expressions of their authors and not those of the Society. Manuscript received at ASME Headquarters, June 3, 1953. This paper was not preprinted.

gions must satisfy the equation of motion. Since, however, the mass of the material involved in the cutting process is so small, the inertia terms may be neglected, and the equation of motion, therefore, reduces to the equation of equilibrium. Furthermore, if the element is in the plastic region then the stress components also must satisfy the yield condition.

It was Saint Venant (11) who first expressed the Tresca yield condition as it applied to plane-strain problems. Using rectangular Cartesian co-ordinates with flow parallel to the x, y-plane, he found that the Tresca yield condition takes the form

$$\left(\frac{\sigma_x - \sigma_y}{2}\right)^2 + \tau^2 = k^2 \quad \ldots\ldots\ldots\ldots [1]$$

where k is the maximum shear stress, equal to one half the tensile yield stress of the material. This expression must be satisfied by the stress components on an element in an elastic region which is stressed up to the yield point, as well as by the stress components on an element in the plastic region where yielding is in progress. The latter condition holds because the stress-strain law is non-work-hardening.

In plane-strain problems it is often convenient to represent the state of stress at a point in an elastic body, as a point on a Mohr-circle diagram (12). If the components of stress are given as σ_x, σ_y, and τ, then (σ_x, τ) and $(\sigma_y, -\tau)$ are two points on the circle, whose radius squared is equal to

$$\left(\frac{\sigma_x - \sigma_y}{2}\right)^2 + \tau^2$$

By comparing this expression with Equation [1], it is found that when yielding occurs the radius of Mohr's circle is equal to k.

It can be seen by looking at a circle diagram drawn to satisfy the yield condition, that there exist two mutually perpendicular directions in which the normal stresses are equal to each other, and shear stress is equal to the maximum value k.

The Shear Line

Let us analyze chip formation during machining, by considering the motion of a particle within the uncut material, which eventually becomes part of the chip. Such an analysis will depend on the relative motion between the particle and the tool and is therefore equally applicable when either the tool or the workpiece is in motion.

Some distance from the tool the particle under consideration is stress-free and moves toward it with a constant velocity. As it approaches its stress increases until it reaches its maximum value at the shear line. There yielding occurs and its velocity is changed so that it will move along the face of the tool. After passing through the shear line, the particle enters a highly stressed region and then soon afterward a nonstressed region. It then continues to move up the face of the tool due to its continuity with the particles behind it.

In order to obtain a complete solution to the machining operation it will be necessary to satisfy both the velocity and stress requirements of the problem, some of which were just described. Therefore the velocity requirements will be studied in this section and the stress requirements will be studied in the next section.

Let us call the velocity of approach for each element in the uncut material U, and the velocity of each element in the chip V. These two constant-velocity regions are separated by the shear line. Since these regions are continuous and do not separate or overtake each other during the cutting process, their velocity components perpendicular to the shear line are equal to each other. It is, therefore, permissible to equate normal components of velocity for an element on either side of the shear line, which is shown to be an arbitrary curve AB in Fig. 1 and obtain the relationship

$$U \sin \theta = V \sin \alpha \sin \theta + V \cos \alpha \cos \theta \quad \ldots\ldots [2]$$

where α is the rake angle, and θ is the angle between the tangent to the curve and the horizontal axis. Divide Equation [2] by

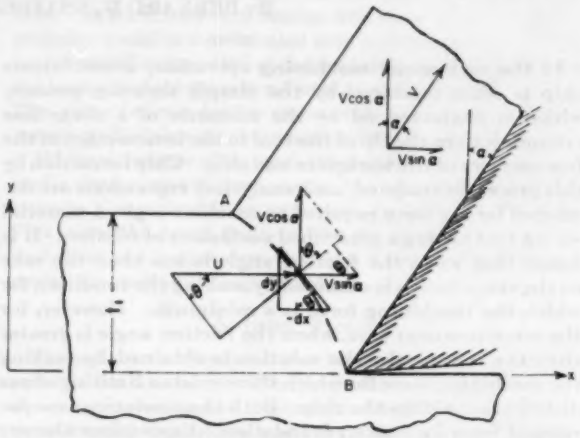

Fig. 1 Relative Velocity Vectors for Particles Within the Material Being Cut

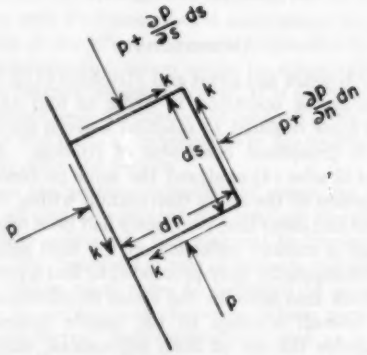

Fig. 2 An Element on the Straight Shear Line

$\cos \theta$, and set $\tan \theta = -dy/dx$, to find the differential equation for the shear line

$$U\,dy = (V \sin \alpha)dy - (V \cos \alpha)dx \quad \ldots\ldots [3]$$

When integrated, it becomes

$$y = -\frac{V \cos \alpha}{U - V \sin \alpha} x + \text{const} \quad \ldots\ldots [4]$$

which is the equation for a straight line. We see, therefore, that in order to satisfy continuity requirements, shear must occur along a straight line.

Every element on this straight shear line is subjected to stresses which satisfy the yield condition. This means that the shear-stress components have reached their maximum value k along the shear line, and the normal stress components p may vary from point to point. At any particular point the normal stresses on two orthogonal surfaces are equal to each other. They are, of course, compressive stresses, because they are induced by pressing the tool against the workpiece.

A typical element on the straight shear line is shown in Fig. 2.

The normal stress is shown to vary arbitrarily along the perpendicular to the shear line, but the shear stress is, of course, constant along the line. Nevertheless, the stress components must satisfy the equilibrium equation, which may be applied in the normal and tangential directions.

The equation of equilibrium in the normal direction reduces to $\partial p/\partial n = 0$ and in the tangential direction reduces to $\partial p/\partial s = 0$. Both these equations are satisfied only if p is a constant.

We have seen, therefore, that for the machining operation under consideration, shear occurs along a straight line along which the shear stress and normal stress are constant.

Force Relationships

During the machining process the resultant force applied to the tool distributes itself along the chip-tool interface and is then transmitted through the chip to the shear line, where yielding occurs. Because of friction between the tool and the chip, the actual force distribution along this surface may be resolved into normal and tangential components which are related by the coefficient of friction. Yielding occurs along the shear line. The stress component along the shear line, therefore, is k while the stress component perpendicular to this line is, of course, p. These surfaces are the only ones on which forces are acting, and since the chip is in equilibrium, these forces are equal to each other.

We are only interested in obtaining an expression for the resultant force necessary for machining. Therefore let us replace the actual force distribution along the tool by a resultant F, which can be expressed in terms of its components F_t and F_n directed parallel and perpendicular to the uncut surface. These components are related to each other by the friction angle β and the rake angle α, for it can be seen in Fig. 3 that if β is the angle between the resultant force F and the normal to the tool surface, then the angle lmn is equal to $(\beta - \alpha)$ and

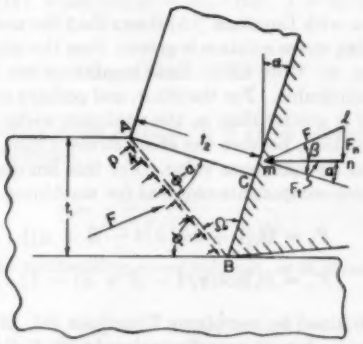

Fig. 3 Force Distribution on the Chip

$$F_n = F_t \tan(\beta - \alpha) \quad [5]$$

As we pointed out earlier in this section, the tool force F is equal in magnitude to the resultant applied along the shear line A-B. For a unit width of tool, this is equal to the vector sum of the normal stress p and the shear stress k, each multiplied by the length of shear line. Its length, from the geometry of Fig. 3, is $t_1/\sin\varphi$, where t_1 is the depth of cut, and φ is the shear angle. The resultant tool force, therefore, has components parallel and perpendicular to the uncut surface equal to

$$F_t = pt_1 + kt_1/\tan\varphi \quad [6a]$$

$$F_n = pt_1/\tan\varphi - kt_1 \quad [6b]$$

When we substitute these expressions into Equation [5] and solve for p, we find

$$p = k\tan(\varphi + \beta - \alpha) \quad [7]$$

The normal stress p is a function of the shear angle φ. This angle, however, has not yet been evaluated. In order to do so, it is necessary to obtain another expression in which these quantities occur.

This other relationship will be found by seeking a solution which will yield a minimum machining force and at the same time result in a satisfactory stress distribution within the chip.

Ernst and Merchant (1, 2, 3) found the angle φ for which the machining force F_t is a minimum by simply setting its derivative equal to zero. Let us apply this same reasoning to our equation.

Machining force, as a function of φ, is obtained by substituting Equation [7] into Equation [6a], and found to be

$$\frac{F_t}{kt_1} = \tan(\varphi + \beta - \alpha) + \cot\varphi \quad [8]$$

When this expression is differentiated[5] and set equal to zero, it becomes

$$\cos^2(\varphi + \beta - \alpha) - \sin^2\varphi = 0 \quad [9]$$

which can be rewritten

$$\cos(2\varphi + \beta - \alpha)\cos(\beta - \alpha) = 0 \quad [10]$$

Equation [10] is satisfied whenever the argument of the cosine is equal to $\pi/2$, that is, whenever

$$\varphi = \frac{\pi}{4} - \frac{\beta}{2} + \frac{\alpha}{2} \quad [11]$$

With an explicit expression for the shear angle, it is now possible to evaluate the normal stress p and of course the force components F_n and F_t. The expression for F_t is found by substituting Equation [11] into Equation [8] thereby obtaining

$$\frac{F_t}{kt_1} = 2\cot\left(\frac{\pi}{4} - \frac{\beta}{2} + \frac{\alpha}{2}\right) \quad [12]$$

while the expression for F_n is found by substituting Equations [11] and [7] into Equation [6b], thereby obtaining

$$\frac{F_n}{kt_1} = \frac{2}{\csc(\beta - \alpha) - 1} \quad [13]$$

We have seen, therefore, that for a given machining operation with a prescribed friction angle β, the minimum machining force F_t is given by Equation [12] and the corresponding shear angle φ is given by Equation [11]. This minimum force is the actual machining force whenever the stress distribution within the chip is satisfactory, that is, whenever the applied force can be transferred to the shear line without exceeding the yield point. Under this condition, yielding will occur only along the shear line. Since it can be shown that the shear angle is directly related to the maximum stress within the chip, let us be sure that the chip stress is satisfactory for any angle φ specified by Equation [11]. This can be done by discussing the importance of the wedge angle Ω.

The wedge angle Ω is the angle between the shear line and the face of the tool. It can be seen from Fig. 3 that Ω is related to the shear angle φ by the expression

$$\Omega = \frac{\pi}{2} - \varphi + \alpha \quad [14]$$

[5] In performing the differentiation, it was assumed, as did Ernst and Merchant in their analysis, that β is an independent variable. This was done so that the expression for φ given by Equation [11] would coincide with their result. Even though this assumption is questionable (5, 13) it is repeated here in order to complete the discussion on the mechanics of the simple shearing process.

As φ increases, the wedge angle decreases. However, this decrease is accompanied by an increase in the stress intensity within the chip itself, because the same force is then distributed through a smaller area. For some limiting value of φ the maximum stress intensity at a point within the chip just reaches the yield point. In terms of the Mohr-circle diagram mentioned earlier, this means the radius of the circle just equals k. For larger values of φ the yield point would be exceeded, and plastic flow would occur. During the machining operation under consideration, plastic flow occurs only along the shear line and not within the chip. Therefore shear angles larger than this limiting value cannot occur.

It is certainly possible that for the shear angle specified by Equation [11] the corresponding wedge angle

$$\Omega = \frac{\pi}{4} + \frac{1}{2}(\beta + \alpha) \quad [15]$$

is so small that the yield condition at the most highly stressed point within the chip is violated (4). The limiting wedge angle should be found, to be sure that the angle Ω specified in Equation [15] is greater than, or at least equal to, the minimum allowable value.

The most highly stressed point within the chip is at the very tip of the tool, because, although elastic unloading will probably encroach into the triangular region between the shear line and the tool, it will not reach the apex.

An enlarged view of this element and the corresponding circle diagram are shown in Fig. 4 (a and b). Its radius is shown equal to the maximum possible value, namely, k, so that the information obtained from this diagram corresponds to the limiting stress condition.

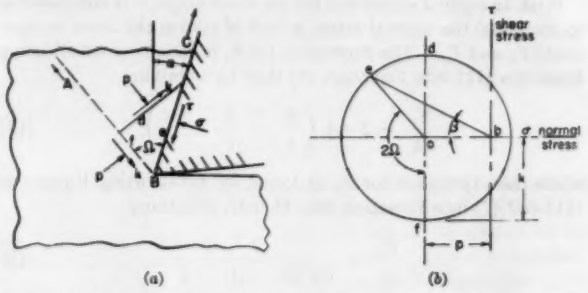

FIG. 4(a) ENLARGED VIEW OF AN ELEMENT IN THE CHIP AT THE BASE OF THE TOOL

FIG. 4(b) CORRESPONDING MOHR CIRCLE DIAGRAM

The points in Fig. 4 were labeled so that their co-ordinates represent the stress components on the corresponding surfaces of the element. For example, the stress components of surface f is given by the co-ordinate of point f. Surface f lies directly on the shear line and is, therefore, subject to a normal stress p and a shear stress k. These values are indicated on the circle diagram.

The stresses on surface e, which is in direct contact with the tool, are also shown on the same diagram. If Ω is the angle between surface e and f, then the stress along the tool at this point is given by the co-ordinates of point e on Mohr's circle, located 2Ω counterclockwise from f. Point e is shown in the upper half plane because the frictional force, which always acts opposite to the direction of motion, is directed toward the point B.

Angle ebo represents the friction angle β between the chip and tool, because the ratio of shear stress to normal stress at the face of the tool gives the coefficient of friction $\mu = \tan \beta$. The friction angle also can be written in terms of the wedge angle

$$\tan \beta = \frac{\tau_e}{\sigma_e} = \frac{-k \cos 2\Omega}{p + k \sin 2\Omega} \quad [16]$$

From this equation, another expression for the normal stress on the shear line can be found by substituting Equation [14] into the foregoing and obtaining

$$p = \frac{k \cos(2\varphi - 2\alpha + \beta)}{\sin \beta} \quad [17]$$

Equation [17] applies only when a limiting stress condition exists in the chip. We saw previously that the normal stress was given by Equation [7] for all stress conditions within the chip, and therefore certainly for the limiting stress condition. An equality can be written between these two expressions

$$\frac{\cos[2(\varphi - \alpha + \beta) - \beta]}{\sin \beta} = \tan(\varphi - \alpha + \beta) \quad [18]$$

only when the limiting stress solution applies. The corresponding shear angle φ can be found by first rewriting[6] Equation [18] to read

$$\frac{\cos 2(\varphi - \alpha + \beta)\cos(\varphi - \alpha)}{\cos \beta \cos(\varphi - \alpha + \beta)} = 0 \quad [19]$$

and then setting the argument of the cosine equal to $\pi/2$. This yields

$$\varphi = \pi/4 - \beta + \alpha \quad [20]$$

an expression for the shear angle for the limiting stress condition.

In view of Equations [14] and [20], the minimum permissible wedge angle is given by the expression

$$\Omega_{min} = \pi/4 + \beta \quad [21]$$

A comparison with Equation [15] shows that the wedge angle for the nonlimiting stress solution is greater than the minimum when β is less than α. Only under these conditions can the previous solution be applicable. For the other, and perhaps more common case, when β is greater than α, the minimum wedge angle determines the solution, because the shear stress within the chip has then attained its maximum value. For this limiting stress condition the force components required for machining are given by

$$F_t = kt_1[1 + \cot(\pi/4 - \beta + \alpha)] \quad [22a]$$

$$F_n = kt_1[\cot(\pi/4 - \beta + \alpha) - 1] \quad [22b]$$

which are obtained by combining Equations [6], [20], and [7].

In order to see how the nondimensional term F_t/kt_1 varies with friction angle β for a given rake angle α, it is plotted against this variable in Fig. 5. For convenience, an auxiliary scale of μ, the coefficient of friction, also is shown. Equation [22a] was used to plot these curves when β is greater than α, whereas Equation [12] was used when β is less than α. It can be seen from these curves that the machining force F_t increases with increasing friction and decreases with increasing rake angle.

It should be noted that for $\beta \geq \pi/4$, the machining force is shown to be constant. This is perfectly valid because for all those cases shown, $\Omega = \pi/4 + \beta$, and the shear stress at the tool-chip interface, given by Equation [16] as $-k \cos 2\Omega$, becomes $k \sin 2\beta$. When $\beta = \pi/4$, the shear stress is, of course, equal to k. However, this is the maximum frictional stress the chip can withstand, because the material itself shears at this point. Therefore, for larger values of β, shear flow occurs within the material rather than frictional slip between the two surfaces, and the force required is, of course, the same as required when $\beta = \pi/4$.

[6] In order to obtain Equation [19], it was found useful to make use of the equality $\cos(2A - B) = \cos 2A \cos B + 2 \sin A \cos A \sin B$.

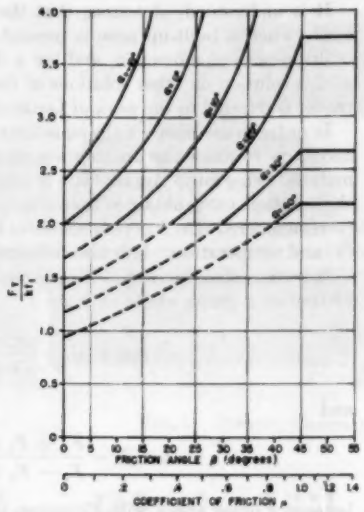

FIG. 5 MACHINING FORCE AS A FUNCTION OF FRICTION

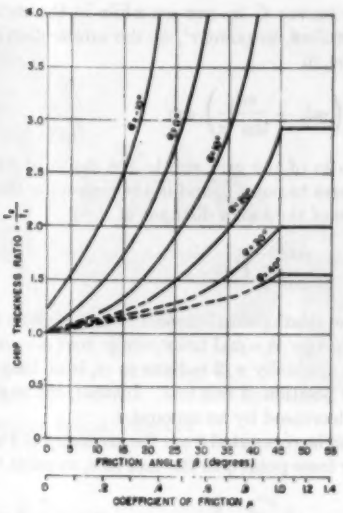

FIG. 6 CHIP-THICKNESS RATIO AS A FUNCTION OF FRICTION

CHIP THICKNESS AND GRID DEFORMATION

The chip-thickness ratio r is defined as the ratio between the thickness of chip t_2 and the initial depth of cut t_1. It can be evaluated by referring to the geometry of our solution.

If in Fig. 3, A-C is drawn perpendicular to the face of the tool, then angle BAC is the complement of angle ABC and, in view of Equation [14], equal to $(\varphi - \alpha)$. But, A-$B \sin \varphi = t_1$, and A-$B \cos (\varphi - \alpha) = t_2$. Therefore,

$$r = \frac{\cos (\varphi - \alpha)}{\sin \varphi} \quad \ldots\ldots\ldots\ldots\ldots\ldots [23]$$

For the limiting stress solution, φ is given by Equation [20] and this ratio becomes

$$r = \frac{\cos (\pi/4 - \beta)}{\sin (\pi/4 - \beta + \alpha)} \quad \ldots\ldots\ldots\ldots [24a]$$

whereas for the nonlimiting stress solution, φ is given by Equation [11] and

$$r = \frac{\cos (\pi/4 - \beta/2 - \alpha/2)}{\sin (\pi/4 - \beta/2 + \alpha/2)} \quad \ldots\ldots\ldots\ldots [24b]$$

These solutions are shown in Fig. 6 where the chip-thickness ratio r is plotted against the angle of friction for tools with various rake angles. It can be seen that the ratio t_2/t_1 increases with increasing friction and decreases with increasing rake angle. This holds true until $\beta = \pi/4$, for above this value it takes on the modified form explained previously.

Grid deformation will depend on the velocity of approach U, and the velocity of the chip V. It was shown previously that these velocities are related by Equation [2]. When that relationship was first written, it was assumed that the shear line might be curved. Since then, however, we have seen that for the machining operation under consideration, it is actually a straight line. Therefore θ is constant and has since been referred to as φ. In view of this, Equation [2] can be rewritten to read

$$U \sin \varphi = V \cos (\varphi - \alpha) \quad \ldots\ldots\ldots\ldots [25]$$

Since this equation gives the relationship between the velocity of all particles in the uncut material and in the newly formed chip,

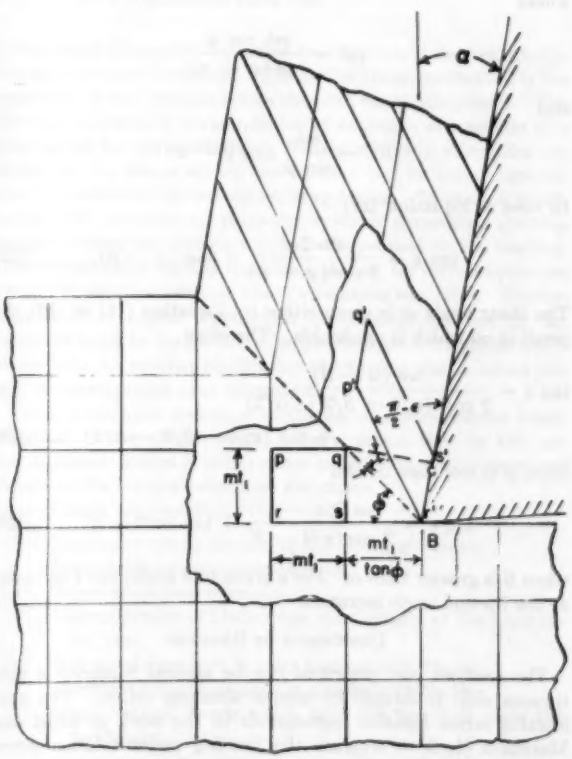

FIG. 7 DEFORMATION OF AN ORIGINALLY SQUARED GRID

it is possible to determine the deformation of an initially squared network embedded in the work material, by calculating the movement of the grid in a finite period of time. After completing such a calculation, it can be seen that all points on a grid line parallel to the uncut surface remain parallel to the tool. Those lines which are perpendicular to the uncut surface do not remain perpendicular to the tool.

This effect can be seen by studying the movement of element

$pqrs$ in Fig. 7. Point r moves U in. per sec while in the uncut material. It moves, therefore, to point r', at the intersection of the tool face and shear line, in

$$\frac{1}{U}\left(mt_1 + \frac{mt_1}{\tan\varphi}\right)\sec$$

The constant m is the ratio of the grid size to the depth of cut. In mt_1/U sec, point p moves to point q, and in the remaining time moves parallel to the face of the tool a distance of

$$\frac{mt_1}{U\tan\varphi}\,V \text{ in.}$$

to the point p'. From the relationship between U and V given in Equation [25] it is seen that qp' is equal to $mt_1\cos\varphi/\cos(\varphi-\alpha)$.

The line pq which was originally $\pi/2$ radians to rs, is no longer perpendicular to the new position of this line. Instead, the angle between these lines has decreased by an amount ϵ.

This angular change can be computed from the geometry of Fig. 7. Drop a perpendicular from point q to the tool face, at point C. Then notice that

$$\tan(\pi/2-\epsilon) = \frac{mt_2}{qp' + BC} \quad \ldots\ldots\ldots\ldots [26]$$

where

$$qp' = \frac{mt_1\cos\varphi}{\cos(\varphi-\alpha)}$$

and

$$BC = \frac{mt_1}{\sin\varphi}\sin(\varphi-\alpha)$$

In view of Equation [23]

$$\tan\epsilon = \frac{\sin 2\varphi}{2\cos^2(\varphi-\alpha)} + \tan(\varphi-\alpha) \quad \ldots\ldots [27]$$

The shear angle φ is given either by Equation [11] or [20], depending on which is applicable. Therefore

$$\tan\epsilon = \frac{\cos(\alpha-\beta)}{2\cos^2(\pi/4-\beta/2-\alpha/2)} + \tan(\pi/4-\beta/2-\alpha/2) \quad \ldots\ldots [28]$$

when β is less than α, and

$$\tan\epsilon = \frac{\cos 2(\alpha-\beta)}{2\cos^2(\pi/4-\beta)} + \tan(\pi/2-\beta) \quad \ldots\ldots [29]$$

when β is greater than α. For a given tool angle, $\tan\epsilon$ decreases as the friction angle increases.

Discussion of Results

The analysis just presented can be applied whenever a continuous chip is formed by simple shearing action. The nonlimiting stress solution corresponds to the work of Ernst and Merchant (1, 2, 3) whereas the limiting stress solution corresponds to work of Lee and Shaffer (4). It is interesting to see that by following the approach presented in this paper, both of these ideas were developable from the same foundation. By doing this, not only were we able to show the similarity between the two solutions, but at the same time it was possible to emphasize the importance of considering the stress within the chip. Furthermore, it should be noted that current, as yet unpublished, work indicates that this approach to the problem is readily extendable to the analysis of other machining operations.

It is understood, of course, that the results described do not apply when a built-up nose is present. For an analysis of the built-up-nose phenomenon, and for a discussion of the influence of this solution on other solutions of the machining problem, the reader is referred to the work of Lee and Shaffer (4).

In order to use many of the equations derived in this paper, it is necessary to know the appropriate maximum shear stress of the material being cut. Appropriate is used here to mean more than the constant value obtained from a simple shear test, for it should be remembered that k is very sensitive to variations in strain rate (9) and temperature. It is also influenced by size effect (13, 14).

It is suggested, in view of these complications, that data can be plotted on a graph whose axes are

$$\tan\varphi = \frac{\cos\alpha}{r-\sin\alpha} \quad \ldots\ldots\ldots\ldots [30]$$

and

$$\tan\beta = \frac{F_n + F_t\tan\alpha}{F_t - F_n\tan\alpha} \quad \ldots\ldots\ldots\ldots [31]$$

because a quick check with Equation [12] or [22] will show that the shear stress k is a common factor in the numerator and denominator of Equation [31] and therefore the axes are independent of the shear stress.

It should be re-emphasized that the simple shearing process is described by the nonlimiting stress solution whenever the friction angle is less than the rake angle. However, whenever the friction angle is greater than the rake angle, the stress distribution within the chip controls, and the machining operation is then described by the limiting stress solution.

BIBLIOGRAPHY

1 "Chip Formation, Friction, and High Quality Machined Surfaces," by H. Ernst and M. E. Merchant, from "Surface Treatment of Metals," Trans. ASM, vol. 29, 1941, pp. 299–378.

2 "Mechanics of the Metal Cutting Process. I. Orthogonal Cutting and a Type 2 Chip," by M. E. Merchant, *Journal of Applied Physics*, vol. 16, 1945, pp. 267–275.

3 "Mechanics of the Metal Cutting Process. II. Plasticity Condition in Orthogonal Cutting," by M. E. Merchant, *Journal of Applied Physics*, vol. 16, 1945, pp. 318–324.

4 "The Theory of Plasticity Applied to a Problem of Machining," by E. H. Lee and B. W. Shaffer, *Journal of Applied Mechanics*, Trans. ASME, vol. 73, 1951, pp. 405–413.

5 "The Shear-Angle Relationship in Metal Cutting," by M. C. Shaw, N. H. Cook, and I. Finnie, Trans. ASME, vol. 75, 1953, pp. 273–288.

6 "The Effect of Cutting Fluid Upon Chip-Tool Interface Temperature," by M. C. Shaw, J. D. Pigott, and L. P. Richardson, Trans. ASME, vol. 73, 1951, pp. 45–56.

7 "Some Factors Affecting the Plastic Deformation of Sheet and Strip Steel and Their Relation to the Deep Drawing Properties," by J. Winlock and R. W. Leiter, Trans. ASM, vol. 25, 1937, pp. 163–205.

8 "High Speed Testing of Mild Steel," by J. H. Hollomon and C. Zener, Trans. ASM, vol. 32, 1944, pp. 111–122.

9 "The Testing of Materials at High Rates of Loading," by G. I. Taylor, *Journal of the Institution of Civil Engineers*, vol. 26, 1946, pp. 486–519.

10 "The Theory of Wedge Indentation of Ductile Materials," by R. Hill, E. H. Lee, and S. J. Tupper, Proceedings of the Royal Society of London, England, series A, vol. 188, 1947, pp. 273–289.

11 "Sur l'Établissement des Équations des Mouvements Intérieurs Opérés Dans les Corps Solides Ductiles au Delà des Limites où l'Élasticité Pourrait les Ramener a leur Premier État," by B. de Saint Venant, Comptes Rendus, Acad. Sci., Paris, France, vol. 70, 1870, pp. 473–480.

12 "Theory of Elasticity," by S. Timoshenko and J. N. Goodier, McGraw-Hill Book Company, Inc., New York, N. Y., 1951, pp. 13–17.

13 "An Analysis of the Mechanics of Metal Cutting," by D. C. Drucker, *Journal of Applied Physics*, vol. 20, 1949, pp. 1013–1021.

14 "The Size Effect in Metal Cutting," by W. R. Backer, E. R. Marshall, and M. C. Shaw, Trans. ASME, vol. 74, 1952, pp. 61–71.

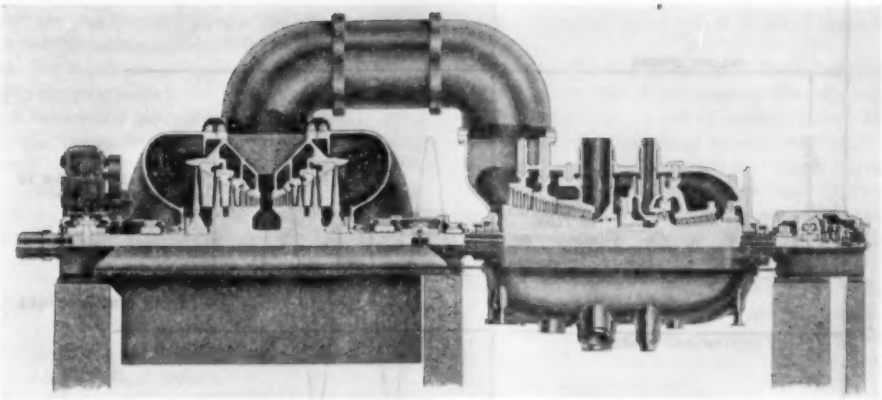

FIG. 1 TYPICAL CENTRAL-STATION STEAM TURBINE

Turbine-Blade Vibration and Strength

BY W. E. TRUMPLER, JR.,[1] AND H. M. OWENS,[2] PHILADELPHIA, PA.

In the design of turbines, the strength of the blades is a matter of great importance since blading is the heart of the turbine. The authors discuss the factors which affect the strength of turbine blades and show what recent progress has been made and what studies are under way toward improved blade designs. The discussion is limited to the full-admission type of blade row which is subjected to steam flow through its full annulus, the most common type of blade row. A discussion of the problems of designing partial-admission rows was given by R. P. Kroon[3] in a paper presented before the Society in 1939.

OF the loads which cause stresses in blades, the three most important are centrifugal force, steam load, and blade vibration. Centrifugal stresses, while they may be large in magnitude, are relatively of secondary importance because they are of a steady nature and can be calculated easily and accurately. Similarly, the steady components of steam load do not cause the designer any great problem. However, vibrational stresses in full-admission blade rows are difficult to analyze and sometimes cause trouble. This is borne out by a review of turbine-blade history which shows that blade failures, other than the fatigue type, rarely occur.

EXCITATION

Vibrational stresses cannot be calculated accurately because of the almost intangible nature of two important factors, excitation and vibratory build-up. The first of these, excitation, is the magnitude of the periodic forces that can cause vibrations. The vibratory build-up is the amplitude of vibration or response of a blade group to this excitation. Nearly all blade vibrations are excited by the steam within the turbine but in some cases external disturbances do set up exciting forces. In marine applications, the turbine-gear-propeller systems sometimes develop strong torsional oscillations which are impressed on the blading. These do not cause blading troubles, however, for their frequencies are so low that no resonant blade vibrations can arise. Excitation forces of higher frequencies occasionally are set up by imperfect teeth in the reduction gears but these are isolated effectively from the turbine blading by the flexible shafts which are used to insure proper gear alignment.

The predominant source of excitation of steam-turbine blade vibrations is the steam itself. Ideally, steam flow in 100 per cent admission stages is uniform but practically many structural features of the turbine cause flow variations.
Some of these are (see Fig. 1):

(*a*) Stationary vanes preceding the rotating blades.
(*b*) Several discrete steam-inlet pipes.
(*c*) Steam-extraction openings.
(*d*) Nonuniformity of blade rings, particularly at the horizontal joint.
(*e*) Structural members in inlet and exhaust pipes.
(*f*) Manufacturing variations in nozzles and blades.
(*g*) Steam-exhaust hoods which turn the flow just after the last blades.

Turbine manufacturers consider all of these items and devote reasonable attention toward minimizing their adverse effects. In all cases the disturbances could be reduced if enough space were used to reduce steam velocities, and if all types of carefully designed guide vanes were installed where desirable. However, this is not always possible because of limitations of weight, size, and manufacturing. Furthermore, the additional size might require mechanical reinforcements which could introduce more flow disturbances as well as create difficult thermal-stress problems.

[1] Manager, Mechanical Design, Westinghouse Electric Corporation. Mem. ASME.
[2] Development Engineer, Westinghouse Electric Corporation, Steam Division. Assoc. Mem. ASME.
[3] "Turbine-Blade Vibration Due to Partial Admission," by R. P. Kroon, *Journal of Applied Mechanics*, Trans. ASME, vol. 62, 1940, pp. A-161–A-165.

Contributed by the Power Division and presented at a joint session of the Power and Applied Mechanics Divisions, and Society of Naval Architects and Marine Engineers, at the Annual Meeting, New York, N. Y., November 29–December 4, 1953, of THE AMERICAN SOCIETY OF MECHANICAL ENGINEERS.
NOTE: Statements and opinions advanced in papers are to be understood as individual expressions of their authors and not those of the Society. Manuscript received at ASME Headquarters, September 21, 1953. Paper No. 53—A-98.

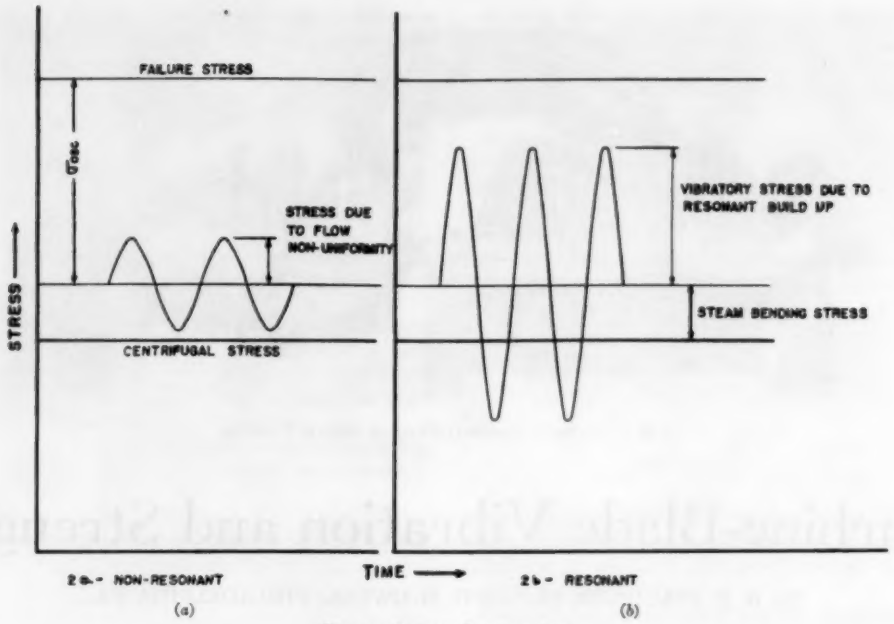

FIG. 2 STRESS COMPONENTS

The magnitude and nature of the flow variation is known, at present, only in general terms. It seems logical that the variation is a periodic wave with a fundamental frequency equal to turbine running speed and containing many harmonics thereof. However, it is not the same for each blade row throughout the machine and it is not a constant percentage of the calculable steam force for all conditions between low load and full load. Up to the present, few experimental data have been available because of the difficulty in making the necessary measurements. Now, though, the recently completed development laboratory of of the authors' company has provided the facilities to conduct the extensive and comprehensive program required to obtain the needed data.

VIBRATORY BUILD-UP

The amplitude of vibration that is developed by blades subjected to the exciting force depends on the vibratory build-up. This in turn is a function of the ratio of the frequency of the exciting force to that of the blade, and of the damping which is present in the vibratory system. It may be represented by the resonance curve given in all textbooks on vibrations. The resonant peak amplitude which depends on damping occurs when a frequency of the exciting force or any of its multiples is close or equal to a natural frequency of the blade. This is applicable to untuned blades which are allowed to run on resonance. The nonresonant vibratory build-up is small and occurs when all frequencies of the exciting forces are different from the natural frequencies of the blades by an adequate margin.

The resonant vibratory build-up is inversely proportional to damping. The order of damping was established some years ago[3] during investigations of partial-admission blading in full-scale rotating tests on a turbine in operation. Values of logarithmic decrement varying from 0.02 to 0.06 were measured on blades made of 12 to 13 per cent chromium steel which has a material damping of approximately 0.02. (The logarithmic decrement is approximately the decrease of amplitude between successive cycles of a free vibration.) In most cases, additional damping due to mechanical friction is available at contact surfaces in both the blade root and shroud. However, experimental values of mechanical damping found in blading while the spindle is stationary are of little value for any looseness under this condition will disappear at speed. The centrifugal force is normally sufficient to fix firmly the root and shroud. Further, the effects of surface finish in contact surfaces, tolerances, and especially the length of operating time, have not been explored sufficiently to provide any reliable data on mechanical damping.

The foregoing description can be summarized by a diagram of the total blade stress and its components, Fig. 2. Here the centrifugal stress and average steam stress are calculated values. The vibratory components, shown qualitatively, could be calculated if the magnitude of the exciting force and vibration build-up were known, but would have to be multiplied by a stress-concentration factor k to allow for stress risers in fillets. The location of the failure line is dependent on the magnitude of the steady stresses and the endurance limit of the material. In this figure the difference between the nonresonant and the resonant cases is in the vibratory build-up.

At this point it is evident that vibratory stress cannot be calculated accurately because of the limitation of our present-day knowledge. Therefore it is necessary to resort to another means of determining the vibratory strength of turbine blading. Fig. 2(b) is applicable to the case of untuned blades which are designed to withstand resonant operation. These untuned blades comprise the large majority of all turbine blades as they are used in all stages except partial-admission stages and long low-pressure stages. Fig. 2(a) is applicable to the tuned blades which are used in the last few rows of low-pressure turbines. The design of these blades is primarily a matter of frequency control rather than strength.

STATISTICAL ANALYSIS OF BLADING HISTORY

The basis for rational design of untuned turbine blades lies in the analysis of operating history of turbine blading. On blading whose performance was unsatisfactory, extensive calculations were made to determine the maximum operating stress and frequency of vibration. Since an average blade, with a frequency of

about 300 cycles per sec (cps), would have a life of less than 10 hours at stresses above the endurance limit, it is necessary to ascertain that an extreme condition of operation for a very small percentage of time is not overlooked.

The factor which represents the ability of a blade to resist vibratory failure is the "magnification factor." It is defined as the ratio of the actual vibratory stress to the steady steam stress multiplied by the stress-concentration factor k. In the case of blades which have failed, the vibratory stress may be taken as the failure which is given by[4]

$$\sigma_{OSC} = \sigma_E - \lambda (\sigma_{CF} + \sigma_S)$$

where

σ_{OSC} = vibratory stress at failure
σ_E = endurance limit of material
λ = slope of failure line (modified Goodman diagram)
σ_{CF} = centrifugal stress
σ_{STEAM} = steady steam bending stress

From this the magnification factor at the time of failure is

$$a = \frac{\sigma_{OSC}}{k\,\sigma_{STEAM}}$$

Magnification-Factor Curves

If we now plot the magnification factor against the harmonic of a large number of rows of blades, these blade rows including as many as possible of those which have failed in service, it is possible to draw a failure curve by the use of statistical analysis. Such a curve, Fig. 3, is useful for a given type of design blading

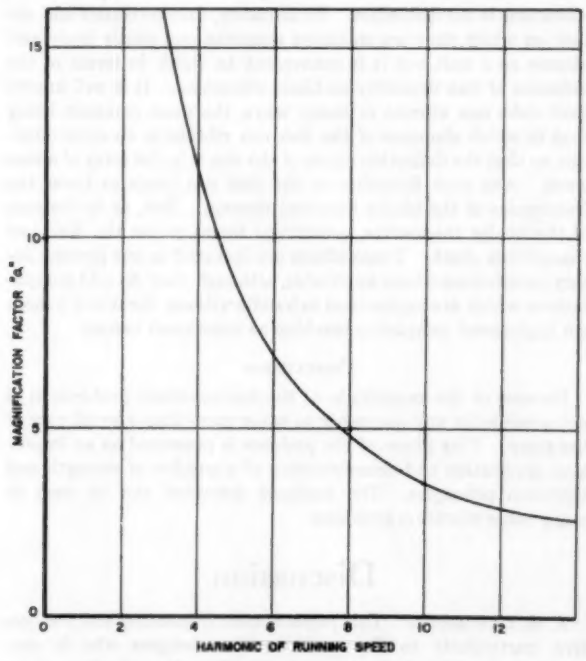

Fig. 3 Typical Magnification-Factor Curve

such as reaction stages having a T-root and shrouded in groups of a similar length. Obviously, a number of curves will fit various locations in a turbine as well as different types of roots, materials, and so on.

It is seen that the accuracy of the calculation depends on the correctness of the stress-concentration factor, which, in turn, depends on the excellence of manufacture. In choosing correct statistical constants it must be realized that in a few cases where the calculated magnification factor would appear quite safe, nevertheless failure occurred. These must be considered as caused by high stress-concentration factors from poor manufacture. Such cases must be few or it would be impossible to draw a satisfactory analysis from statistical data. Naturally, in plotting points on such co-ordinates, we will find that there are blades with low magnification factors in the failure zone where no failure has occurred. This is to be expected since all blades will not be resonant and the excitation may be much less in certain locations and turbine designs.

After the magnification-factor curves become available to the designer, he continues to calculate for each new row the "allowable magnification" by the same formula as given and compares this allowable with the failure curve. If the allowable a is below the curve the stress is too high and the blade will not be used. Several important observations may be made about the magnification-factor equation:

1 The straight-line strength diagram for combined steady and alternating load gives a conservative allowable vibratory strength. This is demonstrated by ample fatigue data which show that if the steady stresses are nearly equal to the yield strength, oscillating stresses of at least 50 per cent of the endurance stress are necessary to cause failure.

2 In the range of centrifugal stresses as required for marine application and often found in other turbines, a 25 per cent increase in σ_{CF} would decrease the allowable σ_{OSC} by only about 10 per cent.

3 Any improvement in design which decreases the stress-concentration factor at any critical point in the blade-shroud system directly increases the steam load which can be carried.

A large amount of the magnification-factor data were assembled and plotted some 12 years ago. The confidence that is placed in the data is demonstrated by the fact that no factor of safety is applied to steam load on the blade as determined by this approach. The proof that this confidence is merited lies in the excellent record of both land and marine turbines, particularly in the past 10 years.

Tuned Blades

Tuned blades must be designed to avoid harmonics of the running speed as illustrated in Fig. 4 which is a plot of blade frequency against turbine running speed. The resonant points which must be avoided are at the intersections of the radial "vibrations per revolution" lines and the vertical "running-speed" lines. In the case of the 1800-rpm turbine depicted in the figure, the resonant blade frequencies are integral multiples of 30 cps and a perfectly tuned blade would have its natural frequencies halfway between these values.

In the case of marine-turbine blading, perfect tuning cannot be achieved because the variable speed of the turbine makes it impossible to avoid blade resonance somewhere within the running-speed range. Long marine blades are tuned out of resonance at maximum speed where maximum centrifugal stress and maximum steam bending stress occur. At a lower speed blade resonance does occur but at this point both centrifugal stress and steam bending stress are reduced so that the blades may be designed with sufficient strength to run resonant by the magnification-factor method described earlier.

In designing tuned turbine blades it is necessary to calculate

[4] "The Effect of Range of Stress on the Fatigue Strength of Metals," by J. O. Smith, University of Illinois Bulletin, vol. xxix, no. 26, February, 1942.

the frequencies of the various natural modes of vibration and the vibratory stress distribution. A method of doing this has been described by G. W. Jarrett and P. C. Warner.[5] These calculations are long, complicated, and tedious to perform by manual computations. However, they can be made readily and fairly rapidly with the aid of a modern computing machine of the "electronic-brain" type. For several years these calculations have been made on a "Card Programmed Digital Computor."

In the design of a turbine blade two sets of natural frequencies are calculated, the "stationary" frequencies which exist when

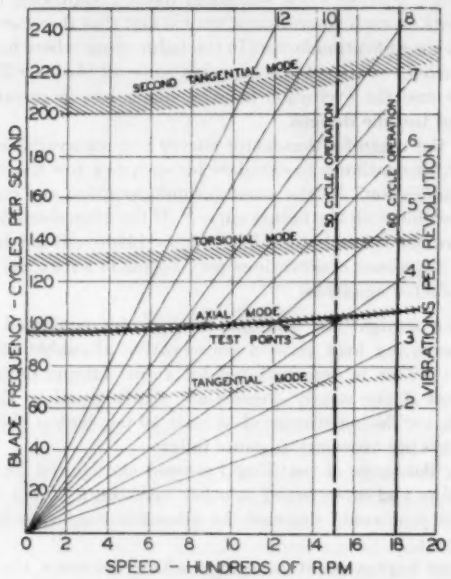

Fig. 4 Turbine-Blade Frequencies

the spindle is not rotating and the "rotating" frequencies which exist when the spindle is rotating at design speed. These frequencies differ because of two effects of rotation. The first is the stiffening effect of centrifugal force on the blade port section. This may be calculated readily. The second effect is a change of blade-root tightness which can be described by means of Fig. 5. This figure shows a type of root which is frequently used on the larger marine-turbine blades. It has a double T arrangement of lugs to provide greater strength to resist centrifugal forces and "straddle" side lugs to prevent spreading of groove walls.

In assembly the blades are placed in grooves and calked in place so that contact pressure exists at points A. There may be a partial clamping on the side lugs B, depending on assembly conditions such as initial clearance and amount of calking. On rotation, centrifugal force tends to spread the groove walls and increase the clamping at points B. Since blade roots cannot be made to exactly the same dimensions, some are assembled more tightly than others. While centrifugal force tightens all roots, it has a greater effect on those which were initially loose than on those initially tight. These changes of blade-root tightness affect the values of the natural frequencies of the blades in a manner that cannot be calculated. However, the effects can be evaluated by tests made on blades under both stationary and rotating conditions.[6]

[5] "The Vibration of Rotating, Tapered-Twisted Beams," by G. W. Jarrett and P. C. Warner, Trans. ASME, vol. 75, 1953, pp. 381–389.

[6] "Mechanical Design and Testing of Long Steam Turbine Blading," by H. M. Owens and W. E. Trumpler, Jr., ASME Paper No. 49—A-64, 1949, not published.

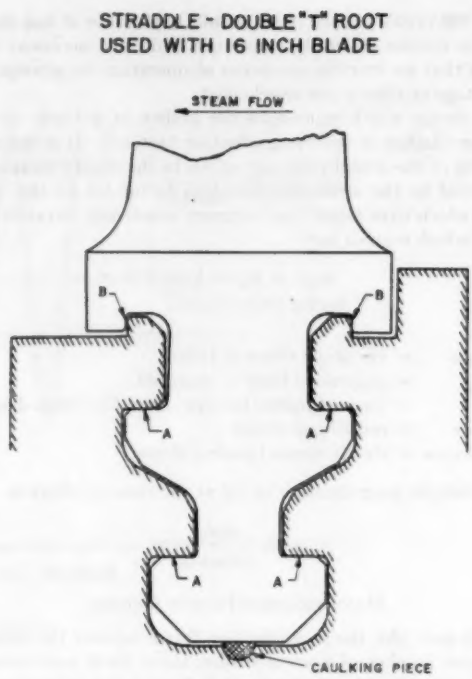

Fig. 5 Typical Turbine-Blade Root

Another factor which has a major effect on frequencies of vibrations is the disk effect. In actuality, turbine blades and the disk on which they are mounted comprise one elastic body and vibrate as a unit but it is convenient to think in terms of the influence of disk flexibility on blade vibrations. It is well known that disks can vibrate in many ways, the most common being that in which elements of the disk rim vibrate in an axial direction so that the deflection curve of the rim is in the form of a sine wave. Any such flexibility of the disk rim tends to lower the frequencies of the blades mounted thereon. But, as in the case of the blades themselves, centrifugal forces stiffen the disk and change this effect. These effects are included in our present design calculations where applicable, although they do add complications which are impractical to handle without the use of a modern high-speed computing machine as mentioned before.

Conclusion

Because of the magnitude of the turbine-blade problem, it is not possible for any one paper to cover more than a small part of the story. This phase of the problem is presented as an important application and demonstration of a number of strength and vibration principles. The methods described can be used in many other vibration problems.

Discussion

J. H. Lancaster.[7] This paper is most interesting and instructive, particularly to the marine-turbine designer who is constantly faced with the problem of providing adequate strength to resist vibratory forces whose magnitude he does not know.

In full-admission blading, variations in steam force are undoubtedly the major source of blade-vibration excitation. However, external sources such as gear-tooth inaccuracies should not

[7] Engineer, Central Technical Department, Bethlehem Steel Company, Shipbuilding Division, Quincy, Mass.

be entirely discounted. In turbine and gear arrangements which have relatively short, stiff, flexible couplings and shafts, it is quite possible for periodic forces resulting from such inaccuracies to be transmitted back to the turbine rotor and blading.

Concerning the stress-concentration factor k used by the authors, it seems reasonable to assume that for a given blade there probably would be several different points of stress concentration each with its particular stress level resulting from a given steady steam load. Conceivably a point having a low stress-concentration factor could be subjected to high stress and vice versa with this given load. However, in higher modes of vibration wherein the deflection curve of the blade is not similar to that produced by a steady steam load, a high stress level might well occur at a point of high stress concentration. It would be of interest to know how the stresses resulting from higher modes are handled when computing the magnification factor a.

Authors' Closure

Mr. Lancaster correctly calls to attention other possible sources of vibration excitation. Gear inaccuracies have been reported to cause blade trouble. This has occurred in a closely connected turbo-gear-generator set in the one case familiar to the authors. The normal vibrations on board ship are, in general, of lower frequency than those of the blading.

Although the magnification-factor data are generally applied to the first-mode vibration pattern they may be applied as well to higher modes. If a blade design is satisfactory for first-mode resonance, it is usually well within the limits for second or higher modes since the energy input is found to be much less in higher modes. It is true, however, that this is based on a concept of uniform flow disturbance along the length of blade. Other types of flow disturbances such as one at the tip of blade only could change the picture. Another source of vibratory excitation always present is the wake following each stationary blade. Should a higher mode resonate with this disturbance it is possible that high stresses may develop. Few cases of failure have been charged to this cause, the reason being that lashing into groups usually minimizes the energy input to the group unless the nozzle and blade pitch are identical. Here, again, if the wake intensity were uniform along the blade, and the displacement diagram had a nodal point, the vibratory energy input would be small.

In a constant-speed application where the first mode is detuned but the second mode is not, then the magnification factor calculation for second mode is used. The allowable a curve for such a condition would be somewhat different from that for first-mode resonance. Also, as proposed by Mr. Lancaster, the critical point would probably be at a different location from the first mode due to the combination of stress-concentration factor and bending-moment distribution.

Manpower and Other Factors Affecting Operating Costs in Steam Generating Stations

By V. F. ESTCOURT,[1] SAN FRANCISCO, CALIF.

The tremendous gains in thermal efficiency which have been achieved by going to higher steam pressures and temperatures with increasingly larger units are now approaching a point where the returns are diminishing at an impressive rate. As these rates of improvement continue to diminish with still further increases in temperature and pressure, it becomes increasingly important to give closer attention to the effect of basic plant design upon the total station payroll. Various philosophies of centralized control are reviewed and evaluated in some detail. Consideration also is given to the interrelation between design and operating concepts and the effect of plant management policies upon operating costs. It is shown that many of these problems are adaptable to economic evaluation and the need for such an approach is greatly emphasized in the light of the present trend of technological advances and changing economic conditions. The effect of the changing requirements in the type of plant operating organization also is discussed in relation to the control of operating costs.

[Following Mr. Estcourt's paper will be found the individual contributions of the panel members.—Editor.]

Introduction

THE principal objective of this paper is to give consideration to certain problems of thermal-electric station operation which deserve increasing attention at management levels as a result of the present trend of diminishing returns from technological advances in the art and also due to changing economic conditions, particularly with respect to labor costs. These problems have to do with the interrelation between design and operating concepts, the effect of specific plant-management policies upon operating costs, and the need for the application of analytical methods to those factors which involve operating manpower.

Trends in Investment Cost and Cycle Efficiency

At the 1952 Annual Meeting of the Society Mr. Herman Weisberg presented an excellent review[2] of the trend in power-plant investment costs. He gave statistical data to show that, although the historical costs per installed kw were only slightly less in 1920 then they are today, tha present replacement cost of a 1920 design, after adjusting for the cost index, would be about $315 per kw as compared with $160 per kw for today's designs of coal-burning plants. This reduction in unit cost has been accomplished, in spite of the more expensive equipment and alloys that must be used for present-day thermal cycles with higher steam temperatures and pressures, and has been made possible largely by increasing the size of turbines and boilers. The largest single-shaft turbine built in 1920 was approximately 45,000 kw as compared with 250,000 kw today. Boiler manufacturers now are willing to build individual boilers as large as the largest turbine being offered up to the present time. This has led to the acceptance of a single boiler per turbine at considerable saving in investment cost with almost as high station availability as formerly was obtained with two or more boilers per turbine. This is particularly true with base-load plants operating over a narrow load band.

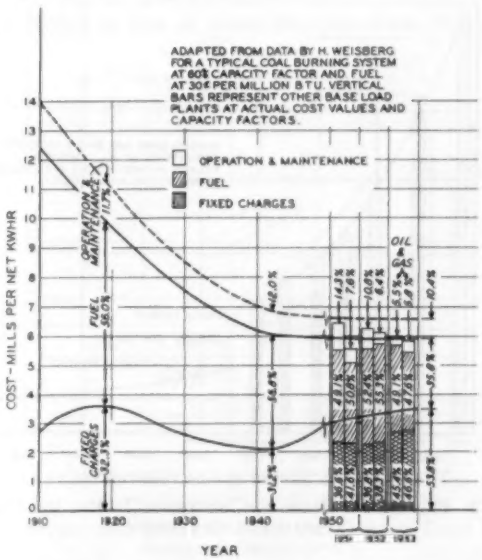

FIG. 1 HISTORICAL TREND OF STEAM-PLANT PRODUCTION COST COMPONENTS

In Fig. 1 the curves from Mr. Weisberg's paper[2] for the trends in capital investment and heat rates for a typical power system have been replotted in terms of mills per kwhr for fixed charges and fuel. The cost of fuel has been taken as 30 cents per million Btu and assumed average values for operating and maintenance costs less fuel have been superimposed upon the other two curves in order to arrive at the general trend in over-all production costs. From these curves it can be seen that, for the typical system under consideration, the average fuel costs per kwhr at 60 per cent capacity factor are still in excess of 35 per cent of the

[1] General Superintendent of Steam Generation, Pacific Gas and Electric Company. Mem. ASME.

[2] "Boiler Construction Costs," by H. Weisberg, Mechanical Engineer, Public Service Electric and Gas Company of New Jersey. Part of panel discussion at 1952 ASME Annual Meeting. Reprinted in *Combustion*, February, 1953, pp. 45–47.

Contributed by the Power and Fuels Divisions and presented at a panel session of the Power and Fuels Divisions at the Annual Meeting, New York, N. Y., November 29–December 4, 1953, of THE AMERICAN SOCIETY OF MECHANICAL ENGINEERS.

NOTE: Statements and opinions advanced in papers are to be understood as individual expressions of their authors and not those of the Society. Manuscript received at ASME Headquarters, October 27, 1953. Paper No. 53—A-95.

total production cost of a kwhr, including fixed charges, or 78 per cent of operating costs only.

The vertical bars represent examples of other modern coal-burning stations on the basis of actual cost values and capacity factors. These show a range of fuel costs between approximately 47 and 55 per cent of total production costs, or between 77 and 90 per cent of operating costs only. The figures clearly illustrate the general magnitude of this component of the total operating cost and the need for still further improvement in the heat cycle. On the other hand, savings due to higher thermal efficiencies inherent in yet higher steam pressures and temperatures probably can be achieved at a justifiable investment cost only if turbines and boilers are increased still further in size. Such large units are restricted to the larger generating systems which can absorb these large blocks of power economically and which have sufficient generating resources so that they can afford a forced outage of units of 250-mw capacity or larger.

With respect to the trend in cycle efficiency, Mr. W. L. Chadwick,[3] in a paper delivered before the Pacific Coast Electrical Association in May, 1953, presented a chart which indicated the trend in station heat rates to an ultimate initial steam condition of 5000 psi at 1600 F, and with double reheat to the same temperature. If it is assumed that the reheat and initial steam temperatures are the same and that the initial pressure conforms approximately to the economic optimum at each temperature level, then the steam temperature is the principal controlling factor and it is reasonable to plot the heat rates as a function of initial and reheat steam temperatures as in Fig. 2. This is merely one

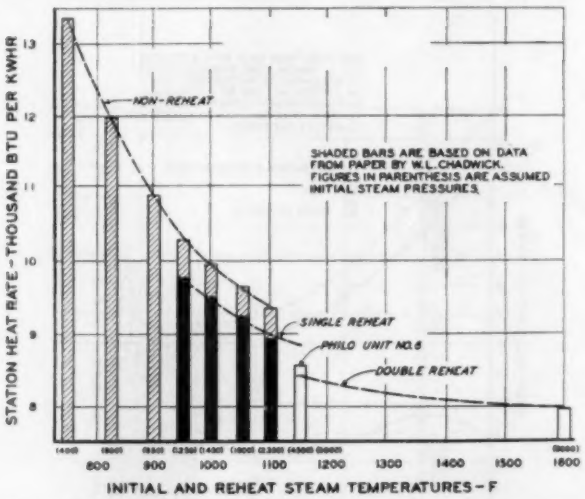

Fig. 2 Plant Heat Rates for Increasing Initial and Reheat Steam Temperatures

method of illustrating the progressive reduction in benefits accruing from a continued increase in steam temperature even though this temperature increase is accompanied by higher steam pressures into the supercritical range.

It is also reasonable to anticipate that design and operating difficulties will continue to increase with the complications associated with progressively higher steam temperatures and pressures, with corresponding increases in operating and maintenance labor costs. Any increases in manpower per kilowatt of capacity will have a progressively larger offsetting effect upon these declining benefits from improved steam conditions. Therefore it will become all the more important to give closer attention to manpower problems and, in particular, to intensify our studies on the effect of basic design and plant layout upon the total station payroll. Such studies should assist in keeping to a minimum any increases in payroll which might result from the adoption of more complicated cycles.

Trend in Manpower Costs

A great deal of thought has been devoted to the economics of improved heat cycles and considerable ingenuity has been exercised in holding initial investment costs to a minimum in order to obtain the full benefit of these improvements in spite of the more expensive materials which adversely affect the initial cost. However, the problem of manpower costs does not render itself as readily to scientific analysis. This is partly due to the difficulty in evaluating human factors. Nevertheless, it is possible to arrive at a reasonable evaluation of the more important components in the plant layout and in management policies which bear directly upon such costs.

The broken line in Fig. 3 shows the trend in plant capacity per man as given by Mr. Weisberg.[2] His curve was intended to

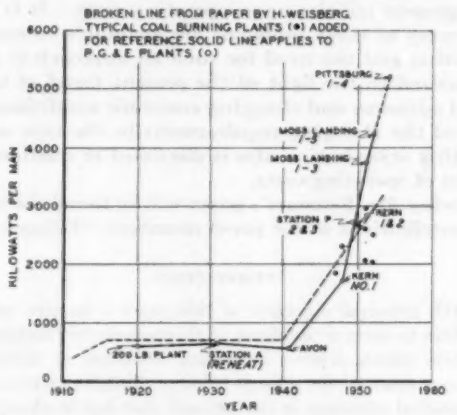

Fig. 3 Historical Trend in Operating Manpower Requirements

represent the trend for large coal-burning units on a typical system. To this have been added by means of black dots several other examples of typical modern coal-burning stations. The solid line shows the actual trend on the Pacific Gas and Electric Company's system for oil and gas-burning plants. In order to correlate these figures, it may be considered that roughly 15 to 20 per cent more manpower is required in a coal-burning station. As will be shown later, these general manpower trends have been the result of a combination of increased size of the units and the more extensive use of some form of centralized control.

Although fully centralized control was adopted by the Pacific Gas and Electric Company in 1940, it did not immediately reflect a manpower saving because of other offsetting factors. However, it can be seen from the solid line in Fig. 3 that the beneficial effects, commencing in 1948, were very pronounced even though the installation was still unfavorable for minimum manpower because of special features in the design for quick load pickup, such as four boilers for two main turbine generators and two condensing-house turbine generators.

In general, plant design, arrangement of equipment, and management policies with respect to operator coverage and training have a pronounced effect upon operating manpower

[3] "What Is Ahead in Generation," by W. L. Chadwick, Vice-President in Charge of Engineering and Construction, Southern California Edison Company. Paper presented at 1953 Annual Convention of Pacific Coast Electrical Association and reprinted in *Electrical West*, June, 1953, pp. 111–114.

costs and can be evaluated with reasonable accuracy. First, however, it is of interest to consider a change in cycle heat rate or a change in the number of shift operators in terms of their equivalent costs, or each in terms of a break-even investment cost. Such a comparison is shown in Fig. 4 wherein these equivalent costs are given for plants ranging in size between 100 and 300 mw and operating at 80 per cent capacity factor.

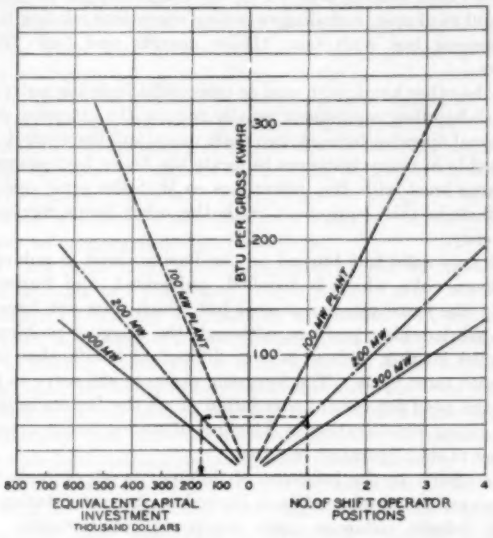

FIG. 4 EQUIVALENT VALUES OF PLANT HEAT RATES, INVESTMENT, AND MANPOWER COSTS

It is clear that for a 300-mw plant, the addition of one man per shift would nullify the fuel savings resulting from a gain of approximately 33 Btu per kwhr in cycle efficiency, or nearly 50 Btu for a 200-mw installation. These figures are based upon operating labor costs on the Pacific Coast and the equivalent values, of course, will be influenced not only by the capacity of the plant but also by prevailing wage rates, the cost of fuel, and the plant load factor. Theoretically, it requires $4^1/_3$ shift operators to fill one operating position for 7 days per week around the clock. When vacations and sick-leave provisions also are taken into consideration as well as possible shift premium pay, the total cost is usually the equivalent of approximately $4^1/_2$ to $4^2/_3$ times the base pay of the payroll classification of each shift-operator position. This may be increased further by the need for a training pool to take care of replacements resulting from resignations or upgrading due to system growth, and the size of this manpower pool is somewhat affected by the number of regular operators on the payroll.

EFFECT OF STATION DESIGN UPON MANPOWER COSTS

By far the greater proportion of any success to date in reducing manpower has been the inherent result of the increased size of modern units in much the same manner as this factor has reduced plant-investment costs per kilowatt. On the other hand, without the adoption of centralized control the effect of the size of units upon manpower would not have been so pronounced. By having the major controls centralized in one control room it has been possible to operate two or more large units with only a very small increase in the number of operators above the requirement for one unit.

The effect upon operating manpower of increasing the size of the main units is illustrated in a general way in Fig. 5. The curve is based upon the requirements for the four 156-mw units at our Pittsburg Steam Plant. If the size of these units were increased to 200 mw each it would have a relatively small effect upon the total manpower requirements based upon a four-unit control room. Conversely, if the size of these units were reduced to 100 mw, or even 50 mw, we would anticipate only a nominal reduction in total manpower. Consequently, for the particular

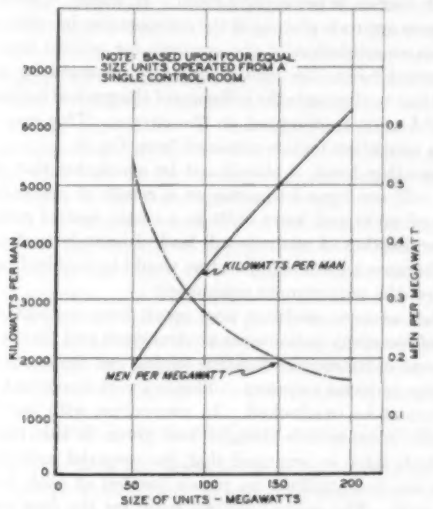

FIG. 5 EFFECT OF SIZE OF UNITS UPON OPERATING MANPOWER

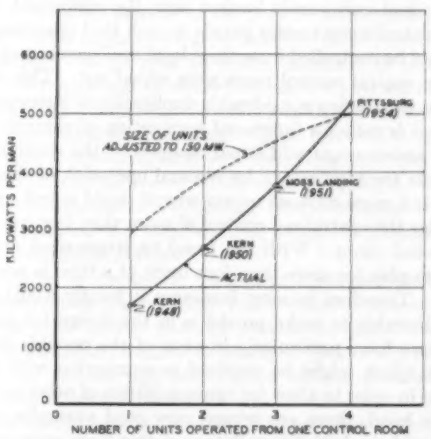

FIG. 6 EFFECT OF NUMBER OF UNITS PER CONTROL ROOM UPON OPERATING MANPOWER

station layout under consideration, it may be estimated that the effect of increasing the size of the units would be to increase the kilowatts per man from approximately 1900 for four 50-mw units to about 6300 for four 200-mw units. This latter figure is equivalent to one sixth of a man per megawatt of installed capacity.

Further manpower savings may accrue from the consolidation of more units within the same control room, but such savings may be very limited or quite substantial, depending considerably upon certain plant-management policies with respect to operator coverage and operator training in relation to a particular plant layout. However, the curves in Fig. 6 illustrate what actually has been accomplished in this respect in certain stations where design and manpower conditions are favorable.

The solid line shows the number of installed kilowatts per man in four actual stations with one, two, three, and four units per control room, respectively.

The four-unit job is nearing construction completion but is not yet in service; therefore the manpower figures are estimated in this instance. The solid line on the chart shows that the kilowatts per man increase from 1700 for one unit per control room to 5200 with four units per control room. However, in order to provide a more accurate picture of the comparative benefits resulting from this consolidation of the controls for several units in the same control room, the broken line was obtained by adjusting the solid line to eliminate the influence of the gradual increase in the size of the units represented on the curves. This was done by applying correction factors obtained from Fig. 5.

On the other hand, it should not be concluded that the same benefits will continue to accrue as a result of centralizing the controls of more and more units in a single control room. The overcentralization of controls will lead ultimately to diminishing returns because additional operators would be required to operate and patrol the very remote equipment.

Another adverse condition may result from concentrating the control of too many units in one control room and that is the danger of some catastrophic situation wiping out the controls of too many large units on a system. This is a very important problem which cannot be overlooked. In connection with our more recent units, considerable thought was given to this matter and the controls were so arranged that the essential individual unit controls are decentralized on panels located at each boiler and turbine unit. The central control room for the four units consists of a so-called master panel from which the normal operation of the four units can be handled. This basic hookup as between the individual unit panels located near the equipment and the central control-room master panels is such that operation of the plant could be controlled from these local unit panels even though the entire central control room were wiped out. This does not mean that there is any considerable duplication of instruments and controls; it is rather a functional segregation of controls so that, with the assistance of additional manpower, the controls on the unit panels are satisfactory for manual operation of the station.

There is a more obvious reason why it is not usually practical to consider the centralized control of more than four units in the same control room. With the trend to larger-sized units it is difficult to plan for more than four units at a time in one system location. Therefore in most instances it hardly would be considered desirable to make provision in the design for additional units above four, particularly in view of the possible added investment which might be required in connection with the first four units in order to allow for future addition of other units. On the other hand, there are several very good examples of plants laid out with an initial installation of two large units with provisions for the future installation of one or two additional units of the same or larger size all operated from the one control room.

Interrelated Factors of Operation and Design Affecting Manpower Requirements

Some features in the plant layout will result in reduced operating manpower only in conjunction with certain operating policies relating to the type of operators and the manner in which their various duties are assigned. This is particularly true, for example, in connection with the foregoing analysis of the effect of increasing the number of units operated from the same control room. Bearing in mind this reservation, it is possible to make certain observations regarding the effect of the type of fuel and the location of certain major auxiliaries upon manpower requirements. For example, with fuel oil and gas it is usually possible to save at least one man per shift by locating the boiler feed pumps and evaporators on the control-room level. This results from the fact that most of the operating manpower is on this floor, there being very little need for operators on the lower floor as a result of the smaller auxiliaries being in duplicate with provision for automatic starting of the stand-by units.

As an illustration, we have on our system stations consisting of five main units with a total capacity of nearly 600,000 kw with only two men looking after all of the equipment on the ground floor and yard area, including switching operations relating to the high-tension bus with four 110-kv circuits and four 220-kv circuits.

On the other hand, with coal or other solid fuels the pulverizer and ash-handling equipment usually require the attention of an additional operator for each two main units, and therefore it may be feasible in many instances to locate the boiler feed pumps on the same level with the pulverizers so that the same operator may include this equipment with the other items mentioned previously.

The only solid fuel burned on the Pacific Coast is pulverized petroleum coke which is handled, pulverized, and burned in exactly the same manner as coal but which does not have the usual ash-handling problem, although the slagging problem on the boiler heating surfaces is more difficult to handle than is the case with most coals. The foregoing example will serve to illustrate the need for careful correlation of all the factors involved when giving consideration to the effect of station design upon the number of shift operators required.

In addition to the influence of different types of fuels upon manpower, the number of fuels burned in the same station also has a definite influence upon manpower requirements. The problem of burning two or more fuels is not at all difficult except for the unusual demand upon the shift operator during the change-over from one fuel to the other. For example, on the Pacific Gas and Electric Company's system, gas is available during the summer months but as the cold weather comes on in the fall the domestic gas-heating load gradually increases so that the amount available for steam-generating stations gradually diminishes. The reverse situation occurs in the spring as gas fuel again becomes plentiful. Each of these two conditions occurring, respectively, in the fall and spring of the year necessitates considerable switching back and forth between gas and oil fuel up to several times per day over a period of months.

Our past practice was to make the fuel change-over of one burner at a time. When changing from oil to gas, considerable handling is necessary in order to retract the oil-burner guns and blow them out with saturated steam to prevent carbonization of hot oil at the burner tip. In general, many burners and auxiliaries are involved in such a change-over and it has been difficult to avoid having additional men on each shift in order to take care of these fuel changes. Recently, however, a system of so-called mass change-over has been developed wherein it is possible to transfer from one fuel to the other in one operation for all of the nine or more burners in one boiler. This not only shortens the actual change-over operation from 20 min to 3 or 4 min per boiler but also makes it possible to handle the operation from the central control room with the aid of television. The solution of this problem is referred to here in some detail as it is a good example of some of the factors involving station design which may have a substantial effect upon operating costs.

Effect of Plant-Management Policies Upon Operating Costs

One example of the effect of plant-management policy upon operating cost relates to shift-operator coverage or the scope of duties assigned to each operator. With centralization of controls and substantially increased automatic stand-by protec-

tion of auxiliaries through automatic starting of the duplicate spare, and the general improvement in instrumentation, alarms, and controls, it is obvious that plant equipment, in general, does not require the same amount of operator attention as formerly. Therefore the trend has been to use considerably fewer equipment operators than in the past.

One good illustration of this already has been given wherein such improvements have made it possible for only two men to patrol and operate the entire main floor and switchyard areas of a large station. There are other examples applying to eastern utilities where even greater reliance is being placed upon controls, instrumentation, and alarms in the central control room to the extent that it is hard to find an operator during the course of a trip through the entire plant having a capacity in excess of 500,000 kw and consisting of a great deal of auxiliary equipment widely dispersed throughout the building on five or six different floor elevations. This latter example goes to a degree which typifies what is sometimes described as a policy of "austerity" with respect to equipment-operator coverage.

In this connection, some companies appear to have taken what amounts to a calculated risk or possibly some sacrifice in reliability by holding the number of control and equipment operators to an almost irreducible minimum for a particular design of station. However, in some instances it has become apparent that the saving in equipment operators has been offset in whole or in part by an increased number of control operators with considerably more elaborate and expensive control rooms.

In base-load stations operating at an annual capacity factor of, say, 70 per cent or better, such austerity measures can be carried out with the expectation of obtaining very acceptable performance from the standpoint of operating reliability. Plants which are required to operate over a very wide load range and designed for quick load pickup due to interconnection with a large percentage of hydro capacity, and burning more than one type of fuel, are in a less favorable position to practice this form of austerity. On the other hand, experience indicates that there is usually an opportunity for reducing the work load of operators by a realistic evaluation of their various duties relating to such activities as patrolling and inspecting equipment, logging of instrument readings, and so on. A simple example of this will be given.

In stations of older design it was usually the practice to take hourly readings of all instruments. With the increased complication of modern power stations there has been not only a substantial increase in the amount of instrumentation but considerably more use has been made of recording instruments. The question then arises as to whether recording instruments need to be read by the operator at regular intervals. A time-honored theory has been that the only guarantee the operator is keeping himself familiar with all of his plant conditions is to require him to log all of the important instrument readings at frequent intervals regardless of whether they are recorded or not.

Although this is still a good basic approach, the considerable increase in instrumentation introduces the problem of overloading a limited number of shift operators so that they do not give sufficient attention to over-all operation of the station. Studies which were made in some of our larger stations have resulted in the reduction in frequency and number of regularly logged instrument readings by as much as 65 per cent without affecting materially the assurance that the operators are being kept closely in touch with the performance of each item of equipment throughout the day.

By analyzing and evaluating carefully the various duties of the shift operators in relation to the functional components of the plant, it is possible to determine with reasonable accuracy the work load on each man under both normal and upset conditions of operation. With this information we can arrive at a so-called austerity-factor rating for a particular plant. At the risk of oversimplifying the problem, the method can be illustrated in a very general way by assuming that two modern reheat units each with one gas and oil-fired boiler and having a capacity of 100 or 150 mw, with a shift crew of 5 men, would have an austerity-factor rating close to 80 or 90 per cent depending considerably upon the plant layout and other factors involving basic operating conditions and plant-management policies. It might be considered further that the addition of 4 or 5 more operators to each shiftwould reduce this austerity factor to zero, and intermediate figures may be obtained by interpolating between these two extremes. However, changes in the design of the plant by more judicious application of instrumentation and controls and improvements in layout for functional simplicity could so reduce the work load on the operators as to bring about an appreciable change in this austerity-factor rating.

This rather elementary example is given merely to suggest the possibilities of this method of appraisal in comparison with the sometimes all too vague and purely qualitative approach to this important problem. As a matter of interest, if this system of evaluation is applied to our postwar plants in northern California, they would have an austerity-factor rating of roughly 50 per cent, even though the kilowatts of capacity per shift operator position are relatively high as already indicated in Fig. 3.

Differing Concepts of Centralized Control

In connection with automatic controls, in order to appreciate fully the factors which influence operating manpower, it is necessary to digress somewhat in detail into the history and differing philosophies of centralized control. The term "centralized control" has been abused by its rather loose application in somewhat the same manner as the popular conception of "stainless steel" when applied as a generalization for any steel containing chromium. Some idea as to the difference in philosophies upon which the designs of centralized-control jobs are based may be obtained by comparing the total number of plant operators per shift required in each instance. In the recent past, these have ranged from a minimum of 6 to a maximum of 17 per shift for two units per control room. This wide disparity in manpower requirements represents a difference of approximately $200,000 per year in payroll or a break-even equivalent capital investment of approximately $1,600,000.

In so far as we are aware, the first attempt to operate a large high-pressure steam-generating plant from a central control point was made at the Holland Station in 1930. This plant, now renamed Gilbert Station, is arranged without a dividing wall between the turbine and boiler areas and is operated from a single group of control panels.

Typical examples of subsequent jobs specifically designed for centralized control are as follows:

1 Oswego, Niagara Mohawk Corporation; initial operation in 1940.

2 Avon, Pacific Gas and Electric Company; initial operation in 1940.

3 Martinez and Oleum, Pacific Gas and Electric Company; initial operation in 1941.

4 Tidd, American Gas and Electric system; initial operation in 1945.

There may have been other examples, but the jobs mentioned were among the first applications of centralized control to high-pressure steam plants of any considerable size and may be considered as fairly typical of the early developments in this field.

As already discussed briefly in connection with the effect of station design upon manpower costs, the type of control-room

layout which is feasible for a particular plant is considerably influenced by prevailing policies with respect to operator coverage. Broadly speaking, shift operators fall into two categories or some combination thereof. The men assigned to the control room usually are known as "control operators" as distinct from "equipment operators" who actually patrol and operate the individual pieces of equipment locally.

Some utilities make a rather definite distinction between these two categories so that the duties of the control operator are specifically confined to the operation of the controls in the central control room; equipment operators, on the other hand, have the exclusive duty of patrolling equipment, handling valves, and performing other physical operations relating specifically to the equipment as distinct from the controls.

More or less of a compromise has been adopted by others wherein one of the control operators occasionally may leave the control room in order to perform certain duties relating to the equipment itself, thereby assisting the equipment operator when necessary.

There is still a third policy wherein the control operators are trained specifically to perform equally well the double function of control operator and equipment operator.

Although varying considerably as to detail, control-room layouts may be classified broadly into the following three basic types:

1 Completely isolated and remote.
2 Semi-isolated and centrally located.
3 Open and centrally located.

In category (1) are included those control-room layouts which provide complete isolation from the plant equipment by means of a fully housed soundproofed room. This appears to be the most popular arrangement at the present time. There are some instances of this type of control room wherein it is located centrally with respect to operation but the complete isolation makes it relatively unimportant whether it is in a central location with respect to turbines and boilers or remotely located in a corner of the building or even on the roof of the plant, as is the case with at least one company.

In such instances, the arrangement would fall in category (2) as "semi-isolated and centrally located." It gives the appearance of only semi-isolation owing both to its proximity to major equipment with adequate access doors and the use of considerable glass paneling to provide a certain amount of visibility with respect to major equipment.

The functional difference between the completely isolated and semi-isolated type of control room is not very great. The number and type of shift operators required in each instance is approximately the same and it might be safe to say that a choice between the two types can be based largely upon considerations of investment cost and personal preference for the particular station. Good success is reported by some companies[4] with layouts which rely almost entirely upon remote control of all equipment operations including the starting up and shutting down of major units.

In either of these two arrangements control operators usually are assigned on a unit basis. Thus in a station consisting of two main units, one half of the control room contains one or more control panels with all of the necessary controls and instrumentation for the mechanical operation of one of the units. One operator is assigned to the operation of such a panel. The other

[4] "Remote Operation Through Centralized Control Rooms—A New Concept Developed on the American Gas and Electric System," by T. T. Frankenburg, Assistant Head, Mechanical Engineering Division, American Gas and Electric Service Corporation, ASME. Paper No. 51—SA-47.

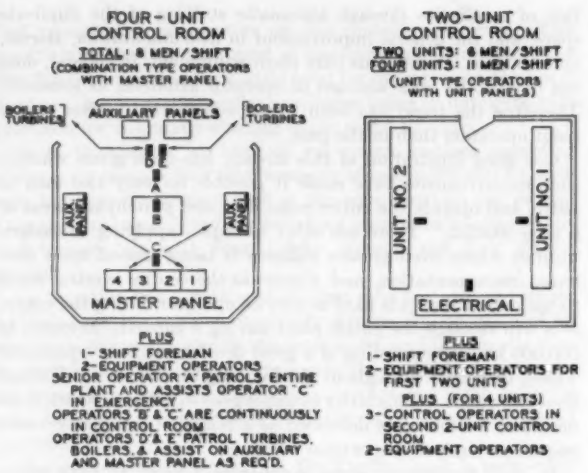

FIG. 7 BASIC COMPARISON SHOWING APPLICATION OF MASTER PANEL VERSUS UNIT PANELS FOR CONTROL OF FOUR UNITS

side of the control room consists of a duplicate set of panels for the other unit, and usually there is a separate group of generator and electrical panels which may be supervised by a third man. This arrangement is illustrated on the right side of Fig. 7. In addition to these control operators there generally are between two and four equipment operators located around the station to patrol the various items of major equipment and auxiliaries. A watch engineer or shift foreman would complete the complement of shift operators making a total of from five to eight men per shift for two main units.

In a certain sense this represents the ultimate of the so-called unit-system concept wherein not only is the boiler-turbine combination considered as an isolated unit, but there also are unit control panels and unit operators. However, some utilities have backed away from this extreme policy of unit operators in order to reduce shift operating labor and are endeavoring to get along without the third man by having the other two men consolidate their duties to some extent.

Category (3) applies to a control room which is not only located centrally with respect to major equipment but also is open on one or more sides in order to provide unrestricted movement of operators between the controls and the various items of major equipment and principal auxiliaries. This type of layout, as illustrated on the left side of Fig. 7, presupposes the use of combination control and equipment operators who are trained to handle the controls and operate the principal electrical and mechanical equipment, most of which is located at the control-room level. Thus it should be clear by now that there is a fairly well-defined correlation between the type of control-room layout, the basic panel arrangement within the control room, and the type of operators.

It should be pointed out that Fig. 7 is intended only to illustrate the basic principles involved. The number of operators might vary appreciably in each of the two schemes, although this would not affect greatly the comparison on the basis of the same austerity factor. On the other hand, the data in Fig. 6 apply specifically to actual stations of a basic design conforming to the philosophy of this third category of centralized control. It is important to emphasize this point because substantially different results might be obtained with other arrangements of centralized control and differently trained operators. As an example, we were advised a year or so ago by the designers of a plant then under construction with a single control room for four units that,

although there was the potential possibility of a labor saving with four units per control room instead of two, there was no certainty that it would materialize, and at best it might amount to one operator per shift. This is fundamentally true with so-called unit panels and unit operators, because each additional pair of units calls for substantial duplication of shift operating personnel.

In order to carry the concept of category (3) to its logical conclusion, careful consideration must be given to the plant layout with respect to the location of various auxiliaries such as boiler feed pumps, evaporators, and so on, so that they are readily accessible from the control room. Fire doors usually are provided to isolate the control room in a major emergency. This open-type arrangement not only allows the operators freedom of movement between the control room and the principal equipment but also permits a predetermined level of normal machinery noises in the control room except in the soundproofed operator booth which is provided for the purpose of efficient communication and necessary desk work. Control operators who also perform the functions of equipment operators, in addition to their duties as push-button operators, must be reasonably noise-conscious if they are to do an intelligent job of operating the equipment.

For maximum effectiveness of this arrangement, it is necessary to obtain a compromise between compactness in the panel arrangement and good readability of instruments, so that the operators are able to see the principal instruments at a reasonable distance as they move about in connection with their diversified duties. In this respect the situation is exactly the opposite of what is required in the isolated unit type of control room. It also should be understood that the location of the control room in a central position with respect to boilers, turbines, and important auxiliaries is not so much for the purpose of seeing them as it is to provide accessibility for those equipment operations which require the personal attention of the operator who, in this type of layout, performs the dual functions just described.

A considerable degree of compactness and functional simplification is achieved by arranging instruments and controls in accordance with a master-panel system as distinct from a unit system. On the master panel are assembled the principal instrumentation and controls for a minimum of two and a possible maximum of four main units. It has been learned through many years of close observation that certain specific instruments and controls are required to operate the plant safely under average day-to-day conditions, and these represent only a relatively small percentage of the total. Therefore the essential instruments for, say, four main units can be grouped on one master panel which is no longer than a panel containing all of the instruments for a single unit. A large proportion of the special instrumentation and controls for individual equipment are located on panels which may or may not be in the control room or even within sight of the operator from the control room. No operators are located permanently at these remote panels. A number of utility companies have adopted this idea of a master panel and in at least one instance it has been designated as a "flight panel."

This functional arrangement of the master panel greatly relieves the psychological strain so that usually a single operator can handle the controls on a master panel for three or four units about as easily as a single operator can take care of the unit type of panel with its considerable concentration and complexity of instrumentation and controls, many items of which are seldom used. The latter frequently includes long rows of neatly arranged control devices all identical in appearance and uniformly spaced on the panel so that it is impossible to identify them without reading the name plates. On the other hand, the tremendous advantage of the inherent diversity factor in the master-panel arrangement becomes most apparent in the event of upset conditions. Since it is usually the case that trouble does not occur simultaneously on all of the three or four units, this diversity of work load with respect to individual units lightens materially the burden upon the operators who are assigned to such a group of units. Furthermore, the problem of the shift foreman, in co-ordinating the over-all operation of three or four units, is simplified greatly by reason of this functional centralization of important instrumentation and operating activity.

Although this third category of centralized-control philosophy appears to favor relatively low operating labor costs, it should be clear that certain conditions are essential for its satisfactory application. Without doubt the initial training of the type of operator required is more costly and its success is dependent largely upon the background and attitude of both first-level supervision and top plant management. It is unrealistic to advocate a particular philosophy of control-room layout and panel arrangement unless all of the local conditions with respect to available personnel and plant-management policies are known in intimate detail. The proper solution in each instance requires painstaking attention to the functional and human realities of the particular job.

Instrumentation and Control Problems

A discussion of control-panel design is outside the scope of this paper except for the purpose of illustrating certain basic principles which may affect manpower costs substantially and indirectly influence other operating costs.

It would be extremely difficult to co-ordinate all of the functional components of present-day thermal cycles without a large degree of centralization of controls and instrumentation. The greatly increased size of boilers with added complications for the control of higher steam temperatures with reheat introduces problems of distance and inaccessibility which can only be solved satisfactorily by means of centralized controls.

However, it should be borne in mind that the principle of diminishing returns applies here as it does in most engineering problems. It is not always desirable to rely upon more and more centralized controls with their added complications to overcome problems of inaccessibility in the basic design which make it difficult for an operator to handle the equipment. It is far better to provide for maximum accessibility to the operator and avoid the use of additional controls when the exercise of greater ingenuity in the fundamental design will accomplish the same objective.

Making everything automatic is not only expensive but does not necessarily improve operating reliability or result in the saving of any manpower. In fact, the reverse may be the case, although the control designer may derive considerable personal satisfaction in the feeling that the plant is fully automatic. The basic objective should be to centralize only those controls which really assist the operator in doing a safe and intelligent job of operation with minimum psychological strain. In this manner the length of the control panels can be kept to a minimum without crowding of the instrumentation and control devices. It would appear difficult to justify the investment in remote controls for such items as lighting off the boiler, bringing the turbine up to speed, and the like, for the reason that these operations are performed so seldom that it is questionable whether any tangible benefits accrue in manpower savings, operating reliability, and so on. On the other hand, it is conceivable that specific situations might justify such extremes.

In connection with individual panel design, it appears to us that there is still a great deal of room for improvement from the standpoint of functional considerations and improved design of control devices. On the Pacific Gas and Electric Company's system, although since 1940 we have followed the basic concept of a

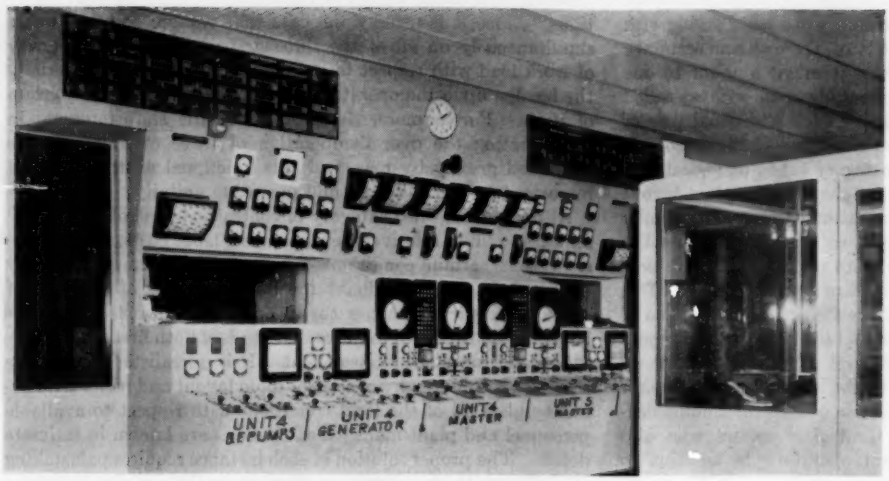

FIG. 8 VIEW OF MASTER CONTROL PANEL FOR TWO 100-MW REHEAT UNITS, 1450 PSI, 1000 F/1000 F

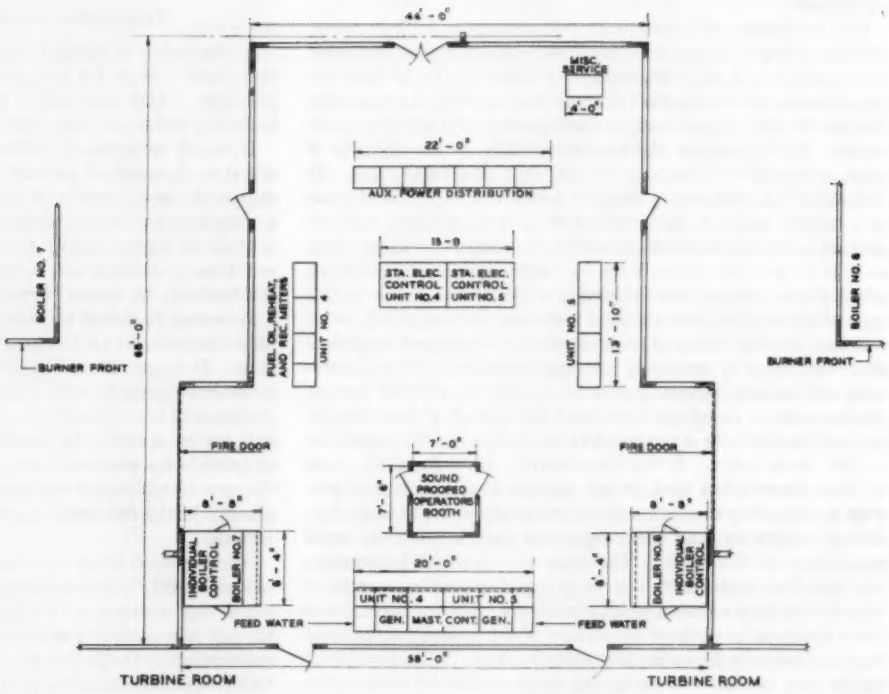

FIG. 9 CONTROL-ROOM ARRANGEMENT FOR TWO 100-MW REHEAT UNITS, 1450 PSI, 1000 F/1000 F

master panel, as described earlier, we have gone through a gradual evolution with respect to details and are continuing to find substantial opportunities for further improvement. As an example of the evolutionary trend of control-panel arrangements on our own system, Fig. 8 shows a master panel for two 100,000-kw reheat units illustrating the use of a certain number of recording instruments as part of the essential instrumentation in cases where it is important to see at a glance the trend as well as the instantaneous value of the particular item. This particular installation is by no means what we would consider representative of the ultimate goal in master-panel arrangement, but it does serve to illustrate certain important principles. For example, the standardization of control devices and instrumentation by shape and color is exemplified, and this functional segregation of control handles by different standard shapes can be seen clearly.

A plan of this control room showing its relation to the boilers and turbines is given in Fig. 9. The total floor area in this instance is approximately 3100 sq ft, which is relatively high. We have an identical two-unit installation with a central control-room area of approximately 2500 sq ft. One eastern company recently designed a control room with less than 1200 sq ft for two 150-mw units or 4 sq ft per mw of capacity. The control room for the Pittsburg Steam Plant of the Pacific Gas and Electric Company covers an area of less than 2200 sq ft for four 156-mw units, or 3 sq ft per mw. This is illustrated in Fig. 10.

In our earlier jobs we included a much larger number of individual panels in the main control room in addition to the master

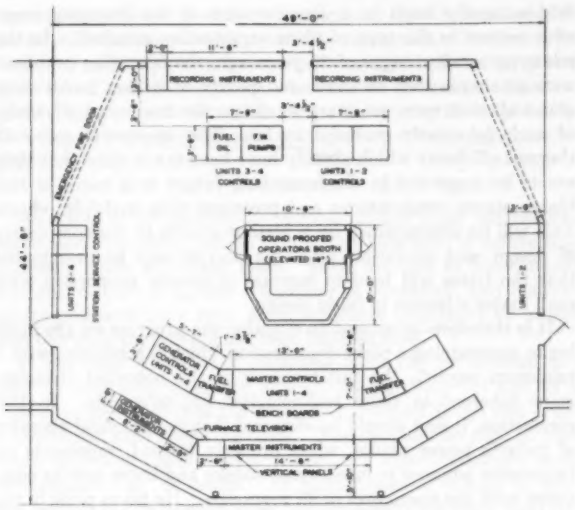

FIG. 10 CONTROL ROOM FOR FOUR 150-MW REHEAT UNITS, 1800 PSI, 1000 F/1000 F

SPACE ECONOMICS AND OTHER CONSIDERATIONS AFFECTING OPERATING COSTS

There are certain conditions affecting operating costs which can be controlled only to a rather limited extent. These include such items as (*a*) location of the plant with respect to available cooling water and its effect upon plant layout, (*b*) the availability of fuels in the general area, and (*c*) the basic operating requirements of the station in relation to the system as a whole. These factors may be reflected substantially in the operating payroll and other costs. The effect upon operating labor of both the type and number of fuels to be burned already has been illustrated by specific examples. The other two items will now be reviewed briefly.

Cooling towers, with problems of chemical control of tower-basin water and inherent dispersal of the equipment itself in relation to the plant proper may be the cause of increased labor costs unless great care is exercised in both the design and management of the installation. On the other hand, with ocean water, in spite of all that has been accomplished by means of thermal control of mussels, it is usually necessary to maintain a crew of condenser men for cleaning accumulations of marine growth from the tube sheets and sometimes dead mussel shells lodged within the tubes. The latter are particularly objectionable

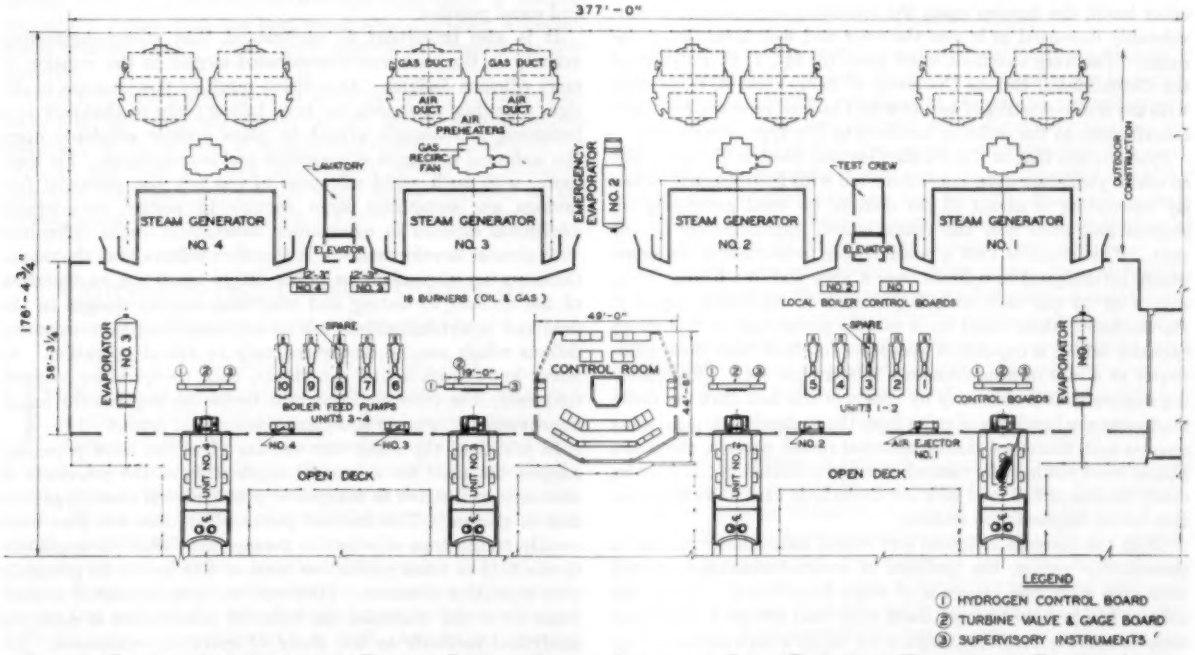

FIG. 11 GENERAL ARRANGEMENT OF CENTRAL CONTROL ROOM IN RELATION TO LOCAL PANELS AND EQUIPMENT IN GENERAL AREA

panel. As the effectiveness of the basic arrangement became more apparent we decided to move the individual boiler panels out of the control room entirely. This is illustrated in Fig. 11 wherein the location of the local boiler panels can be seen in relation to the central control room as well as the general arrangement of equipment on the control-room level. It is interesting to note that each individual boiler panel has approximately the same length as the master panel which is only 13 ft long for all four boilers and turbines. Thus a very short master panel has been achieved by simplification and elimination of seldom-used instruments and controls rather than by reducing the size of the instruments. However, this should not be interpreted as being unfavorable to the judicious use of miniature instruments.

because they become the cause of rapid tube failures due to so called impingement attack. In connection with river or ocean sources of supply for condenser cooling water, if local conditions with respect to the site make it necessary to build a pumping plant, traveling screens, and the like, at a location remote from the turbine and its condenser, this may well lead to additional payroll and other operating costs together with added difficulties relating to operating co-ordination.

Such problems as these are examples involving principally the factor of distance and accessibility, and their solution falls under the general heading of space economics. Since the lowest over-all cost is what is desired, the optimum design must take into consideration both the investment fixed charges and the actual cost

of operation and maintenance. Frequently there is an opportunity to exercise ingenuity in keeping investment costs low for the particular layout which also favors minimum operating costs. In such economic studies it seems that the tendency is to err on the high side in the estimate of incremental investment costs and on the low side in considering the related operating and maintenance costs. Fixed charges on the original investment continue through the years at approximately the same value, but it should be borne in mind that the trend in labor costs is consistently upward. It therefore behooves us to exhaust all the possibilities in attempting to arrive at an economic design which also will satisfy the condition of a minimum payroll.

The basic operating requirements of the plant such as the load pattern may also have a considerable effect upon both operating and maintenance costs.

Many plants are required to operate on a base load around the clock for at least five days per week except for some reduction between the hours of approximately 11:00 p.m. and 6:00 a.m. Other plants are required to take units off the line not only over the week end but also at night. This latter requirement provides an opportunity to perform maintenance work without experiencing forced shutdowns when the capacity may be needed on the system. From a statistical standpoint this results in what appears to be better equipment availability records. On the other hand, the burden upon the operating organization is considerably increased as is also the wear and tear upon the equipment. The very excellent work done by Mr. J. C. Falkner[8] of the Consolidated Edison Company of New York, in connection with the quick-starting of turbines and boilers, represents a major contribution to the problem involved in this type of operation.

Systems like that of the Pacific Gas and Electric Company not so many years ago were interconnected with hydroelectric capacity amounting to about 65 per cent of its total generating resources and even now the figure is still approximately 38 per cent. This requires that a considerable proportion of its steam plants be designed to operate over a very wide load range from, say, 5 or 10 per cent to 100 per cent of maximum capacity. Furthermore, there must be a certain percentage of this steam capacity which is capable of accepting full load from these minimums at a rate of approximately 2000 kw per sec. This operating requirement is necessary by reason of the fact that the dense load areas are hundreds of miles from the hydroelectric generating sources and, therefore, during seasonal runoff periods, the steam plants must not only be backed down to a minimum but must be ready to accept full load in a few seconds in case of an interruption in the transmission system.

With the increase in initial and reheat steam temperatures to present-day values, the problem of steam-temperature control over such wide load ranges is of major importance. Unless this control is adequate to meet these wide load swings it is not possible to operate turbines designed for today's high initial and reheat steam temperatures without sacrificing some of the efficiency which is associated with them. Therefore boilers must be designed to give reasonably constant initial and reheat steam temperatures over a very wide load range. This severe operating requirement not only tends to increase the initial investment cost but also reflects unfavorably upon the cost of maintenance and operating labor.

The Changing Scene in Plant Organization

The discussion of these various operating and management problems in the light of the rapidly advancing technology in this field naturally leads to a consideration of the changing scene with respect to the type of plant organization required. In the relatively crude designs of 30 years ago, the operating problems were so simple that an Orsat and plenty of willing hands were about all that were necessary to obtain the maximum efficiency of such inherently wasteful cycles. The impressive gains in thermal efficiency which already have been made since that time are to be surpassed in the immediate future as a result of still higher steam temperatures and pressures with multiple reheat. This will be accompanied by a further growth in the complexity of design and operating problems and it may be anticipated that the latter will tend to increase in greater proportion with each major advance in basic design.

It is therefore important to examine the progress we are making in maintaining a plant organization which can achieve, with a minimum payroll, the full measure of the potential economic gains inherent in these technological improvements. In this connection, it first should be observed that the practical operator of today's power plants, when properly trained, represents an impressive advance in intellectual stature and know-how as compared with the manpower of 30 years ago. He takes pride in the rapid progress being made in his chosen field and fully appreciates that, in our expanding economy, these advances are reflected in greater employment and a general elevation of his economic and social position.

It is also important to understand that power-engineering activity in the past was concentrated largely in the creation of more efficient designs. As a direct result of this progress in design, a gradual evolution has been taking place so that now it is becoming increasingly urgent to place greater emphasis upon the technical problems of operation and management. Furthermore, with such rapid advances in the art, the potential fuel savings are sometimes large enough to justify considerable additional expense in overcoming substantial initial difficulties with pioneer developments. It therefore follows that the manufacturers are dependent as never before upon the co-operation of the utilities in testing and analyzing untried designs in the field and in obtaining their advice and assistance in overcoming defects which can be discovered only in actual operation. As many know from actual experience, such co-operative research frequently has been an important factor leading toward major improvements in basic equipment design and layout.

In addition, the manpower studies which we have presented suggest the need for a broader application of the principles of economic evaluation to manpower problems and plant organization in general. The thermal power plant does not lend itself readily to the type of scientific management which is applicable in the field of mass production because this has to do primarily with repetitive processes. However, we have attempted to illustrate by a few examples the inherent possibilities of applying analytical methods to the study of operating manpower. Although the subject of maintenance has been omitted purposely, it is simpler to apply these same basic methods in that field because it is not so involved with the relatively intricate problems of operation.

This pressing need for greater activity in the technical fields of operation and plant management should be a challenge to the young engineer who possesses both a high academic record and above-average qualities of initiative, imagination, and leadership. He not only must be trained to be familiar with designs which are made with the aid of plans principally in two dimensions to accomplish a job which is to be constructed in three dimensions, but he also must learn how to create and sustain life in the finished product in four dimensions—three in space plus the human dimension. The medical student knows that the study of human anatomy must be followed by a period of internship and

[8] "Quick-Starting of Large High-Pressure, High-Temperature Boilers," by J. C. Falkner, Manager, Electric Production Department, Consolidated Edison Company of New York, Trans. ASME, vol. 75, 1953, pp. 1407–1460.

supervised practice in order to understand its functional significance and the innumerable types of malfunction which must be reckoned with. There is a very close analogy in the field of power generation, and the engineer must follow his study of power-plant anatomy by five or more years of internship in the plant before he can hope to produce anything of significant value in this field.

Conclusion

As stated at the outset, the purpose of this paper has been to focus attention upon certain problems which have a substantial influence upon operating costs. Such matters as incremental loading of units, economic scheduling of overhauls, and maintenance problems have been given extensive treatment by others and therefore purposely have been omitted here.

It has been shown that operating costs can be reduced not only by exercising ingenuity in plant management but also by a clearer understanding of the effect of equipment design and plant layout upon such operating costs. The reverse also may be true when operating policies do not meet the objectives which were contemplated in the design. In such instances, it may or may not be possible to modify these policies depending upon the type of operating labor available and other factors which to some extent may control existing plant-management policies. This merely serves to emphasize the extreme importance of co-ordinating the design with the best obtainable operating situation. Some utilities already have made impressive progress in this direction.

Finally, we have attempted to show that many of these problems, although involving human factors, are to a large extent adaptable to the process of economic evaluation. The need for such an approach is being emphasized greatly by changing economic conditions and by the technological advances of the recent past as well as those which are now in the making.

Consolidated Edison Looks at the Manpower Situation

By J. C. FALKNER,[6] NEW YORK, N. Y.

THE quest of the public utilities to decrease over-all costs is apparently endless. In the past, effort has been made in individual fields, i.e., design, construction, and operation. Now the industry is co-ordinating two or more fields—specifically, endeavoring to design plants so that manpower will be at a minimum. We are now thinking of how each man must function as we design. This is progress.

As an example, to show how this thinking has reduced manpower, Table 1 is given comparing the manpower requirements for the two units at the Astoria Station now under construction with two units at Waterside built in 1949. Astoria has a control room centrally located and Waterside has separate boiler, turbine, and electrical boards.

Notice that at Astoria there are only two equipment operators for two units. We feel that this will provide sufficient protection because we not only have all bearings supervised by thermocouples with alarms in the control room, but the station is divided into areas, and lights on 28 area alarm panels located throughout the plant indicate the functioning of any alarm. Thus the roving equipment operator knows immediately the area in which there may be trouble and proceeds there as the control-room operator, via public-address system, tells him of the details. If we did not have the bearing-alarm installation, at least two more men per watch would be required.

[6] Manager, Production Department, Consolidated Edison Company of New York. Fellow ASME.

TABLE 1 MANPOWER REQUIREMENTS FOR TWO UNITS AT ASTORIA STATION COMPARED WITH TWO AT WATERSIDE STATION

Station	Astoria	Waterside
Size of units	2-180 mw	2-110 mw[a]
Boilers	1 for each turbine	1 for each turbine
Fuel	coal, oil, and gas	coal and oil
Conditions	1800 psi, 1000 F — 1000 F	1600 psi, 1000 F
Manpower per watch for operation on coal:		
Supervision	2	6
Control-room men	2	4
Equipment operators	2	13
Operating mechanics	4	1
Ash handlers	1	2
	11	26
Coal handling (one shift)	10	13
Men per mw	0.15	0.55
Kw per man	6400	1800

[a] These topping units each rated at 50 mw supply sufficient exhaust steam to generate 60 mw in 200-psi low-pressure turbines. The manpower for these has been included in the table.

The plan at Astoria is to use the operating mechanics primarily as mechanics and as operators only for start-ups, shutdowns, and when operating difficulties arise. As mechanics they will do any required maintenance work within their physical and mental abilities. After the station is in firm service, since these units will operate around the clock, we expect that practically all their time will be spent on maintenance work.

The Astoria Control Room

The Astoria control room has a centralized flight panel whereon all instruments and controls for current operation are mounted. Recorders and less-used instruments are on other panels in the control room. This arrangement saves manpower because the men do not have to travel far to secure the information they need.

If one of the two units is shut down for an extended period for some reason, not more than one man would be freed from operating duties. In other words, approximately the same number of men are required for either one or two-unit operation.

We question the advisability of mass change-over of burners from one fuel to another because of the difficulty of maintaining constant load on the generator while the change-over is in progress. Naturally, if change-overs are very frequent, money may be spent economically to save manpower. For the changes now necessary on our boilers we prefer to change over one burner at a time.

Saving Manpower by Modernizing Control Systems

In the older stations a fertile field exists for saving manpower by changing instrumentation and control systems. For example, at Hudson Avenue, 32 boilers, 8 rows of 4 each, required 6 water tenders per watch to supervise the drum levels. We are now installing the control and observation of the drum levels on the operating floor under the eyes of the boiler operators, with only one water tender per watch to check the controls and to take care of some odd duties formerly covered by the six water tenders. Thus five men per watch are saved. This should cast no reflection on the original designers because of the increased cost of labor and the improvements in instrumentation and controls over the years.

TABLE 2 STATION CREW—MEN PER MW CAPACITY[a]

Year	Hudson Avenue	Waterside	Hell Gate	East River
1928	2.15	..	1.44	2.65
1932	0.85	..	..	1.45
1936	0.83	2.35	1.25	..
1940	0.80	1.75	1.13	1.29
1944	0.80	1.15	1.01	1.12
1948	0.73	1.13	0.87	..
1952	0.69	0.90	0.83	0.60

[a] Excluding supervision.

Table 2 indicates the progress made in reducing manpower requirements in the major stations of the Consolidated Edison Sys-

tem by installation of modern units and by reducing manpower on the older installations.

Another means of saving manpower is by laying out equipment so that it can be maintained easily and efficiently. This includes hoist beams, trolleys, and good access for removing pump covers, bearings, and so on. Frequently, too little thought is given to this in the original design. Also, as a means of reducing maintenance labor, thought should be given, in buying equipment, to the ease or difficulty of making repairs. If the equipment buyers would penalize the vendor for "hard to work on" equipment, the vendor would soon make design improvements.

Planning for Efficient Use of Manpower

By W. V. DRAKE[7] and D. H. RILEY,[8] PITTSBURGH, PA.

WHEN studying the factors affecting operating costs in steam-electric generating stations, it is almost superfluous to say that each system or company is unique in that it faces problems different, to a greater or lesser degree, from those of its neighbor. For in reality, the problems differ from station to station.

In discussing manpower and operating costs, it would be foolhardy, in an attempt to reduce factors at each station to the lowest common denominator for comparative purposes, to divorce each power station from its parent company. System or company-wide policies are important, if not the most important, factors which dictate the size of station crews.

System-Wide Factors Affecting Manpower

Consider, then, some of the factors which are really system-wide in nature and which can affect manpower and operating costs at individual generating stations:

1 System location is a prime factor in so far as wage rates are concerned. The supply and demand of skilled and unskilled labor directly affect the flexibility with which a system can operate. Where the labor market is tight, a larger permanent crew may be required; and where the labor supply is plentiful, hiring can be done on a more temporary basis.

2 The existence of a strong labor union can and does have a great effect on operating costs. Although labor unions are almost universal, it would be senseless to deny their importance where wage rates and permissible organizational setups are concerned. Labor unions frequently have a strong voice in determining the size of the operating force, particularly in determining the size of the reserve operator group. In nonunion plants, supervisory personnel often can be used for fill-in work during vacations and illnesses. Manpower requirements are affected further by whether or not a supervisor actually can operate during busy periods, i.e., turn valves, switches, and so on.

3 System or company policies concerning the location of technical and administrative help affect the size of station crews. The first of two obvious alternatives is to do as much technical and administrative work as possible in a central location. The second alternative is, of course, to keep at least part of the technical and administrative help in the field at the various power stations. Quite often, geographical distances and locations preclude choosing the first alternative. The use of a central force, needless to say, does have merit where it can be effected in a reasonable manner.

4 Much the same arguments as applied to technical and administrative work can be applied to chemical and research work; that is, it can be done centrally or in the field at the various power stations. A third alternative, however, where chemical and research work is concerned, is that it may be contracted totally or in part to outside firms.

5 Frequently, where geographical limitations permit, the use of a roving maintenance crew or crews becomes practicable. Under this system, one or more of the larger generating stations may employ an abnormally large maintenance crew, part of which can be sent out to the smaller or more remote stations for major maintenance work. The smaller or more remote stations need then employ only a skeleton maintenance force for minor repair work.

6 System philosophy regarding reserve capacity will affect manpower requirements and operating costs at the individual stations. Where reserve capacity is plentiful, maintenance work can be done during weekdays and usually fewer men are required. Where reserve capacity is scarce, much of the maintenance work must be done on week ends, at overtime rates, and by a crew large enough to complete the work in the allotted time.

7 The matter of minor construction jobs at power stations can affect its manpower requirements. With some companies, the policy is to maintain a force sufficiently large to take care of minor construction jobs. The alternative here, of course, is to contract all construction work.

Problems at Older Stations

Next, to consider other factors affecting operating costs in power stations, it is well to realize that the problems at an older station differ from and may be appreciably more complex than those at a new station. Consider some of the problems common to, if not inherent to, older stations.

Table 3 and Figs. 12 and 13, herewith, show a history and growth pattern for Station A, which is typical of many stations throughout the country. The station started about 1920 and was enlarged until in 1936 it was a 340-psi station of 180,000-kw capacity. The equipment consisted of 5 turbogenerators and 14 boilers. The operating crew numbers 92 men, which is equivalent to 1957 kw per operating man.

It may be well to mention here the maintenance setup. At Station A the maintenance force was organized as three distinct and separate groups, i.e., mechanical maintenance, boiler-room maintenance, and electrical maintenance. This was fairly common practice at the time and appeared to be a reasonable and logical approach to the problem. With the coming of labor unions, certain areas of responsibility were assigned to each group. As the plant continued to grow, with the addition of more modern equipment, the maintenance setup using the three distinct groups was no longer the most efficient setup. To merge the three groups into one over-all maintenance group presented many problems, both from the personnel standpoint and from the equipment or plant-facilities standpoint.

In 1937, at Station A, six of the low-pressure boilers were removed and replaced by three 1240-psi boilers which feed a 50,000-kw topping unit. Although a topping unit often can be added at a relatively low capital cost per kw of capacity, it invariably leads to a complicated operating setup. The complication involves not only operation, but maintenance as well.

With the addition of the No. 7 unit, which is a one-unit one-boiler job, much the same operating and maintenance setup was extended to take care of the unit. The No. 7 unit has a turbine board and boiler board separate from one another and on two different levels, the design being an extension of the old plant. The unit required four operating men per shift.

When the No. 8 unit goes into service in 1954, it will have its own central control room. In so far as is possible, it is planned to divorce the No. 7 and No. 8 units from the older part of the sta-

[7] Vice-President, West Penn Power Company. Mem. ASME.
[8] Manager of Power Production, West Penn Power Company. Mem. ASME.

TABLE 3 MANPOWER REQUIREMENTS AT STATION A

Date	Description	Station kw capability	Shift operators	Coal and ash-handling crew	Maintenance crew	Others: superintendent, technical, labs, clerical, storerooms, etc.	Total force	Kw per shift operator	Kw per man (total)
July, 1936	5 turbines—340 psi 12 stoker boilers—340 psi 2 pulv coal boilers—340 psi	180000	92	17	88	34	231	1957	779
July, 1945	5 turbines—340 psi 1 superposed turb—1240 psi (added in 1937) 3 boilers—1240 psi (added in 1937) Removed six 340-psi boilers in 1937 Retained 8—340-psi boilers	230000	110[a]	13[a]	104[a]	38[a]	265[a]	2091	868
July, 1953	Added unit job (no. 7 unit) Dec., 1945—1240 psi	315000	140	15	131	49	335	2250	940
July, 1954	Add unit job (no. 8 unit) May, 1954; reorganize operating crew to operate Nos. 7 and 8 units separate from rest of plant	450000	132	16	131	51	330	3409	1364
Future	Possible future unit job (no. 9 unit) which will use same control room as no. 8 unit	585000	144	16	131	51	342	4063	1711

[a] Wartime manpower shortage—the total force would undoubtedly have been larger had the men been available.

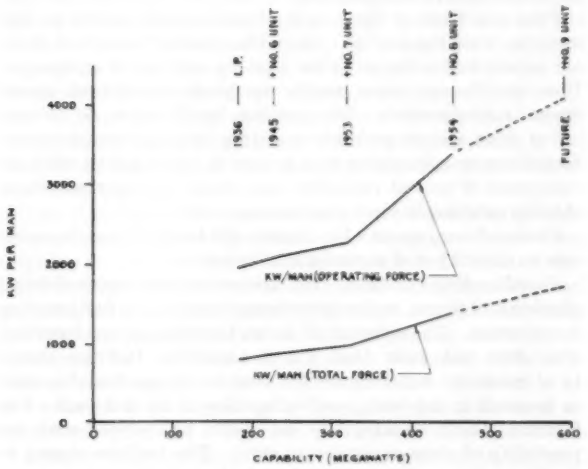

FIG. 12 KILOWATTS PER MAN VERSUS PLANT NET CAPABILITY AT STATION A

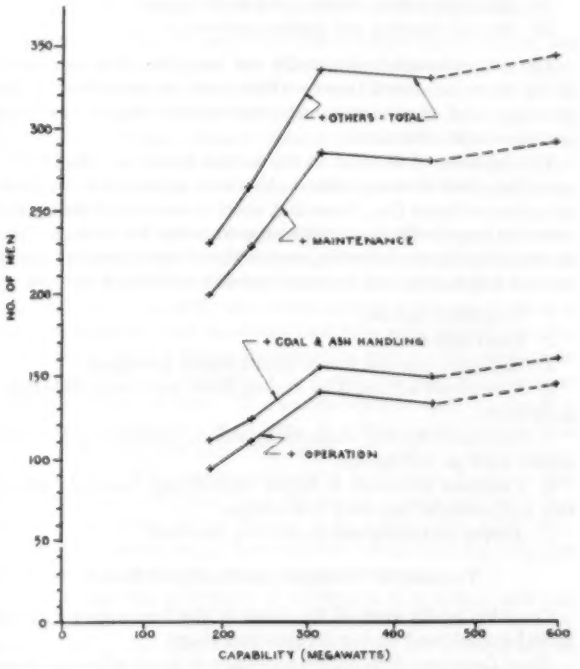

FIG. 13 MANPOWER VERSUS CAPABILITY AT STATION A

tion and to operate the two units as a separate station, thereby effecting an appreciable saving in manpower. It is planned to operate the two units with eight operating men per shift. In the event a No. 9 unit is added, it will be controlled from the same central control room as the No. 8 unit and should require only three additional men per shift, making a total of eleven operating men per shift for the three units.

Table 3 shows that the maintenance crew at Station A is quite large. Some of the factors which result in the large crew should be mentioned here. (1) The older part of the station requires a large maintenance crew, not only because of the age of much of the equipment, but the older equipment is used for peak loads which tends to increase the maintenance requirements. (2) Station A provides a maintenance crew for major repairs at some of the other stations on the system. (3) The fact that the maintenance crew is divided into the three separate parts, as mentioned, contributes to the size of the crew. (4) Station A is one of the oldest stations on the system and the average age of the men employed there is appreciably higher than that for the newer stations. The average age of employees not only affects productive effort, but also affects the length of the vacation period and amount of time out due to illness.

FACTORS AFFECTING OPERATING COSTS

Now, consider the factors affecting operating costs in new steam-electric generating stations. These factors logically fall into two main categories:

1 Factors to be taken into consideration during the initial planning, engineering design, and construction of a power station.

2 Factors which affect costs during the manning, operation, and maintenance of a power station.

Consider the first category, which experience shows to be the most important, because good initial planning, plant layout, equipment design, control-room layout, and the like, mean less manpower for operation and maintenance. The factors to be considered are quite numerous and some are impossible to evaluate

fully as yet; for example, the semioutdoor or completely outdoor plant as compared to the totally enclosed plant. The service record of outdoor plants, particularly those located in the northern part of the country, is not long enough to determine definitely whether or not a true long-time saving is effected by this design or whether the operation, maintenance, and other costs, some not now even considered, will outweigh the savings in initial investment.

There are, without doubt, some very definite factors which if considered, studied, and built into a station will tend to keep operating costs down. The major factors are listed as follows and will be discussed separately later:

1 Plant location.
2 Plant construction.
3 Plant layout.
4 Type and make of equipment.
5 Control-room layout.
6 Fuel-handling facilities.
7 Maintenance facilities.
8 Storeroom and storage space.
9 Adequate office, shower, and locker space.
10 Special cleaning and janitor equipment.

The list, although undoubtedly not complete, does give some of the more important factors which must be considered in the planning, and engineering, and construction stage if operating costs are to be minimized.

The following lists some of the factors which can affect costs, once the plant is in operation. It would appear that the foregoing factors listed (i.e., those that must be considered during the planning stage) offer the greatest opportunities for savings. The factors listed in the following are worthy of consideration and if studied and carried out do make possible additional savings.

1 Employee morale.
2 Good supervision.
3 Adequate but not excess maintenance personnel.
4 Permanent additions to station force made only after thorough study.
5 Minimum testing, engineering, clerical, purchasing, and personnel work at the station.
6 Constant attention to better engineering, materials, methods, and material handling and storage.
7 Proper and adequate accounting methods.

Factors to Consider in Planning Stage

Consider briefly each of the items in the first category which must be considered during the planning stage.

Plant Location. It is hardly necessary to expound on the three fundamental principles of nearness to load or transmission, adequate water supply, and nearness to a good fuel supply or transportation. Generally, within a given locale, the problem of plant location reduces itself to a choice among several logical sites. Once the choice of site is made, there are several less obvious factors which should be considered. Purchase of sufficient property for plant expansion and efficient fuel handling should not be overlooked. Another factor is the location of the plant itself on the property; this is especially important with respect to future considerations, such as plant expansion, expansion of fuel-handling facilities, cooling-water facilities, transportation and transmission facilities, and so on. Quite often, through lack of foresight, companies have sufficient acreage at a plant site for expansion, only to find that the location on the site of the existing plant is so awkward as to preclude plant expansion.

Plant Construction. Needless to say, a fireproof building, low in upkeep, is highly desirable. The outdoor and semioutdoor construction appears to be growing in favor at present, but all the factors are not known as yet on this type of building. Even as high as construction costs are, the savings in initial cost could be overcome quickly by high maintenance costs if such should occur due to cheap or inadequate construction. The use of noncorrosive materials where possible and the minimizing of painting are of importance. Another important factor is to have the construction force do as complete a job as possible. Frequently, owing to an incomplete job on the part of the construction people, a large maintenance crew is required during the initial period of service. Once the initial phase is passed, the operating company finds itself with an oversized maintenance crew.

Plant Layout. Much has been written and said concerning plant layout. The trend is to keep as much equipment as possible within easy access of the operating personnel. This is, of course, a basic consideration to be followed wherever possible. A point often overlooked in plant and equipment layout is the future maintenance of the equipment. Maintenance costs, high versus low, are often the direct result of plant and equipment layout, bad versus good. Equipment spacing and location of lifting equipment also deserve consideration.

Type and Make of Equipment. Opinions vary widely on this subject. Once the over-all cycle of the plant is determined, there are certain limitations as to the capacity and size of equipment. However, the equipment usually can be purchased from one of several manufacturers. The problem is, of course, to balance initial costs against probable operating and maintenance costs. Experience usually proves that it pays to spend a little more for equipment of proved reliability, and made of proper materials, thereby resulting in lower maintenance costs.

Control-Room Layout. No attempt will be made here to elaborate on the subject of control-room layouts.

Fuel-Handling Facilities. The circumstances at each individual plant will, of course, be the determining factor where fuel handling is concerned. The criterion of design is minimum fuel handling. This does not mean that the fuel-handling facilities should be of minimum requirements but that the design should be such as to result in the least possible handling of the fuel itself. The facilities should be adequate and should be designed with the possibility of plant expansion in mind. The facilities should be flexible enough to permit receipt of the fuel by different methods.

Maintenance Facilities. The maintenance shop should be laid out as near as possible in a centralized location with easy accessibility to the plant equipment. Such things as electrical test boards, special shop tools, special plant tools, inspection platforms, and the like, should be considered and if possible installed during the initial construction of the plant. Monorail beams and chain blocks or other hoists over the larger equipment will reduce maintenance costs materially, although the initial cost of installation may seem excessive.

Storeroom and Storage Space. The storeroom and adjacent storage space if possible should be planned to accommodate the ultimate storage. Although such a procedure may appear to be wasteful initially, over the long haul a saving usually can be realized. Where the storage of precision machine parts, such as bearings, is concerned, consideration should be given to dehumidifying the storage space to eliminate corrosion of steel parts which are not protected from moisture. There also should be adequate space for storing large slow-moving material. The space should be provided with adequate handling facilities.

Adequate Office, Shower, and Locker Space. If possible, the office should be centralized in the station, or possibly centralized but separated from the station proper. Consideration should be given to building with the ultimate station capacity in mind. If possible, the shower and locker space should be located in a single spot in the administration building, in order to minimize

the janitor and cleaning costs. Simplified design and construction also help to minimize janitor and cleaning costs.

Special Cleaning and Janitor Equipment. Inasmuch as cleaning and janitor work in a power station is a continuous and daily function, it is wise to install initially adequate facilities to do the work. Equipment such as a centralized vacuum-cleaning system with outlets strategically located throughout the station undoubtedly entails a high initial expenditure, but the time saved and the more effective cleaning made possible with such an installation may more than repay the initial cost. The installation of adequate storage space and sinks for cleaning work also should not be overlooked. A gathering place for janitors and laborers, where work assignments can be issued, should also be provided.

After Plant Is in Operation

Consider now the factors which apply once the station is in operation.

Employee Morale. This factor does not lend itself to definition and has an intangible quality; nonetheless its importance, from a cost standpoint, cannot be overemphasized. Basically, the problem here is to instill in all employees a desire to be part of the team, and to keep each individual aware of the importance of his particular job to the over-all picture. If for any reason any man or group feels that he or it has been treated unjustly, and the morale deteriorates, the effect, although not immediately obvious, will show up in high operating costs. Admittedly, it would be difficult to assign a dollar-and-cents value to a thing so intangible as employee morale, but its importance should not be overlooked.

Good Supervision. It should be almost unnecessary to mention the importance of good supervision, for without good supervision employee morale is certain to be bad. Aside from its effect on employee morale, good supervision can manifest itself in many ways such as good planning, technical proficiency, and the like, which must necessarily show up in terms of low operating costs.

Adequate but not Excess Maintenance Personnel. The line between adequate and excess is difficult to define. It is well to be aware that it is false economy to keep the maintenance force so small that equipment deteriorates to the point where continuity of operation is jeopardized. It is possible, however, to overload the maintenance force when confronted with major breakdowns or overhauls. This problem often can be overcome through the use of a centrally located roving maintenance force. The local or permanent maintenance force should be sufficiently large to keep all equipment in a good state of repair. The problem of maintenance-force size is not a static one, for the problem changes as the station becomes older.

Permanent Additions to Station Force Made Only After Thorough Study. During the initial starting of a plant, the operating, labor, maintenance, and all groups are frequently overburdened with work. As operating conditions stabilize, the duties are correspondingly decreased and clarified. Therefore it is probably better, when starting up a new plant, to retain at least part of the personnel on a temporary basis. Permanent assignments can then be made, after thorough study under stable operating conditions indicates the size of force required.

Minimum Testing, Engineering, Clerical, Purchasing, and Personnel Work at Station. Frequently a saving can be realized if as much of the work listed in the foregoing as possible is done on a system-wide basis by a centrally located force. Care should be taken that none of the listings mentioned is neglected, but if each station is manned so that it is completely self-sufficient in this regard, there is apt to be duplication of effort when viewed from a system standpoint.

Constant Attention to Better Engineering, Materials, Methods, Material Handling, Storage. As the plant grows older, the wear on equipment and breakdown of equipment become a larger factor in the operation of the station. As these problems arise, if they are analyzed with regard to the types of materials used and the reasons for the breakdowns, considerable savings in operating costs can be effected by wise substitutions of material or change in design or method either to eliminate or decrease materially the cost of such maintenance. In a large plant, consuming great quantities of fuel and large amounts of material each month, there are savings in operating costs which can be realized by studying the methods of handling and storing such material in order to decrease the time and money spent in this phase of operation.

Proper and Adequate Accounting Methods. A point, frequently overlooked, that applies to much if not to all that has been said is that of accounting procedures and methods. Obviously, little or nothing can be done to correct or to prevent a situation when the accounting methods do not permit as complete an understanding of the situation as possible. The ramifications of cost accounting in power stations are many, and although no attempt is made here to broach the subject, its importance should be recognized.

Effect of Station Design on Manpower Requirements

Table 4 and Figs. 14 and 15 of this comment show some of the effects of station design on manpower requirements. When studying the figures, it should be kept in mind that it is impossible to reduce all the stations to the same basis for comparison purposes. Although there are many varied and extraneous factors which enter the picture, as shown in Table 4 and Figs. 14 and 15, the figures do serve to show some general but interesting characteristics.

Stations B and C are of essentially the same design, with the exception of a few minor differences. The only major difference is in the size of the two plants (Station B has two 75,000-kw net capability unit jobs with one central control room, and Station C has two 22,500-kw net capability unit jobs with one central control room). Table 4 shows the operating crew at both stations to be 18 men. This is equivalent to 4 men per shift and 2 reserve operators at each station. The maintenance force at Station B is 13 men and at Station C is 10 men. It should be pointed out that both stations require help from other stations for major maintenance jobs. The maintenance force at Station B also is distorted because of the fact that the station is new and there is a construction force at the station now, adding the third unit. Generally, it can be seen, however, that incremental capacity can be added at little cost in manpower requirement.

The comparison of Station E to Station C is also of interest. Station E is of similar design and nearly the same capacity as Station C. The difference is that Station E has one unit job as compared to Station C's two unit jobs. Both stations have a central control room. Station E requires 13 operating men as compared to Station C's 18 operating men, which is equivalent to a difference of one operating man per shift. Station E also has a minimum maintenance crew of 8 men and draws on other stations for help during major overhauls.

Station F is of unit design with a central control room, but it also has a separate electrical control room which requires one operating man per shift. Hence Station F has 4 operating men on each shift, which is the same as Stations B and C, even though Stations B and C both have two units as compared to Station F's one unit.

Station D, which has a net capability of 170,000 kw, has three boilers and two turbogenerators and can be compared to Station B, which has a net capability of 150,000 kw but consists of the two unit jobs. Station D has a 27-man operating crew which is equivalent to 6 operating men per shift, which compares to the 4 operating men per shift at Station B. Both stations have a central

TABLE 4 EFFECTS OF STATION DESIGN ON MANPOWER REQUIREMENTS

Station	Year in service	Description	Station kw capability	Shift operators	Coal and ash-handling crew	Maintenance crew	Others: superintendent, technical, labs, clerical, storeroom, etc.	Total force	Kw per shift operator	Kw per man (total)
B	1952	2-unit jobs 1 central control room	150000	18	5	13	8	44	8333	3409
C	1950	2-unit jobs 1 central control room	45000	18	3	10	6	37	2500	1216
D	1949	3 boilers 2 turbogenerators 1 central control room	170000	27	6	33	18	84	6296	2024
E	1949	1-unit job 1 central control room	30000	13	3	8	4	28	3000	1393
F	1949	1-unit job 1 central control room + 1 electrical control room	60000	17	5	13	8	43	3529	1395

NOTES: 1 Station B and C are similar with respect to station layouts, but differ in the size of the units:
Station B..... 2-75000-kw units
Station C..... 2-22500-kw units
2 Stations E and C are similar with respect to equipment, but differ in the size of the units:
Station E..... 1-37000-kw unit
Station C..... 2-22500-kw units
System conditions dictated the use of 2 units at Station C.

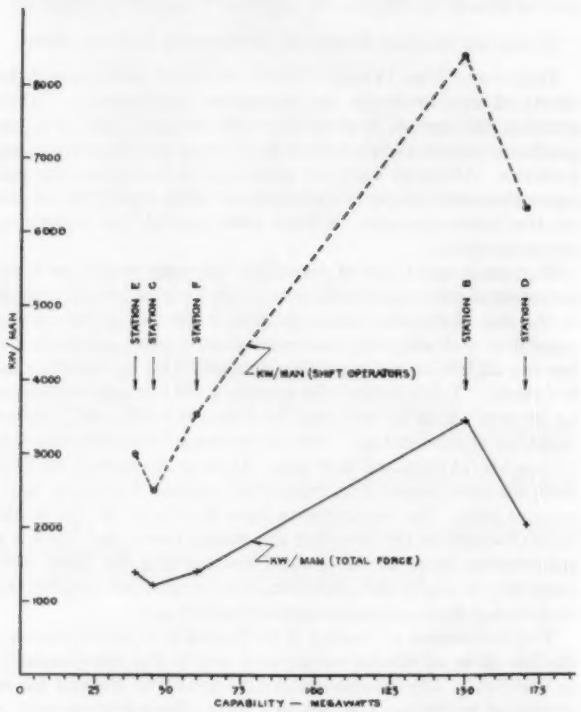

FIG. 14 EFFECTS OF STATION DESIGN ON MANPOWER REQUIREMENTS

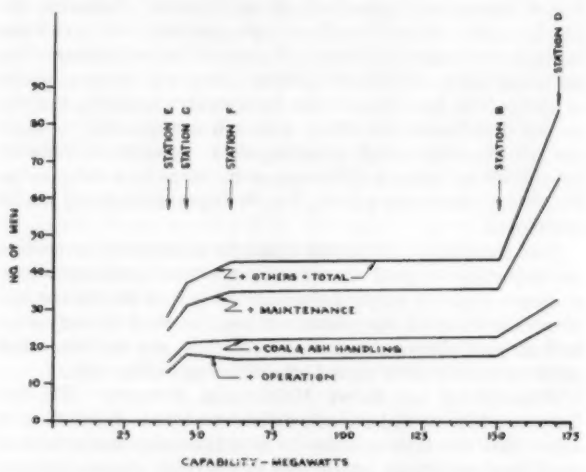

FIG. 15 STATION MANPOWER VERSUS CAPABILITY

control room, but the added complication of three boilers and the subsequent cross connections require an additional man in the control room and an additional roving man. It will be noted from Table 4 that the maintenance force at Station D is relatively large. It should be pointed out, however, that of the stations listed in the table, Station D is the only one which has a self-sufficient maintenance crew.

CONCLUSION

The obvious conclusion to be drawn from Table 4 and Figs. 14 and 15 is that design considerations can and do affect manpower requirements. In the past, the manning of many stations came as an afterthought to design. Advancement of the art has shown, however, that co-ordination of design and manpower requirements can result in substantial savings. Furthermore, system policies with regard to maintenance and other personnel at power stations can result in increased savings.

Maintenance and Effect on Manpower and Power-Production Costs

By G. V. WILLIAMSON,[9] ST. LOUIS, MO.

MAINTENANCE of steam-electric power generating plants has received little attention from the technical societies or associations. Yet, as all powerhouse engineers know, it is a vital part of his operations, and one which affects not only manpower and cost results but station dependability and productivity. This is a short outline of these problems, as seen by one whose company has given intensive study to the problem in the past few years.

Maintenance Manpower and Cost Factors

The manpower and costs for maintenance are, typically, secondary to plant dependability. Also, they are more strongly affected by local conditions and practice than are operating problems. This has made comparison of maintenance results among plants or systems, in such terms as mills per kilowatthour or cents per ton coal, unfruitful on the whole. Yet it is a vital part of good power operations and design. Maintenance manpower and costs are affected by many things, but particularly by the following:

1 Plant design and selection of original equipment.

2 Work conditions, such as the use of traveling crews and outside contractors. This variation has made it almost impossible to obtain comparable data on maintenance crews.

3 Load-base versus peaking.

4 Local coal and circulating-water characteristics.

5 Age of plant; necessity for keeping it on load; overloads.

6 The operator's administration and engineering skill in maintenance policies and practices.

Costs of maintenance on six older and three younger plants are shown in Table 5 of this comment. It is apparent from the variation in this pattern that no dependable guides can be given as to the size of crew needed for maintenance in a given plant.

TABLE 5 MAINTENANCE COSTS; COAL POWER PLANTS

Plant	Size class, megawatts	Age class, years	Cents per kwhr — Maintenance labor	Cents per kwhr — Material other than coal
A.....	400	Over 10	0.020	0.013
B.....	500	Over 10	0.020	0.013
C.....	500	Over 10	0.030	0.025
D.....	300	Over 10	0.035	0.035
E.....	500	Over 10	0.035	0.035
F.....	300	Over 10	0.030	0.020
G.....	300	Under 10	0.015	0.008
H.....	200	Under 10	0.013	0.008
J.....	100	Under 10	0.010	0.008
Average	350		0.025	0.018

The manner in which the author's company has analyzed maintenance costs has been organized around the following:

1 Cost Records. A machine accounting system, now in effect for six years, giving breakdown by boiler and turbine number at each plant, each type of pulverizer, and the like.

2 Organization of a maintenance analysis division, working directly with plant people on man-hour records for specific jobs; holding intra and interplant meetings on maintenance methods and cost results.

3 Organization of plant maintenance departments under assistant general superintendent—maintenance.

4 Development of toolroom storeroom, scooter delivery system to improve productivity of maintenance forces.

5 Development of a traveling group of turbine overhaul experts.

6 Close organization between load scheduling by power supervisors and steam-plant betterment department and "equipment overhaul committee" for true, most economical maintenance and outage plan.

[9] Superintendent of Steam Engineering, Power Production, Union Electric Company of Missouri. Fellow ASME.

Realizing Full Benefits of Centralized Control

By J. D. WILLIAMSON,[10] DAYTON, OHIO

IN his paper Mr. V. F. Estcourt points out that the principal reason for centralized control is to reduce manpower and thereby reduce operating costs.

Judging by the number of operators assigned per shift, many companies do not take full advantage of these savings, even allowing for variations in management policy in regard to equipment coverage.

An extreme example is the use of 12 men per shift, including watch engineer, in a postwar coal-fired station with two units operated from one control room. Electrical controls are in a separate room. The number of operators assigned to the second pair of units is not known.

It is doubtful if that number of men would have been required in the conventional station of a few years ago. Other stations may be cited which vary from this extreme coverage only in degree. These stations have not derived full benefit from the costly automatic equipment so necessary in centralized control.

Conversely, one company's management is satisfied with a crew of three operators and a watch engineer covering a two-unit gas-fired station.

On-the-spot studies of stations using minimum coverage by companies who plan to use centralized control are highly recommended. Adjustments to conform with design differences and management policy will result in adequate coverage without overmanning.

Minimum Personnel for Other Jobs

The same careful study should be made with regard to the strength of other crews. It is far easier to increase the force than to decrease it, particularly if one must reckon with a unionized station. Starting with a minimum crew may require occasional overtime work, but this is an inexpensive method of determining the need for an increased force.

When we started a new station 5 years ago, our coal-handling crew consisted of five men and a working foreman. They handled rail shipments, belt conveyers, bulldozers, and the job was operated 7 days per week.

This was deliberate undermanning. We kept this crew on the light side until we finally arrived at the present force of eight men and the working foreman. We are certain that this is the minimum crew that can perform this work properly with virtually no overtime. This same procedure should be applied to practically every job in the station.

Effect of Union Contract

The contract between the company and the union can have a very definite effect on generating costs. Perhaps this is subject to less control than other factors but an effort should be made to do the best job possible.

When writing or amending a contract, avoid language which may hamper future developments. For example, an agreement specifying the number of operators "per unit," or per unit of

[10] Assistant Manager, Power Production, Dayton Power & Light Company. Mem. ASME.

TABLE 6 TOTAL PRODUCTION EXPENSES EXCLUDING FUEL OF SOME TYPICAL PLANTS

Station	Number and size of units, mw	Fuel burned—coal, oil, gas	Plant factor, per cent	Generating cost other than fuel: Actual, mills/kwhr	Generating cost other than fuel: Adj to 100 per cent plant factor, mills/kwhr
A	4–60	C	64	0.42	0.27
B	3–90	O	64	0.41	0.26
C	2–100	C	91	0.67	0.61
D	4–110	C—O—G	65	0.65	0.42
E	3–125	C	97	0.56	0.54
X	6–40 to 60	C	79	0.36	0.28

boiler horsepower may have appeared harmless a few years ago, but imagine its effect on the labor required in a modern high-capacity station.

The power-production division must be represented on the management committee in any union negotiation. An apparently innocuous demand which would cost little in some departments might assume major proportions when applied to shift workers.

In some instances the control operator's job has been rated too high. This not only increases costs but may create dissatisfaction among those having similar responsibilities in older stations. It is our opinion, shared by the control operators on the job and by the union, that this classification should not rate higher than other top operating jobs in any type of station.

An Evaluation of Some Postwar Stations

Mr. Estcourt points out three factors which affect manpower in central-control stations:

1 Large units tend to reduce men/mw.

2 More units operated from a single control room have the same effect.

3 Coal-burning stations require 20 per cent more men on the payroll than oil or gas-fired stations.

These are sound principles and it is interesting to examine the results as reported in the latest (1951) Federal Power Commission report, "Steam-Electric Plant Construction Cost and Annual Production Expenses."

The item compared in Table 6 is "total production expenses exclusive of fuel." While it is conceded that factors such as central maintenance crews will affect this cost, it should form a reasonable basis for comparison. All have been converted to the equivalent of 100 per cent plant factor in order to simplify the comparison.

With one exception, the figures in Table 6 represent some of the largest, postwar, central-control-type stations in the country that were operating in 1951. Why isn't there some consistency in the "costs other than fuel" when the precepts laid down by Mr. Estcourt are applied? While an equal number of examples could be cited to prove Mr. Estcourt's thesis, particularly as applied to fuel, that does not explain away the ones listed in this comment. There are evidently some cost factors which are escaping our attention. Possibly this panel discussion will bring them to light.

Incidentally, Station X in Table 6 simply adds a bit of confusion—it does not have centralized control.

Discussion

F. W. Argue.[11] The author has made a stimulating contribution to the important study of the effect of manpower on reliability and operating expenses. His use of the quantitative "austerity factor" is especially interesting as it introduces possibilities of assigning values to what have always been considered as solely matters of judgment.

As centralized control has extended to more units in a station, each of increasing complexity, the feeling has grown among many operators and designers that the capability of human operators to deal with adverse or upset conditions may well be exceeded. Students of the subject report that only an astonishingly small number of facts or separate communications can be absorbed in rapid succession before the human brain becomes "overloaded," so to speak, and not only refuses to receive further intelligences, but rejects those which have already been received. The author points out that his company recognizes this human limitation by utilizing a master panel on which are mounted only a relatively few instruments and controls.

While arrangement and disposition of controls may vary, the concepts are similar, namely, that if the equipment or controls deviate from normal, the human operator takes over and institutes corrective measures and uses his judgment as to whether continued operation might endanger the equipment.

While it is recognized that a power station is vastly more complex than an electric circuit, in the case of the latter it is accepted without question that, under faulty conditions, the circuit is automatically opened. Here the concept is not continuity of service at all costs, but rather to safeguard the equipment so that full service can be restored as soon as the fault can be cleared.

Applying this latter concept to power-station design might result in utilizing automatic controls somewhat along established lines but adding more provisions for automatically tripping a unit if predetermined limits of variation were exceeded. Instrumentation in such a plant probably would consist chiefly of recorders, as the principal human-operator function would be to analyze troubles after the fact.

While at first glance this may appear to be a drastic and somewhat ill-considered method of dealing with manpower problems, a review of some of the automatic tripping features already adopted in power stations indicates that possibly we are approaching this condition by the rear door. Design criteria which were applicable to common header stations, where a trip-out frequently involved the whole plant, are not equally valid with a unit system, where temporary loss of one unit is not necessarily catastrophic.

An oversimplified example of this principle applied to familiar equipment is the domestic heating system, where boilers or water heaters are completely automatic but are also equipped with tripping devices which shut the unit down if normal conditions are not maintained.

It is believed that power-station control functions could be monitored in a similar manner using, for the most part, available control and safety devices. While still in the conjectural stage it is entirely possible that one of the so-called "electronic brains" could be adapted to this service, with the prescribed operating conditions punched out or marked on a series of tapes. Carrying this one step further might see the "brain" capable of starting and stopping a unit on the daily cycle required in many plants.

This comment is not made with the thought that a system of this type, representing an austerity factor approaching 100 per cent, is presently feasible. It does emphasize, however, that critical analysis and review, such as are presented in this paper, are necessary in order to keep operating and design practices in proper perspective in the face of a rapidly changing technology.

[11] Assistant Engineering Manager, Stone & Webster Engineering Corporation, Boston, Mass. Mem. ASME.

F. S. Helfter.[12] The author has performed a worth-while service in discussing the various items that affect steam-generating-station operating costs.

Centralized control rooms have become almost standard design and the question arises as to how many unit controls should be brought together into one room. Dunkirk and Albany, the last two new plants built by Niagara Mohawk, have continued the practice employed at Oswego of bringing the controls from two units to one operating point. This has worked out satisfactorily and, although this arrangement may require a little more manpower, it is believed there are many advantages in this system to justify it. Lower costs due to controls being nearer the equipment, less generating capacity affected in case of a catastrophe in the control room, design for future units not limited by present units, are but a few important advantages of a two-unit control room.

How a plant is to be loaded is a factor to be considered when deciding on a design. A fluctuating load and one that necessitates units to be taken out of service frequently, justifies many features that a base-loaded plant would not require. The more variations in load or in types of fuel burned, the more facilities should be made available to the operators.

Just how far one can go in centralization and reducing operating personnel may depend to a great extent on the amount of spare generating capacity available to the systems. If the loss of a unit may require a cut in customer load, every precaution must be taken to forestall a unit failure, and even more so, a multiunit failure.

Radical departures from past practices are much more difficult to incorporate in an extension to an old plant than they are to put into effect in a new plant. The policies of management can be changed in most cases more easily than those of the union. To eliminate a position or to increase even slightly the responsibility of an operator without an increase in remuneration very often results in a grievance.

In staffing a new station, the higher-type operators from the parent plants usually are transferred to fill the key operating positions. When adding units to an old station, it is customary to upgrade the existing personnel according to job or company seniority almost irregardless of qualifications or physical capabilities. Unless operators can be hand-picked for the job, it would be quite a handicap for everyone concerned to attempt to operate a plant with what might be called a skeleton crew. In a modern plant with only a few operators on a shift, each man must shoulder his own load and cannot be "carried" by fellow employees or his foreman. It is the responsibility of management to employ a higher-type man for operation and give him the necessary training to bring him up to the modern standards of the equipment he is to operate.

The writer agrees with the author that with the great increase in hourly wage rates and the many fringe benefits now in effect, every effort must be made to reduce the operating force to a practical minimum but this should be done without jeopardizing plant output as continuity of service is of prime importance to the electrical household of today.

G. A. Porter.[13] The author is to be commended for his excellent paper on the efforts that have been taken in the design of new large steam-electric generating stations to reduce operating costs by reducing manpower requirements. This is one of the most comprehensive papers on this subject that has come to the writer's attention.

There can be no argument with the general theme of the paper that we must design for the minimum practical operating and maintenance manpower. Care must be taken, however, to avoid reducing manpower so much that reliability is sacrificed or that operating economies are lost.

In the design of new thermal plants employing large generating components and centralized controls, there is not too great a difference in the number of required operating jobs. The type of fuel, as has been mentioned, can be more of a factor than the type of control center.

Our new St. Clair Power Plant is of this type. When completed in 1954, there will be four 150,000-kw turbine generators supplied with steam from four steam generators. The units will be controlled from two mechanical control rooms and one central electrical control room. There will be 13 jobs per shift including supervision.

A plant such as River Rouge, planned for service in 1955, with two 260,000-kw reheat units, is being designed with a mechanical-control center for each turbine-boiler unit and a common electrical-control center for the plant. This is in contrast to the St. Clair arrangement where two turbines and two boilers are controlled from one operating center. With each unit consuming as much as $6,000,000 of fuel annually, such an arrangement of controls, properly manned, will permit obtaining maximum economy. It is proposed that there will be 13 jobs per shift together with supervision.

The author has not discussed the worth-while savings that are possible when old stations are modernized or capacity is increased by high-pressure additions. The capacity of two stations of the writer's company has been increased materially by additions within the past five years. The reduction in manpower per megawatt resulting from the addition and modernization of the coal-handling systems were as follows:

Plant A

Original capacity, 300 mw	Men per mw, 1.4
Final capacity, 500 mw	Men per mw, 0.9

Plant B

Original capacity, 310 mw	Men per mw, 1.4
Final capacity, 510 mw	Men per mw, 0.8

Author's Closure

The author is very much indebted to the other members of the panel who have added considerable factual information on the problem of manpower costs, and also to Messrs. Argue, Helfter, and Porter for their thoughtful comments.

Several of the discussers have called attention to the manpower savings which can be effected by modernization and reorganization in older stations, and the statistics which they have furnished should be of considerable value to others. Mr. Falkner's statement regarding the reduction in shift manpower resulting from a bearing-alarm installation is also interesting. Although the saving of two men per watch at Astoria as a result of this installation may not always be attainable, it is a good example of what can be accomplished by careful consideration of the functional components of the plant.

In connection with Mr. Falkner's comment regarding the possible difficulty of maintaining constant load on the generator during mass change-over of burners from one fuel to another, it should be stated that we have not encountered any such difficulty and our experience with this system during the past two years has led to the conclusion that it is not only a quicker method of changing fuels but is less vulnerable to operating errors. As is usually the case with this type of control problem, the results obtained may vary widely because the degree of success will depend largely upon the ability to achieve a functional and realistic design.

[12] General Superintendent of Steam Stations, Niagara Mohawk Power Corporation, Buffalo, N. Y. Mem. ASME.

[13] Vice-President, The Detroit Edison Company, Detroit, Mich. Mem. ASME.

When making comparisons of manpower requirements at different plants, it is important to make sure that the data are set up on a comparable basis. The figures which were given in our paper for the number of men per megawatt and the kilowatts per man include all maintenance manpower except for the relatively small amount of work which is handled by outside contracts. However, it is our understanding that almost the entire maintenance force required for Astoria is part of the manpower pool which is headquartered at the Hellgate Station. Therefore it is assumed that the unit manpower figures given for Astoria include very little, if any, maintenance labor. Presumably the same comment applies in some degree to the figures given for Waterside Station. This is mentioned primarily for the purpose of emphasizing the extreme care which must be exercised in using figures of this type for basic studies. On the other hand, the beneficial effect of such manpower pools in reducing labor costs is emphasized by G. V. Williamson. We are also indebted to Mr. Williamson for his thought-provoking contribution on some of the basic problems of maintenance and their effect upon production costs. He has made an able condensation of a subject which might well be expanded into a major paper.

Messrs. Drake and Riley have contributed some valuable manpower statistics applying to plants operated by their company. They have also enumerated various groups of factors which affect manpower under the headings of (*a*) System-Wide Factors, (*b*) Design Factors, and (*c*) Plant-Management Factors. The influence of these various factors is fairly well understood today in a qualitative way, but this type of information is of relatively little use unless a basis can be established for arriving at a quantitative evaluation in terms of their relative economic significance. When the latter type of approach is made it will be found that many of the factors, although logically associated with the problem, in reality cannot be assigned any significant dollar value.

Mr. Argue calls attention to the apparently increasing complexity of centralized control so that "the feeling has grown among many operators and designers that the capability of human operators to deal with adverse or upset conditions may well be exceeded." Mr. Argue is not alone in this opinion. Other utility engineers have expressed increasing concern with the complications of controls for unit boiler-turbine installations, stating that, when considered along with the centralized control system, the complexity of relays, interlocks, controls, etc., becomes such a maze of delicate control equipment that it borders on inviting hazards rather than warding against them. Fundamentally, this is a problem of physical bigness and is analogous to the present-day problem of administrative bigness. In the latter instance the trend of modern management is toward decentralization with the aid of special administrative devices for the co-ordination of the various localized activities.

A similar solution can be applied to the physical problem, and it would appear that plant performance and availability are sometimes adversely affected not only by unexpected complexities of the so-called unit system, but also from the over-centralization of controls which in turn results in excessive concentration and isolation of operating manpower. In the author's paper, examples were given to illustrate the possibility of decentralization of seldom-used controls together with the grouping of the principal controls for several large main units on a single control panel not much longer than a completely centralized control panel for a single unit. Furthermore, this type of master panel can be made far less complicated for the operator than a completely centralized panel for a single large unit. This arrangement, if properly designed, can result in a substantial reduction in average work load per man due to the diversity factor between the number of operators in terms of the number of units affected by trouble simultaneously.

Mr. J. D. Williamson cites specific examples of the extremes in the number of shift operators which result from differing policies and design philosophies affecting manpower requirements. The magnitude of this problem in terms of dollars has been emphasized in our paper under the heading of Differing Concepts of Centralized Control. In considering the number of operators which are required for a particular plant, it would appear that the word "required" is used rather loosely and too often refers to the number of men *assigned* to a particular plant rather than the minimum number of men actually *required* as a result of an objective analysis of all the factors. The very nature of the problem appears to invite an oversimplified approach supported largely by broad generalizations. One of the analytical devices which we have suggested for use in arriving at a realistic evaluation of manpower requirements is the so-called austerity-factor rating. A realistic application of such a factor is not easy but does suggest a form of approach to the problem which in some instances will result in rather surprising conclusions.

The wide differences in manpower "requirements" cited by both Mr. Williamson in his discussion and also in the author's paper, serve to further emphasize that there is a real need for more reliable methods of operating-manpower evaluation. It has already been pointed out that these discrepancies are due not only to management policies with respect to the scope of operator duties, but also to the general plant layout with particular reference to the control center. Any conclusion that the latter does not materially influence the number of operators required for reliable plant performance may well lead to costly operating experiences.

The author fully agrees with Mr. Porter that operating manpower can be reduced to the point where operating reliability and economy are sacrificed. As a general example, although it is safe to say that it is possible to operate two large reheat units with entire satisfaction and reliability with five men per shift with oil and gas fuel, or six men per shift with coal fuel, attempts to operate with this number of men have not always been entirely successful. It can be shown that the number of operating errors, equipment outages, and maintenance costs may increase appreciably by merely cutting down the number of operators per shift without due regard to the problems of station layout and operating management which are involved. A realistic and more analytical approach to the evaluation of such factors has been one of the principal objectives of the author's paper.

The Economics of Large Reheat Turbine-Exhaust-End Size Selection

By D. W. R. MORGAN, JR.,[1] and S. D. FULTON,[2] PHILADELPHIA, PA.

The purpose of this paper is to provide a method and tools for making a study, at capability performance, of large reheat-steam-turbine exhaust-end size, and of those other plant components which are affected by the heat rejected to the condenser. The result of this type of study will lead to an economic evaluation and selection of appropriate turbine-exhaust ends. It is often desirable to investigate the effect on over-all plant performance and gross cost of operation, including investment and fixed charges of the various turbine-exhaust-stage annuli available on alternative units of large ratings. This paper does not attempt to provide exact or final answers; but it will measure principal factors and indicate whether a given situation warrants a more detailed study.

Nomenclature

The following nomenclature is used in the paper:

C = total justifiable increased plant cost, dollars
C_{fh} = evaluated fuel savings, from ΔHR_p, dollars
C_{fw} = evaluated fuel savings, from $\Delta kwhr_w$, dollars
C_p = plant cost, dollars per kw of capability
ΔC_c = condenser surface cost difference, dollars
ΔC_w = circulating-pump cost difference, dollars
E_c = steam-generator efficiency, per cent
E_m = circulating-pump motor efficiency, per cent
E_w = circulating-pump efficiency, per cent
F = fuel cost, cents per million Btu
FC = fixed charges, per cent
G = turbine-exhaust flow, lb/hr
G_a = approximate turbine-exhaust flow, lb/hr
H_c = approximate condenser duty, Btu/lb
ΔH_c = difference in heat rejected to condenser, Btu/hr
HR_p = plant heat rate, Btu/kwhr
HR_t = turbine heat rate (based on output at generator terminals), Btu/kwhr
ΔHR_p = plant heat-rate difference, Btu/kwhr
ΔHR_t = turbine heat-rate difference, Btu/kwhr
K = exhaust-flow correction factor (Fig. 1)
kw_t = turbine capability at generator terminals, kw
Δkw_t = kilowatt difference at turbine coupling, kw
$\Delta_w kw$ = difference in circulating water-pump power, kw
$\Delta kwhr_w$ = kilowatthours per year difference for circulating water pumps based on full-capacity pump operation, kwhr
L = auxiliary loss, per cent
L_b = boiler feed-pump power, per cent of kw output at generator terminals (Table 5)
LF = load factor, per cent
P = correction factor for one-half circulating-pump capacity operation
R_b = capability credit for reduced boiler feed-pump power, dollars
R_w = capability credit for reduced circulating-pump power, dollars
S_m = condenser surface per million Btu/hr heat transfer, sq ft
ΔS = condenser-surface difference, sq ft
Sp gr = specific gravity
TDH = total dynamic head, ft of water
W_m = circulating water, gpm per million Btu/hr of heat rejected
ΔW = circulating-water difference, gpm

Introduction

The heat rate of a turbine generator unit measured in Btu consumed per kilowatthour generated is, among other items, dependent upon the turbine-exhaust-stage annulus area selected for the installation. Because load factors, fuel costs, condensing-water temperatures, interest charges, and other factors vary between different localities, there is no one-and-only proper exhaust size for a given turbine capability. Table 1 shows those turbine exhaust-end annuli now considered as standard by the authors' company and the corresponding reheat-cycle turbine capabilities for which they are applicable.

Note that for 150 megawatts capability, as an example, there is available a range of nearly 2 to 1 in relative exhaust-stage areas

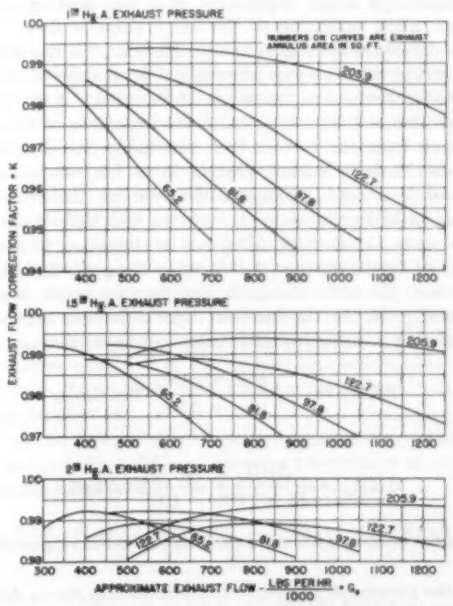

Fig. 1 Curve of Exhaust-Flow Correction Factor Versus Approximate Exhaust Flow in Pounds Per Hour

[1] Manager, General Engineering Section, Westinghouse Electric Corporation. Assoc. Mem. ASME.

[2] General Engineering Section, Westinghouse Electric Corporation. Mem. ASME.

Contributed by the Power Division and presented at the Annual Meeting, New York, N. Y., November 29–December 4, 1953, of The American Society of Mechanical Engineers.

Note: Statements and opinions advanced in papers are to be understood as individual expressions of their authors and not those of the Society. Manuscript received by ASME Headquarters, October 21, 1953. Paper No. 53—A-93.

TABLE 1 EXHAUST END-CAPABILITY COMBINATIONS FOR REHEAT TURBINES

Number of exhaust ends	Exhaust annulus, sq ft	Capability megawatts 100	125	150	175	200	250	300
3600-rpm tandem compound								
2	65.2	X	X	X				
2	81.8	X	X	X				
3	97.8		X	X	X	X		
3	122.7		X	X	X	X	X	
3600/1800 rpm cross compound								
2	205.9			X		X	X	X

for the 3600-rpm tandem-compound unit, and over 3 to 1 for the corresponding cross-compound unit with an 1800-rpm low-pressure element. The evaluation of this variable, in terms of relative thermal performance and cost, is the purpose of this paper. The results of this evaluation by the method given in this paper should be considered only as a first approximation indicating a broad line of demarcation between economic and uneconomic turbine-exhaust ends.

Data for preliminary studies ordinarily do not include information on partial-load performance or seasonal water-temperature variations, both of which have an appreciable effect on the fuel saving realizable with a larger exhaust end. The lower heat rates obtained with larger exhaust ends are the result of lower exhaust loss. This difference in exhaust loss decreases as the volumetric exhaust flow decreases and becomes negative under some conditions. Therefore load and exhaust pressure, both of which affect exhaust volumetric flow, have a sizable effect on the relative thermal performance of units employing different size exhaust ends.

Preliminary studies usually will be based on the thermal performance at capability and design exhaust pressure. Fortunately, the errors introduced by this procedure all favor the larger exhaust end; therefore they do not affect materially the usefulness of the data in defining the field where more detailed study will be required.

Basis of the Method

It can be assumed that the exhaust flow for two turbine generator units having different exhaust-end annuli, designed for the same capability, steam conditions, and feed-heating cycle, is the same when operating at the same throttle flow. Therefore the difference in exhaust loss (in kilowatts) is the difference in kilowatts at the generator terminals, if generator efficiency and difference in mechanical losses are disregarded. Exhaust flows can be determined from heat-balance calculations or closely approximated from the turbine heat rate as described later. Exhaust-loss-difference curves, plotted as a function of exhaust flow, provide a ready means of determining the exhaust-loss difference in kilowatts between turbines with different exhaust-annulus areas. If desired, Δkw_t can be corrected to generator output; but for the purpose of this paper the generator efficiency is neglected. Since the change in heat rate for small changes in load is negligible, the turbine heat-rate[3] difference between two units differing in exhaust-end annulus can be written as

$$\Delta HR_t = (-)\frac{HR_t \times \Delta kw_t}{kw_t + \Delta kw_t}, \text{ Btu/kwhr} \quad \ldots\ldots [1]$$

and

$$\Delta HR_p = \frac{\Delta HR_t \times 10^4}{E_s \times (100 - L)}, \text{ Btu/kwhr} \quad \ldots\ldots [2]$$

The plant heat-rate difference is used for fuel-saving evaluation.

[3] For the purpose of this paper the turbine heat rate is defined as the heat added to the motive fluid by the steam generator divided by the kilowatt output at tgenerhe ator terminals.

Determination of heat-rate difference from exhaust-loss difference is the basis of the method presented in this paper.

Development of the Method

In order to make an economic comparison, by the method presented in this paper, of two turbine-generator units with different exhaust-end annuli, it is necessary to determine or assume the following data:

1 Initial and reheat steam conditions.
2 Exhaust pressure, inches Hg abs.
3 Capability, kw.
4 Exhaust-annulus areas, sq ft.
5 Heat rate at capability (for unit with smaller exhaust-annulus area), Btu/kwhr.
6 Fuel cost, cents per million Btu.
7 Load factor, per cent.
8 Fixed charges, per cent.
9 Plant cost, dollars per kw of capability.
10 Steam-generator efficiency, per cent.
11 Auxiliary loss, per cent.
12 Circulating-water temperature, deg F.
13 Condenser-tube size, gage, and length.
14 Circulating-water velocity, fps.
15 Circulating-water total dynamic head, ft of water.
16 Percentage of year with one-half circulating-pump-capacity operation.

All of the foregoing factors influence the final result. However, exhaust-annulus area, exhaust pressure, fuel cost, load factor,

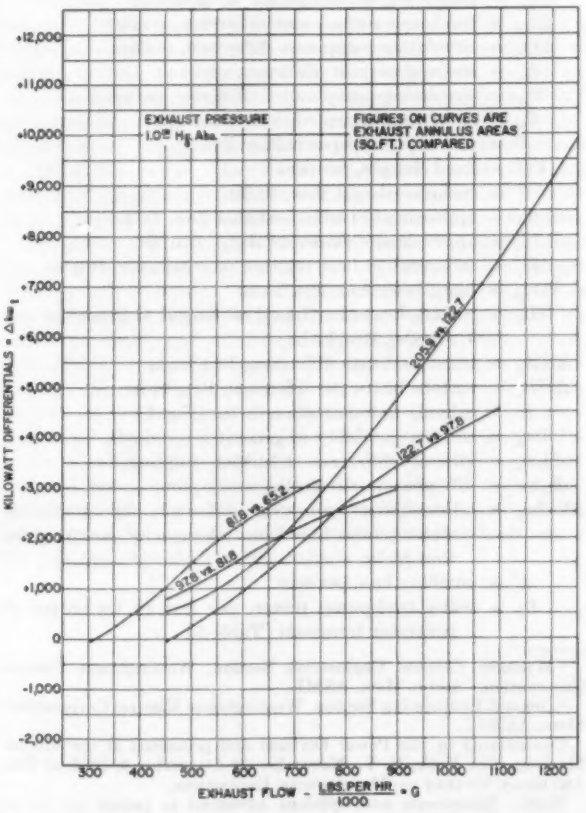

Fig. 2 Curve of Kilowatt Differentials Versus Exhaust Flow in Pounds Per Hour at 1.0 In. Hg Abs

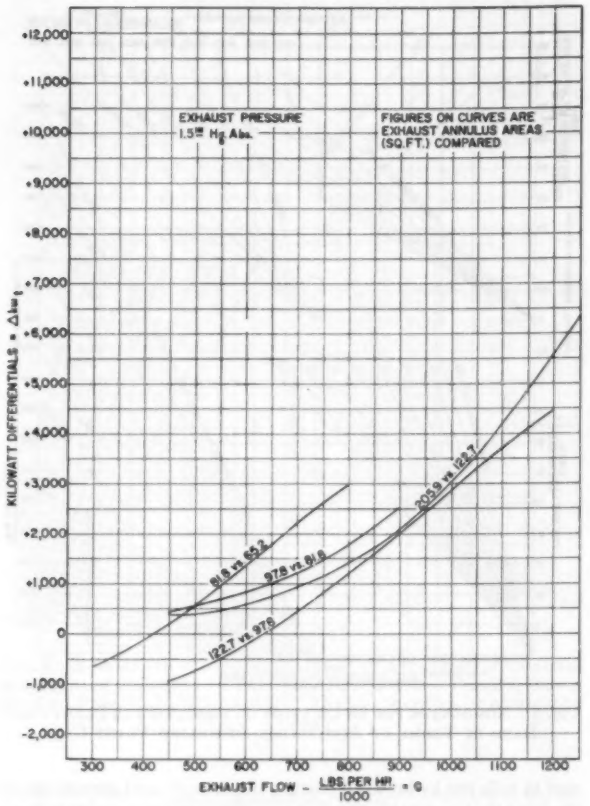

FIG. 3 CURVE OF KILOWATT DIFFERENTIALS VERSUS EXHAUST FLOW IN POUNDS PER HOUR AT 1.5 IN. HG ABS

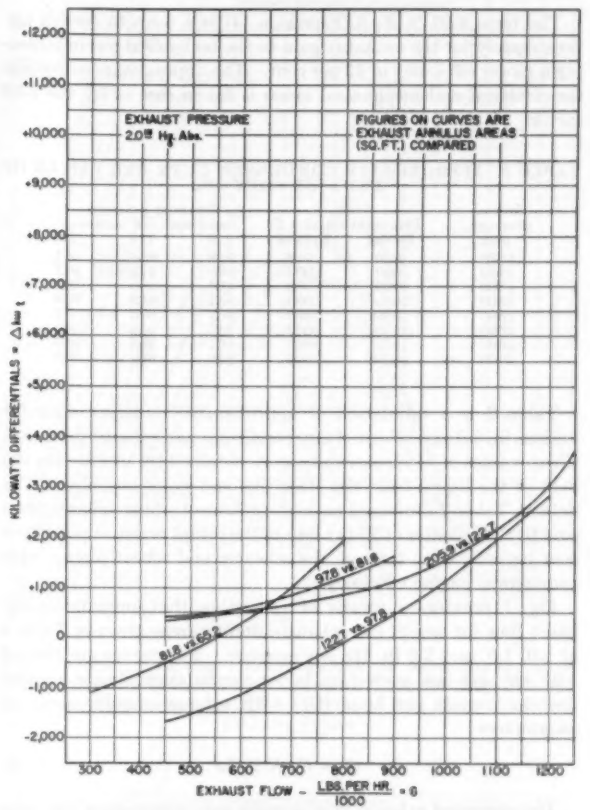

FIG. 4 CURVE OF KILOWATT DIFFERENTIALS VERSUS EXHAUST FLOW IN POUNDS PER HOUR AT 2.0 IN. HG ABS

and fixed charges will have the greatest effect. These items generally are known, with the exception of load factor and fuel cost, which must be estimated.

A complete economic analysis for any given situation involves the following elements:

a Difference in building and foundation cost.

b Difference in piping, boiler-feed system, and steam-generator cost.

c Difference in turbine-generator cost.

d Evaluated fuel saving from reduced plant heat rate.

e Evaluated fuel saving from reduced circulating-water-pump power.

f Difference in cost due to reduced condenser surface and circulating-pump capacity.

g Pumping-power capability credit (boiler feed and circulating water).

Items (*a*) and (*b*) are beyond the scope of this paper. Item (*c*) can be obtained readily from the turbine manufacturer.[4]

Cost evaluation for items (*d*), (*e*), (*f*), and (*g*) can be obtained from the data herein, subject to the limitations cited in evaluating item (*d*).

Omitting consideration of items (*a*) and (*b*), justification of the purchase of a turbine with a larger exhaust annulus requires that item (*c*) must be less than the algebraic sum of items (*d*), (*e*), (*f*), and (*g*). The total justifiable increased plant cost C, is

$$C = C_h + C_{tw} + \Delta C_s + \Delta C_w + R_w + R_b, \text{ dollars} \ldots [3]$$

Solution of Equation [3] requires determination of the plant heat-rate difference. Equation [1] gives the turbine heat-rate difference as a function of the difference in kw output with equal exhaust flows. Equation [2] converts turbine heat-rate difference to plant heat-rate difference.

Figs. 2, 3, and 4 show the kilowatt differentials at the turbine coupling between selected exhaust-annulus areas as a function of exhaust flow in pounds per hour at 1.0, 1.5, and 2.0 in. Hg abs exhaust pressure. It will be noted that each exhaust-annulus area is compared to the next larger exhaust-annulus area. If it should be desired to compare other combinations, the algebraic sum of the kilowatt differentials at the same exhaust flow, pounds per hour, and back pressure may be used; however, the maximum permissible exhaust flow of the smaller exhaust-annulus area, as indicated by the termination of the curves in Figs. 2, 3, and 4, must not be exceeded.

The exhaust flow, as determined by heat-balance calculations, should be used if available; otherwise the exhaust flow may be approximated closely from the turbine heat rate

$$G_a = \frac{(\mathrm{HR}_t + 34.13 \times 0.92 \times L_b - 3413 \times 1.02)\,\mathrm{kw}_t}{H_e}, \text{ lb/hr}$$

$$G_a = \frac{(\mathrm{HR}_t + 30.80 \times L_b - 3481)\mathrm{kw}_t}{H_e}, \text{ lb/hr} \ldots\ldots [4]$$

[4] See Fig. 10 for approximate cost differentials between various exhaust-end annuli. These cost differentials are in effect with the authors' company at the time of writing. They are subject to change and should be verified with the manufacturer.

The term $0.92 \times L_b$ in Equation [4] is a term to correct approximately for the enthalpy gain in the boiler feed pump assuming a motor efficiency of 92 per cent. The approximate correction for electrical and mechanical losses is taken care of by the 1.02 factor.

TABLE 2 APPROXIMATE CONDENSER DUTY BTU PER LB OF EXHAUST FLOW—H_e

Initial pressure, psig	Temperature, deg F		Exhaust pressure, in. Hg abs		
	Initial	Reheat	1.0	1.5	2.0
1250	950	950	959	966	971
1450	1000	1000	965	972	977
1800	1000	1000	953	960	965
1800	1050	1000	953	960	965
1800	1050	1050	963	970	975
2000	1050	1000	946	954	959
2000	1050	1050	957	963	967
2400	1050	1050	948	956	961

Table 2 is a tabulation of approximate condenser duty for various initial and reheat-steam conditions and exhaust pressures. These values of condenser duty were obtained by subtracting the heat of the liquid from the state line end point enthalpy. The data in Table 2 are based on high-pressure-turbine exhaust pressure to the reheater at 25 per cent of the initial pressure and 10 per cent pressure drop through the reheater and reheat piping, with commercial engine efficiency.

Fig. 1 provides a means of correcting the approximate exhaust flow for any of the exhaust-annulus areas given in Table 1 at 1.0, 1.5, and 2.0 in. Hg abs pressure. The curves are plotted with exhaust-flow correction factor versus approximate exhaust flow in pounds per hour (G_a) with exhaust-annulus areas as parameters

$$G = G_a K \text{ lb/hr} \quad [5]$$

The corrected exhaust flow permits determination of the kilowatt differentials from Figs. 2, 3, and 4. This value, when substituted in Equation [1], determines the turbine heat-rate difference. The evaluated fuel saving, item C_{ft} of Equation [3], may now be determined

$$C_{ft} = (-)\frac{F \times \Delta HR_p \times LF \times 8760 \times kw_t}{FC \times 10^6}, \text{ dollars} \quad [6]$$

Fig. 5 is a graphic solution for C_{ft}, Equation [6].

In order to establish the terms of Equation [3] which are affected by heat rejected to the condenser, it is necessary to determine the difference in total heat, in Btu per hour, rejected to the condenser

$$\Delta H_e = \Delta HR_t \times kw_t, \text{ Btu/hr} \quad [7]$$

The error introduced by neglecting the boiler feed-pump power is of no consequence since Equation [7] deals with a heat-rate difference.

Figs. 6 and 7 are nomographs for determination of S_m, the condenser surface required to transfer 1,000,000 Btu per hr, and W_m, the difference in circulating water required in gallons per million Btu per hr difference in heat rejected.

Fig. 6 is for $^7/_8$-in-OD condenser tubes, and Fig. 7 for 1-in-OD condenser tubes. The figures are based on 85 per cent clean, 18 BWG admiralty tubes, with absolute pressure, circulating-water temperature, circulating-water velocity, and active tube length as parameters.

There is an annual saving in fuel consumption owing to the reduction in kilowatthours of circulating-water-pump power required. Fig. 8 is a nomograph for determination of justifiable increased plant cost C_{fw}, resulting from the reduction of circulating-water quantity required. The total dynamic head in feet, fuel

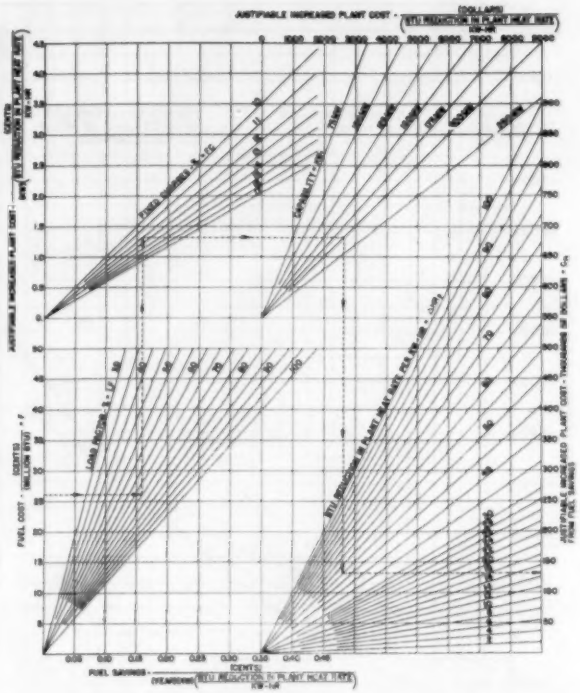

FIG. 5 NOMOGRAPH FOR EVALUATION OF REDUCTION IN PLANT HEAT RATE IN TERMS OF JUSTIFIABLE INCREASED PLANT COST

cost in mils per kwhr, fixed charges in per cent, and percentage of the year that one-half pumping capacity is used, are parameters. In Fig. 8 pump efficiency varies as a function of total dynamic head at levels consistent with those obtainable in commercially available pumps. An algebraic expression of Fig. 8 is

$$C_{fw} = (-)\frac{F \times HR_p \times \Delta kwhr_w \times P}{FC \times 10^6}, \text{ dollars} \quad [8]$$

where

$$\Delta kwhr_w = \frac{\Delta W \times TDH \times Sp\ gr \times 16{,}500}{E_w \times E_m}, \text{ kwhr/yr} \quad [9]$$

$$P = 1 - 0.55\left[\frac{\text{Per cent time } ^1/_2 \text{ circ-water-pump operation}}{100}\right] \quad [10]$$

The power consumption with one-half circulating-water-pump capacity in service will be less than 50 per cent of the full-capacity pump operation. For the purpose of this paper a figure of 45 per cent has been assumed.

The difference in circulating-water-pump capacity is

$$\Delta W = \frac{\Delta H_e}{10^6} W_m, \text{ gpm} \quad [11]$$

The change in condenser surface is

$$\Delta S = \frac{\Delta H_e}{10^6} S_m, \text{ sq ft} \quad [12]$$

Table 3 gives the approximate cost of incremental condenser surface in dollars per square foot which, used in Equation [13], determines the difference in condenser cost

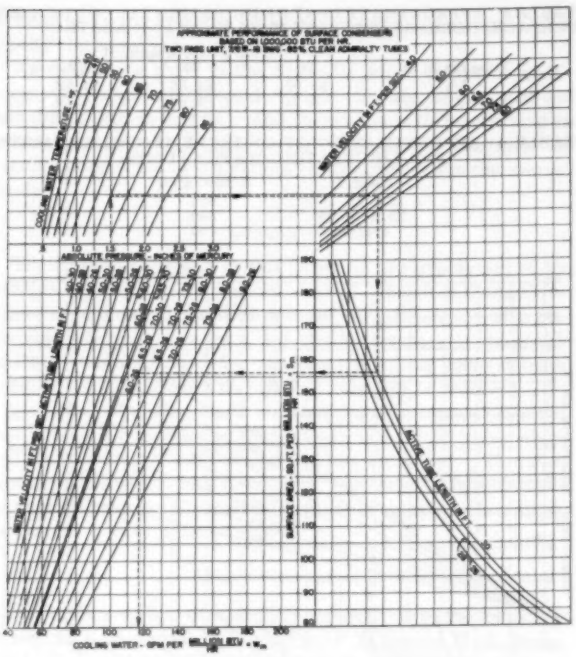

FIG. 6 NOMOGRAPH FOR DETERMINATION OF APPROXIMATE CONDENSER SURFACE REQUIRED TO TRANSFER 1,000,000 BTU PER HR, BASED ON TWO-PASS, 7/8-IN-OD, 18-BWG, 85 PER CENT CLEAN ADMIRALTY TUBES

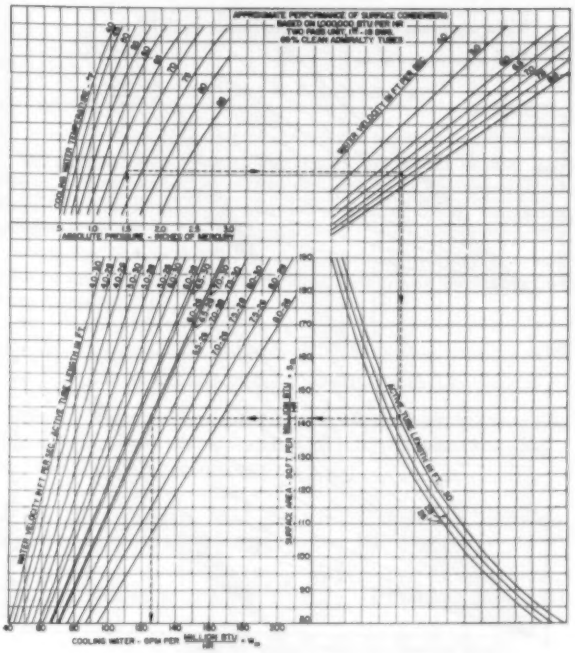

FIG. 7 NOMOGRAPH FOR DETERMINATION OF APPROXIMATE CONDENSER SURFACE REQUIRED TO TRANSFER 1,000,000 BTU PER HR, BASED ON TWO-PASS, 1-IN-OD, 18-BWG, 85 PER CENT CLEAN ADMIRALTY TUBES

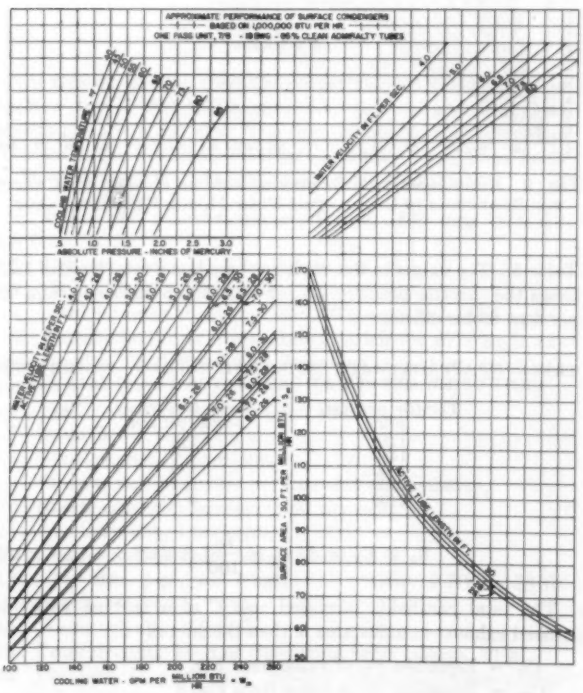

FIG. 6(a) NOMOGRAPH FOR DETERMINATION OF APPROXIMATE CONDENSER SURFACE REQUIRED TO TRANSFER 1,000,000 BTU PER HR, BASED ON SINGLE-PASS, 7/8-IN-OD, 18-BWG, 85 PER CENT CLEAN ADMIRALTY TUBES

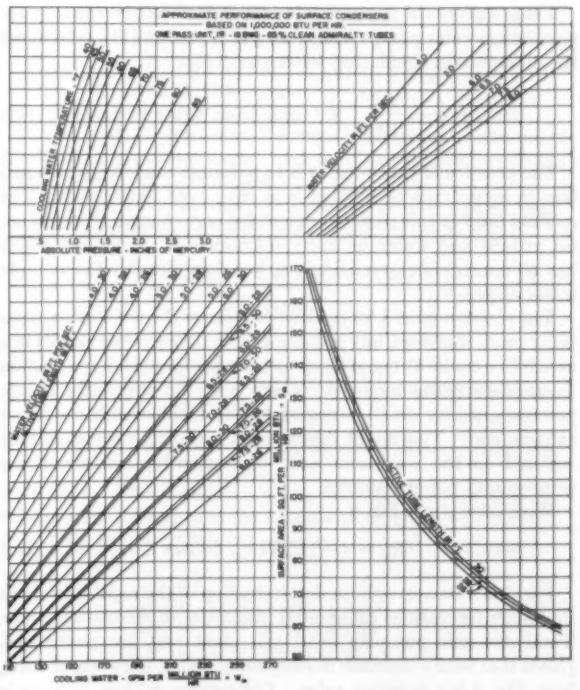

FIG. 7(a) NOMOGRAPH FOR DETERMINATION OF APPROXIMATE CONDENSER SURFACE REQUIRED TO TRANSFER 1,000,000 BTU PER HR, BASED ON SINGLE-PASS, 1-IN-OD, 18-BWG, 85 PER CENT CLEAN ADMIRALTY TUBES

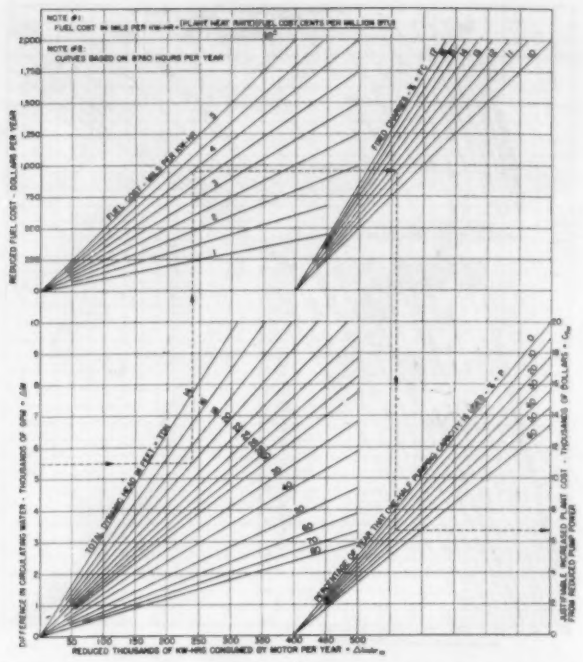

FIG. 8 NOMOGRAPH FOR EVALUATION OF DECREASED CIRCULATING-PUMP POWER COST IN TERMS OF JUSTIFIABLE INCREASED PLANT COST

$$\Delta C_s = (-)\,\Delta S \times (\text{value from Table 3}), \text{ dollars} \ldots [13]$$

Table 4 gives the approximate cost of incremental capacity for circulating-water pumps which, used in Equation [14], determines the difference in circulating-water-pump cost

$$\Delta C_w = (-)\frac{\Delta W}{1000} \times (\text{value from Table 4}), \text{ dollars} \ldots [14]$$

The practice of the industry is to purchase condensers with surface in increments of 5000 sq ft in sizes over 50,000 sq ft. The method used in this paper to determine cost changes of incremental surface and water quantity introduces a small error which has no appreciable over-all effect, but does simplify the solution materially.

The power required for auxiliaries reduces the net station capability; and, therefore, any reduction in auxiliary power results in a capability credit at the station cost per kw for each kw reduction in auxiliary power required. There is then a circulating pump-power-capability credit accruing to the turbine with the larger exhaust end. This credit results from a smaller amount of heat rejected to the condenser and, consequently, less circulating water-pump power required.

With Δkw_w from Fig. 9

$$R_w = (-)\,C_p \Delta kw_w, \text{ dollars} \ldots [15]$$

Fig. 9 is a nomograph for determination of the capability credit in dollars for various differential quantities of circulating water. Total dynamic pumping head and plant cost are parameters. (Note that with a decrease in circulating water, the value of Δkw_w from Fig. 9 is a negative value. Conversely, with an increase in circulating water, Δkw_w is a positive value.)

There is also a capability credit for the reduced boiler-feed-pump power. The approximate boiler feed-pump power L_b on a percentage basis, for various throttle pressures is given in Table 5. The values in this table are based on a total head of 1.25 times the throttle pressure, 75 per cent pump efficiency, and 92 per cent motor efficiency.

TABLE 3 APPROXIMATE COST OF INCREMENTAL CONDENSER SURFACE, DOLLARS PER SQ FT 50,000 SQ FT AND ABOVE

Tube diam, in.	Active tube length, ft 26	28	30
7/8	$5.03	$4.83	$4.62
1	5.21	4.99	4.79

TABLE 4 APPROXIMATE COST OF INCREMENTAL CAPACITY FOR CIRCULATING-WATER PUMPS

Head, ft	$/1000 gpm
15 to 25	475
25.01 to 55	540
over 55	560

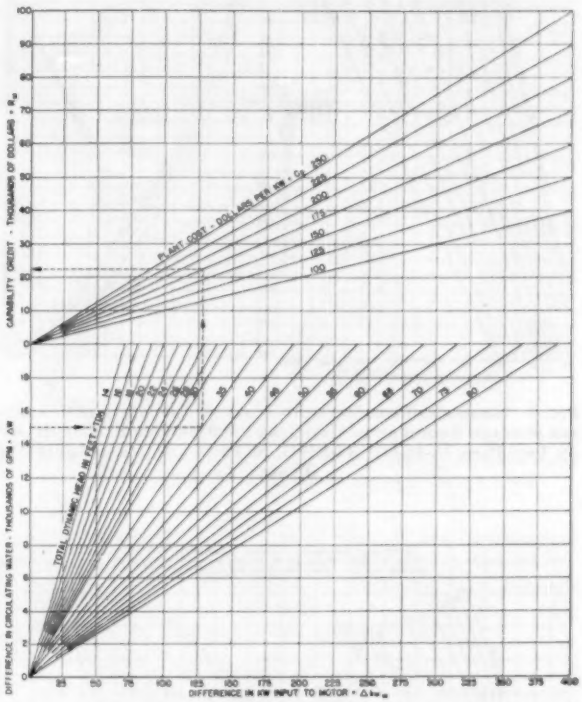

FIG. 9 NOMOGRAPH FOR DETERMINATION OF CAPABILITY CREDIT FOR REDUCTION IN CIRCULATING-PUMP-MOTOR KILOWATT INPUT

TABLE 5 APPROXIMATE BOILER-FEED-PUMP POWER PER CENT OF KW OUTPUT AT GENERATOR TERMINALS—L_b

Throttle pressure, psig	Boiler-feed-pump power, per cent
1250	1.3
1450	1.5
1800	1.9
2000	2.1
2400	2.5

$$R_b = C_p \times \Delta kw_t \times \frac{L_b}{100}, \text{ dollars} \ldots [16]$$

The total justifiable increased cost C of a turbine with increased exhaust-annulus area is then the sum of

C_{ft} = Equation [6] or value from Fig. 5
C_{tw} = Equation [8] or value from Fig. 8
ΔC_s = Equation [13]
ΔC_w = Equation [14]
R_w = Equation [15] or value from Fig. 9
R_b = Equation [16]

C must be greater than the difference in turbine-generator cost to justify the larger exhaust-end annulus.

An example is given in the Appendix which compares a 200-megawatt tandem-compound turbine having an exhaust-end annulus of 97.8 sq ft with a tandem-compound turbine having an exhaust-end annulus of 122.7 sq ft. The example illustrates the relative importance of the various factors involved in the over-all study.

Conclusion

The method presented in this paper for the evaluation of the relative economy of the various sizes of exhaust-end annuli requires a minimum amount of data for the preparation of a preliminary analysis. However, a degree of accuracy is obtainable which is sufficient to define the areas requiring more detailed analysis. In many cases no further study will be required.

The effect of partial loads, reduced vacua in summer months, and increased building and foundation cost, are all items which will make the larger-size exhaust end less attractive. Therefore any situation which does not appear economically feasible from an analysis made by the method outlined in this paper is unlikely to warrant a more detailed study.

Acknowledgment

The authors wish to express their appreciation to the following: Messrs. C. B. Campbell, J. R. Carlson, F. J. Heinze, H. R. Reese, and C. C. Christensen for their advice and constructive criticism; Dr. W. J. Cope and Messrs. V. P. Buscemi, K. C. Wein, M. L. Russell, and R. E. Gaunt for the preparation of data; Miss E. D. J. Campen for the preparation of curves.

Appendix

Example

It is desired to determine the proper exhaust-end annulus to purchase for a 200,000-kw-capability turbine generator unit operating at 1.5 in. Hg abs. The sizes of exhaust ends offered at 3600 rpm in this rating are 97.8 sq ft and 122.7 sq ft, from Table 1. The following data are available for the study:

1 Initial and reheat-steam conditions, 1800 psig 1000 F/1000 F.
2 Exhaust pressure, 1.5 in. Hg abs.
3 Capability, 200,000 kw.
4 Annulus areas of exhaust ends, 97.8 sq ft and 122.7 sq ft.
5 Turbine heat rate at capability, using the 97.8 sq ft exhaust annulus, 7850 Btu/kwhr (based on output at generator terminals).
6 Fuel cost, 40 cents per million Btu.
7 Load factor, 70 per cent.
8 Fixed charges, 14 per cent.
9 Plant cost, 150 dollars per kilowatt of capability.
10 Steam-generator efficiency, 90 per cent.
11 Auxiliary loss, 6 per cent.
12 Design cooling-water temperature, 65 F.
13 Tube size, gage, and length: $^7/_8$-in. OD, 18 BWG, 28 ft active length, two-pass.
14 Water velocity, 6 fps.
15 Total dynamic head of circulating-water pumps, 30 ft.
16 Per cent of year that one-half circulating-water-pump capacity is used, 20 per cent.

Step 1. The exhaust flow G, in lb/hr, at turbine capability must be determined. To obtain this value, the approximate exhaust flow G_a in lb/hr is determined from Equation [4]

$$G_a = \frac{(\mathrm{HR}_t + 30.80 \times L_b - 3481)\mathrm{kw}_t}{\mathrm{H}_e}, \text{ lb/hr} \quad [4]$$

$$G_a = \frac{(7850 + 30.80 \times 1.9 - 3481)200{,}000}{960} = 922{,}300$$

The approximate exhaust flow G_a is then used in Fig. 1 to obtain the exhaust-flow correction factor K, for the exhaust annulus corresponding to the heat rate of 7850 Btu/kwhr, namely, 97.8 sq ft at 1.5 in. Hg abs.

From Fig. 1, $K = 0.977$.

Then the corrected turbine-exhaust flow G can be determined from Equation [5]

$$G = G_a \times K, \text{ lb/hr} \quad [5]$$

$$G = 922{,}300 \times 0.977 = 901{,}100 \text{ lb/hr}$$

Step 2. After the exhaust flow G is determined, the kilowatt differential between the two exhaust annuli is obtained from Fig. 3 for 1.5 in. Hg abs exhaust pressure.

From Fig. 3, $\Delta\mathrm{kw}_t = 2000$ kw.

With the foregoing data, the turbine heat-rate difference $\Delta\mathrm{HR}_t$ can be determined from Equation [1]

$$\Delta\mathrm{HR}_t = (-)\frac{\mathrm{HR}_t \times \Delta\mathrm{kw}_t}{\mathrm{kw}_t + \Delta\mathrm{kw}_t}, \text{ Btu/kwhr} \quad [1]$$

$$\Delta\mathrm{HR}_t = (-)\frac{7850 \times 2000}{200{,}000 + 2000} = (-)77.7 \text{ Btu/kwhr}$$

The plant heat-rate difference $\Delta\mathrm{HR}_p$ can be determined from Equation [2]

$$\Delta\mathrm{HR}_p = \frac{\Delta\mathrm{HR}_t \times 10^4}{E_s \times (100 - L)}, \text{ Btu/kwhr} \quad [2]$$

$$\Delta\mathrm{HR}_p = \frac{(-)\ 77.7 \times 10^4}{90 \times (100 - 6)} = (-)91.8 \text{ Btu/kwhr}$$

Step 3. With the heat-rate difference determined, the terms of Equation [3] can be calculated to determine the total justifiable increased plant cost, C, in dollars.

The evaluated fuel savings, C_{fi}, resulting from the plant heat-rate difference, can be obtained from Equation [6] or Fig. 5

$$C_{fi} = (-)\frac{F \times \Delta\mathrm{HR}_p \times \mathrm{LF} \times 8760 \times \mathrm{kw}_t}{\mathrm{FC} \times 10^8}, \text{ dollars} \quad [6]$$

$$C_{fi} = (-)\frac{40 \times (-)\ 91.8 \times 70 \times 8760 \times 200{,}000}{14 \times 10^8} = 321{,}700 \text{ dollars}$$

Note that the value of C_{fi} can be obtained directly from Fig. 5.

Step 3(a). The remaining terms in Equation [3] are dependent on the difference in the exhaust heat rejected to the condenser, ΔH_e, Btu/hr. This value can be obtained from Equation [7]

$$\Delta H_e = \Delta\mathrm{HR}_t \times \mathrm{kw}_t, \text{ Btu/hr} \quad [7]$$
$$\Delta H_e = (-)77.7 \times 200{,}000$$
$$\Delta H_e = (-)15{,}540{,}000 \text{ Btu/hr}$$

Step 3(b). The difference in condenser surface S_m, and the difference in circulating water per million Btu rejected W_m, corresponding to the difference in heat rejection to the condenser ΔH_e, can now be obtained from Fig. 6 for $^7/_8$-in-OD tubes.

From Fig. 6, $S_m = 139$ sq ft, $W_m = 96$ gpm.

Step 3(*c*). Having determined S_m and W_m, the circulating-water difference in gpm, ΔW, and the condenser-surface difference in square feet, ΔS, can now be obtained from Equations [11] and [12]

$$\Delta W = \frac{\Delta H_s}{10^6} \times W_m \quad \text{[11]}$$

$$\Delta W = \frac{(-)\ 15{,}540{,}000}{10^6} \times 96$$

$$\Delta W = (-)1492 \text{ gpm}$$

$$\Delta S = \frac{\Delta H_s}{10^6} \times S_m \quad \text{[12]}$$

$$\Delta S = \frac{(-)\ 15{,}540{,}000}{10^6} \times 139$$

$$\Delta S = (-)2160 \text{ sq ft}$$

Step 3(*d*). The evaluated fuel savings C_{fw}, resulting from reduced circulating-pump power Δkwhr_w, can be determined from Equations [8], [9], and [10] or can be determined graphically from Fig. 8.

$$C_{fw} = (-)\ \frac{F \times \text{HR}_p \times \Delta\text{kwhr}_w \times P}{\text{FC} \times 10^6} \quad \text{[8]}$$

$$\Delta\text{kwhr}_w = \frac{\Delta W \times \text{TDH} \times \text{Sp gr} \times 16{,}500}{E_p \times E_m}, \text{ kwhr} \quad \text{[9]}$$

$$\Delta\text{kwhr}_w = \frac{(-)\ 1492 \times 30 \times 1 \times 16{,}500}{85 \times 90} = (-)\ 96{,}600 \text{ kwhr}$$

$$P = 1 - 0.55 \left[\frac{\text{Per cent time } 1/2 \text{ circ-pump operation}}{100} \right] \quad \text{[10]}$$

$$P = 1 - 0.55 \times \frac{20}{100} = 0.89$$

Then

$$C_{fw} = (-)\ \frac{40 \times 9280 \times (-)\ 96{,}600 \times 0.89}{14 \times 10^6}$$

$$C_{fw} = 2280 \text{ dollars}$$

Note that the value of C_{fw} can be obtained directly from Fig. 8.

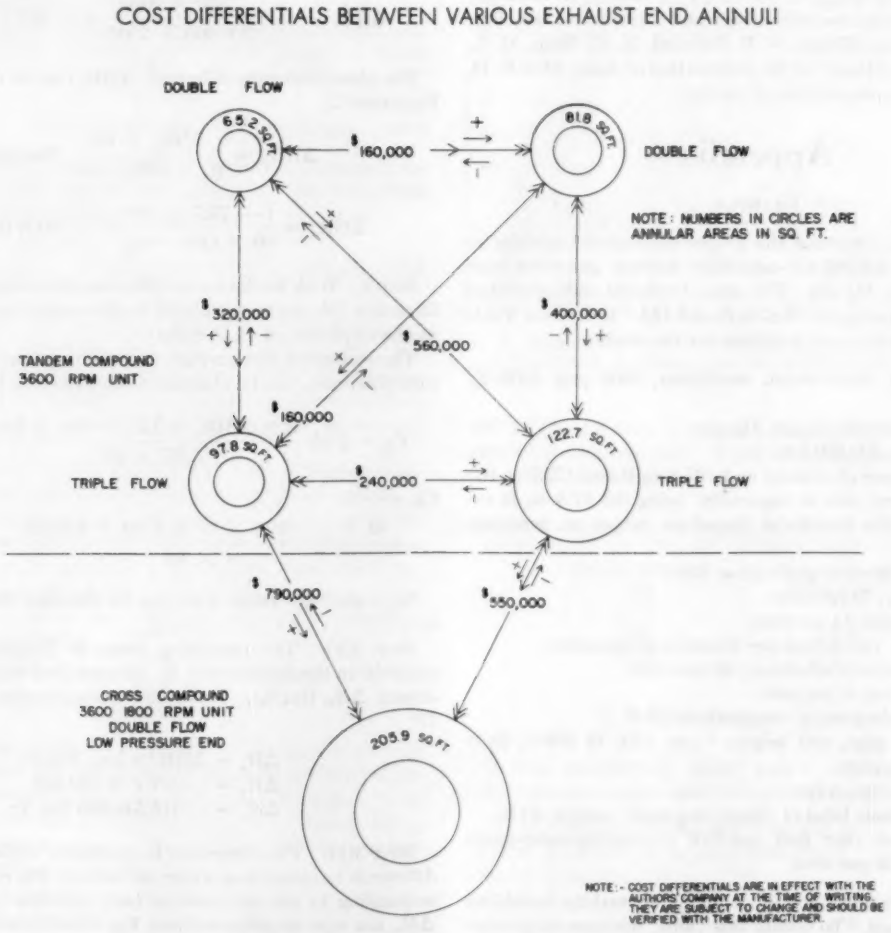

FIG. 10 COST DIFFERENTIALS BETWEEN VARIOUS EXHAUST-END ANNULI

Step 3(e). The condenser-surface cost difference ΔC_s, in dollars, can be determined from Equation [13]

$$\Delta C_s = (-)\ \Delta S \times \text{value from Table 3, dollars} \ldots \quad [13]$$

$$\Delta C_s = 2160 \times 4.83$$

$$\Delta C_s = 10{,}430 \text{ dollars}$$

Step 3(f). The circulating-pump cost difference ΔC_w, in dollars, can be determined from Equation [14]

$$\Delta C_w = (-)\ \frac{\Delta W}{1000} \times \text{value from Table 4, dollars} \ldots [14]$$

$$\Delta C_w = \frac{1492}{1000} \times 540$$

$$\Delta C_w = 805 \text{ dollars}$$

Step 3(g). The capability credit for reduced circulating-pump power, R_w, can be determined from Equation [15] or Fig. 9

$$R_w = (-)\ C_p \times \Delta \text{kw}_w, \text{ dollars} \ldots\ldots\ldots\ldots [15]$$

$$\Delta \text{kw}_w = (-)\ 11.0 \text{ from Fig. 9}$$

$$R_w = (-)\ 150 \times (-)\ 11.0$$

$$R_w = 1650 \text{ dollars}$$

Step 3(h). The capability credit for reduced boiler-feed-pump power R_b, in dollars, can be determined from Equation [16]

$$R_b = C_p \times \Delta \text{kw}_t \times \frac{L_b}{100}, \text{ dollars} \ldots\ldots\ldots\ldots [16]$$

$$R_b = 150 \times 2000 \times \frac{1.9}{100}$$

$$R_b = 5700 \text{ dollars}$$

Step 3(i). Solving Equation [3] for total justifiable increased plant cost in dollars

$$C = C_{ft} + C_{fw} + \Delta C_s + \Delta C_w + R_w + R_b$$

$$C = 321{,}700 + 2280 + 10{,}430 + 805 + 1650 + 5700$$

$$C = 342{,}565 \text{ dollars}$$

From Fig. 10 the cost differential for the larger exhaust-end annulus is \$240,000. Since the total justified increased plant cost C is greater than the cost differential for the larger exhaust-end annulus by approximately \$102,000, it appears probable that a more detailed analysis, involving partial-load operation, seasonal water-temperature variations, and changes in plant cost not accounted for herein, would show a satisfactory return on the additional investment.

Discussion

S. M. Arnow.[5] This paper discusses a situation that frequently occurs in studies which are being made to determine the basic thermal cycle of large central stations. The exhaust-annulus area of a turbine determines the leaving loss which has a very sensitive effect on generation. A relatively small change at this point will have a considerable bearing on the efficiency of the turbine plant.

[5] Senior Engineer, Mechanical Division, Philadelphia Electric Company, Philadelphia, Pa. Mem. ASME.

The basic analysis presented in the paper is applicable not only to the size and number of exhaust ends, but also to the broader problem of tandem versus cross-compound machines. It is obvious that a large increase in annular areas may be obtained by cross-compounding, using an 1800-rpm low-pressure exhaust in a 3600/1800-rpm combination. For this reason the authors are to be commended both for the choice of subject and the manner of approach for determining the factors involved.

While the analysis is clear and easy to follow, especially with the help of the example at the end of the paper, it must be noted that some of the factors have but a minor effect on the problem. For instance, in the example worked out in the paper, the evaluated fuel saving is \$321,700. The cost differential of the larger exhaust is \$240,000, the difference amounting to \$81,700 which should be quite sufficient to justify consideration. Incidentally, these two items are most easily obtained. The other factors are circulating-pump power saving (\$2280), condenser-surface and circulating-pump price reduction (\$11,235), and increase in plant-capability credits (\$7350). Inasmuch as capability due to the reduction in boiler-feed-pump use is given, consistency dictates that reduction in size and saving in fuel also should be included.

One must be impressed with the enormous amount of work which was put into the development of the several nomographs and yet the authors themselves say that condenser and pump sizes are standardized. In the example given the flow is reduced by about 1 per cent. Is one to assume that where a 100,000-sq ft condenser or two 50,000-gpm circulating pumps are called for, a 99,000-sq ft condenser or 49,500-gpm pumps will be bought when the installation of a larger exhaust has been decided upon? Thus the largest of these factors is eliminated. Again, a system which utilizes a 200,000-kw machine would hardly be affected by increase in capabilities of 11 or 38 kw which are those credited to the circulating and boiler-feed pumps, respectively. The conclusions must be reached that these very complicated factors may be disregarded in so far as end results are concerned.

While pointing out the many acts of commission, they are also guilty of one very significant sin of omission, wherein they make no mention of the effect of possible increased cost of building, foundations, and so on, which may result from larger annuli. If, for example, in the case of a 3600-rpm machine, the larger area is obtained by providing an extra exhaust, it may mean an addition of some 8 to 10 ft to the length of the unit, resulting in a longer building, more expensive foundations, and possibly a longer span of the crane. These considerations may well become the determining factor in making the final decision.

It is easy to see that larger exhaust areas present many factors not included in this paper, and it is hoped that the authors will remedy this situation at some time in the future.

Authors' Closure

The authors wish to thank Mr. Arnow for his constructive comments. The purpose of the authors in including some seemingly insignificant items is merely to show the relative magnitude of the factors involved. It serves the purpose of cataloging items with regard to significance.

The fallacy in the method of evaluating the reduction of condenser duty is acknowledged in the paper and justified on the basis of introducing only an insignificant error. It should be noted that while small changes in the condenser surface or the circulating-water quantity required may not change the capital expenditure, there will be a change in the operating expense which could have been evaluated.

The effect of exhaust-end-annulus area on building, foundation, and piping cost was recognized in the paper but specifically omitted as being too complicated and controversial for inclusion.

Economic Determination of Condenser and Turbine-Exhaust Sizes

By E. H. MILLER[1] AND A. SIDUN[2]

There are many combinations of condensers and turbine exhaust-annulus areas available to the engineer studying alternate large steam-station designs. The proper selection from among these many combinations is a broad economic problem which can best be solved by considering initially only those few basic variables that apply directly to the problem. It is the purpose of this paper to present these basic data on turbine and condenser performance in a form that will help the user to determine quickly the most economical turbine-condenser combination for a given situation.

Introduction

IDEALLY, the pressure at which a steam power plant exhausts its steam flow should be equal to the saturation pressure of the circulating-water temperature. The size and cost of the turbine-condenser combination, however, increase rapidly as this pressure is approached and, at the same time, the gain in performance diminishes.

Thus, to choose the most economical combination of turbine and condenser in a practical case, the point must be determined where the additional investment resulting from larger condensers and larger turbine-exhaust area can no longer be balanced economically by an improvement in station performance. The method of finding this economic balance point can be separated logically into three parts:

1 Find the difference in station performance between combinations.

2 Find the difference in station costs between combinations.

3 Place a dollar value on the differences in station performance and compare this value with differences in cost.

Each of these problems will be covered in detail in the following sections of the paper. In addition, an example showing the use of this method has been included in the Appendix.

Station Performance

There are two separate and distinct improvements in station performance to be gained by a more efficient turbine-condenser combination. One of course is a reduction in the amount of fuel burned. The more efficient combination also has a lower steam rate at maximum capacity, with attendant saving in the cost of the steam-generator equipment.

Change in station heat rate, which is the measure of both these gains, is obtained by correcting the change in gross turbine heat rate for boiler efficiency and station auxiliary-power requirements as follows

$$\text{Change in station heat rate, Btu/kwhr} = \frac{\text{Change in gross turbine heat rate, Btu/kwhr}}{\text{Boiler efficiency, } \frac{\%}{100} \times \left(1 - \frac{\text{Auxiliary power, kw}}{\text{Turbine output, kw}}\right)} \quad [1]$$

Boiler efficiency for a given steam condition, feedwater-heating cycle, and steam output will not change with exhaust pressure or turbine-exhaust size. Generally 85 to 90 per cent efficiency may be used in making economic studies. Auxiliary-power requirements that do not change with exhaust pressure or exhaust size can be assumed to total approximately 6 per cent. The additional circulating-water-pump power can be calculated from data included in this paper.

Turbine heat rates usually are obtained by calculating heat balances for a specific situation with given steam conditions, feedwater-heating cycle, turbine capability, exhaust size, and exhaust pressure. Turbine efficiencies for use in calculating heat balances have been presented by Messrs. Elston and Knowlton.[3] More recently Messrs. Keller and Downs have published a method of modifying easily any heat balance for changes in exhaust pressure.[4]

The first of these two methods has been used to calculate, with representative feedwater-heating cycles and exhaust pressures, the differences in gross turbine heat rate for turbines built with various exhaust sizes and capacities. The second method was used to calculate the changes in heat rate with exhaust pressure for each of these turbine alternates. The combined heat-rate differences due to changes in exhaust size and exhaust pressure have been tabulated for initial steam conditions of 850 psig, 900 F; 1450 psig, 1000 F; 1450 psig, 1000/1000 F; and 2000 psig, 1050/1000 F; in Tables 1, 2, 3, and 4. The gross heat rate for the base turbine usually will be available from specific heat-balance calculations. If this is not the case, the approximate gross turbine heat rate may be obtained from Fig. 1.[5]

The exhaust pressure at which a turbine will operate can be calculated by the method detailed in the "Standards of Heat Exchange Institute."[6] This method has been used to calculate, for a large range of condenser sizes and two types of pass arrangements, the exhaust pressure that can be obtained with a given circulating-water temperature and quantity of heat rejected to the condenser. Figs. 2, 3, 4, 5, 6, and 7 show this calculated exhaust pressure for single-pass and two-pass condensers of representative design.

The method of selecting water temperature for making economic comparisons varies with location. This can be appreciated readily when one considers that the peak system load and the peak circulating-water temperature may occur simultaneously in one section of the country, as against peak system load and low

[1] Supervisor, Turbine Advance Engineering, Large Steam Turbine-Generator Department, General Electric Company, Schenectady, N. Y. Assoc. Mem. ASME.

[2] Manager, Condenser Division, Foster-Wheeler Corporation, New York, N. Y.

Contributed by the Power Division and presented at the Annual Meeting, New York, N. Y., November 29–December 4, 1953, of The American Society of Mechanical Engineers.

Note: Statements and opinions advanced in papers are to be understood as individual expressions of their authors and not those of the Society. Manuscript received at ASME Headquarters, October 26, 1953. Paper No. 53—A-94.

[3] "Comparative Efficiencies of Central Station Reheat and Non-reheat-Steam-Turbine Generator Units," by C. W. Elston and P. H. Knowlton, Trans. ASME, vol. 74, 1952, pp. 1389–1399.

[4] "The Effect of Exhaust Pressure on the Economy of Condensing Turbines," by A. Keller and J. E. Downs, Trans. ASME, vol. 76, 1954, pp. 445–451.

[5] It should be understood that the heat rates and efficiencies referred to in this paper apply to turbines as built by the General Electric Company.

[6] "Standards of Heat Exchange Institute," third edition, Heat Exchange Institute, 122 East 42nd St., New York 17, N. Y., 1952.

water temperature in another. To consider these local conditions properly, a method which evaluates the maximum-capacity station performance at the circulating-water temperature that coincides with the system peak load, and that evaluates the average fuel saving at the average water temperature, will give more realistic results than a method that uses the average water temperature for both evaluations.

The heat rejected to the circulating water at a given kilowatt load is obtained by deducting the heat equivalent of the turbine output plus its generator and fixed losses from the total heat input to the turbine.

In most cases the following simplified formula, which uses the base gross turbine heat rate directly from Fig. 1, and a heat equivalent corrected for fixed and generator losses, will give the total heat rejected with sufficient accuracy

TABLE 1 GROSS TURBINE HEAT-RATE DIFFERENCES, BTU/KWHR

Initial Steam Conditions: 850 PSIG 900 F, Variable Exhaust Pressure, Inch Hg Abs

Number and Length of Last-stage Buckets	2-20″	2-23″	2-26″	3-23″
80-MW Turbine Capacity				
@½″ Hg Abs	5	−125	−300	−405
@1″ Hg Abs	−10	−130	−285	−355
@1½″ Hg Abs	Base	−80	−170	−190
@2″ Hg Abs	50	25	−10	0
@2½″ Hg Abs	130	155	160	205
100-MW Turbine Capacity				
@½″ Hg Abs	140	5	−145	−270
@1″ Hg Abs	125	−10	−150	−255
@1½″ Hg Abs	115	Base	−95	−155
@2″ Hg Abs	130	55	25	−10
@2½″ Hg Abs	170	145	155	150
125-MW Turbine Capacity				
@½″ Hg Abs	.....	155	5	−110
@1″ Hg Abs	.....	135	−10	−120
@1½″ Hg Abs	.....	125	Base	−75
@2″ Hg Abs	.....	140	60	25
@2½″ Hg Abs	.....	185	155	145

Total heat rejected, Btu/hr = [turbine output, kw] [(turbine heat rate — 3500) Btu/kwhr] ..... [2]

Circulating-water velocities of 7 and 8 fps have been selected as

TABLE 2 GROSS TURBINE HEAT-RATE DIFFERENCES, BTU/KWHR

Initial Steam Conditions: 1450 PSIG 1000 F, Variable Exhaust Pressure, Inch Hg Abs

Number and Length of Last-stage Buckets	2-20″	2-23″	2-26″	3-23″	3-26″
80-MW Turbine Capacity					
@½″ Hg Abs	−10	−120	−255	−320	.....
@1″ Hg Abs	−20	−120	−215	−260	.....
@1½″ Hg Abs	Base	−50	−85	−90	.....
@2″ Hg Abs	60	55	65	85	.....
@2½″ Hg Abs	150	180	240	270	.....
100-MW Turbine Capacity					
@½″ Hg Abs	85	−15	−135	−230	−335
@1″ Hg Abs	70	−25	−135	−205	−270
@1½″ Hg Abs	75	Base	−65	−90	−90
@2″ Hg Abs	100	70	50	45	95
@2½″ Hg Abs	155	170	185	205	295
125-MW Turbine Capacity					
@½″ Hg Abs	.....	95	−10	−110	−240
@1″ Hg Abs	.....	80	−25	−110	−210
@1½″ Hg Abs	.....	85	Base	−55	−90
@2″ Hg Abs	.....	115	70	45	55
@2½″ Hg Abs	.....	175	180	170	220
150-MW Turbine Capacity					
@½″ Hg Abs	.....	190	70	−10	−135
@1″ Hg Abs	.....	170	50	−25	−135
@1½″ Hg Abs	.....	165	60	Base	−65
@2″ Hg Abs	.....	175	95	70	50
@2½″ Hg Abs	.....	205	170	170	185

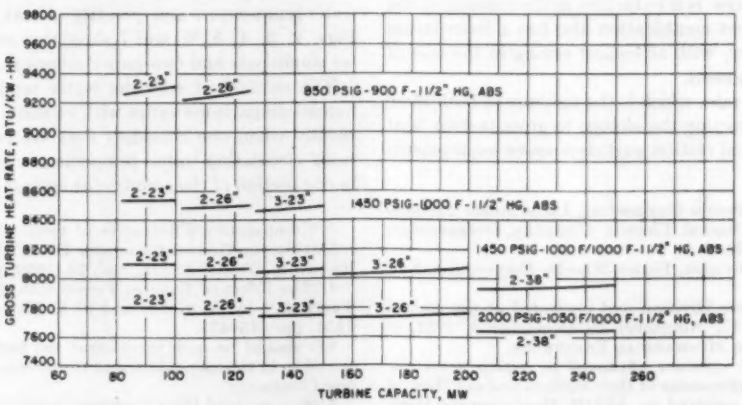

FIG. 1 TYPICAL GROSS TURBINE HEAT RATES

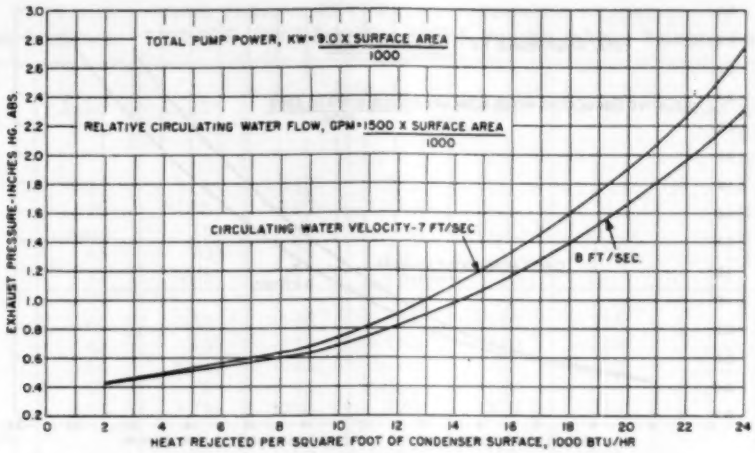

FIG. 2 SINGLE-PASS CONDENSER PERFORMANCE WITH 40 F INLET WATER

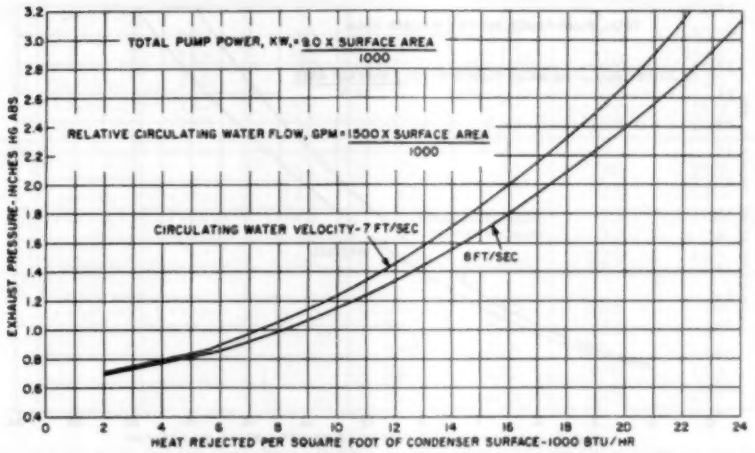

FIG. 3 SINGLE-PASS CONDENSER PERFORMANCE WITH 60 F INLET WATER

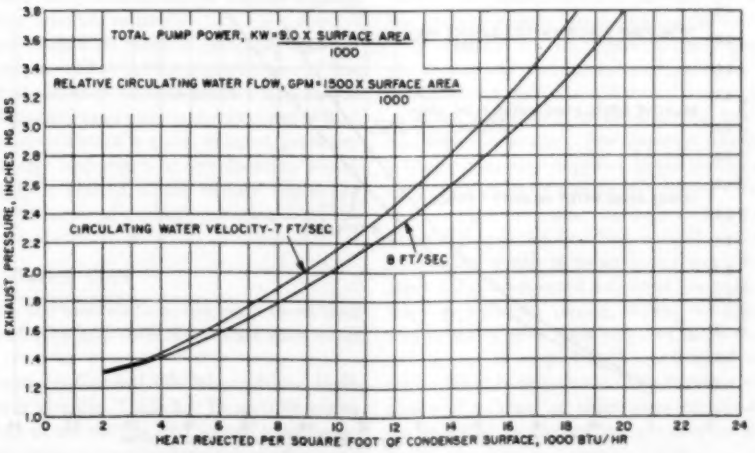

FIG. 4 SINGLE-PASS CONDENSER PERFORMANCE WITH 80 F INLET WATER

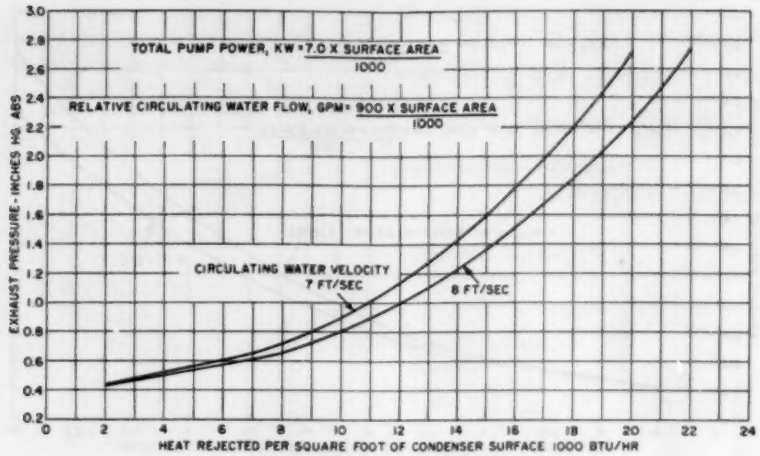

FIG. 5 TWO-PASS CONDENSER PERFORMANCE WITH 40 F INLET WATER

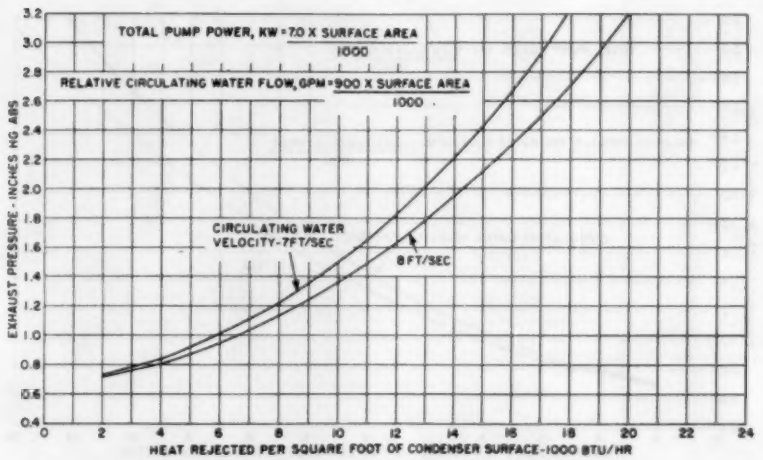

FIG. 6 TWO-PASS CONDENSER PERFORMANCE WITH 60 F INLET WATER

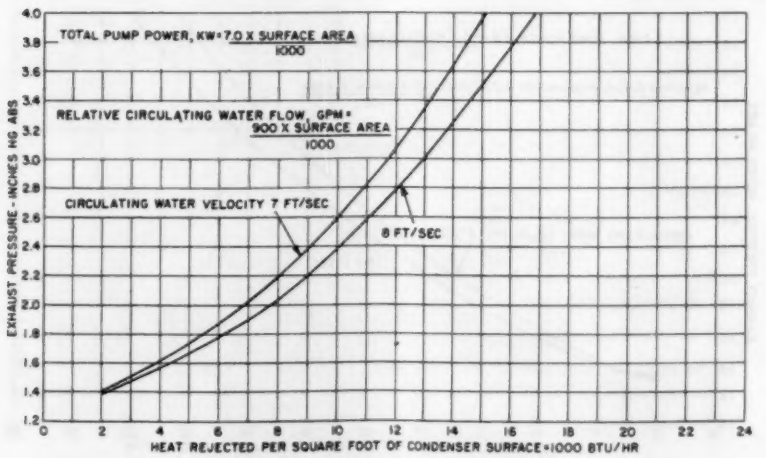

FIG. 7 TWO-PASS CONDENSER PERFORMANCE WITH 80 F INLET WATER

TABLE 3 GROSS TURBINE HEAT-RATE DIFFERENCES, BTU/KWHR

Initial Steam Conditions: 1450 PSIG 1000 F Reheat to 1000 F, Variable Exhaust Pressure, Inch Hg Abs

Number and Length of Last-stage Buckets	2–20″	2–23″	2–26″	3–23″	3–26″	1–43″	2–35″	2–38″	2–43″
80-MW Turbine Capacity									
@ ½″ Hg Abs	−25	−125	−235	−265	.....	.....	.....	.....	.....
@ 1″ Hg Abs	−30	−105	−185	−170	.....	.....	.....	.....	.....
@ 1½″ Hg Abs	Base	−35	−55	−0	.....	.....	.....	.....	.....
@ 2″ Hg Abs	65	90	120	200	.....	.....	.....	.....	.....
@ 2½″ Hg Abs	155	225	295	380	.....	.....	.....	.....	.....
100-MW Turbine Capacity									
@ ½″ Hg Abs	60	−30	−135	−195	−310	−315	.....	.....	.....
@ 1″ Hg Abs	45	−35	−110	−160	−210	−220	.....	.....	.....
@ 1½″ Hg Abs	55	Base	−40	−40	−30	−50	.....	.....	.....
@ 2″ Hg Abs	90	75	90	120	180	150	.....	.....	.....
@ 2½″ Hg Abs	135	175	235	275	370	330	.....	.....	.....
125-MW Turbine Capacity									
@ ½″ Hg Abs	.....	65	−30	−100	−200	−215	.....	.....	.....
@ 1″ Hg Abs	.....	50	−35	−85	−165	−180	.....	.....	.....
@ 1½″ Hg Abs	.....	60	Base	−25	−40	−60	.....	.....	.....
@ 2″ Hg Abs	.....	100	80	90	130	100	.....	.....	.....
@ 2½″ Hg Abs	.....	150	185	225	295	260	.....	.....	.....
150-MW Turbine Capacity									
@ ½″ Hg Abs	.....	140	40	−30	−135	−150	−305	−360	−515
@ 1″ Hg Abs	.....	115	30	−35	−110	−130	−235	−280	−330
@ 1½″ Hg Abs	.....	110	40	Base	−40	−60	−85	−110	−90
@ 2″ Hg Abs	.....	125	90	75	90	65	100	70	135
@ 2½″ Hg Abs	.....	160	155	175	235	200	280	225	360
200-MW Turbine Capacity									
@ ½″ Hg Abs	.....	.....	155	75	−20	−40	−200	−265	−415
@ 1″ Hg Abs	.....	.....	130	65	−30	−55	−180	−235	−320
@ 1½″ Hg Abs	.....	.....	125	65	Base	−25	−100	−140	−150
@ 2″ Hg Abs	.....	.....	135	95	65	35	30	−5	50
@ 2½″ Hg Abs	.....	.....	165	140	160	125	170	125	230
250-MW Turbine Capacity									
@ ½″ Hg Abs	.....	.....	.....	305	215	165	10	−60	−185
@ 1″ Hg Abs	.....	.....	.....	280	195	150	10	−50	−150
@ 1½″ Hg Abs	.....	.....	.....	270	195	150	45	Base	−30
@ 2″ Hg Abs	.....	.....	.....	280	225	180	125	95	130
@ 2½″ Hg Abs	.....	.....	.....	305	275	225	235	205	285

the range in velocity most widely used by the industry. With relatively clean fresh water, velocities up to 8 fps are used without serious effect on tube life. For brackish water, sea water, and more corrosive conditions, 7 fps velocity represents the accepted maximum. For most situations it is desirable to use the highest velocity that does not affect tube life seriously.

An economic comparison should be made in each case between one and two-pass condensers as well as between condensers of the same pass arrangement but different surface areas. The major advantage of the more commonly used two-pass condenser is that it uses less circulating water to obtain a given exhaust pressure. This advantage is particularly important in any location where the circulating-water supply is limited or the supply works are expensive, such as cooling tower or other high-pumping-head installations.

Station Cost

Of the factors making up the total station cost, only those that change with alternate condenser and turbine-exhaust sizes need be considered.

The price increment between General Electric turbines built with various exhaust sizes is given in Table 5. These differences generally apply to turbines of all ratings and steam conditions. Table 5 also shows the difference in turbine-foundation plan area and length between each exhaust size.

The price addition for successive sizes of condensers as well as the price difference between one and two-pass condensers of the same surface is given in Table 6. The price increments are based on the following equipment, completely erected: Surface condenser and tubes, steam-jet air ejectors, and the normal circulating and condensate pumps, motor drives, and minor auxiliaries.

In addition to the apparent price changes due to additional condenser and turbine-exhaust areas, a thorough study of the conditions at each site will reveal several miscellaneous costs that must be considered in determining the correct condenser and turbine-exhaust size. For instance, a larger turbine exhaust with a longer span may require a larger building. If the larger exhaust area is obtained by a cross-compound turbine the turbine foundation or plan area may be larger; but because of the turbine's shorter length the building actually may become smaller when the station width is dependent upon other factors than turbine size. Cross-compound machines normally require additional electrical equipment, piping, wiring, and supervisory instruments, and in many cases they will cost more to erect at the station.

The cost of supplying the additional circulating water is generally the only important miscellaneous effect resulting from the choice of a larger or single-pass condenser, since in most cases the required condenser surface can be fitted into the available space.

The following approximate values of these miscellaneous costs

TABLE 4 GROSS TURBINE HEAT-RATE DIFFERENCES, BTU/KWHR

Initial Steam Conditions: 2000 PSIG 1050 F Reheat to 1000 F, Variable Exhaust Pressure, Inch Hg Abs

Number and Length of Last-stage Buckets	2–20″	2–23″	2–26″	3–23″	3–26″	1–43″	2–35″	2–38″	2–43″
80-MW Turbine Capacity									
@½″ Hg Abs	−25	−120	−215	−225	.....	.....	.....	.....	.....
@1″ Hg Abs	−30	−100	−160	−130	.....	.....	.....	.....	.....
@1½″ Hg Abs	Base	−25	−30	45	.....	.....	.....	.....	.....
@2″ Hg Abs	65	90	140	235	.....	.....	.....	.....	.....
@2½″ Hg Abs	155	225	305	405	.....	.....	.....	.....	.....
100-MW Turbine Capacity									
@½″ Hg Abs	55	−30	−130	−170	−280	−280	.....	.....	.....
@1″ Hg Abs	40	−35	−110	−125	−175	−185	.....	.....	.....
@1½″ Hg Abs	50	Base	−30	−10	10	−10	.....	.....	.....
@2″ Hg Abs	85	75	90	145	215	180	.....	.....	.....
@2½″ Hg Abs	145	175	235	295	395	350	.....	.....	.....
125-MW Turbine Capacity									
@½″ Hg Abs	.....	55	−30	−100	−200	−210	.....	.....	.....
@1″ Hg Abs	.....	40	−35	−90	−150	−165	.....	.....	.....
@1½″ Hg Abs	.....	50	Base	−20	−30	−50	.....	.....	.....
@2″ Hg Abs	.....	90	80	90	130	100	.....	.....	.....
@2½″ Hg Abs	.....	160	185	220	295	255	.....	.....	.....
150-MW Turbine Capacity									
@½″ Hg Abs	.....	125	35	−30	−135	−150	−270	−325	−480
@1″ Hg Abs	.....	100	15	−35	−115	−135	−200	−235	−300
@1½″ Hg Abs	.....	100	35	Base	−35	−55	−50	−75	−45
@2″ Hg Abs	.....	115	85	75	85	60	130	95	180
@2½″ Hg Abs	.....	170	160	175	230	195	300	250	380
200-MW Turbine Capacity									
@½″ Hg Abs	.....	.....	135	65	−20	−45	−185	−245	−385
@1″ Hg Abs	.....	.....	110	45	−25	−50	−160	−205	−290
@1½″ Hg Abs	.....	.....	110	55	Base	−25	−80	−115	−115
@2″ Hg Abs	.....	.....	120	90	65	35	40	10	75
@2½″ Hg Abs	.....	.....	165	145	160	130	180	140	245
250-MW Turbine Capacity									
@½″ Hg Abs	.....	.....	.....	270	185	140	5	−65	−185
@1″ Hg Abs	.....	.....	.....	240	165	120	0	−50	−140
@1½″ Hg Abs	.....	.....	.....	240	175	130	40	Base	−25
@2″ Hg Abs	.....	.....	.....	245	210	165	120	90	130
@2½″ Hg Abs	.....	.....	.....	280	270	220	225	200	280

TABLE 5

Number and Length of Last-stage Buckets	Differential General Electric Turbine Price	Differential Turbine Foundation Plan Area	Differential Turbine Foundation Length
2–20″			
2–23″	$120,000	40 sq ft	+ 1 ft
2–26″	$160,000	80 sq ft	+ 2½ ft
3–23″	$160,000	280 sq ft	+10½ ft
3–26″	$240,000	160 sq ft	+ 5 ft
1–43″	0	410 sq ft	−30½ ft
2–35″	$315,000*	720 sq ft	+21½ ft
2–38″	$115,000*	60 sq ft	+ 2 ft
2–43″	$300,000*	90 sq ft	+ 3 ft

* Cross-compound, double-flow turbine price differentials are for 200,000-kw maximum capacities and above.

are given as being fairly representative of modern station costs and practices. They should be supplemented by detailed cost studies of the particular location under consideration in order to be reasonably certain that the most economical selection has been made.

The cost of circulating-water-supply equipment varies from approximately $3 to $10 per gpm for a river or lake installation, to $9 to $15 per gpm for a cooling-tower installation. The incremental cost for supplying additional water for a larger condenser should be less than this base cost, possibly only one half as much.

The difference in turbine plan area given in Table 5 generally increases the building and foundation cost by approximately $50 per sq ft for outdoor and $100 per sq ft for indoor stations.

It will cost approximately $150,000 more to provide for station erection and the additional electrical equipment, piping, wiring, and supervisory instruments needed for the average cross-compound unit than it will for a 3600-rpm tandem-compound unit.

Evaluation

Station performance normally improves with a reduction in exhaust pressure or with an increase in turbine-exhaust area, or both. The improvement in average-load performance between alternate turbine-condenser combinations that results in less fuel being burned must be evaluated and deducted from the difference in station cost.

The following formula frequently is used to evaluate this fuel

TABLE 6

Condenser Surface Area Square Feet	Price Increase Single-pass Arrangement Compared to Two-pass Arrangement
40,000	$28,000
50,000	$35,000
60,000	$42,000
70,000	$49,000
80,000	$56,000
90,000	$63,000
100,000	$70,000
110,000	$77,000
120,000	$84,000
130,000	$91,000
140,000	$98,000

NOTE: Price increase for changes in condenser surface area:
$57,000/10,000 sq ft increase for 2-pass condenser arrangement
$64,000/10,000 sq ft increase for single-pass condenser arrangement

saving and obtain a corrected station-cost difference

$$\text{Evaluated Fuel Savings} = \frac{\text{(Change in station heat rate, Btu/kwhr)(average turbine output, kw)(8760) (fuel cost, cents per million Btu)}}{10^6 \text{ (Capitalization rate, per cent)}} \quad [3]$$

Comparison

The more efficient turbine-condenser combination also demands less steam from the boiler to meet its maximum capacity. Thus the size and cost of each piece of equipment associated with steam generation and feedwater heating can be reduced by a corresponding amount without deducting from the expected capacity or reliability of the station. This method of determining the most economical combination by comparing the saving in steam-generation investment with the corrected station-cost difference is particularly difficult, involving incremental costs of many items of equipment.

The method that follows in the Appendix avoids this difficulty and is, therefore, much more convenient. The steam-generation equipment and steam flow are kept constant, letting any improvement in efficiency increase the station kilowatt capacity.

The value of this extra capacity, which is to be compared with the corrected station-cost difference, will depend somewhat on local conditions, but is generally equal to the incremental cost of adding kilowatts to the system with a larger unit at the same efficiency.

Conclusion

The basic data presented in this paper on turbine and condenser performance should help in obtaining a better appreciation of the proper and economical size of steam-station components.

Appendix

A detailed procedure is given for finding the most economical turbine-condenser combination for a specific location where the maximum capacity and the steam condition of the turbine have been selected and data on fuel cost, water temperature and availability, and expected turbine average loading are available (Table 7).

Step 1. For a given steam flow, find the differences in the maximum station capacity for several turbine-condenser combinations. In selecting these combinations initially use the base turbine-exhaust size from the turbine-performance tabulations and, as an alternate, the size smaller or larger depending upon the availability of warm or cold circulating water. Choose several condenser sizes from Table 6 at $^1/_2$ to $^3/_4$ sq ft per kw of maximum turbine capacity

The approximate heat rejected at maximum station capacity is then calculated, using Equation [2], and is used with the appropriate condenser-performance curve to establish the exhaust pressure for the various condenser alternates. For the example given, the curve corresponding to the circulating-water temperature which occurs at peak system load has been used in order to make the capacity comparison at the conditions that will occur when the capacity is needed most.

At these exhaust pressures the differences in gross turbine heat rate are obtained from the proper turbine-performance tabulation and added to the base heat rate to give the relative gross turbine heat rate. For steam conditions other than those for which differences have been tabulated, use the steam condition nearest to design. For example, the differences in gross turbine heat rate with exhaust pressure and exhaust size for 2000 psig, 1050/1000 F usually can be used for calculating the most economical turbine-condenser combination at 1800 psig 1000/1000 F with negligible error.

Keeping the same throttle flow or heat input, the gross turbine heat rate determines the turbine capacity for each alternate. Assign the base capacity to the smallest turbine-condenser combination in order to simplify the following steps of the evaluation.

Auxiliary-power requirements are calculated to correct the turbine output to the net station output. Circulating-water-pump power is calculated from the formula shown on the condenser-performance curves, holding other auxiliary power constant for alternate combinations at a total of approximately 6 per cent of the base turbine capacity.

Step 2. For each of the turbine-condenser alternates, evaluate the saving that will result from the more efficient alternates. The fuel saving is based on the turbine-condenser performance calculated at the expected average load and the weighted average circulating-water temperature.

The heat rejected at average load is calculated using Equation [2] and the heat rate at capacity from Fig. 1. The exhaust pressure is calculated for each condenser alternate at the weighted average circulating-water temperature and is used in determining the changes in gross turbine heat rate from the base heat rate. Equation [1] is used to correct this change into change in station heat rate. The value of this change is calculated using Equation [3] and the change in station heat rate relative to the smallest combination.

Step 3. This value of future fuel savings expected with the more efficient combinations is deducted from the higher cost of these combinations to obtain a corrected station-cost difference. Again, these differences should be relative to the smallest combination. Turbine and condenser-price differentials are obtained from Tables 5 and 6, respectively. Other costs cover the change in plan areas and the additional expenses for cross-compound turbines, additional length, additional circulating water, and so on.

TABLE 7 PROBLEM: DETERMINE THE ECONOMIC CONDENSER AND TURBINE-EXHAUST SIZE

Given: **150-MW Capacity Addition with Steam Conditions of 2000 PSIG 1050 F, Reheat to 1000 F.**
100-MW Average Load with 60 F Inlet Water, 30¢/million BTU Fuel Cost and 15% Capitalization Rate.
Peak Station Load Expected with 80 F Circulating Water.

Alternate Number and Length—Last-stage Bucket Condenser Surface in Sq Ft for 2-pass Arrangement and Circulating Water Velocity of 7 ft/sec		Base 2–26″ 60,000	2 2–26″ 80,000	3 2–26″ 100,000	4 3–23″ 60,000	5 3–23″ 80,000	6 3–23″ 100,000
Step No. 1 Difference in Capacity							
(1) Approximate Heat Rejected @ Capacity	BTU/Hr	637×10^6	→	→	→	→	→
Heat Rejected per sq ft of Condenser Surface	BTU/Hr/Sq Ft	10,620	7960	6370	10,620	7960	6370
(2) Exhaust Pressure @ 80 F Water	Inch Hg Abs	2.76	2.17	1.91	2.76	2.17	1.91
(3) From Fig. 4, △HR @ 150-MW	BTU/Kw-hr	196	106	75	218	108	60
(4) Relative Gross Heat Rate (△HR+Base)	BTU/Kw-hr	7946	7856	7825	7968	7858	7810
(5) Gross Turbine Output	Kw	150,000	151,718	152,319	149,586	151,680	152,612
Total Heat Input	BTU/Hr	1191.9×10^6	→	→	→	→	→
(6) Circulating Pump	Kw	420	560	700	420	560	700
(7) Other Auxiliary	Kw	9000	9000	9000	9000	9000	9000
(8) Total Auxiliaries	Kw	9420	9560	9700	9420	9560	9700
(9) Net Station Output	Kw	140,580	142,158	142,619	140,166	142,120	142,912
Step No. 2 Evaluated Fuel Saving							
(10) Approximate Heat Rejected @ Average Load	BTU/Hr	425×10^6	→	→	→	→	→
Heat Rejected per sq ft of Condenser Surface	BTU/Hr/Sq Ft	7080	5320	4250	7080	5320	4250
(11) Exhaust Pressure @ 60 F Water	Inch Hg Abs	1.14	0.95	0.86	1.14	0.95	0.86
(12) From Fig. 4, △HR @ 100-MW	BTU/Kw-hr	−92	−116	−121	−100	−132	−142
Change in Turbine HR from Base Alternate	BTU/Kw-hr	0	−24	−29	−8	−40	−50
(13) Change in Station HR from Base Alternate	BTU/Kw-hr	0	−30	−36	−10	−50	−62
(14) Value @ 1750 $/BTU		0	$52,500	$63,000	$17,500	$87,500	$108,500
Step No. 3 Net Difference in Station Cost							
(15) Difference in Turbine Cost		0	0	0	$160,000	$160,000	$160,000
(16) Difference in Condenser Cost		0	$114,000	$228,000	0	114,000	228,000
(17) Difference in Miscellaneous Cost @ $100/sq ft Plan Area		0	0	0	28,000	28,000	28,000
Difference in Cost of Circulating Water @ $4/GPM		0	72,000	144,000	0	72,000	144,000
(18) Total Difference in Station Cost		0	186,000	372,000	188,000	374,000	560,000
Less Evaluated Fuel Savings		0	52,500	63,000	17,500	87,500	108,500
(19) Corrected Difference in Station Cost		0	$133,500	$309,000	$170,500	$286,500	$451,500
Step No. 4 Compare:							
(20) Difference in Corrected Station Cost Between Base and Alt. 2		$133,500					
(21) Difference in Net Station Output		1578 Kw					
(22) Cost of Incremental Capacity, $/Kw		$85/Kw					

Step 4. This corrected station cost represents the additional investment that can be made in more efficient turbines beyond that which will be returned directly by fuel savings. For this additional investment the purchaser may get additional station capacity cheaper than could be obtained in any other way.

Step 5 (Summary). Select the condenser and turbine-exhaust size which results in the largest station output that does not cost more than approximately 80 per cent of the finished station cost in dollars per kilowatt for its incremental capacity. For the example shown, only the base alternate and alternate (1) have been compared. At an estimated station cost of $135 per kilowatt, it appears that alternate (2) is a more economical alternate than the base combination. The comparisons should be carried further in a practical case to include single-pass condensers and a turbine with two 23-in. last-stage buckets.

Acknowledgments

The authors gratefully acknowledge the assistance of E. Goitein and W. B. Bumbarger in the preparation of material for this paper.

Discussion

S. Baron.[7] The authors should be congratulated for presenting a paper that contains all the necessary cost and thermal data that would permit the reader to apply the information for his own investigations. The method presented is simple and straightforward and allows rapid solution of the problem. Furthermore, the authors' use of incremental costs for condensers, turbine exhausts, circulating-water flows, turbine foundations, and station costs as applied to this type of problem is far better than the method practiced by many engineers of expressing total costs on a per unit basis such as area, kilowatts, or gallons per minute.

It is common practice to size condensers and study the thermal gains in power-plant cycles based on yearly average circulating-water temperatures. Of course, where the circulating-water temperature varies only a few degrees throughout the year, the average as applied to the problem is correct. However, consider the case where the temperature varies from 40 to 80 F during the year as is so common in this part of the country. For example, let us consider a case where the water temperature is 40 F for 6 months, and 80 F for the remaining 6 months, thus giving an average of 60 F for the year. Based on the same problem presented in the paper, the following data would have resulted as shown in Table 8 of this discussion.

The writer was not able to check the magnitude of values for line 12 of the authors' calculation at 60 F although the differences of the various cases with the base were about the same.

It is apparent from the comparison that the change in heat rate is definitely related to the circulating-water temperature variation. The results may or may not change the optimum selection. However, to be certain, the writer would recommend that the average circulating-water temperature for each month be used and the monthly net savings calculated. The results of each month can be totaled to determine the yearly savings.

The authors chose the arrangement of turbine-exhaust and condenser size which gave them the minimum cost per additional kilowatt capacity. This method of evaluation is probably correct if the unit being considered is the only one in a station. However, it is more probable there are other units in the station, or tied in with the station, which are less efficient than the unit being considered. Therefore the writer would have evaluated the additional kilowatts as a fuel saving over operating with less efficient units. This is probably the truer situation.

The formulas for gallons per minute and circulating-water-pump kilowatts are approximations and probably in most cases are correct. For the case under study, it is suggested that the gallons per minute and pump kilowatts be calculated carefully from the actual conditions that exist.

G. A. Hendrickson.[8] One approach to the question of larger turbine-exhaust and condenser sizes is to consider simply that the customer is buying kilowatts. On this basis the charges for the larger exhaust-end sizes are quite high, ranging up to $300 per kw of increased capacity. Compared to a total station cost in the order of $150 per kw, increased costs of such magnitude are difficult to overcome, particularly when the item of expense is not in the direction of progress, as in the present case.

When economic comparisons are close, it is more to the point to put extra investment in such items as increased throttle pressures and temperatures, for such investments lay the foundation for future reductions in heat rates.

Attention is directed to the authors' use of heat rates at the average load and at the average circulating-water temperatures. Naturally, in a question with so many factors varying independently, it is not possible to give a final solution for all combinations of circulating-water-temperature distributors and load-duration data. Instead of giving a comparison based on weighted averages for a particular location and load requirement, it is just as significant to give an illustration comparison at average load and average circulating-water temperature as the authors have done, provided sufficient data are given for determining a weighted-average heat rate for any particular situation.

The paper would be much strengthened if data were complete for obtaining a weighted-average heat rate with any combination of circulating-water temperatures and load-duration data for the different condenser and turbine-exhaust sizes. This is particularly true of data for heat rate at reduced turbine loads, since the customer is dependent on the manufacturer for authentic information of this kind. Such information necessarily might be restricted to a particular design type, but this is no great handicap as similar data for other types could be sought at the proper source.

Data on the variation of condenser pressures with circulating-

[7] Burns and Roe, Inc., New York, N. Y.

[8] Dean, College of Engineering, Lawrence Institute of Technology, Dearborn, Mich. Mem. ASME.

TABLE 8 RE-EVALUATION OF AUTHORS' PROBLEM, TABLE 7

	Base	2	3	4	5	6
Line 11:						
Exhaust pressure at 40 F	0.66	0.58	0.54	0.66	0.58	0.54
Exhaust pressure at 80 F	2.02	1.71	1.56	2.02	1.71	1.56
Line 12:						
Change in heat rate						
At 40 F	−124	−127	−128	−156	−163	−166
At 80 F	+96	+20	−16	+151	+55	+9
Average of 40 F + 80 F	−14	−54	−72	−3	−54	−79
Change in Tb HR	0	−40	−58	+11	−40	−65
Change in Tb HR at 60 F from paper	0	−24	−29	−8	−45	−54
Difference in Tb HR	0	−16	−29	+19	+5	−11
Difference in Tb HR in per cent, authors' figure as base	0	66.7	100	235	11	20.4

water temperatures are not so vital as such information is available in recent literature. It would be a great convenience, however, to have it under one cover.

The writer desires to commend the authors for the presentation of data on a timely subject and to express the hope that we will have more along the same line in the future.

H. R. REESE.[9] The authors are to be commended on presenting a fine paper which outlines a simplified method for determining the economical combination of condenser and turbine-exhaust sizes.

The gross turbine heat rates plotted against turbine capability in Fig. 1 of the paper, together with the tabulation of gross turbine heat-rate differences, make it very easy to compare the change in heat rate for different number and length of last-row blades.

Although the form is good there are a few questions which the authors may be able to answer with regard to Tables 1 to 4, and Fig. 1.

1 In Fig. 1 wouldn't it be better if the heat-balance arrangement and number of stages of feed-heating were specified?

2 In Fig. 1 it is noted that the base gross turbine heat-rate curve for the 2 to 23 ends are flat for the top three steam conditions. Correcting for leaving loss and size factor it is expected the heat rate at 100 mw for the 1450 psig 1000 F steam conditions would be approximately 20 to 30 Btu/kwhr poorer than the 82-mw load point. And for the same reasons, it is expected the 2000 psig, 1050 F/1000 F curve would improve while increasing from 82 to 100 mw. For steam conditions of 1450 psig, 1000 F/1000 F, the flat curve for the 2–23 ends and between 82 and 100 mw appears to be correct. Do the authors have an explanation why these three heat-rate curves are flat between the 82 and 100-mw loads?

3 In Fig. 1 why isn't the 1450 psig, 1000 F/1000 F heat-rate curve flat for the 3–23 ends similar to the flat curve for the 2–23 ends, since the leaving losses are approximately the same?

4 Was the heat-rate difference between the 1450 psig 1000 F and 1450 psig 1000 F/1000 F intentionally made greater than the published standardized heat rates for the same steam conditions?

5 In Table 2 the heat-rate difference between 1.5 and 1.0 in. Hg abs for a 100-mw turbine capacity with 2–23 ends is listed as —25, while the published standardized difference is —40. In Table 3 the heat-rate difference for the same rating and exhaust ends is —35, as compared to —75 for the published standardized rates. These differences are great enough to affect the evaluation of both the turbine and particularly the condenser. Which one is correct?

Time did not permit other comparisons, although it is noted the heat-rate differences for 1800-rpm units are greater than those used by the writer's company. The art of designing the last stage is gradually reaching the optimum, so that one would expect very little difference in leaving losses between the turbine manufacturers.

We agree with the authors that the cross-compound machines require additional electrical equipment, piping, and supervisory instruments and they will cost more to erect at the station. We question the statement that the longer span on tandem-compound units may require a larger building, while a cross-compound machine with the shorter span may have a smaller building. It has been concluded generally that the auxiliaries determine the size of the building. Therefore it would be expected that the size of the building for tandem or cross-compound units would be approximately the same. However, in most cases the cross-compound units to date have required larger buildings.

[9] Assistant Manager, Central Station Section, Land Turbine Engineering, Steam Division, Westinghouse Electric Corporation, Lester, Pa. Mem. ASME.

Some station designers have estimated the extra cost for a cross-compound-unit building and foundation to be approximately $500,000. This, added to the $150,000 for station erection, additional electrical equipment, wiring, and supervisory instruments, makes a total of $650,000. The extra cost for the cross-compound unit is around $550,000 making a grand total of $1,200,000. It would be rather difficult to justify this extra cost except in regions where cold circulating water is available for the entire year and fuel costs are high. This example may be a little on the high side but it is made to caution those designing plants for units from 150 to 250 mw to evaluate the facts carefully.

One more point should be discussed. "Any improvement in efficiency increases the station kilowatt capacity. The value of this extra capacity is generally equal to the incremental cost of adding kilowatts to the system with a larger unit at the same efficiency." It is believed this method of analysis is incorrect because the electric utilities sell kilowatthours, not kilowatts of installed capacity. For example, assume steam conditions of 1800 psig, 1000 F/1000 F, 1 in. Hg abs for a 3600-rpm 200-mw tandem-compound unit with a station heat rate of 9350 Btu/kwhr and a net station cost of $30,000,000, and a cross-compound unit 3600/1800 rpm with a heat rate of 9140 Btu/kwhr and an evaluated station cost of $30,450,000 and 4500 extra kilowatts capacity. Other factors are fuel 20 C/mm Btu, 60 per cent load factor, 15 per cent capitalization rate and load duration over a 35-year period.

The average capital investment for each kilowatthour sold for the 3600-rpm tandem-compound unit is

$$\text{Net kw} \times \text{hr} \times \frac{\%\ \text{load factor}}{100} \times \text{years} = \text{kwhr sold}$$

$$200{,}000 \times 8760 \times \frac{60}{100} \times 35 = 3.68 \times 10^{10}\ \text{kwhr}$$

Then the mils capital investment per kwhr sold is

$$\frac{\text{Plant cost} \times \dfrac{\text{cents}}{\text{dollar}} \times \dfrac{\text{mils}}{\text{cents}}}{\text{kwhr}} = \text{capital charge per kwhr}$$

$$\frac{30{,}000{,}000 \times 100 \times 10}{3.68 \times 10^{10}} = 0.82\ \text{mils/kwhr capital investment}$$

Based on a 35-year life the additional kilowatthours which can be sold for the cross-compound unit would be for the first 7 years

$$4500 \times 8760 \times 7 = 2.75 \times 10^{8}\ \text{kwhr}$$

Since the evaluated additional cost is $450,000, the cost per kilowatthour is

$$\frac{450{,}000 \times 100 \times 10}{2.75 \times 10^{8}} = 1.64\ \text{mils/kwhr capital investment}$$

In order for a cross-compound unit to be justified it appears that the capital investment should not exceed 0.82 mils/kwhr in this case.

The result obtained by this method of analysis will be influenced by fuel cost, load factor, capitalization rate, and the increased station cost for the cross-compound unit.

It appears in the foregoing case the maximum justifiable increase evaluated cost would be

$$\frac{0.82 \times 2.75 \times 10^{8}}{100 \times 10} = \$225{,}000$$

In conclusion, it would appear that the method of evaluating extra capacity in this paper should be studied further.

Authors' Closure

The authors are gratified that so much worth-while discussion of the paper was submitted. Several refinements in the method of using the data on the turbine and condenser performance have been suggested and they should prove helpful to the station designer in making the final selection of condenser and turbine-exhaust sizes. Other discussion points that deal directly with the problem of evaluating different exhaust sizes and condensers at the same turbine rating and steam conditions will be explained and amplified.

Mr. Baron has rightly called attention to the difficulty of properly determining an "average" circulating-water temperature and makes an excellent suggestion that the evaluated fuel savings could be obtained more accurately by totaling the monthly fuel savings calculated at monthly average circulating-water temperature. It would appear that this is also a good way to avoid the problem of obtaining a weighted "average" yearly load; and for those station designers who must contend with large seasonal variations in either circulating-water temperatures or load, the authors recommend this variation of the basic method to help make the final selection of exhaust-end equipment.

Professor Hendrickson seems to suggest that a choice must be made between getting the optimum steam conditions and the optimum exhaust size and condenser. On the contrary, it appears to the authors that the method of appraisal suggested in the paper is desirable at any steam condition, and as the gains in heat rate at high pressures and temperatures become more costly, it becomes particularly necessary to derive all the possible economic benefits from the exhaust end of the turbine.

Although no data have been specifically included in the paper to give turbine heat rates at partial load, it was the authors' intention that the differences in heat rate with exhaust pressure and exhaust size would be obtained from Table 1 through Table 4, at both maximum load and at partial loads. The method of weighting this partial load heat rate for seasonal variations will vary with location but it appears that Mr. Baron's suggestion for calculating monthly fuel saving deserves consideration.

Mr. Reese has raised several questions about the typical heat-rate curves in Fig. 1 which are described in the paper as an alternate method to using actual heat balances of obtaining an estimate of the heat rejected to the condenser. The authors have no reservations as to the accuracy of these curves for the purpose intended, although it is agreed that if these heat-rate curves are to be used to calculate performance differences between the various turbine ratings or steam conditions, the heat-balance arrangements must be defined and the scale and size of Fig. 1 expanded.

The four tabulations of heat-rate differences, including those whose accuracy were questioned, have been rechecked and are found to be in close agreement with our most recent field tests. A complete discussion of the performance of condensing turbines with changes in exhaust pressure can be obtained from the paper by A. Keller and J. E. Downs published in 1954.[4]

The authors thoroughly agree with Mr. Reese in cautioning those designing power plants to "evaluate the facts carefully." On the other hand, the rather high estimated figures that he has cited to show an extra cost of $1,200,000 for cross-compound units should not discourage station designers from investigating and obtaining the facts on heat-rate and station-capacity gains that may be realized with a more liberal exhaust size.

One additional point discussed was the method of evaluating the extra capacity resulting from increased efficiency. Mr. Reese suggested an alternative system of evaluation, which is based on comparing the capital investment per kilowatthour for additional capacity with the capital investment per kilowatthour for the base capacity. This method is a simplification of one sometimes used to help the station designer select the optimum-capacity addition to meet the expected load growth. However, as it has been used in the example, Mr. Reese has incorrectly compared the base-station capital investment per kw spread over a 35-year period with the capital investment per kw of incremental capacity, calculated for only the first seven years of operation. A more proper evaluation is made if the capital investments are both compared on the same basis. For example, if the additional capacity is used at 60 per cent load factor, the extra kilowatts that can be sold over the 35-year life of the station becomes

$$4500 \times 8760 \times \frac{60}{100} \times 35 = 8.25 \times 10^8 \text{ kwhr}$$

Using Mr. Reese's figure for capital investment of 0.82 mil per kw for the base capacity, it appears that the maximum justifiable evaluated cost for the more efficient station would be equal to

$$\frac{0.82 \times 8.25 \times 10^6}{100 \times 10} = \$675{,}000$$

or

$$\frac{\$675{,}000}{4500 \text{ kw}} = \$150 \text{ per kw}$$

Thus, when the evaluation is made on a comparable basis, even this simplified method gives results in close agreement to the authors' example; although in a specific case a careful analysis should be made of the expected future-station loading and its effect on load factor and rate-of-investment return.

This same problem of comparing the value of additional capacity with its cost confronts the station designer when he selects the optimum turbine rating; it thus follows that the value of additional capacity obtained with better station efficiency is equal to the value of additional capacity obtained with larger station components and is therefore closely equal to the incremental cost of station kilowatts at a particular station capacity.

Perhaps the authors' calculation that incremental station costs are approximately 80 per cent of the base station cost is true only in the general case, and in specific cases and for the final calculation a more accurate analysis of the cost or value of incremental kilowatts may be needed. A variation of Mr. Reese's suggested method, correctly taking into account load factors and capitalization rates, or the suggestion of Mr. Baron, that extra kilowatts should be evaluated in comparison to less efficient system capacity, may prove on further study to be a more accurate analysis.

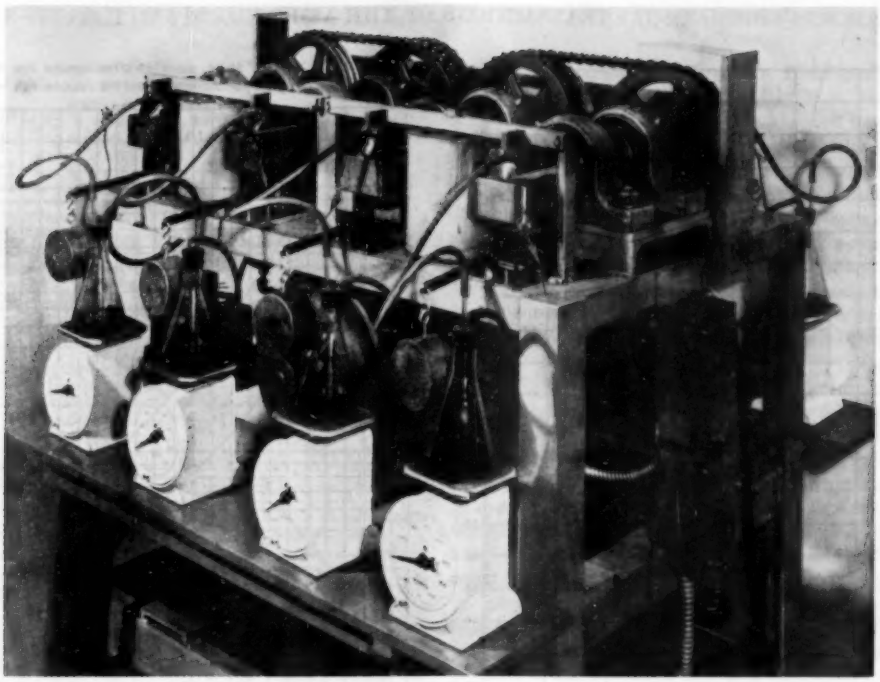

FIG. 1 APPARATUS USED IN STUDY OF WICKING CHARACTERISTICS OF WASTE

Effect of Viscosity of Car-Journal Oils on Running Temperature and Other Characteristics of Journal-Bearing Performance

BY W. M. KELLER,[1] CHICAGO, ILL.

The effect of viscosity in journal oil has been the subject of discussion for many years. Until recent years no data had been obtained with sufficient accuracy and in sufficient quantity to establish the optimum viscosity for oils in the journal box. In more recent years with laboratory test equipment, it has been possible with controlled conditions to isolate the oil as a variable and obtain reliable data on this subject. A consideration of this problem shows that with full hydrodynamic lubrication the asperities of journal and the bearing are separated by a film of oil. While there may be minor areas in which this condition does not obtain, the general separation of the two surfaces must take place, as it is evident that if large areas of the bearing were in metal-to-metal contact the wear which results would be of a much higher order and bearing failure more frequent. When bearings have a hydrodynamic film and the metal surfaces are not in contact, the heat developed in a journal box is from two sources, i.e., the pressure of the waste against the bottom of the journal and the viscous shear of the oil film between the bearing and the journal.

[1] Director of Mechanical Research, Association of American Railroads, Mechanical Division. Mem. ASME.

Contributed by the Railroad Division and presented at a joint session of the Railroad Division and Lubrication Activity at the Annual Meeting, New York, N. Y., November 29–December 4, 1953, of THE AMERICAN SOCIETY OF MECHANICAL ENGINEERS.

NOTE: Statements and opinions advanced in papers are to be understood as individual expressions of their authors and not those of the Society. Manuscript received at ASME Headquarters, July 31, 1953. Paper No. 53—A-111.

EFFECT OF VISCOSITY

THE 8-spindle machine of the Association of American Railroads (AAR) employs a half-size $5^1/_2$-in. × 10-in. journal having $2^3/_4$-in. × 5-in. dimensions and is shown in Fig. 1. This machine has been used to develop much information regarding wicking characteristics of waste and a series of tests were conducted to determine the effect of viscosity on bearing temperature and the oil feed. Full-scale testing equipment also has been used to obtain data. Fig. 2 shows a comparison of oil viscosities between 34 and 69 SU viscosity at 210 F, plotted against bearing temperatures and oil feed. From this figure it will be noted that two general trends are evident; the first being that the stabilized bearing temperature increases with an increasing viscosity and the oil feed to the bearing from the waste pack decreases. On the

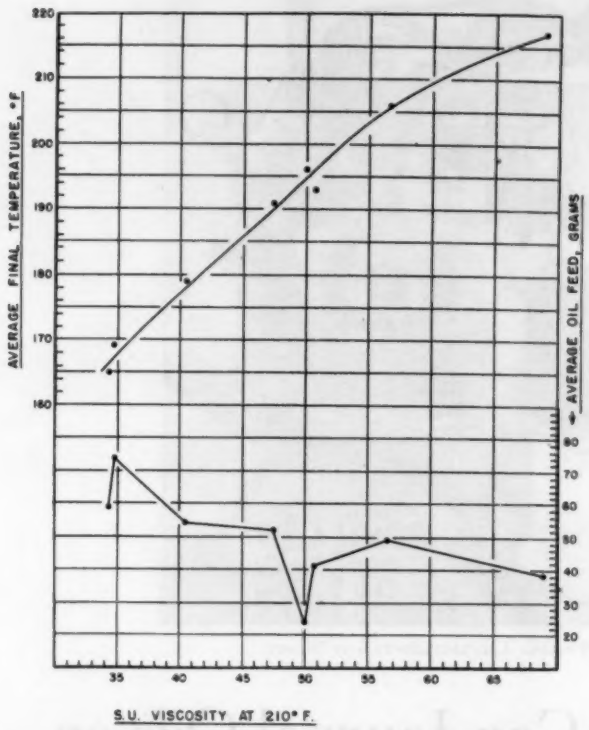

FIG. 2 COMPARISON OF OIL VISCOSITIES BETWEEN 34 SU AND 69 SU VISCOSITY AT 210 F, PLOTTED AGAINST TEMPERATURES AND OIL FEED

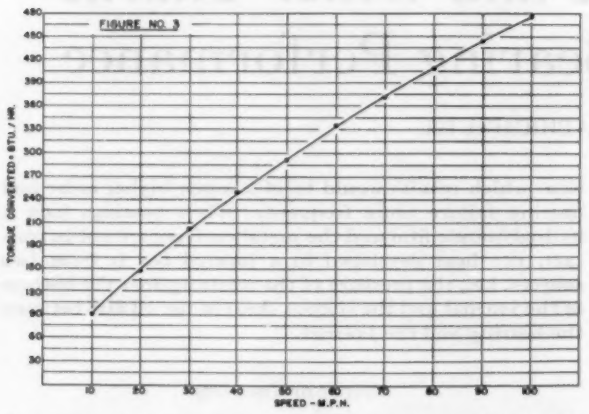

FIG. 3 AVERAGE CURVE SHOWING RELATIONSHIP OF TORQUE AS CONVERTED TO BTU PER HOUR TO SPEED (MPH)

basis of this consideration it appears evident that the viscosity of journal-box oil should be reduced to the minimum possible in order to get high oil feed and low operating temperatures. There are numerous factors, however, that prevent using oils below a certain viscosity, and these factors involve the ability of the oil to maintain separation of the bearing surfaces by maintaining a full hydrodynamic film.

The heat generated in the oil film and by the box packing is a function of speed and bearing load. In a series of tests the torque was measured and this torque translated in terms of energy in Btu.

Fig. 3 shows a curve of the relationship between speed and the

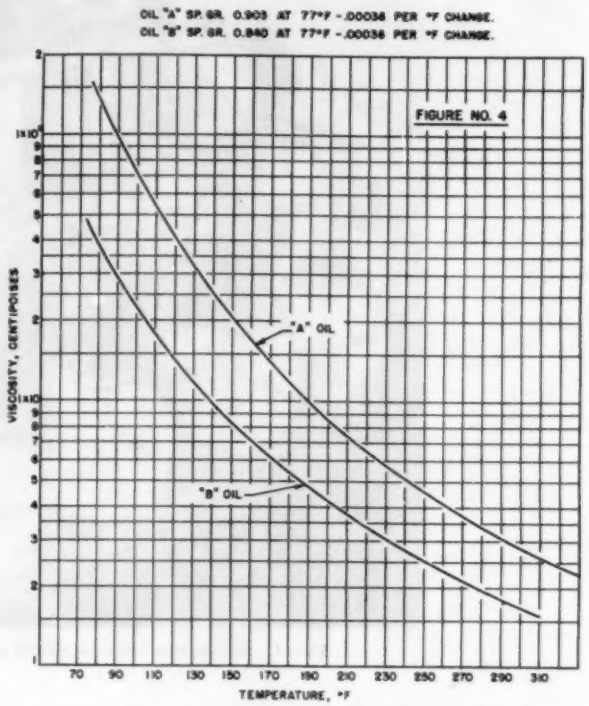

FIG. 4 VISCOSITY VERSUS TEMPERATURE RELATIONSHIP OF TWO OILS OF DIFFERENT VISCOSITY

heat generated by a $5^1/_2$-in. × 10-in. journal bearing. The equation for this curve is $Y = C(x)^{0.72}$ where C is a constant equal to 17. In considering this equation it must be remembered that there is a wide spread between the readings obtained because of uncontrollable conditions and variations in maintaining a hydrodynamic oil film and, therefore, the equation represents only an average of the wide band that is obtained in the laboratory. Some of this variation is due to the method of obtaining the torque readings which, while as precise as it is possible to develop to date, is not a perfect system of measurement. The heat generated by the bearing lowers the viscosity and the film cannot be maintained under high loads. It is apparent from the value of the exponent that the heat developed is in almost direct linear proportion to the speed.

Fig. 4 shows the relationship between two oils labeled A and B arbitrarily selected which indicates the viscosity change with temperature. Oil A is a 50–55-sec-viscosity oil at 210 F and oil B is a 40–42-sec-viscosity oil at the same temperature.

Fig. 5 shows the calculated maximum load in pounds per square inch that will be supported by an oil film of the viscosity of oil A and oil B. It is evident from these data that a relationship between the journal load and the oil viscosity must be maintained so that the optimum bearing operating temperature is not always obtained and the higher temperature is accepted in order to obtain the film required to support the bearing. The principal objection to oils of higher viscosity is that during extremely cold weather the more viscous oil has a tendency to cause the waste pack to be displaced from under the journal and also higher-viscosity oils have a poorer wicking action than the lighter-viscosity oils. The journal bearing operates in atmospheres from minus 40 to 120 F.

HEAT DISSIPATION

Because of the design of the box there is a severe temperature

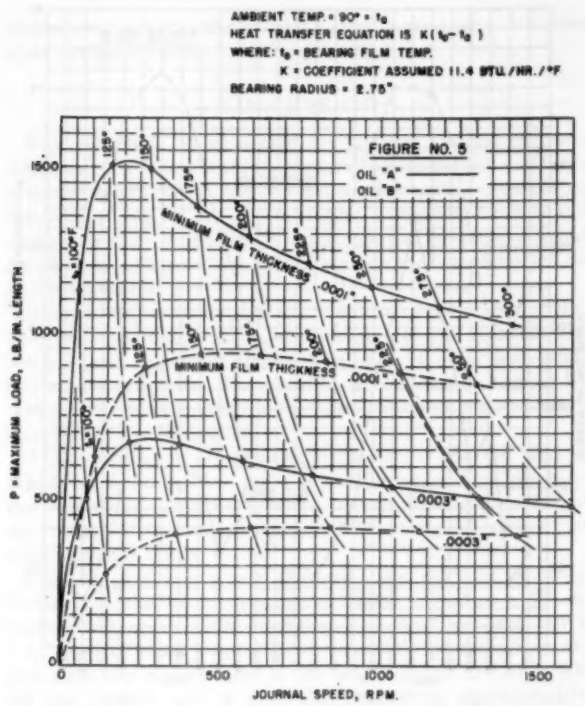

FIG. 5 COMPUTED VALUES OF EQUILIBRIUM BEARING OPERATING TEMPERATURE AND MAXIMUM LOAD CAPACITY VERSUS SPEED WITH TWO DIFFERENT VALUES OF LIMITING MINIMUM FILM THICKNESS

gradient between the journal surface and the exterior of the box. It is possible to have a journal box operating at abnormally high temperatures of 275 to 300 F with an outer box temperature of 125 to 150 F. The path of heat flow through the axle provides some heat dissipation. While the mass temperature of the bearing is a function of the heat generated, the temperature of the bearing varies with heat-transfer conditions of the outside air.

The introduction of outside air into the box would allow too much dirt to enter the box to provide a satisfactory means of cooling the bearing. Where cooling air is brought into the box through a screen to prevent dirt from entering the box, the screen would soon be clogged with foreign matter and make such a system ineffective. To dissipate the heat developed in the bearing by cooling with air would require some means of circulating the air within the bearing itself and exclude the air from the interior of the box.

The journal bearing is the only high-capacity high-speed bearing which is not bored to fit its journal. It is possible to have up to $^1/_2$ in. greater diameter in the bearing surface than that of the journal although such differences are rare; differences of $^3/_{16}$ in. are common. This journal diameter tolerance creates high unit pressures but the lining metal used in the bearing is soft enough to allow these unit pressures to be reduced rapidly by the wearing-in process so that they can be brought quickly to the point where the bearing will operate satisfactorily. Table 1 gives the composition of the bearing lining.

TABLE 1 BEARING-LINING COMPOSITION

	Per cent
Antimony, not less than	8.0
Tin and antimony	10.0 to 14.0
Arsenic, max	0.2
Copper, max	0.5
Sum-tin, antimony, lead, and arsenic, min	99.25
Remainder, max	0.75

The projected area of a $5^1/_2$-in. × 10-in. bearing is 37.73 sq in. and, based on full journal load of 20,000 lb, the load per square inch is 530 lb. This is a relatively low unit load, but when only a small bearing area exists at the top of the bearing as is the case when a new bearing is applied to a worn axle, the unit load may be several times that of a fully "worn-in" bearing.

The Brinell hardness of this lining is approximately 19.0 at 68 F and 8.5 at 212 F and has a melting point of about 460 F. Consequently, the oil film must be maintained properly in order to prevent temperatures of sufficient elevation to increase the coefficient of friction to the point where the heat cannot be dissipated rapidly enough to prevent an overheated bearing.

Viscosity Index

While establishing the proper viscosity for journal-box work is, as in other lubrication problems, important, the viscosity index is also very important because of the extreme operating temperature range of the ambient temperatures encountered by the journal box. As a rule of thumb it may be considered that under normal bearing operating conditions the average temperature of the bearing is about 100 deg F higher than the ambient. However, oil-film temperatures are much higher than the mass temperature of the bearing. Ambient temperatures on United States railroads are in the general range of from —40 to 127 F. During hot summer weather in the Southwestern region, particularly in the Nevada desert area, temperatures of 110 to 120 F are not uncommon. In addition, there is a sun load which aggravates the temperature condition. Thus a temperature spread of 160 deg F or more is present in the atmospheres in which journal bearings must operate.

The viscosity index, VI, is calculated by the equation

$$\text{VI} = \frac{L - U}{L - H} \times 100$$

where

L = viscosity at 100 F of an oil with 0 viscosity index having the same viscosity at 210 F as the oil whose VI is to be calculated

U = viscosity at 100 F of the oil whose viscosity index is to be calculated

H = viscosity at 100 F of an oil of 100 viscosity index having the same viscosity at 210 F as the oil whose VI is to be calculated

In the values of H and L, H represents a crude oil with a small viscosity-temperature coefficient and rated at 100 VI, and L an oil with a large one rated zero VI. The larger the viscosity index, the smaller is the tendency of oil to thin out with temperature increase. The AAR specifies a minimum VI of 80 for journal-box oil. It is obvious that a very high VI is desirable and if it were possible to develop an oil whose viscosity was unaffected by temperature change, it would assist greatly in eliminating hotboxes.

Viscosity Defined

Viscosity may be described as the property of a fluid which is such that, when flow occurs inside it, forces arise within the fluid to oppose its flow; it is a measure of the combined effect of adhesion and cohesion within the fluid. Viscosity is usually thought of in terms of the seconds required for a given quantity to pass through an orifice, but it is much more significant than the means of measurement might indicate. The depth to which oil molecules can be stacked is dependent on the cohesion between the molecules and this cohesion is directly related to viscosity. Cohesion between molecules is great in solids, very much reduced in liquids, and scarcely exists in gases. Liquids therefore might be thought of as being in two groups, one as true liquids, such as

water, and the second as boundary liquids, such as very viscous oils and greases. The ability to maintain an oil film under a bearing means that it must have sufficient adhesion to the bearing and journal and sufficient cohesion between molecules to generate a hydrodynamic film. The greater the unit load the more difficult film generation becomes.

Referring to Fig. 4, it will be noted that the viscosity of oil A (50–55 viscosity) at 220 F is the same as oil B (40–42 viscosity) at 167 F. Thus the ability to support high bearing loads is greater for oil A at higher temperatures, the oils being approximately equal—viscositywise—at about a 50-deg F temperature spread within the operating-temperature range of the bearing. A variable, however, which must be considered is the difference in heat developed by viscous shear in the film between bearing and journal. Oil B has been found to operate at about a 20-deg F lower bearing temperature under normal conditions than oil A. If this figure is subtracted from the temperature spread the temperature difference at which viscosities are equal, in so far as bearing operation is concerned, is about 30 deg F.

Temperatures in bearings and journals are not uniform over the bearing length. At the wheel fit of the axle, the wheel provides a mass of 600 to 800 lb which provides a path for heat flow. As the wheel revolves in air, a large air-cooling surface is provided which permits heat exchange to the surrounding air. At the outer end of the axle the journal face is enclosed by the box and air blast is prevented by the enclosure. Therefore the heat conducted away from the end of the axle is a relatively small percentage of the total.

As a consequence of these conditions the heat flow is normally inboard or toward the wheel. In a laboratory test, where the journal was intentionally overheated, it was found by measuring with a contact pyrometer that the following temperatures existed on the journal surface 10 min after the journal stopped rotating:

$1^1/_2$ in. from axle-journal collar (outer end)	400 F
$1^1/_2$ in. from axle-journal fillet (inner end)	370 F
Axle dust-guard seat	270 F
Middle of wheel hub on outboard face	175 F

While sufficient data do not yet exist to prove the case completely, it is evident that the outer end of the journal normally operates at a somewhat higher temperature than the inboard end. While the mass temperature of a bearing may appear to be within the proper operating limits of a given-viscosity oil, isolated bands or areas frequently exceed these limits. As the hysteresis effect of conducting the heat from localized areas to the entire bearing mass is high, oil-film failures need not be general to cause a hotbox. A consideration of the geometry of the bearing would support a conclusion that if there were localized oil-film failure, the remainder of the oil film would support the bearing and the local area at the point of film failure merely would be suspended above the bearing, and the point of failure would be avoided. However, oil films are so small in thickness (in the order of 0.0001 in. to 0.0005 in.) that the deflection of the bearing and depth of the asperities are great enough to allow metal-to-metal contact. When this occurs local heated areas cause the immediate surrounding oil film to change in viscosity to the failure point and the failed area grows into what might be termed a chain reaction, as the failure progresses.

In this situation higher-viscosity oils have a better chance of "healing" the defective area before failure occurs. However, such defects as waste grabs, insufficient oil in the box, packing out of contact with the bearing, and so forth, are all beyond any help from oil viscosity regardless of how advantageous it may be under normal conditions.

Atmospheric-temperature effect on journal bearings is critical. Fig. 6 shows the incidence of hotboxes experienced by one railroad in relation to the outside temperature. The increase in hotboxes is generally proportional to the temperature increase, and is from 3 to 5 times as great in July as it is in January. The waste grab is specified as the cause of a great many hotboxes and there is no doubt that this defect is responsible for a high percentage of the total number of overheated bearings. However, the warmer summer weather results in conditions less conducive to waste grabs, and there is no evidence to suggest that waste grabs should be more prevalent in hot weather than they are in cooler weather, but rather, waste grabs should be fewer.

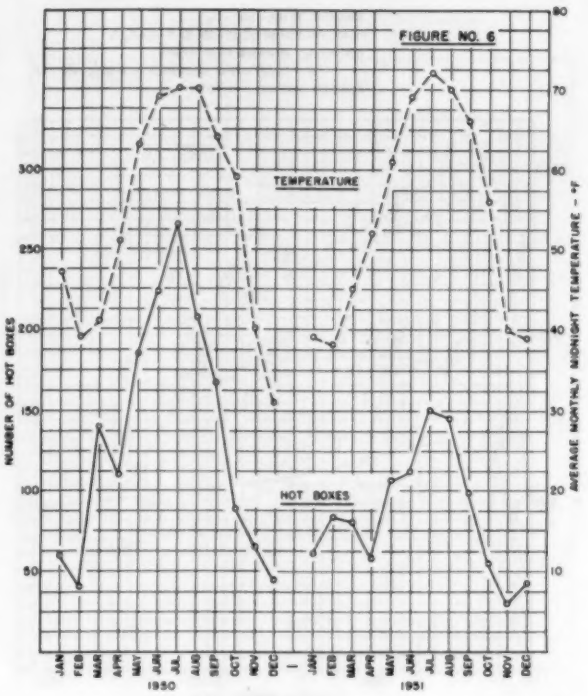

FIG. 6 TOTAL HOTBOXES BY MONTHS AND AVERAGE TEMPERATURES RECORDED

Therefore the reason for the increase in hotboxes during warm weather must be other than that of waste grabs. Consequently, since the oil viscosity has a greater variation with temperature changes than any other single item in the journal-box assembly, it logically suggests itself as a subject that can be profitably investigated further.

CONCLUSIONS

The railroad industry needs an oil that can be used satisfactorily in all the extreme temperatures of summer and winter weather. Using two grades of oil, one for summer and one for winter weather, has been tried in the past. Using one grade of all-year-round oil is preferable. Such an oil must, however, have a high viscosity index and a very low pour point. It appears that the present range of 50–55 viscosity at 210 F as specified by the Association of American Railroads is about correct.

In boundary lubrication the oiliness factor somewhat transcends the viscosity and viscosity index in importance. The lubricity quality of the oil assumes greater importance when there is only partial separation of the bearing and journal by the oil film. The obvious objective in journal-box lubrication is to keep the bearing on a fluid film. In starting trains before oil is carried under the bearing there is a period of metal-to-metal contact, followed by boundary lubrication and, with proper supporting conditions, finally into full hydrodynamic lubrication. Full

hydrodynamic lubrication obtains a large percentage of the time when optimum viscosity of oil is present.

Discussion

V. C. Barth.[2] There is only one physical and one chemical dimension of a car oil that influences proper lubrication and functional behavior in the indirect self-lubrication media: The proper viscosity of the oil for the operating temperature range and load range where lubrication is in the region of fluid film or about 5 mph; and, oiliness where lubrication is in the boundary-film region below 5 mph.

Because car journals operate at wide variations in load, speed, and, therefore, temperatures, the selection of the optimum viscosity is not so readily apparent as in most other high-grade lubrication practices. The problem is complicated further by the necessity of oil mobility in the waste vehicle in order to insure a supply of oil to the journal.

This combination of operating requirements and the lubricator phase of the problem must be considered in their true relation before any solution is possible, because the basic problem of car-journal lubrication is entirely a lubricator problem and not a lubrication problem.

Considering viscosity from the load angle, a $5^1/_2$-in. × 10-in. bearing broached to $5^{17}/_{32}$ in. under 20,000 lb load on a $5^1/_2$-in. journal will, under static condition, Brinell to approximately a 1-in. crown or about 9 sq in. This area rapidly increases in operation until bearing pressures in the neighborhood of 750 or 800 psi are reached and is gradually reduced to approximately 435 psi when the bearing has attained a full crown or an angular length of 113 deg. It is apparent that the maximum load imposed on a car-journal bearing is not very great.

From the speed angle a $5^1/_2$-in. journal operating at 60 mph with a 33-in. wheel turns at 611 rpm or a peripheral velocity of 880 fpm. This is in no sense an excessive operating speed.

Under the maximum condition encountered in freight-train-car operation, car oils in the range of 42 to 45 sec Universal Saybolt at 210 F have sufficient viscosity to satisfy all the requirements for viscous-film lubrication with a minimum of generated heat. In order to insure true wear rather than wiping under boundary operation, fortifying the oil with a polar compound insures an oriented film that offers little resistance to tangential motion because of its pilelike structure. This oil with a nominal viscosity index will have a viscosity at zero in the range of 5000 to 7000 sec and, therefore, have extremely good mobility in the waste over the ambient-temperature range encountered in country-wide interchange service and completely satisfies the functional relation between the oil and waste as an adequate lubricator.

Approximately 50 per cent of the heat generated in a journal-box assembly is viscous shear, the remainder being packing-journal friction. The higher the viscosity of the oil the higher the generated heat with its attending effect of lowering the factor of lubrication safety.

One study covering series of oils furnished by a major oil company was made and the oils were tested under identical conditions for their stabilized viscosity and produced the following:

Initial viscosity, SUS	Stabilized viscosity, SUS	Journal temperature, deg F
46	48	201
53	49	230
70	47	275
80	46	283
90	49	280

[2] Assistant Engineer of Tests, Chicago and North Western Railway System, Chicago, Ill.

It is apparent that regardless of the initial viscosity of the oil under any sustained operating condition, the resultant viscosity will approximate closely that of any other oil having a lower or higher initial viscosity and that the higher the viscosity the greater the wasted energy and the more heat to dissipate.

In general, the foregoing gives the answer to the question of the effect of ambient temperature on the oil. However, it may be well to point out that while ambient temperature does affect mobility of the oil in the lubricator, this can be minimized greatly by a proper-viscosity oil. The real problem of temperature variation is in the waste and not in the oil. Packing in the months of low atmospheric temperatures is entirely different in its functional behavior from that during the warm and hot seasons of the year. Resilience of the pack increases with lowering temperatures and decreases with elevating temperatures. The ratio of sustained pressure of the pack against the journal between zero and 100 F is in the neighborhood of 4 or 5 to 1 or about the same as winter hotboxes to summer heatings.

The tabulation of comparative viscosities and journal temperatures quoted were taken from a report of Mr. A. A. Schafer in the Test Department of the New York Central Railroad, from which the following also is quoted:

"It does not necessarily follow that upon the basis of this report that raising the viscosity of the oil is a logical procedure. To do that would aggravate causes which, on their face value, may seem to make higher viscosities necessary. Lint influences and capillary at varying atmospheric temperatures are these causes. They result in elevated bearing temperature and it in bearing deformation. Raising the viscosity indiscriminately is, in effect, an attempt to run away from the cause of heatings. These causes simply become worse with higher viscosity."

J. T. Burwell, Jr.[3] The author is to be congratulated upon having elucidated so clearly through his careful experimental work the effect of the very important factor of viscosity on the operation of the railroad-car journal bearing. It is systematic information such as this upon which careful conclusions can be drawn that will provide the best approach to a final solution to the hotbox problem.

The primary purpose of this comment is to draw particular attention to the interesting families of curves given in Fig. 5 of the paper. While the author refers to these curves in one paragraph of his paper, they are so extremely interesting and important in analyzing the effect of viscosity grade of oil on the bearing performance that further elucidation of them might be in order.

There are essentially two independent families of curves plotted in Fig. 5. It is important to note that both families of curves take account of the round-robin effect of viscosity affecting the friction which in turn affects the temperature of the film which in turn affects the viscosity of the oil. Hence these curves represent exactly what the bearing does in practice with a given grade of oil and no further hypothesizing about these interactions is required.

The first family of curves, consisting of the four curves which show more or less of a hump toward the left of the diagram, represent the load that the journal can carry at any speed at a given minimum film thickness, using a particular grade of oil. However, along each of these curves the operating temperature of the bearing changes, in general rising as one proceeds toward the right.

The second family of curves which are not so clearly distinguished, since they are all shown dashed, again represent the load which the bearing can carry for a given speed and maintain the

[3] Associate Director of Research, Horizons Incorporated, Cleveland, Ohio.

same operating temperature, again using the same viscosity grade of oil. Along these curves, however, the minimum film thickness at which the bearing will be operating changes, in general increasing as one goes down and to the right along these curves. (It is presumed that the curves in this family which intersect circles with the full curves of the other family apply to oil A and those which intersect circles on the dashed curves of the other family apply to oil B.)

In other words, both curves represent limiting safe conditions of operation, the one the minimum film thickness below which surface contact and very high friction set in, and the other the temperature above which the oil or bearing surface may deteriorate in one way or another. Only the area below and inside the specified minimum film thickness and maximum temperature represents the region of safe load-speed conditions in both respects. This method of analysis and presentation was first reported by McKee.[4]

In the light of these curves, the remarks of Mr. Barth are extremely interesting. His data indicate that with five different viscosity grades of oil, the bearing, under the same load and speed, reached different temperatures such that the viscosity at temperature was approximately the same in the five cases. This would suggest that the operating minimum film thickness in the five cases was also approximately the same since it is known from hydrodynamic theory that the same value of load divided by the product of speed and operating viscosity in the same bearing will always yield the same minimum film thickness. If this is so, this is a very important finding because then, as Mr. Barth points out, the less viscous grade of oil is the better one to use since the bearing will be running cooler, even in hot weather, and less energy is wasted. This solution would obviously also take care of the cold-weather situation.

Since this is somewhat opposite to Mr. Keller's conclusion, it would be interesting to see whether we can obtain a theoretical confirmation of it or not. The curves in Mr. Keller's Fig. 5 are not appropriate to use to test this finding, but the same data from which they were plotted should, if replotted in a different manner, serve this purpose very well. The curves in Fig. 5 represent curves of constant film thickness and constant viscosity grade in one case, and constant operating temperature and constant viscosity grade in the other, all plotted on a load-speed diagram. To test Mr. Barth's finding, it is suggested that the same data be replotted in the following manner: A family of curves of constant film thickness and constant load in the one case, and a family of constant operating temperature and constant load in the other, be plotted on a speed-viscosity-grade diagram. In this case, for the viscosity-grade ordinate, one may arbitrarily use the viscosity of the particular oil at some standard temperature such as 100 or 210 F. On such a plot, Mr. Barth's finding would be represented by the curves of constant minimum film thickness being parallel to the viscosity-grade axis in the region of speeds that Mr. Barth used. For the constant load for the two families of curves, the load used in Mr. Barth's experiments should preferably be chosen.

Such plots should be extremely interesting in possibly confirming this experimental finding and, in any case, would be an easier form of presenting the data calculated by Mr. Keller in order to decide this very important question of selecting the proper viscosity grade of oil for varying ambient-temperature conditions.

G. L. PIGMAN.[5] The author is to be commended for his paper, which is believed to represent a significant step forward in placing the railroad journal-bearing problem upon a foundation of sound scientific principles.

It also is desired to present comments based on preliminary conclusions which have been reached in the research program being carried out by Armour Research Foundation for the Association of American Railroads on the hotbox problem. These comments relate particularly to those factors which have most direct influence on heat generation and heat dissipation in the railroad bearing, including bearing friction and conditions for oil-film breakdown, waste-pack friction, and bearing-cooling properties.

The friction characteristics of the railroad bearing as determined in our tests are shown in Fig. 7 of this discussion. In Fig. 7 the coefficient of friction f is plotted against a nondimensional load factor $(P/\mu U)\ (c/R)^2$, where P = bearing load, lb per in. journal length; μ = oil viscosity, reyns; U = linear velocity of journal surface, ips; c = difference between journal and bearing radii, in.; and R = journal radius, in. This type of plot is similar to that commonly used to describe bearing friction characteristics, and curves of similar shape normally are obtained in other applications, but some difference in scales has been used

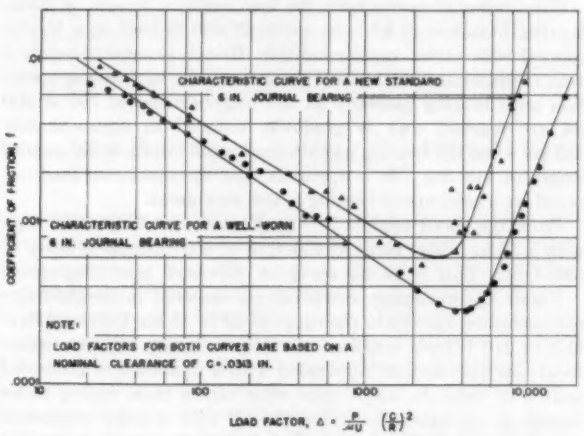

FIG. 7 DIFFERENCE IN OPERATING CHARACTERISTICS OF A NEW AND A WELL-WORN JOURNAL BEARING

which will not now be discussed. The curves may be considered to show the variation of friction coefficient with bearing load divided by oil viscosity times journal speed. The curves show that any combination of these latter quantities which produce a given value of the nondimensional load factor will produce the same coefficient of journal friction.

The straight-line portion of the curves at low values of load factor covers the region of hydrodynamic oil-film lubrication, with decreasing oil-film thickness being obtained as the load factor increases. The minimum point on the curves corresponds to the beginning of oil-film breakdown, after the oil-film thickness has decreased to approximately 0.0001 in. The rising portion of the curves at large values of load factor corresponds to increasing oil-film breakdown and increasing boundary friction. These curves extended to greater load factors will rise rapidly to coefficient-of-friction values of 0.15 to 0.20 with oil present, or to values of 0.35 to 0.40 for a completely dry condition, and then remain essentially constant. The right ends of the curves thus represent an approach to the "hotbox" region.

The minimum point on the lower curve, occurring at a load factor of about 4000, corresponds in practical terms, as one

[4] "Friction and Temperature as Criteria for Safe Operation of Journal Bearings," by S. A. McKee, *Journal of Research*, National Bureau of Standards, vol. 24, 1940, pp. 491–508.

[5] Supervisor, Heat-Power Research Department, Armour Research Foundation, Chicago, Ill.

example, to a bearing load of 22,000 lb, a temperature of 200 F with EM–906–50 type car oil, and a speed of 18 mph.

It is believed that these curves illustrate certain points brought out in the paper. For example, the general effect of oil viscosity can be observed in the region of low load factors (hydrodynamic-film lubrication). A decrease in oil viscosity moves the operating point to the right on the curve. The lower oil viscosity results in decreased friction, but with a thinner oil film closer to the point of oil-film breakdown. Lowest operating friction and greatest operating efficiency may be obtained with low oil viscosity at the minimum point on the curve, but this minimum point also corresponds to beginning of oil-film breakdown and small factor of safety.

With regard to waste-pack friction it has been found that this type of friction is associated with shearing of a thin oil film and follows the physical laws for such phenomena. In particular, it is found that the frictional heating associated with the waste pack varies with $\mu^{0.3} P_w^{0.3} U^{1.3}$ where μ and U are as defined previously and P_w is the pressure force between the waste pack and the journal. The important point for the present discussion is that the heating effect resulting from waste friction is predictable with reasonable accuracy for any given operating condition.

With regard to journal-box cooling, tests have been conducted on a full-scale railroad truck wherein electric heat was supplied in measured amounts to simulate friction heating. Temperatures were measured at different speeds of cooling air as supplied by a blower. From these test results, cooling curves have been plotted which show the relationship between friction horsepower, journal temperature, and car speed at different ambient-air temperatures. It also has been shown in these tests, as discussed in the paper, that the outer end of the journal under some circumstances may have a temperature more than 100 deg F greater than the inner end of the journal.

With these waste-friction data and cooling curves it is possible to answer the question raised previously concerning the range of load-factor values, in Fig. 7, which correspond to normal railroad operating conditions.

Operation curves based on the measured friction and cooling data have been plotted and show, first, that under normal conditions the bearing operates at relatively low load factors, see Fig. 7, or well into the hydrodynamic-film region. The point of particular interest is to define those factors or combinations of factors which tend to move the operation point into the oil-film breakdown region. The test results show that the following factors are among those which tend to have such effect: (1) bearing overload; (2) use of new unfitted bearing; (3) high waste-packing pressure; (4) high ambient temperature; (5) low oil viscosity at high temperature, such as obtained with low-viscosity oil or oil with low viscosity index; (6) sudden decrease in speed while at high temperature.

It is indicated that a combination of several of the foregoing factors can carry the bearing operation into a critical region, although each factor by itself may not always be serious.

Author's Closure

The author wishes to thank Messrs. V. C. Barth, J. T. Burwell, Jr., and G. L. Pigman for the thorough review they made of this paper and the worth-while comments presented.

It is noted that the temperature spread due to viscosity increase shown in Mr. Barth's tabulation is much greater than that of Fig. 2, although the trend is similar. This apparent disagreement might be due to testing conditions, but it indicates the need for more data that can be reconciled in order to reach agreement on the basic principles of journal-box lubrication. It is of interest to note Mr. Barth's comment on viscosity increase affecting capillarity and lint influence adversely and yet while this statement is undoubtedly true Fig. 6 shows that hotbox occurrence is lowest at the time such conditions prevail. This of course cannot be concluded to indicate that lint and poor capillarity are desirable, but that the higher viscosity maintained by cool-weather conditions is helpful in reducing hotboxes.

Mr. Burwell's suggestion that the data of Fig. 5 be plotted on a speed viscosity diagram suggests an approach that promises worth-while results.

As pointed out by Mr. Pigman, a decrease in the oil viscosity moves the operating point on the curves of Fig. 7 to the right on the curve, and while the lower viscosity results in less oil-film shear and consequently, decreased friction, the resultant decrease in oil-film thickness may result in oil-film breakdown and a subsequent hotbox.

Separation of Immiscible Liquids by Means of Porous Membranes

By G. V. JORDAN, JR.,[1] PHILADELPHIA, PA.

In the process industry, porous media are generally associated with filtration and diffusion. However, porous membranes also can be utilized for the separation of immiscible fluids—liquids from gases—gases from liquids—liquids from liquids. The phenomenon of interfacial tension separation as applied to liquid-liquid separatory systems is explained, together with a description of the porous membranes employed. Basic design data and operational features of liquid separatory units and systems are presented. Interesting applications and installations in the process industries are included.

Introduction

THE principal mechanical methods presently employed by the process industries to effect a phase separation of immiscible liquids without alteration of mutual solubilities include gravitational, inertial, and centrifugal systems. All of these methods depend primarily on the differences in the specific gravities of the liquids to be processed and require considerable energy, time, or space for successful operation. These methods are in contrast to distillation, adsorption, and absorption which affect the mutual solubilities of the liquids and, in addition, require the use of heat, specific adsorptives, or deliquescent materials.

Recent evaluations of certain basic principles of capillary physics and surface chemistry, in the light of their possible use as a fluid separatory tool, have brought about an additional mechanical method of separating immiscible liquids without altering mutual solubilities which utilizes, primarily, the interfacial tension value between the liquids and requires a minimum amount of energy, time, and space to effect a complete phase separation.

Basic Principles of Interfacial Tension Separation

We are all familiar with the effects of surface and interfacial tension in our everyday life. The shedding of water droplets from water-repellent garments, the difficulties of wiping up water with an oily cloth, the hazards of driving on a macadam road following a rain, the presence of an interface between two immiscible liquids such as gasoline and water. All of these phenomena are based on the fact that the interface between a liquid and a gas or between two immiscible liquids has strength and will resist rupture. Interfacial tension separation is dependent entirely on methods to support this interface, rendering it more resistant to rupture, thereby allowing the utilization of practical separatory systems under variable flow and pressure conditions.

The entire concept of interfacial tension separation is based on the fact that any porous membrane is pervious to the flow of any liquid under certain conditions, provided the size of the capillaries through the membrane is larger than the molecular size of the liquid; conversely, any porous membrane is impervious to the flow of any liquid under certain other conditions. The conditions which determine whether a porous membrane is pervious or impervious to the flow of a liquid depend primarily on the following:

1 The interfacial tension value between the liquids.

2 The size of the maximum opening in the porous membrane.

3 The degree of wetting, nonwetting, or preferential wetting of the porous membrane by the liquids.

4 The pressure drop of the liquid system across the porous membrane.

A fuller understanding of the basic mechanisms of interfacial tension separation prompts a brief presentation of facts relative to the liquid-liquid interface; the liquid-liquid interface support; and a few fundamental relationships which exist between the liquid-liquid interface and the interface support.

The Liquid-Liquid Interface. When two immiscible liquids are in contact with each other, the molecules of each liquid exert an attraction upon those of the other liquid at the interface (1).[2] This molecular attraction reduces the inward pull of each liquid upon the molecules of its own kind present at the interface. A molecule of either liquid present at the interface will be under different forces from a similar molecule located at some distance from the interface. Under such conditions the liquid-liquid interface will have a surface energy. This surface energy is termed the "interfacial tension." Its value is generally expressed in terms of dynes per centimeter.

The interfacial tension value between two immiscible liquids can be reduced considerably by the presence of surface-active agents such as soaps, detergents, and alcohols. This interference can be so great as to render the interface useless as a separatory factor.

Miscible liquids have no interface and, therefore, no interfacial tension value. Under such conditions they do not render themselves to separation by means of the mechanics of interfacial tension separation.

When a liquid-liquid interface is supported across the surface openings of the capillaries of a porous membrane, the pressure differential across that interface which causes it to rupture completely determines the maximum pressure drop across the porous membrane, which will allow for complete separation.

The liquid which is miscible with that filling the capillaries of the porous membrane will pass through readily according to the basic laws of capillary flow. The liquid which is immiscible with that filling the capillaries of the porous membrane will be retained at the interface formed at the surface opening of the capillaries and therefore will not pass through the porous membrane.

The Liquid-Liquid Interface Support. The liquid-liquid interface support is always a porous membrane which receives one of the immiscible liquids or phases of a mixture and allows it to pass through its capillaries while simultaneously repelling the passage of the other phase. It must not only be wetted by the liquid to pass through but also must be preferentially wetted by that liquid so that the other liquid phases will never displace the first.

In detailing briefly the phenomena of wetting, nonwetting, and

[1] Assistant Manager, Fluid Processing Division, Selas Corporation of America, Philadelphia, Pa.

Contributed by the Process Industries Division and presented at the Annual Meeting, New York, N. Y., November 29–December 4, 1953, of The American Society of Mechanical Engineers.

Note: Statements and opinions advanced in papers are to be understood as individual expressions of their authors and not those of the Society. Manuscript received by ASME Headquarters, September 8, 1953. Paper No. 53—A-221.

[2] Numbers in parentheses refer to the Bibliography at the end of the paper.

preferential wetting, it is necessary to consider the surface chemistry of the liquid-solid boundaries at the surface openings of the capillaries present in a porous membrane. The liquid-solid molecular attraction, or more precisely, the pressure of the ultimate layer of liquid molecule against the solid surface can vary from several thousand atmospheres, as in the case of complete wetting, to lesser values (incomplete wetting), to negative values or actual repulsion.

When two or more immiscible liquids, both of which are capable of wetting a solid surface, are initially in contact with that solid surface, one will displace the other from the solid surface owing to its greater specific molecular attraction to the solid. Under such conditions, that solid surface is preferentially wetted by the more strongly attracted liquid. The surface of the liquid-liquid interface supports are basically classified as hydrophilic (preferentially wetted by water) and hydrophobic (completely water-repellent).

The size of the largest capillary opening in the interface support determines, to a great extent, the maximum pressure that the interface will withstand before rupture occurs. Basically, the smaller the capillary opening in the interface support, the higher the pressure the interface will withstand before rupture occurs. Conversely, the larger the maximum capillary opening, the smaller the allowable pressure before the interface will rupture. The actual relationship between these two variables is hyperbolic.

The ideal liquid-liquid interface support constitutes a porous membrane with controlled maximum pore size. Sufficient open area to permit practical flow rates and a smooth external surface to enable uniform support of the interface are also requirements of the interface support.

Relationship Between Liquid-Liquid Interface and Liquid-Liquid Interface Support. The basic relationship between a liquid-liquid interface and a liquid-liquid interface support may be best explained by examining closely the entrance of a single capillary opening of a porous membrane which is supporting an interface between two immiscible liquids. Specifically, let us consider the distortion of an interface while an external pressure tends to drive one of the phases through the capillary filled with and completely wetted by the other phase. The liquid which preferentially wets the capillary surface lies in intimated contact with the walls of the capillary and the surface adjacent to the entrance of this capillary. Under such conditions the actual interface does not come in contact with the solid surface; therefore we are dealing specifically with a two-phase liquid system and the interface support is utilized only as a means of imposing a dimensional limitation upon that system.

The thickness of the liquid film which preferentially wets the capillary depends upon several factors; however, it is assumed that this thickness is inconsequential in comparison to the size of the opening. The strength of this film is great enough to overcome any molecular attraction between the liquid molecules at the surface of the solid and the nearest molecules of the liquid immiscible with the liquid which wets the capillaries.

Fig. 1 illustrates, schematically, a single capillary of a liquid-liquid interface support which is preferentially wetted by liquid A and supports the interface formed by contact with liquid B which is immiscible with liquid A. Note the presence of the liquid film at location L, which is formed by the complete wetting of the capillary C by liquid A which prevents liquid B from contacting the surface of the capillary.

Section 1 indicates the normal distortion of the interface at a safe operating pressure. In this position the component of the interface parallel to the capillary axis at the flex point X of the distortion, is strong enough to resist the pressure P, which tends to force the liquid B through the capillary C.

Section 2 indicates the position of the distortion of the interface

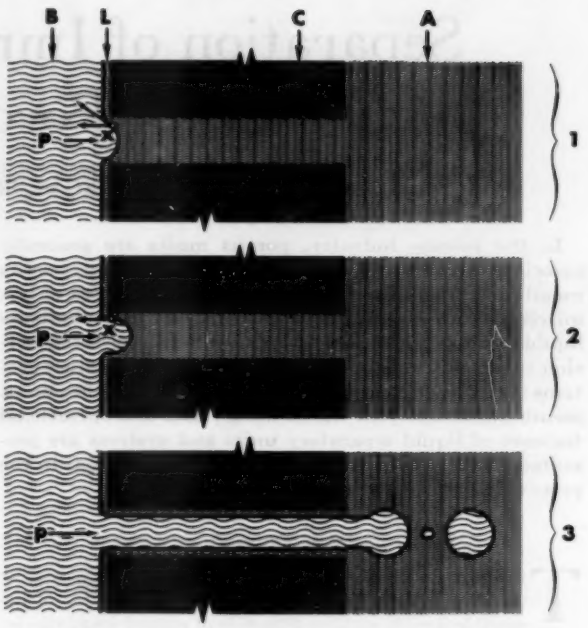

FIG. 1 THE LIQUID-LIQUID INTERFACE SUPPORT

at a critical operating pressure at which liquid B begins to flow through the capillary C. In this position, the interface surface has just become parallel to the axis of the capillary, at flex point X. Under such conditions, the entire interface surface is directly opposed to the pressure P.

Section 3 indicates complete rupture of the interface resulting from an increase in pressure P above the critical range, which allows liquid B to pass through capillary C. This condition will cause incomplete separation.

The maximum safe operating pressure for any given liquid-liquid separatory system, across a system of circular capillaries of a known maximum capillary radius, can be calculated on the basis that the force which tends to cause rupture of the interface is a product of the pressure P and the effective capillary cross-section area A. The force-resisting rupture of the interface is a product of the interfacial tension value σ and the circumference of the capillary opening C. Thus $\sigma C = PA$. For a circular capillary of radius r, then $2\pi r\sigma = \pi r^2 P$ or $P = 2\sigma/r$.

Fig. 2 outlines the relationship between the maximum capillary radius of the interface support, the rupture pressure of the interface, and the interfacial tension value of the liquids forming the interface. The maximum capillary radius of the liquid-liquid interface supports were determined by the "bubbling pressure method" (2) based on an equation developed by Herbert Freundlich (3). The interfacial tension value of the several immiscible liquids were derived from published data. This graph can be utilized readily to determine the maximum pressure differential that can be employed across an interface support of a known maximum pore radius for the complete separation of immiscible liquids of known interfacial tension value.

EMULSIONS

For successful continuous practical operation, the mechanics of interfacial tension separation demand that the liquids be presented to the interface supports in clearly defined phases. For example, if we utilize a hydrophobic interface support to separate water from a hydrocarbon, the hydrocarbon phase will wet the interface

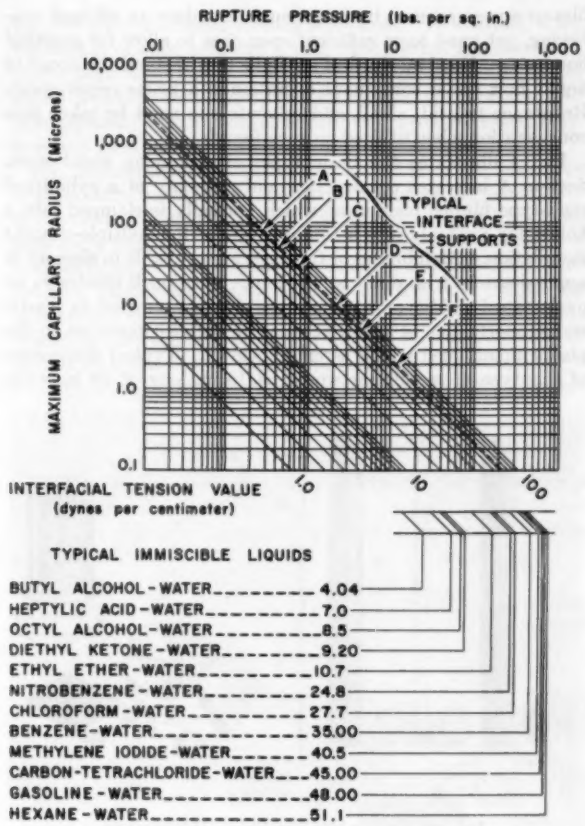

FIG. 2 RELATIONSHIP BETWEEN MAXIMUM CAPILLARY RADIUS AND INTERFACE SUPPORT; RUPTURE PRESSURE OF INTERFACE; AND INTERFACIAL TENSION VALUE OF LIQUIDS FORMING INTERFACE

support preferentially since the support is water-repellent; therefore the hydrocarbon will readily pass through the capillaries of the interface support and any water phase will be retained at the interface at any pressure differential up to the specified rupture pressure.

However, if this same hydrocarbon-water mixture is presented directly to a hydrophobic interface support in the form of an unstabilized emulsion, there would be an interference to the flow of the hydrocarbon through the hydrophobic interface support until the hydrocarbon freed itself from the confusion of the emulsion and formed a clearly defined continuous phase which would be received by the hydrophobic interface support and passed through its capillaries.

A brief description of emulsions and how they are processed for presentation to the interface supports is presented.

An emulsion is generally defined as a dual-phase liquid system in which fine droplets of one liquid are dispersed in a second liquid with which it is completely immiscible or incompletely miscible (4). Generally they are formed by the mixing or agitating of the liquids as would occur during process operations or transportation. The components of an emulsion consist of a continuous or predominant phase and a dispersed phase. The continuous phase is generally, but not necessarily, that phase which is in excess of the dispersed phase. The size and shape of the droplets, relative viscosity of the liquid, the presence of surface-active agents, and several other factors can determine which of the liquids constitutes the continuous or dispersed phase (5). The dispersed phase is generally present in the continuous phase in the form of fine droplets which tend to rise or fall as a result of variation in droplet size and density difference. There is always a tendency for these droplets to concentrate, conglomerate, and separate out as a continuous phase.

Emulsions generally are classified as stable or unstable. The stability of emulsions is determined by the permanence of the dispersed droplets in the continuous phase and if the dispersion remains permanent then it is considered a stable emulsion. This permanence of the dispersion is entirely dependent on factors which prevent contact between the droplets and therefore prevent them from conglomerating.

The important factors which determine the permanence of the dispersion are the presence of electrical charges on the surface of dispersed droplets or a capsulating film around the droplets which is both protective and resistant but not adhesive (6). The film is the result of the effects of surface-active agents present in the form of liquids or fine solid particles which surround the droplets and prevent the conglomeration of the droplets on collision by virtue of the mechanical strength of the film. The droplets or particles constituting the dispersed phase of a stable emulsion are generally in the range of 1.5 microns diam or less (7).

When the effects of the electrical charge or the capsulating film are sufficient to reduce considerably or destroy almost entirely the interfacial tension value between the liquids, separation by the mechanics of interfacial tension separation is improbable.

Unstable emulsions, to a great extent, are formed in the same manner and have the same general physical characteristics and appearance as stable emulsions. In many instances the size of the dispersed droplets is as small as those encountered in stabilized emulsions but there also may be present droplets of much larger size, in the range of 1 mm (8). However, the total interfering effect of any surface activity or electrical charge that may be present is not great enough to render the dispersion permanent.

The basic difference between a stable and an unstable emulsion is the fact that in an unstable emulsion the interfacial tension value between the liquid has not been reduced drastically or destroyed entirely; therefore the dispersed droplets can be induced to conglomerate by physical means. Under such conditions, the mechanics of interfacial tension separation are applicable to the complete phase separation of such unstable emulsions.

COALESCING

The liquid mixtures presented to the mechanics of interfacial tension separation for complete phase separation are generally in the form of unstable or partially stabilized emulsions. However, as previously indicated, the interface support is not capable of effecting a separation of mixtures presented directly to it in the form of an emulsion. Therefore a preconditioning operation is necessary for the presentation of the mixture to the interface support for final separation. This preconditioning operation is termed "coalescing."

Coalescing is basically that operation which causes the droplets of the dispersed phase of an unstabilized emulsion to conglomerate and form a clearly defined phase. The most important contributing factor to this operation is the interfacial tension value between the liquids. Generally, the greater the interfacial tension value, the more readily the liquids will coalesce. The presence of surface activity, fine dirt particles in the dispersed phase, and a relative viscous continuous phase will reduce considerably the rate at which coalescing will occur.

The process industry utilizes a variety of methods to effect coalescing of emulsions, the principal one being the simple settling tank which reduces the velocity of the emulsion stream presenting a quiescent state which enables the dispersed droplets to conglomerate and form clearly defined phases. Modifications of the simple settling tank employing vessels of various shapes and in-

corporating baffles and flow directional inducers are also utilized. Addition and recycling of excess dispersed phase is another method of assisting coalescing (9). Flow of emulsions through beds of rather coarse porous materials such as steel wool, wire mesh, excelsior, and glass fibers also is effective (10).

Observations and tests have indicated, however, that the most effective and rapid coalescing is brought about by causing the emulsion to pass through comparatively fine rigid-type porous membranes possessing a fibrous structure. Coalescing through such membranes is effected initially by the removal of the surface film surrounding the dispersed-phase droplets by a filtration operation. This phase occurs at or near the external surface of the membrane. The channeling effect of the fibrous structure of the coalescing membrane then comes into play by inducing the dispersed-phase droplets to conglomerate at an accelerated rate by intimate contact through the restricting openings.

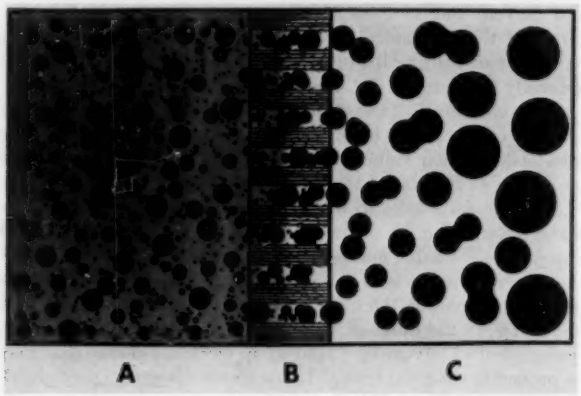

FIG. 3 COALESCING IN OPERATION

Fig. 3 illustrates, schematically, the sequence of coalescing operations as they occur through the porous section of a rigid-type coalescing membrane. Section A indicates the normal structure of an unstable emulsion before processing. In section B the droplets minus the capsulating film are going through exaggerated openings of a coalescing membrane. Note induced conglomeration by intimate contact. Section C illustrates coalesced droplets in a conditioned continuous phase. Note the formation of larger droplets by additional collision as they travel from the membrane.

Because of variations in interfacial tension values, relative viscosities, and strength of the capsulating film, it is extremely difficult to predetermine the maximum safe velocity and rates of flow through coalescing membranes. The presence of an excessive amount of solid particles, particularly of a gelatinous nature, will interfere greatly with coalescing since it will tend to plug the membranes prematurely. The interfering effect of these factors can be determined only by actual tests.

DESCRIPTION OF POROUS MEMBRANES

A basic separatory system incorporating interfacial tension separation generally employs three distinct types of porous membrane—coalescing membranes, hydrophobic separatory membranes, and hydrophilic separatory membranes. A description and the basic characteristics of each type are presented.

Coalescing Membranes. The basic requirements of a coalescing membrane are that it must possess a fibrous structure to initiate coalescing and sufficient depth of fibrous structure to complete this operation. The fibrous structure must be uniform to eliminate the by-passing of any uncoalesced stream. Further, the fibrous structure must be fine enough to induce an efficient coalescing, yet must have sufficient open area to allow for practical flow rates. Good mechanical strength to withstand the abuse of liquid flow under continuous operation is a prime requirement. Resistance to acid, alkali, and solvents also must be taken into consideration when utilized on such liquids.

Fig. 4 illustrates the basic types of coalescing membranes. Section A indicates construction and assembly of a cylindrical rigid-type fibrous membrane which normally is clamped into a holder for assembly into a common header for multiple-element installation. Membranes of this type are available in sizes up to approximately 4 in. diam × 4 ft long. Section B illustrates an oval-shaped rigid-type membrane which is cemented to plastic end supports, one of which acts as the outlet connection to the plastic manifolded holder assembly shown. Typical dimensions of this type of membrane would be 15 in. long × 10 in. wide.

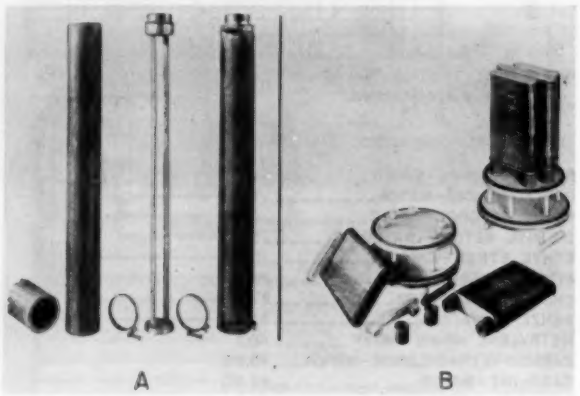

FIG. 4 GROUP OF COALESCING MEMBRANES

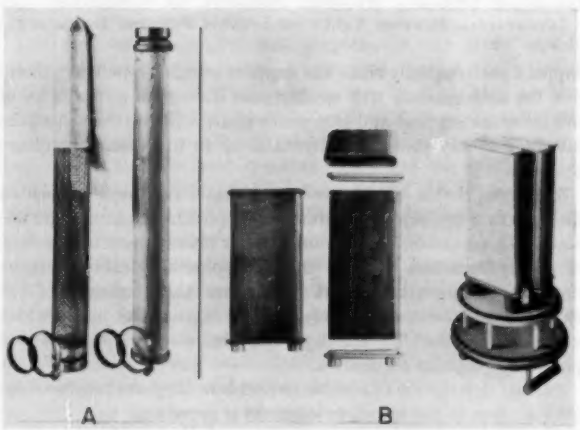

FIG. 5 GROUP OF SEPARATORY MEMBRANES

Variations of these designs also are utilized depending on the particular operating conditions to which they are applied.

Separatory Membranes. Since the prime function of the hydrophobic separatory membrane is to retain the aqueous phase, its most important requirement obviously is that it be water-repellent. Conversely, the hydrophilic membrane must be readily and preferentially wetted by water in order that it allow the passage of the aqueous phase and retain the organic or hydrocarbon phase.

Since both the hydrophilic and hydrophobic separatory membranes are utilized as liquid-liquid interface supports, control over

the size of the maximum opening is required. In addition, a high percentage of open area and a thin cross section are desirable to enable high flow rates of liquids through the membranes at the lowest possible pressure drop to minimize the possibility of interface rupture. Good mechanical strength, a smooth external surface, and good chemical resistance are also required.

Fig. 5 illustrates construction and assembly of the basic types of separatory membranes. Section A indicates the construction of a cylindrically shaped flexible-type hydrophobic or hydrophilic separatory membrane supported by a wire screen which forms an adapter to which the membrane is clamped and assembled into a common header for multiple-element installation. Rigid-type cylindrically shaped hydrophobic or hydrophilic separatory membranes also are utilized requiring a minimum of internal support. Section B illustrates an oval-shaped rigid-type hydrophobic or hydrophilic separatory membrane equipped with plastic connecting end supports.

The Basic Separatory System

The basic separatory system incorporating the mechanics of interfacial tension separation employs two operations in sequence, primary operation being coalescing, the final operation, complete phase separation.

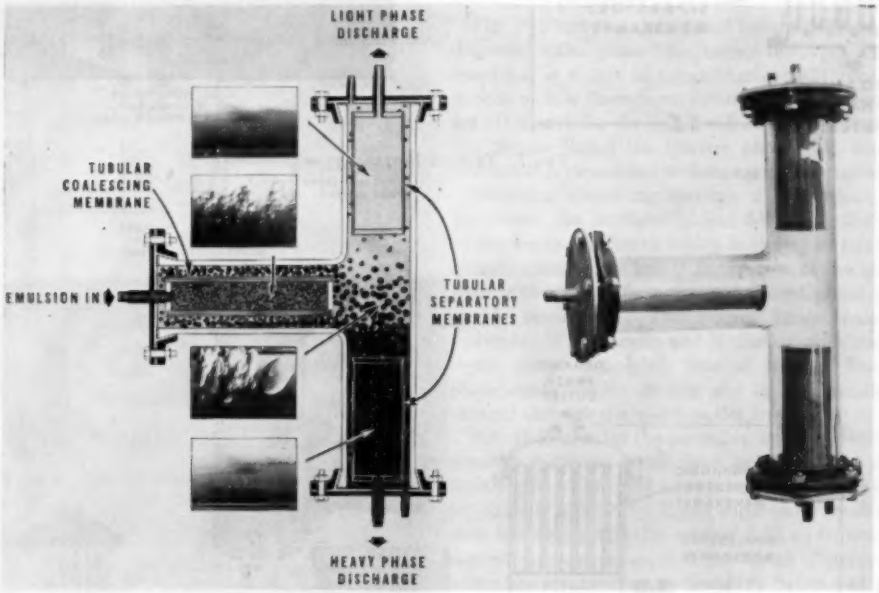

Fig. 6 Basic Separatory System

Fig. 6 illustrates the arrangement of a simple separatory unit incorporating a coalescing membrane, a hydrophobic separatory membrane, and a hydrophilic separatory membrane. The accompanying diagram illustrates the various operations that occur during the course of flow of an emulsion through the several sections. As indicated, the emulsion enters the unit, passes through the coalescing membrane and is discharged to the separatory section as clearly defined phases with a well-defined interface. Natural division of the liquids according to respective values of specific gravity will bring the heavier phase in contact with the lower membrane which has been selected (hydrophobic or hydrophilic) to pass that liquid and retain the other. Rise of the lighter phase to the upper section will bring it in contact with the membrane located there and selected (hydrophobic or hydrophilic) to pass only the lighter phase. Entrained droplets of the foreign phase due to the velocity of the stream will be retained by the selected membrane, coalesce with additional droplets, and return to their respective phase. Thus there is always an exchange of droplets occurring in the comparative quiescent area formed by the separatory section. The interface is generally held at a point midway between the separatory membrane and its position is controlled by relative throttling of the flow of the separated phases.

Typical Applications and Installations

The mechanics of interfacial tension separation are utilized in the chemical and pharmaceutical industries to separate emulsions encountered in steam distillations, solvent extractions, and organic reactions, as well as for the recovering of costly organic materials in a variety of processing operations. They also are utilized for the removal of water from hydrocarbons such as gasoline, kerosene, jet fuel, diesel oil, and fuel oil in the petroleum, aviation, automotive, and marine industries.

Fig. 7 illustrates a typical installation in a chemical plant to separate an organic-water emulsion and recover the costly organic liquid. In this installation the organic phase is the continuous and heavier phase and the water is the dispersed and lighter phase. The emulsion is fed to the separatory unit at a pressure of 25 psig and at a rate of 600 gph. Following coalescing, the heavier organic phase travels to the bottom of the separatory section, passes through the hydrophobic membranes which render it completely water-free, down to the range of solubilities, and is discharged to a holding vessel for further processing. The lighter water phase rises to the top of the separatory section, passes through the hydrophilic separatory membranes which render it completely free of the organic liquid, and is discharged directly to the drain. This unit employs four coalescing membranes each $2^1/_2$ in. diam × 24 in. long and seven hydrophilic and hydrophobic separatory membranes each $2^1/_2$ in. diam × 16 in. long. The position of the interface is indicated by the sight-glass arrangement and controlled manually by throttling the flow of the organic phase.

Fig. 8 illustrates construction and assembly of a unit to sepa-

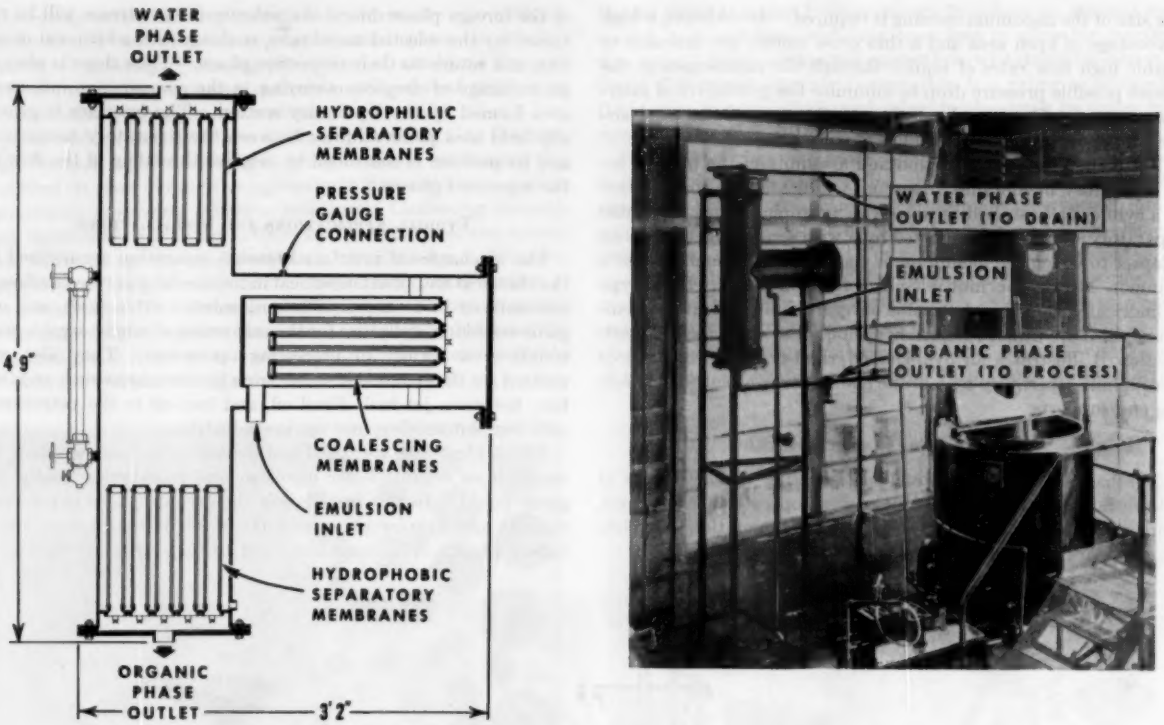

FIG. 7 TYPICAL INSTALLATION

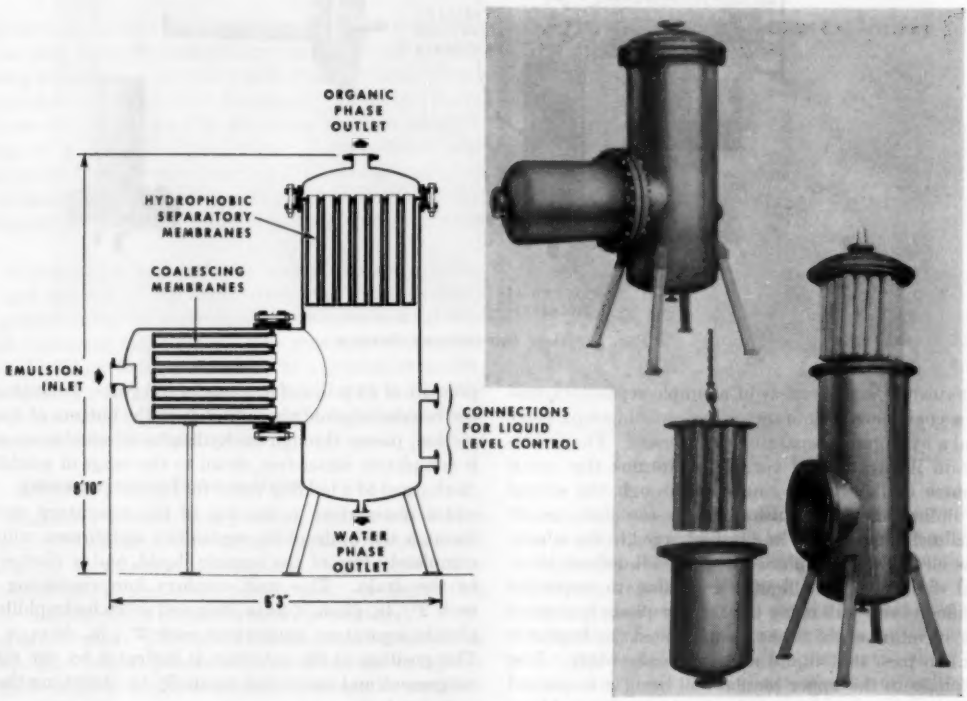

FIG. 8 UNIT TO SEPARATE BUTADIENE-WATER EMULSION AT A RATE OF 6000 GPH

rate a butadiene-water emulsion at a pressure of 125 psi at the rate of 6000 gph. In this case, the heavier water phase is dispersed in the butadiene in an amount of 0.7 to 1 per cent. This is reduced to an amount of 500 to 700 ppm of water in the butadiene which approaches the solubility range. In this installation, coalescing is so effective that the hydrophilic membranes are not required for the removal of butadiene from the water. The interface is located at the bottom of the unit and its position is controlled automatically by a liquid-level controller (not shown) which in turn controls the discharge rate of water as it accumulates. This unit employs nineteen rigid-type coalescing membranes each 3 in. diam × 32 in. long and thirty-seven hydrophobic separatory membranes, each 3 in. diam × 28 in. long.

FIG. 9 UNIT TO PROCESS HAZARDOUS LIQUIDS

A departure from the normal inverted T-structure design is illustrated in Fig. 9. This unit is utilized to separate an extremely hazardous nitrated organic liquid-water emulsion at the rate of approximately 700 gph at a maximum pressure of approximately 25 psi. In this emulsion, the water is the continuous and lighter phase while the heavier, viscous, nitrated, organic liquid constitutes the dispersed phase. Because of space limitations and necessity to minimize total liquid hold-up the unit was designed to permit coalescing and separation in a vertical plane. The novel design of the coalescing and separatory membranes incorporating plastic end supports permitted connection and assembly to an all-plastic carrier for quick and safe membrane exchange. The hazardous nature of the emulsion demanded that all surfaces be highly polished to eliminate the presence of any minute pockets where emulsions may be trapped. This requirement also forbids the use of any threaded sections.

There are cases where it is not possible to utilize the difference in specific gravity between the liquids which make up the emulsion to assist in the formation of clearly defined phases following coalescing. In some instances the specific gravities are equal

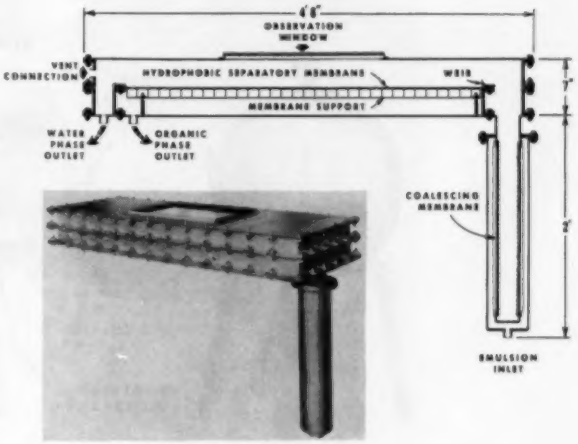

FIG. 10 ZERO GRAVITY DIFFERENTIAL UNIT

and there are occasions where the differences are not sufficient or the specific gravities will change owing to variations in temperature during processing.

Fig. 10 illustrates design and assembly of a unit to separate a dispersed water phase from benzol following a steam-distillation operation at a rate of approximately 500 gph. During certain periods of flow there is no difference in the specific gravity; during other periods, the water will constitute the lighter phase and the organic liquid the heavier phase. At times, this relative position is reversed due to temperature variations.

Following coalescing through a cylindrical, rigid coalescing membrane, the coalesced phases flow along the top surfaces of a hydrophobic membrane which is sloped in relation to the angle of inclination of the unit. Inclination of the unit assists in controlling the rate of flow of the coalesced phase across the hydrophobic membrane. The benzol phase passes through the hydrophobic membrane and is discharged through the organic-liquid outlet completely free of water. The retained water phase continues on to the end of the membrane and is discharged through the water outlet free of any undissolved benzol.

Fig. 11 illustrates the assembly and construction of a unit to separate dispersed water from gasoline of jet fuel at a rate of 60,000 gph. This unit has over-all dimensions of approximately $3^1/_2$ ft × $6^1/_2$ ft × $7^1/_2$ ft and employs 80 coalescing membranes, each having an effective area of 3.25 sq ft, and 30 hydrophobic separatory membranes, each having an effective area of 8.5 sq ft which are arranged on an assembly flange and positioned as set forth in the illustration. After coalescing, the lighter hydrocarbon phase passes through the hydrophobic membranes and is discharged to the hydrocarbon-phase outlet. The rejected heavier water phase accumulates in the vessel attached to the bottom of the unit and is discharged automatically or manually depending on the type service. The interface is generally held at a point midway between the sight-glass arrangement and its position is maintained by automatic or manual throttling of the discharge rate of the water phase. Similar units are in operation for the separation of dispersed water from gasoline and jet fuel at rates up to 120,000 gph and for the removal of water from fuel oil, diesel oil, and kerosene at rates up to 60,000 gph.

CONCLUSIONS

The mechanics of interfacial tension separation employing porous membranes constitutes a practical, economical method of separating unstable emulsions on a production basis. Perhaps a

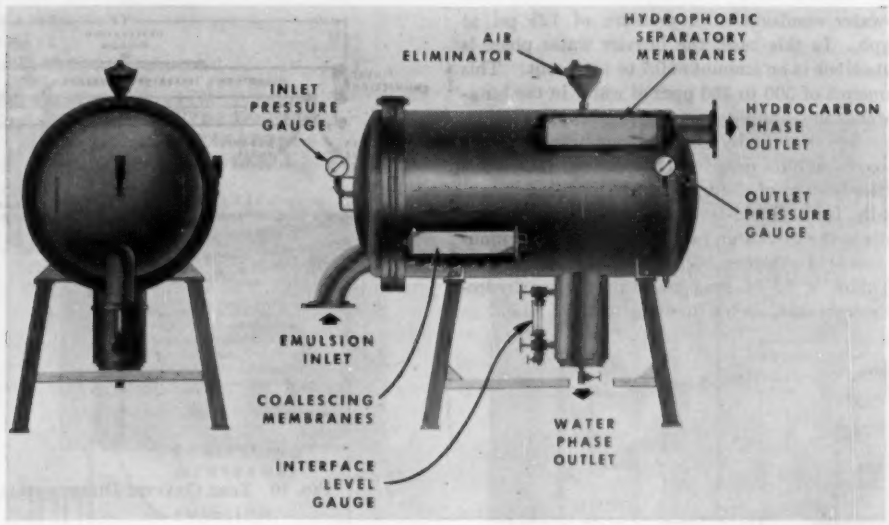

FIG. 11 UNIT TO SEPARATE GASOLINE-WATER EMULSION AT A RATE OF 60,000 GPH

more intimate knowledge of the basic principles of surface chemistry and capillary physics will enable the process industry to devise practical, economical methods to accomplish an even more difficult operation, namely, the separation of stabilized emulsions.

BIBLIOGRAPHY

1 "Industrial Chemistry of Colloidal and Amorphous Material," by W. K. Lewis, L. Squires, and G. Broughton, The Macmillan Company, New York, N. Y., first edition, 1942, p. 47.

2 "Experiment Bestimmung der Kanalweite von Filtern," by A. Einstein and H. Muhas, *Deutsche Medizinische*, BA XLIX, 1923, S 1012.

3 "Colloid and Capillary Chemistry," by H. Freundlich, E. P. Dutton and Co., New York, N. Y., second edition, 1922, pp. 18–22.

4 Reference (1), p. 250.

5 "Liquid Extraction," by R. E. Treybal, McGraw-Hill Book Company, Inc., New York, N. Y., first edition, 1951, p. 282.

6 Reference (1), p. 250.

7 "Emulsions and Foams," by S. Berkman and G. Egloff, Reinhold Publishing Corporation, New York, N. Y., first edition, 1941, p. 105.

8 "Science of Petroleum," by T. G. Hunter, Oxford University Press, London, England, vol. 3, 1938, p. 1779.

9 "Accelerated Breaking of Unstable Emulsions," by H. P. Meissner and B. Chertow, *Industrial and Engineering Chemistry*, vol. 38, 1946, pp. 856–859.

10 "Desalting of Petroleum by Use of Fiberglas Packing," by T. A. Burtis and C. G. Kirkbride, Trans. AIChE, vol. 42, 1946, pp. 413–439.

Important New and Forthcoming Publications

ASME TRANSACTIONS FOR 1954
Published March, 1955 $15.00; $7.50 to ASME members

This massive reference places at your fingertips a vast amount of authoritative and factual information on significant developments in processes, materials, equipment, and techniques of production. Problems dealt with in its 207 papers and discussions are those associated with automatic control and servomechanisms, aviation, applied mechanics, fuels, fluid flow, gas turbine power, heat transfer, hydraulic control, lubrication, machine design, metal cutting, metal testing, power plants, steam piping, thermal stresses, etc. Bibliographies are keyed to many of the articles.

PROCEEDINGS OF THE SECOND U. S. NATIONAL CONGRESS OF APPLIED MECHANICS
Publication date—May, 1955 $9.00 to ASME members and nonmembers

This book will prove invaluable to those investigating any of the major problems of applied mechanics. Its 99 papers, which have been prepared by a group of eminent specialists, give details of original researches in dynamics, kinematics, vibration, wave motion, mechanical properties of materials, stress analysis, elasticity, plasticity, fluid mechanics, and heat transfer; and provide information on some of the new analytical tools and procedures used.

SAFETY CODE FOR INDUSTRIAL POWER TRUCKS (B56.1—1955) $1.00*

Like the earlier edition, rules of this code apply to both the driver-ride and driver-lead types, such as platform trucks, tractors, low-lift trucks, high-lift trucks, fork trucks, special industrial trucks, etc. Part 1 covers the construction and design features of the industrial trucks and types of accident prevention guards and guarding devices. Part 2 contains rules and regulations applicable to industrial trucks of both the driver-lead and powered hand-type, including those powered by gasoline engines, gas-engine generating equipment, or storage battery. Part 3 supplies thirty-five safety rules and regulations for truck operators. The Code also defines and illustrates the various types of trucks.

AN ASME PAPER Published 1955 50c*

This pamphlet gives suggestions for the preparation, submission and presentation of a paper. While written for the guidance of those preparing papers to be given at ASME meetings, it will be found helpful to others who wish to become familiar with the principles of good technical writing.

NATIONAL PLUMBING CODE (A40.8)
Published March, 1955 $3.50*

Here, at last, is the first true national code. It was developed through a careful study of existing codes and examination of their provisions in the light of new data obtained from extensive investigations. Its requirements, which are set forth in fourteen chapters and seven appendixes cover materials and the standards to which they should conform; joints and connections; traps and cleanouts; interceptors, separators and backwater valves; plumbing fixtures; hangers and supports; indirect waste piping and special wastes; water supply and distribution; drainage system; vents and venting; storm drains; inspection, tests, and maintenance; individual water supply; individual sewage-disposal system; sizing the water-supply system; trailer park plumbing; plumbing installation within a trailer coach; and air gaps, backflow preventers, and drinking fountains.

GAS TRANSMISSION AND DISTRIBUTION PIPING SYSTEMS (B31.1.8)
Publication date—April, 1955 $2.50*

A general revision of the 1952 Code, this 1955 document covers design, fabrication, installation, inspection, testing, and the safety aspects of operation and maintenance of gas transmission distribution systems including gas pipe lines, gas compressor stations, gas metering and regulating stations, gas mains, and gas service up to the customer's meter set assembly. It also covers the conditions of use of the elements of the piping systems including pipe, valves, fittings, flanges, bolting, gaskets, regulators, pressure vessels, pulsation, dampeners, and relief valves.

SURFACE ROUGHNESS, WAVINESS AND LAY (B46.1—1955) $1.25*

This document is a revision and consolidation of the standards on Surface Roughness and Physical Specimens published in 1947 and 1952 respectively. It establishes definite classifications of roughness, waviness and lay; presents a set of symbols for drawings specifications and reports; gives specifications for surfaces intended as precision roughness specimens of roughness height and for surface finish specimens intended to illustrate commonly used machines surfaces. Important new additions to the standard are the requirements for tracer type instruments; the supplementary notes on their use; methods of producing, controlling, and inspecting surfaces; and criteria for the selection of surface qualities.

* 20% discount to ASME members

From The American Society of Mechanical Engineers 29 W. 39 St., New York 18, N. Y.